

Electronic Thesis and Dissertation Repository

6-17-2015 12:00 AM

Non-Linear Chirp Spread Spectrum Communication Systems of Binary Orthogonal Keying Mode

Quan Wang
The University of Western Ontario

Supervisor
Jin Jiang
The University of Western Ontario

Graduate Program in Electrical and Computer Engineering
A thesis submitted in partial fulfillment of the requirements for the degree in Doctor of Philosophy
© Quan Wang 2015

Follow this and additional works at: <https://ir.lib.uwo.ca/etd>



Part of the [Systems and Communications Commons](#)

Recommended Citation

Wang, Quan, "Non-Linear Chirp Spread Spectrum Communication Systems of Binary Orthogonal Keying Mode" (2015). *Electronic Thesis and Dissertation Repository*. 2898.
<https://ir.lib.uwo.ca/etd/2898>

This Dissertation/Thesis is brought to you for free and open access by Scholarship@Western. It has been accepted for inclusion in Electronic Thesis and Dissertation Repository by an authorized administrator of Scholarship@Western. For more information, please contact wlsadmin@uwo.ca.

**NON-LINEAR CHIRP SPREAD SPECTRUM COMMUNICATION
SYSTEMS OF BINARY ORTHOGONAL KEYING MODE**

by

Quan Wang

Graduate Program in Engineering Science

Department of Electrical and Computer Engineering

A thesis submitted in partial fulfillment
of the requirements for the degree of Doctor of Philosophy

The School of Graduate and Postdoctoral Studies
The University of Western Ontario
London, Ontario, Canada

Abstract

Chirp spread spectrum (CSS) is a suitable choice of modulation signals for wireless communications, due to its inherited advantages such as low transmission power, simplicity of implementation, good interference rejection capability. Linear chirps are common choices in practical CSS systems of binary orthogonal keying (BOK) mode. However, linear chirps generally require the time-bandwidth product of each chirp signal to be 60 sHz or more in order to achieve desirable orthogonality requirements. Thus, a BOK CSS system based on linear chirps has to occupy very wide bandwidth, which is a very precious resource for wireless communication. Clearly, the requirement on broad frequency bandwidth is a major limiting factor for the widespread adoption of the BOK linear CSS system in practice. To overcome this drawback, it is worthwhile to explore other types of chirp signals outside the linear domain, which can potentially reduce the bandwidth requirement without jeopardizing the system performance. This is the main objective of the current research. In this dissertation, a pair of non-linear chirps has been discovered, which has the potential to replace linear chirps for BOK CSS systems.

After exploring desirable properties of non-linear chirps, it is demonstrated that a significant performance advantage on orthogonality over linear chirps can be achieved by a pair of sine or cosine chirps. Subsequently, properties of sine and cosine chirps are analyzed mathematically. Derivations of spectral characteristics, autocorrelation and cross-correlation for both sine and cosine chirps are carried out respectively. Finally, comparison of sine chirps of four different time periods (i.e. half time period, full time period, triple time period, and quadruple time period) are made in terms of their cross-correlation and autocorrelation properties. It has been concluded that full period sine (FPS) chirps are the better choice for this particular application among the sine chirps.

Performance of a BOK CSS system based on FPS chirps has been evaluated in three typical scenarios. Firstly, BER (bit error rate) performance of the BOK FPS CSS system in an additive white Gaussian noise (AWGN) channel is derived. Furthermore, performance comparison in terms of BERs between linear chirps and FPS chirps is examined. Secondly, effects of Doppler shift on the BOK FPS CSS system are analyzed. The effect of Doppler

shift between linear chirps and FPS chirps has been compared. Thirdly, BER performance of the BOK FPS CSS system in a fading environment (Rayleigh channel) has been analyzed. Moreover, BER performance comparisons between linear chirps and FPS chirps in the AWGN+Rayleigh channel with and without a Doppler shift have also been studied.

Using analytic means and numerical simulations, this dissertation has conclusively demonstrated that a pair of orthogonal FPS chirps has the capability of replacing linear chirp in BOK CSS systems.

Keywords: CSS; non-linear chirp; sine chirp; cosine chirp; orthogonality; conditional orthogonality; periodic orthogonality

Acknowledgments

Firstly, I would like to extend my sincerest gratitude to my supervisor, Professor Jin Jiang, for his continuous help, patience and guidance throughout the entire duration of my Ph.D. studies at the University of Western Ontario. Without his time, encouragement, efforts, and knowledge, this thesis would not have been completed. I could not wish for better or friendlier supervisors.

Secondly, I must express my appreciation to Dr. Xinhong Huang for her comments and suggestions in improving the quality of this thesis. Special thanks also go out to Dr. Sree Ram Valluri for helping me on the mathematical derivations in my thesis. I also would like to thank members of the Control, Instrumentation and Electrical Systems (CIES) research group at the University of Western Ontario, for their help and advice.

Of course, the greatest appreciation of all goes to my family whose insightful advice, strongest support, utmost understanding and endless patience inspired me to overcome any hurdles in my way. My beloved wife, Shugui Yang, did everything she could to support my study and never complained about my long hours work at school. Many thanks go out to my little daughter, Mandy Shiqi Wang, for her love. In addition, the love and believing from my parents played the major role in making me who I am today.

Finally, I would like to express my great gratitude to NSERC and UNENE Canada for supporting this work.

Table of Contents

Acknowledgments.....	iv
Table of Contents.....	v
List of Tables.....	x
List of Figures.....	xi
Acronyms.....	xvi
Nomenclature.....	xix
1. Introduction.....	1
1.1 Chirp Spread Spectrum Systems.....	1
1.2 Previous Work.....	3
1.3 Problems, Motivations and Objectives.....	4
1.3.1 Problems.....	4
1.3.2 Motivations.....	5
1.3.3 Objectives.....	5
1.3.4 Methodology.....	6
1.3.5 Scope.....	7
1.4 Contributions of the Thesis.....	7
1.5 Organization of the Thesis.....	8
2. Chirp Spread Spectrum.....	10
2.1 Matched Filter.....	10

2.2	Pulse Compression.....	12
2.3	Principle of the BOK CSS System.....	14
2.4	The BOK Linear CSS System.....	17
2.5	Summary	23
3.	Non-Linear Chirps for the BOK CSS System	24
3.1	Method to Explore Non-Linear Chirps for the BOK CSS System	24
3.1.1	General Representation for Arbitrary Chirps.....	24
3.1.2	Representation for a Pair of Chirps for the BOK CSS System.....	26
3.1.3	Method to Determine Non-Linear Chirps for the BOK CSS System	27
3.2	Non-Linear Chirps	28
3.2.1	3rd Power Function Chirps	28
3.2.2	Sine Chirps.....	32
3.2.3	Cosine Chirps.....	37
3.2.4	Exponential and Other Non-Linear Chirps	41
3.3	Conclusions.....	41
4.	Properties of Sine and Cosine Chirps	42
4.1	Introduction.....	42
4.2	Spectral Characteristic	42
4.2.1	Sine Chirps.....	43
4.2.2	Cosine Chirps.....	45

4.2.3	Summary	46
4.3	Autocorrelation Properties	48
4.3.1	Sine Chirps	48
4.3.2	Cosine Chirps	52
4.3.3	Summary	56
4.4	Cross-correlation Properties	56
4.4.1	Cross-correlation Coefficient	56
4.4.2	Orthogonal Characteristics	61
4.4.3	Simplification of the Cross-correlation Coefficient	66
4.5	Sine Chirps of Different Time Period	69
4.5.1	Half Period	70
4.5.2	Triple Period	73
4.5.3	Quadruple Period	76
4.5.4	Summary	79
4.6	Comparison with the Linear Counterpart	80
4.6.1	Spectral Characteristic	80
4.6.2	Autocorrelation Property	82
4.6.3	Cross-correlation Property	82
4.6.4	Summary	83
5	Performance of the BOK FPS CSS System	85

5.1	The BOK FPS CSS System	85
5.2	Performance of the BOK FPS CSS System in an AWGN Channel	87
5.2.1	Analysis of the BOK FPS CSS System	87
5.2.2	Performance Comparison in the AWGN Channel.....	93
5.3	Effect of Doppler Shifts	94
5.3.1	Linear Chirps	95
5.3.2	Full Period Sine Chirp	98
5.3.3	Comparison of BER Performance under Different Frequency Shifts	109
5.4	Performance in a Rayleigh Fading Channel	110
5.5	Summary	112
6	Conclusions.....	113
6.1	Summary of Contributions.....	113
6.2	Suggestions for Future Research	115
	References.....	116
	Appendix A: Formulas Used	121
	Appendix B: Spectrum of Sine Chirps	131
	Appendix C: Spectrum of Cosine Chirps	135
	Appendix D: Autocorrelation of Sine Chirps	139
	Appendix E: Autocorrelation of Cosine Chirps	147
	Appendix F: Cross-correlation of Sine Chirps.....	156

Appendix G: Cross-correlation of Cosine Chirps.....	165
Appendix H: Doppler Effect on Matched Output of Sine Chirps	173
Appendix I: Doppler Effect on Unmatched Output of Sine Chirps.....	182
Curriculum Vitae	190

List of Tables

Table 4.1: Roots of Bessel function of the first kind of order zero	61
Table 5.1: System and channel parameters.....	111

List of Figures

Figure 1.1: Principle of a BOK CSS system.....	2
Figure 1.2: Principle of a DM CSS system.....	3
Figure 2.1: Principle of a matched filter	11
Figure 2.2: Output of a matched filter for a cosine signal	13
Figure 2.3: Output of a matched filter for a linear chirp signal	14
Figure 2.4: Model of a BOK CSS system.....	15
Figure 2.5: Linear chirps and their output waveforms.....	18
Figure 2.6: Matched and unmatched output waveforms of a linear chirp	20
Figure 2.7: Cross-correlation coefficient vs. $T_c B$ for linear chirps	21
Figure 2.8: Eb/No vs. BER of the BOK linear CSS system in the AWGN channel	22
Figure 3.1: Frequency of a pair of 3rd power function chirps	29
Figure 3.2: Comparison of the cross-correlation coefficient vs. $T_c B$ for linear and 3rd power function chirps	31
Figure 3.3: Comparison of the cross-correlation coefficient between the linear chirps and 3rd power function chirps	31
Figure 3.4: Frequency of sine chirps with different Ω	34
Figure 3.5: Comparison of the cross-correlation coefficient vs. $T_c B$ for linear chirps and Sine chirps for four different Ω	34
Figure 3.6: Comparison of the cross-correlation coefficient of linear chirps and HPS chirps when $T_c B = 5.5$ sHz.....	36

Figure 3.7: Comparison of cross-correlation coefficient of linear chirps and FPS chirps when $T_c B = 5.5$ sHz	36
Figure 3.8: Frequency functions of cosine chirps with different Ω	38
Figure 3.9: Cross-correlation coefficient vs. $T_c B$ for linear chirps and cosine chirps with different Ω	40
Figure 3.10: Cross-correlation coefficient of linear chirps and FPC chirps when $T_c B = 5.5$ sHz	40
Figure 4.1: Bessel functions of the first kind at different orders	47
Figure 4.2: Discrete amplitude spectra of a sine chirp.....	47
Figure 4.3: Values of the terms in Eqn. (4.18).....	50
Figure 4.4: Value of the first term in Eqn. (4.18) vs. different Ω	50
Figure 4.5: Comparison between the all terms and the second term defined in Eqn. (4.18) when $\Omega = 1$	51
Figure 4.6: Comparison between the all terms and the second term defined in Eqn. (4.18) when $\Omega = 2$	51
Figure 4.7: Values of the terms in Eqn. (4.23).....	54
Figure 4.8: Value of the first term in Eqn. (4.23) vs. different Ω	54
Figure 4.9: Comparison between all terms and the second term defined in Eqn. (4.23).....	55
Figure 4.10: Bessel function of the first kind of order zero.....	61
Figure 4.11: Autocorrelation & cross-correlation for FPS chirps when $B_{2-1} = 5.5201$ MHz..	64
Figure 4.12: Autocorrelation & cross-correlation for FPS chirps when $B_{2-2} = 8.6531$ MHz. .	64

Figure 4.13: Autocorrelation & cross-correlation for FPS chirps when $B_{2-3} = 10$ MHz.....	65
Figure 4.14: Autocorrelation & cross-correlation for FPS chirps when $B_{2-4} = 11.7915$ MHz	65
Figure 4.15: Value of the first term in Eqn. (4.29) vs. different values of Ω	67
Figure 4.16: Value of the first term in Eqn. (4.35) vs. different values of Ω	68
Figure 4.17: Autocorrelation & cross-correlation for HPS chirps when $B_{1-1} = 5.8957$ MHz	71
Figure 4.18: Autocorrelation & cross-correlation for HPS chirps when $B_{1-2} = 9.0351$ MHz	71
Figure 4.19: Autocorrelation & cross-correlation for HPS chirps when $B_{1-3} = 10$ MHz.....	72
Figure 4.20: Autocorrelation & cross-correlation for HPS chirps when $B_{1-4} = 12.176$ MHz	72
Figure 4.21: Autocorrelation & cross-correlation for TPS chirps when $B_{3-1} = 8.2802$ MHz.	74
Figure 4.22: Autocorrelation & cross-correlation for TPS chirps when $B_{3-2} = 10$ MHz	74
Figure 4.23: Autocorrelation & cross-correlation for TPS chirps when $B_{3-3} = 12.9796$ MHz	75
Figure 4.24: Autocorrelation & cross-correlation for TPS chirps when $B_{3-4} = 17.6872$ MHz	75
Figure 4.25: Autocorrelation & cross-correlation for QPS chirps when $B_{4-1} = 4.8096$ MHz.	77
Figure 4.26: Autocorrelation & cross-correlation for QPS chirps when $B_{4-2} = 10$ MHz.....	77
Figure 4.27: Autocorrelation & cross-correlation for QPS chirps when $B_{4-3} = 11.0402$ MHz	78

Figure 4.28: Autocorrelation & cross-correlation for QPS chirps when $B_{4-4} = 17.3062$ MHz	78
Figure 4.29: Central parts of the cross-correlation for sine chirps with different Ω	79
Figure 4.30: Comparison of the spectra for linear chirp and FPS chirp when $T_c B = 30$ sHz.	81
Figure 4.31: Comparison of the spectra for linear chirp and FPS chirp when $T_c B = 50$ sHz.	81
Figure 4.32: Autocorrelation coefficient of linear chirps vs. FPS chirps	82
Figure 4.33: Cross-correlation coefficient of linear chirps vs. FPS chirps	83
Figure 5.1: A BOK FPS CSS system in the AWGN channel	87
Figure 5.2: E_b/N_0 vs. BER of the BOK FPS CSS system for different $T_c B$	92
Figure 5.3: BER of the BOK FPS CSS system vs. $T_c B$ for different E_b/N_0	92
Figure 5.4: Theoretical and simulated BER for the BOK FPS CSS system	93
Figure 5.5: Performance of linear chirp and FPS chirp with different bandwidths in the AWGN channel	94
Figure 5.6: Output of the matched filter with different frequency offsets	97
Figure 5.7: Output of the unmatched filter in the BOK linear CSS system with different frequency offsets	97
Figure 5.8: Value of the first term in Eqn. (5.36) vs. different Doppler shifts and $T_c B$	100
Figure 5.9: Comparison of the matched output of the BOK FPS CSS system with no frequency offset and 78 kHz frequency offset	102
Figure 5.10: Comparison of the matched output of the BOK FPS CSS system with no frequency offset and 250 kHz frequency offset	103

Figure 5.11: Value of Eqn. (5.49) vs. time-frequency offset product.....	105
Figure 5.12: Comparison of the unmatched output of the BOK FPS CSS system between no frequency offset and 50 kHz frequency offset.....	107
Figure 5.13: Comparison of the unmatched output of the BOK FPS CSS system between no frequency offset and 100 kHz frequency offset.....	107
Figure 5.14: Comparison of the unmatched output of the BOK FPS between no frequency offset and 200 kHz frequency offset.....	108
Figure 5.15: Comparison of the unmatched output of the BOK FPS CSS system between no frequency offset and 300 kHz frequency offset.....	108
Figure 5.16: E_b/N_o vs. BER performance in the Gaussian channel for linear and FPS chirps with different frequency shifts	110
Figure 5.17: E_b/N_o vs. BER performance for linear and FPS chirps in a Rayleigh+Gaussian channel	112

List of Theorems

Theorem 4.1	48
Theorem 4.2	49
Theorem 4.3	52
Theorem 4.4	53
Theorem 4.5	56
Theorem 4.6	57
Theorem 4.7	58
Theorem 4.8	59
Theorem 4.9	66
Theorem 4.10	68
Theorem 5.1	98
Theorem 5.2	99
Theorem 5.3	101
Theorem 5.4	103
Theorem 5.5	104
Theorem 5.6	105

Acronyms

AWGN	Additive White Gaussian Noise
BER	Bit Error Rate
BOK	Binary Orthogonal Keying
CSS	Chirp Spread Spectrum
DS	Direct Sequence
DM	Direct Modulation
DSSS	Direct Sequence Spread Spectrum
E_b/N_o	The energy per bit to noise power spectral density ratio
EMI	Electromagnetic Interference
FH	Frequency Hopping
FSK	Frequency-Shift Keying
FPC	Full Period Cosine
FPS	Full Period Sine
HPS	Half Period Sine
IEEE	Institute of Electrical and Electronics Engineers
LR-WPAN	Low-rate Wireless Personal Networks
MAC	Media Access Control
NBI	Narrowband Interference

OFDM	Orthogonal Frequency-Division Multiplexing
PHY	Physical Layer
PSK	Phase-Shift Keying
PN	Pseudo Noise
QPS	Quadruple Period Sine
QPSK	Quadrature Phase-Shift Keying
RTLS	Real Time Location Systems
SAW	Surface Acoustic Wave
SNR	Signal-to-noise Ratio
TPS	Triple Period Sine
UWB	Ultra Wideband
WSN	Wireless Sensor Network

Nomenclature

$s(t)$	Signal which is sent out at the sender side
$y(t)$	Received signal by the receiver
$h_m(t)$	Impulse response of the matched filter to signal $s(t)$
$g(t)$	Output of the matched filter without Doppler shift
$F(\omega)$	Spectrum of the signal $s(t)$
$H_m(j\omega)$	Transfer function of a matched filter
$s^*(t)$	Complex conjugate of the signal $s(t)$
$c(t)$	Chirp signal
f_0	Carrier frequency
B	Frequency sweeping band
T_c	Duration of the chirp signal in seconds
$T_c B$	Time-bandwidth product
$n(t)$	An additive channel noise
Ω	Number of sweep cycles of sine or cosine chirp during the signal time period T_c
$R(\tau)$	Autocorrelation of a signal $c(t)$

r_L	Autocorrelation coefficient of a linear chirp
r_S	Autocorrelation coefficient of a sine chirp
r_C	Autocorrelation coefficient of a cosine chirp
$C(\tau)$	Cross-correlation of a signal $c(t)$
ρ_L	Cross-correlation coefficient of linear chirps
ρ_S	Cross-correlation coefficient of sine chirps
ρ_C	Cross-correlation coefficient of cosine chirps
$T_c B$	Time-bandwidth product
$J_n(x)$	The Bessel function of the first kind of order n
f_d	Doppler shift
f_{dS}^t	The tolerable frequency shift for the BOK CSS system of full period sine chirp
f_{dS}^{mt}	The tolerable frequency shift for the BOK CSS system of full period sine chirp to the matched output
f_{dS}^{ut}	The tolerable frequency shift for the BOK CSS system of full period sine chirp to the unmatched output

1. Introduction

1.1 Chirp Spread Spectrum Systems

Three techniques have been accepted for implementing spread spectrum modulation: frequency hopping (FH), direct sequence (DS) and chirp spread spectrum (CSS). Unlike FH and DS that employ pseudorandom coding to spread the spectrum of the information-bearing signal, CSS does not require additional coding to spread the spectrum since it can use chirp signal for coding. In addition, CSS signals exhibit a higher degree of interference rejection capability than a pure sinusoidal signal, thus making this class of signals a good candidate for use in spread-spectrum type communication systems [1]. CSS has also shown to be resistant to Doppler and other distortive effects [2, 3]. CSS-based wireless systems can transmit the signal at low transmission power by spreading the spectrum [4]. Therefore, CSS is a good choice for wireless communications, due to its innate advantages such as low transmission power, simplicity of implementation, good interference rejection capability.

The chirp spread spectrum uses chirps for signaling in data transmission, and uses associated pulse compression technique for decoding information. Chirp is a signal in which the frequency changes over a certain time interval, and the pulse compression technique is a practical implementation of matched filtering. Even though the pulse compression technique had been applied in radar systems since the early fifties, the first known paper suggesting it for applications other than radar was not published until 1962 [5]. The inherent property of interference rejection makes chirps (with the associated modulation scheme) suitable candidates in spread spectrum communication systems [1]. Chirp spread spectrum, used in radar systems in the past, has received more and more attention for low-rate wireless personal networks (LR-WPAN). The chirp spread spectrum modulation has been touted as a method of sending data through indoor channels in dense multipath environments [6]. In March 2007, the Institute of Electrical and Electronics Engineers (IEEE) has adopted CSS as a physical layer (PHY) in its new wireless standard IEEE 802.15.4a [7]. This has laid the foundation for the widespread

adoption of CSS in various applications, such as real time location systems (RTLS) [8], industrial control [9], and sensor networking [10].

Chirp spread spectrum systems can be grouped into two categories: binary orthogonal keying (BOK) and direct modulation (DM). The BOK CSS system uses two different chirps with the same bandwidth and duration but opposite sweep polarity, e.g. linear up-chirp and linear down-chirp. A block diagram of a BOK CSS system is shown in Figure 1.1. There, the up-chirp and down-chirps are used to represent different data symbols. For example, bits '1' and '0' can be represented by chirps with positive and negative instantaneous frequency change rates, respectively. At the receiver end, corresponding matched filters are used to decode the received signal.

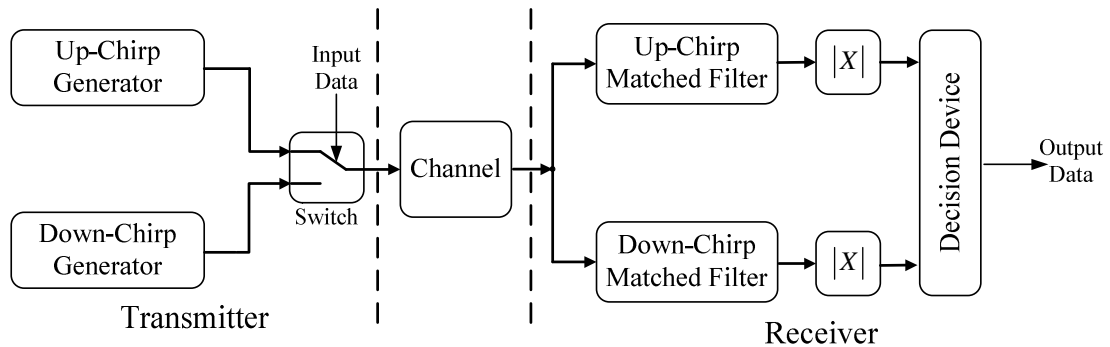


Figure 1.1: Principle of a BOK CSS system

A DM CSS system uses chirps as a time-spreading mechanism rather than signaling. This system is similar in concept to the DSSS systems. Like a pseudo noise (PN) sequence in the DSSS systems, a chirp signal performs a similar function in the DM CSS system [11]. In the DM CSS systems, chirps are only used for the purpose of spreading and de-spreading, while data is modulated using a conventional non-coherent modulation scheme. Therefore, a DM CSS system is more complicated to implement as compared with a BOK CSS system. A block diagram of a DM CSS system with quadrature phase-shift keying (QPSK) modulator/demodulator is shown in Figure 1.2.

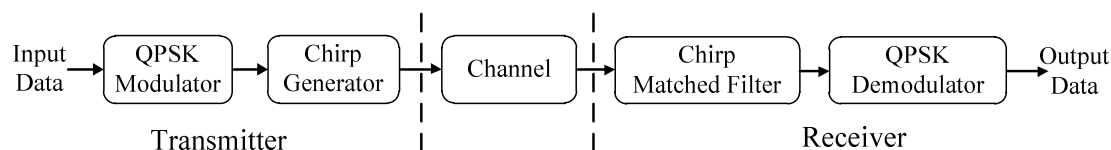


Figure 1.2: Principle of a DM CSS system

The DM method has to combine with other digital modulation schemes for data transmission, while the BOK method does not. Thus, the modulation scheme of the BOK method for wireless data communication is simpler than that of the DM method. Moreover, the BOK chirp method uses two different chirps for data modulation, while the DM chirp method can just use one chirp signal for spreading. Hence, the DM method focuses on the autocorrelation of the chirp signal, which is the same as in a radar system, while the BOK method depends not only on autocorrelation characteristics but also on cross-correlation characteristics between the two chosen chirps. The BOK method is more suitable for analyzing chirps, since its performance depends more on the characteristics of chirps than the DM method does. Therefore, the BOK method is chosen in this research.

1.2 Previous Work

The BOK CSS systems have been studied in the past decades. The BOK CSS system based on linear chirps was first proposed for wireless data communication by Winkler [5] in 1962. In 1973, Berni and Gregg compared the linear chirp BOK modulation with PSK (phase-shift keying) and FSK (frequency-shift keying) modulation in [12], and concluded that the BER performance of the chirp BOK for coherent reception is better than that of FSK but worse than that of PSK. In 1994, many problems of chirp BOK systems have been studied such as the overlap in the multipath channel. Tsai [13] evaluated the BER performance of the linear chirp BOK and proved that a chirp system can be used to greatly reduce the effect of multipath environment on the BER performance. With the development of surface acoustic wave (SAW), which can be used to generate linear chirps, SAW chirped delay lines can be realized at a small size and low cost [14, 15]. The design and performance of a low-cost BOK CSS system for indoor and industrial environments using SAW chirped delay lines are presented in [6, 16]. In 2002, Hengstler [17] proposed a multi-access for chirp direct modulation. Pinkney [18] presented a

scheme of expanding the data throughput of a BOK CSS system by increasing the signal constellation from binary to N-ary piece linear chirps. All of these studies use linear chirps for the BOK CSS systems.

Currently, non-linear chirps have attained little acceptance for the CSS system mainly due to the following reasons: (1) limited development of nonlinear-FM generation and processing devices; (2) mathematical derivation of performance analysis for non-linear chirp signals can be cumbersome; (3) greater system complexity; (4) the linear chirp already has acceptable performance, especially for wide time-bandwidth product.

Despite these factors, many attempts have been made to explore the non-linear chirps. A method of suppressing narrowband interference in ultra wideband (UWB) systems is realized using sine chirp in [19]. Several attempts to design the exponential chirp for radar applications have been published in [20, 21]. Sinh and tan function chirps are investigated for active sonar in [22]. Atan and asinh chirps are studied in [23] to construct UWB pulses and alleviate narrowband interference (NBI). Modified sine chirps and modified tanh chirps are proposed to be used in cognitive UWB system in [24]. Range and Doppler resolutions for Gaussian and Rayleigh chirps are compared in [25]. However, none of these investigations are for the BOK CSS system. Since no non-linear chirps are proven to have potential to replace linear chirps in the BOK CSS system, as of writing this paper, very few works introduce non-linear chirps into the BOK CSS system. Multiuser chirp spread spectrum communication systems using quadratic and exponential chirps are considered in [26]. However, in this paper, the assumption of orthogonality for these chirps has not been validated.

1.3 Problems, Motivations and Objectives

1.3.1 Problems

The performance of the BOK CSS systems is dependent upon the type of chirp waveform selected and the method of generation and processing. The chirp waveforms can be classified into two types: linear chirps in which the frequency increases or decreases linearly with time, and non-linear chirps in which the frequency varies in a

nonlinear manner with time. Most of current works on the CSS systems are based on linear chirps [3, 27]. The performance of a BOK CSS system, such as bit error rate (BER), depends significantly on the orthogonality of the chirp signals used. The better the orthogonality of the chirp signals is, the better the BER performance of the BOK CSS system will be when other factors remain the same. Linear chirps generally require the time-bandwidth product of each chirp signal to be 60 sHz or more in order to achieve satisfactory orthogonality requirements between the chirp signals. Thus, a BOK CSS system based on linear chirps has to occupy a wide bandwidth, which is a precious communication resource. For instance, Nanotron's CSS module nanoPAN 5360, which uses linear chirps, occupies 64 MHz bandwidth for one channel with 1 μ s time period for up to 2 Mbps data rate [28]. Clearly, the requirement on broad frequency bandwidth is a significant limiting factor for a linear CSS system. The question being investigated in this thesis research is to explore if there exist other forms of chirps, which provide improved orthogonality over linear chirps for the BOK CSS system.

1.3.2 Motivations

To address the above problem, it is worthwhile to explore other types of chirp signals outside the linear domain, which can potentially reduce the bandwidth requirement without jeopardizing the system performance.

1.3.3 Objectives

Based on the above motivation, the objectives of this research can be summarized as follows.

- Develop the general representations to construct arbitrary kind of chirps, and construct a pair of chirps for use in the BOK CSS systems
- Determine a pair of non-linear chirps, which can potentially be used to improve the BOK CSS system over linear chirps
- Analyze the properties or characteristics of the chosen non-linear chirps theoretically

- Evaluate the performance of the BOK CSS system based on the chosen non-linear chirps

1.3.4 Methodology

The following methods will be used respectively to carry out the above objectives:

- Although some non-linear chirps are presented in some literature, there is no general representation to construct a pair of non-linear chirps for the BOK CSS system. Therefore, the first task for the first objective is to find a general way to represent an arbitrary chirp, and then construct a pair of chirps to be used in the BOK CSS system. Thus, some pairs of non-linear chirps can be determined for further research.
- To be a good candidate to replace linear chirps in the BOK CSS systems, a pair of non-linear chirps should have a better orthogonal property than that of linear chirps. Thus, a comparison of cross-correlation of linear chirps and the proposed non-linear chirps can be an efficient way to determine if the non-linear chirps are a good candidate.
- To be a good candidate, the chosen chirp signals should have the following desirable properties: (1) They should have better orthogonal property than that of linear chirps; (2) they should have a similar autocorrelation property to linear chirps; and (3) they should lead to a reduced bandwidth requirement without jeopardizing system performance. Therefore, the properties (such as spectrum, cross-correlation, and autocorrelation) of the proposed pair of non-linear chirps need to be theoretically analyzed, so that their characteristics can be validated.
- Accurate BER performance is a crucial parameter to evaluate the performance of a digital communication system. Therefore, in order to prove the proposed non-linear chirps can outperform their linear counterpart for the BOK CSS system, BER performance of the BOK CSS system based on the chosen non-linear chirps in different channel models (e.g. Gaussian, Rayleigh, effect of Doppler shift) needs to be analyzed and validated by a comparison to linear chirps.

1.3.5 Scope

Since there are infinite number of non-linear chirps, it is not possible to investigate all non-linear chirps in this research. Instead, the scope of this thesis is limited to finding a pair of non-linear chirps, which can potentially be used to improve the BOK CSS system by replacing linear chirps.

1.4 Contributions of the Thesis

- One general representation is developed to construct an arbitrary kind of chirp for a given spectral bandwidth. Another general representation is generated to construct a pair of chirps for the BOK CSS system. With these two general representations, a class of non-linear chirps can be constructed and explored for the BOK CSS system.
- A method is developed to observe if a pair of candidate chirps has improved orthogonal property over their linear counterpart.
- Preliminary results have shown that significant performance advantage on orthogonality over linear chirps can be obtained using the pair of cosine or sine chirps. Thus, the properties of sine or cosine chirps are analyzed analytically. The derivations of the spectral characteristics, autocorrelation and cross-correlation for sine chirps are carried out. Similarly, the derivations of the spectral characteristics, autocorrelation and cross-correlation for cosine chirps are also carried out. A significant discovery is validated through mathematical derivation and simulation: a pair of sine or cosine chirps can become orthogonal under some conditions.
- It is found that a pair of full period sine (FPS) chirp is the better choice among the different periods of sine chirps for the BOK CSS system, in terms of the cross-correlation and autocorrelation properties.
- The effect of a Doppler shift on the BOK FPS CSS system is derived, and then validated by simulation.
- BER performance of the BOK CSS system based on FPS chirps in an additive white Gaussian noise (AWGN) channel is derived and then validated. Furthermore, a BER performance comparison between linear chirps and FPS chirps for the BOK CSS system in AWGN+Rayleigh channel has also been analyzed. The

corresponding results show that a pair of orthogonal FPS chirps can achieve better BER performance than its linear counterpart in these two types of channel.

1.5 Organization of the Thesis

The organization of this dissertation is as follows:

Chapter 2 introduces the fundamental theory of the BOK CSS system, which includes: matched filter, pulse compression technique, principle of a BOK CSS system, and characteristics of linear chirps.

Chapter 3 proposed two general representations to construct arbitrary kinds of chirps, and to construct a pair of chirps for using in the BOK CSS system. In this chapter, several non-linear chirps are constructed, and their capabilities of outperforming linear chirps are explored by analyzing their cross-correlation properties. Finally, two kinds of non-linear chirps, i.e. sine and cosine chirps, have shown some interesting characteristics that are more appealing than linear chirp signals for the BOK CSS systems. This interesting finding makes sine or cosine chirps a suitable choice for chirp based signaling approach. Hence, they are chosen for further investigation in this thesis.

In Chapter 4, the properties of sine or cosine chirps are further investigated analytically. The derivations of the spectral characteristics, autocorrelation and cross-correlation for both sine chirps and cosine chirps are carried out, respectively. Finally, by comparing sine chirps with four different time periods (half time period, full time period, triple time period, and quadruple time period) in terms of the cross-correlation and autocorrelation properties, it is concluded that full period sine (FPS) chirps have greater potential for the current applications.

In Chapter 5, the performance of the BOK CSS system based on FPS chirps (BOK FPS CSS system) is evaluated in three scenarios. Firstly, BER performance of the BOK FPS CSS system in an additive white Gaussian noise (AWGN) channel is derived. Furthermore, a comparison of BER performance in the AWGN between linear chirps and FPS chirps is given. Secondly, the effect of a frequency shift on the BOK FPS CSS

system is analyzed. The derivation of the effect of a Doppler shift on the FPS CSS system is carried out. The effect of Doppler shifts between linear chirp and FPS chirp is compared. Thirdly, BER performance of the BOK FPS CSS system in a fading environment (Rayleigh channel) is analyzed. Moreover, BER performance comparisons between linear chirps and FPS chirps in the AWGN+Rayleigh channel, with and without Doppler shift, are also carried out.

The conclusions of the dissertation are summarized in Chapter 6. Several topics of interest are presented as potential subjects of future investigation as well.

2. Chirp Spread Spectrum

A definition of spread spectrum that adequately reflects the characteristics of this technique is as follows [3]: “Spread spectrum is a means of transmission in which the signal occupies a bandwidth in excess of the minimum necessity to send the information; the band spread is accomplished by means of a code which is independent of the data, and a synchronized reception with the code at the receiver is used for despreading and subsequent data recovery”. Similarly, chirp spread spectrum derives its name from using modulated chirps for transmission, and the associated pulse compression techniques for encoding information. The matched filter and pulse compression concepts are fundamental to the CSS system. According to the pulse compression theory [29], the pulse compression of a chirp signal can be realized using a matched filter, which is the optimal filter in terms of achieving the maximal SNR (signal-to-noise ratio) at the filter output for performing signal detection in a white Gaussian noise environment.

2.1 Matched Filter

Since a matched filter has a principle position in the pulse compression technique, its concept and properties are briefly introduced firstly. Matched filters are commonly used in radar in which a known signal is sent out and the reflected signal is examined for common elements of the outgoing signal. The receiver uses a matched filter to pass the effected signal that matches the pattern of the outgoing signal and rejects noise and other signals at the same time [30]. In short, matched filtering (correlation filtering) is a method to detect a known signal. The principle of the matched filter is shown in Figure 2.1. As shown, $s(t)$ is the transmitted signal, which is generated by the signal generator and is then sent from the transmitter, $y(t)$ is the received signal by the receiver, $h_m(t)$ is impulse response of the matched filter, and $g(t)$ is the output of the matched filter without Doppler shift.

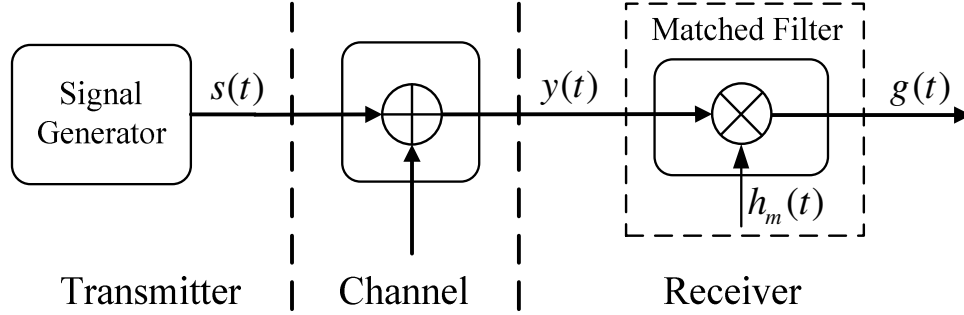


Figure 2.1: Principle of a matched filter

The criterion for the matched filter has been defined by Klauder in [31] as:

$$H_m(j\omega) = F^*(j\omega) \quad (2.1)$$

where $H_m(j\omega)$ is the transfer function of a matched filter, $F(\omega)$ is the spectrum of the signal $s(t)$, which is supposed to be inputted into the matched filter, and $*$ denotes the complex conjugate. From this equation, a filter is matched to the signal when its frequency response is equal to the complex conjugate of the signal spectrum. The impulse response of the matched filter to a general signal $s(t)$ is:

$$h_m(t) = s^*(-t) \quad (2.2)$$

It can be seen that $h_m(t)$ is equal to the complex conjugate of the transmitted signal $s(t)$ after time reversion [32]. Therefore, if a signal is a real even function, i.e. $s(t) = s^*(-t)$, then the impulse response of the matched filter is the transmitted signal itself, i.e. $h_m(t) = s(t)$.

When $y(t)$ is processed by the matched filter, the output of the matched filter without Doppler shift, $g(t)$, can be expressed by the convolution integral between the filter's impulse response and the signal $y(t)$:

$$g(t) = \int_{-\infty}^{+\infty} y(u)h_m(t-u)du \quad (2.3)$$

By combining Eqn. (2.2) and Eqn. (2.3), the output of the matched filter can be written as:

$$g(t) = \int_{-\infty}^{+\infty} y(u)s^*(u-t)du = C(y, s) \quad (2.4)$$

where $C(y, s)$ is a cross-correlation between the received signal $y(t)$ and the transmitted signal $s(t)$. Therefore, the output of the matched filter can be calculated by performing a cross-correlation between the received signal and the transmitted signal. If the received signal is the same as or similar to the transmitted signal, i.e. $y(t)=s(t)$, the output of the matched filter would be the autocorrelation function of the received (or transmitted) signal [33].

In other words, output of a matched filter can be achieved by convolving the incoming signal with a conjugated and time-reversed version of the transmitted signal, or can be obtained by convolving the incoming signal with the transmitted signal if the transmitted signal is a real even function. A practical implementation of matched filtering is pulse compression because the impulse response is matched to the input pulse signals.

2.2 Pulse Compression

Pulse compression is a classical signal processing technique to increase the range resolution as well as the signal to noise ratio without having to increase the peak transmission power [34]. The critical functions in a pulse compression system are modulating the transmitted pulse in the transmitter, and the matched filtering (pulse compression) in the receiver.

The simplest transmitted pulse can be a cosine signal. The pulse is transmitted periodically, but only a single pulse is considered here as an example. Assuming the pulse starts at $t=0$, the signal $s(t)$ can be defined by the following equation, where f_0 is the carrier frequency, and T is the duration of the signal in second.

$$s(t) = \begin{cases} \cos(2\pi f_0 t) = \cos(\omega_0 t) & 0 \leq t \leq T \\ 0 & \text{otherwise} \end{cases} \quad (2.5)$$

A matched filter is used in the receiver to detect the incoming cosine signal. A cosine pulse to be transmitted and the corresponding output of the matched filter are shown in Figure 2.2, respectively.

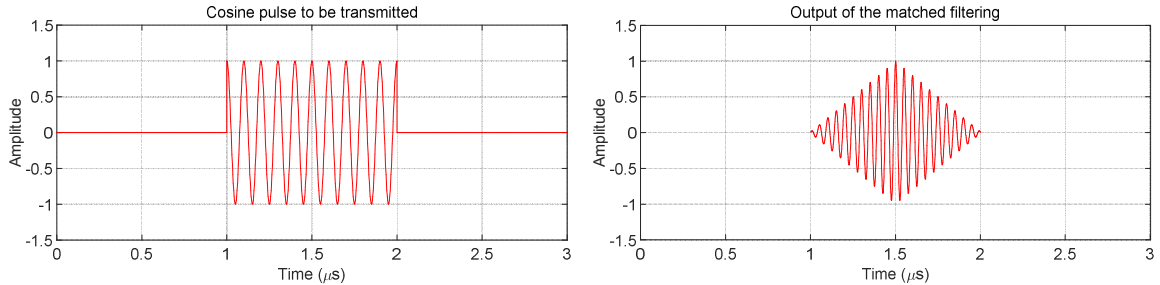


Figure 2.2: Output of a matched filter for a cosine signal

Instead of a fixed frequency signal, such as a cosine signal, a short pulse can be achieved after the matched filter if the transmitted signal is implied by the wide bandwidth, which can be called spread spectrum. Linear chirp, the frequency of which increases or decreases linearly with time, is the most typically used signal in the pulse compression system. The common representation of a linear chirp can be written:

$$c_L(t) = \begin{cases} \cos \left[2\pi \left(f_0 t + \frac{B}{2T_c} t^2 \right) \right] & 0 \leq t \leq T_c \\ 0 & \text{otherwise} \end{cases} \quad (2.6)$$

where f_0 is the carrier frequency, B is the frequency sweeping band, and T_c is the duration of the chirp in seconds. This linear chirp signal and its output after the matched filter are shown in Figure 2.3.

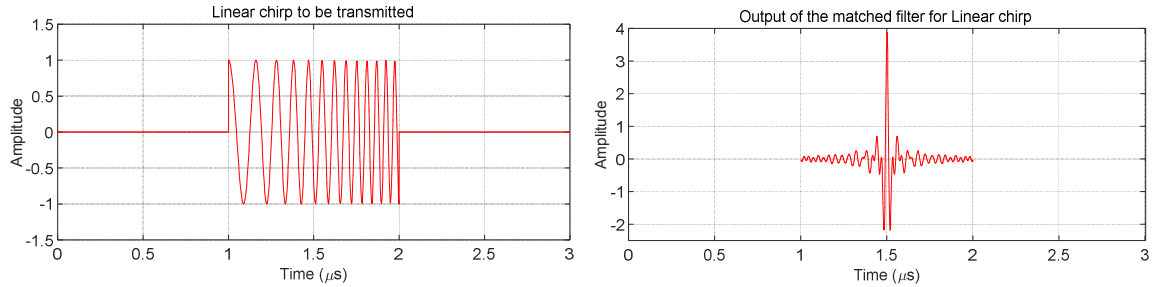


Figure 2.3: Output of a matched filter for a linear chirp signal

By comparing the outputs after the matched filter in Figure 2.2 and Figure 2.3 respectively, a narrow pulse is achieved for the linear chirp signal but not for the cosine signal. Therefore, the energy of the linear chirp signal is compressed into a short pulse by the matched filter, is from which the term, pulse compression, is derived. Since the energy of the signal can be preserved during pulse compression [35], the short pulse will have a large increase in magnitude as shown in Figure 2.3.

Pulse compression technique associated with a chirp signal has the capability of accumulating the energy of this signal into a short pulse with an amplification in magnitude [36]. Therefore, it is more likely to be detected by the corresponding receiver when operating at low power in order to avoid use of high peak power signals. Moreover, the transmission of chirps and the use of the associated pulse compression technique make the system highly robust against interference and multipath distortions [3]. Since the chirp spread spectrum system (CSS system) is based on chirps and pulse compression technique, it inherits these advantages.

2.3 Principle of the BOK CSS System

The pulse compression technique is used in the CSS system for decoding information. A signal model of the BOK CSS system is depicted in Figure 2.4.

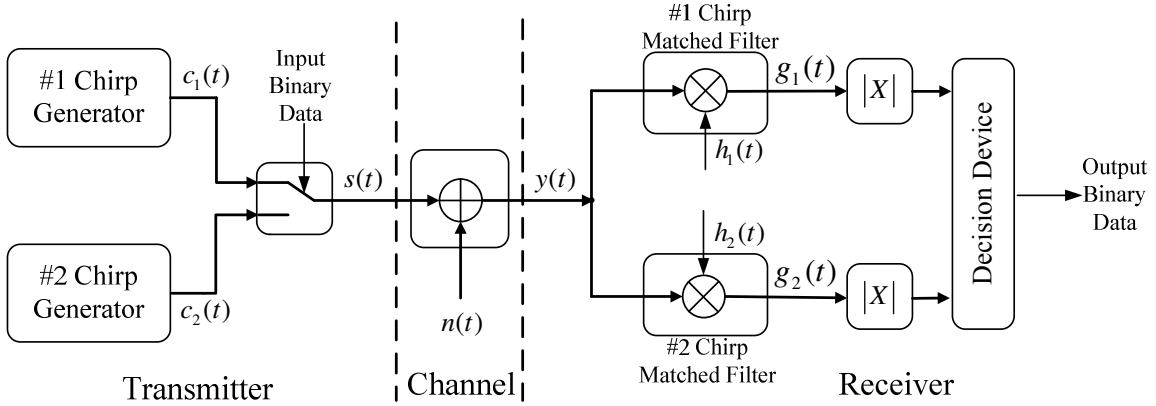


Figure 2.4: Model of a BOK CSS system

At the transmitter side, a switching circuit is triggered by a bit stream. If a bit "1" is to be sent, the switch will be connected to the #1 chirp generator and chirp signal $c_1(t)$ will be transmitted. If a bit "0" is to be sent, the switch will be connected to the #2 chirp generator and chirp signal $c_2(t)$ will be transmitted. Thus, the transmitted signal $s(t)$ is either $c_1(t)$ or $c_2(t)$ within a symbol period. $y(t)$ is the received signal at the receiver end. This signal becomes the input to both matched filters. The received signal $y(t)$ may be corrupted by an additive channel noise, $n(t)$. In this research, the effect of $n(t)$ is not explicitly considered to simplify the analysis of the BOK CSS system, and will be considered in Section 5. Outputs of the filters can be expressed by the convolution integral between the impulse response of the filter and the received signal:

$$\begin{cases} g_1(t) = \int_{-\infty}^{+\infty} y(u)h_1(t-u)du \\ g_2(t) = \int_{-\infty}^{+\infty} y(u)h_2(t-u)du \end{cases} \quad (2.7)$$

where $h_1(t)$ is the matched filter to the #1 chirp signal and $h_2(t)$ is the matched filter to the #2 chirp signal. Thus, according to Eqn. (2.2), these two matched filters can be represented as:

$$\begin{cases} h_1(t) = c_1^*(-t) \\ h_2(t) = c_2^*(-t) \end{cases} \quad (2.8)$$

By combining Eqn. (2.7) and Eqn. (2.8), the outputs of the matched filters can be written as:

$$\begin{cases} g_1(t) = \int_{-\infty}^{+\infty} y(u)c_1^*(u-t)du = C(y, c_1) \\ g_2(t) = \int_{-\infty}^{+\infty} y(u)c_2^*(u-t)du = C(y, c_2) \end{cases} \quad (2.9)$$

where $C(y, c_1)$ is a cross-correlation between the received signal $y(t)$ and the transmitted chirp signal $c_1(t)$, while $C(y, c_2)$ is a cross-correlation between the received signal $y(t)$ and the transmitted chirp signal $c_2(t)$. When $c_1(t)$ is transmitted, the received signal $y(t)$ will be the #1 chirp signal, i.e. $y(t) = c_1(t)$. In this case, the filter $h_1(t)$ is the corresponding matched filter, while the filter $h_2(t)$ does not match to the received signal. The outputs of the filters as defined in Eqn. (2.9) become:

$$\begin{cases} g_1(t) = C(c_1, c_1) = g_1^m(t) \\ g_2(t) = C(c_1, c_2) = g_2^u(t) \end{cases} \quad (2.10)$$

where $g_1^m(t)$ represents the output of filter $h_1(t)$ which is a matched output, while $g_2^u(t)$ is the output of filter $h_2(t)$ which is an unmatched output. From Eqn. (2.10), the matched output is the autocorrelation of the #1 chirp signal $c_1(t)$; while the unmatched output is the cross-correlation between $c_1(t)$ and $c_2(t)$. The output of the corresponding matched filter can be represented as the autocorrelation function of the received (or transmitted) chirp signal, while the output of the corresponding unmatched filter can be represented as the cross-correlation function between the two chirp signals.

Given a signal $c(t)$, its autocorrelation function $R(\tau)$ can be defined as [37]:

$$R(\tau) = c(\tau) * c^*(-\tau) = \int_{-\infty}^{\infty} c(t)c^*(t-\tau)dt \quad (2.11)$$

where τ is the time shift. Further, autocorrelation coefficient $r(\tau)$ of the signal $c(t)$ can be defined in Eqn. (2.12).

$$r(\tau) = \frac{R(\tau)}{E(c)} = \frac{\int_{-\infty}^{\infty} c(t)c^*(t-\tau) dt}{E(c)} \quad (2.12)$$

where $E(c) = \int_{-\infty}^{\infty} c^2(t)dt$ is the energy of the signal $c(t)$ [12].

Similarly, for any two signals, $c_1(t)$ and $c_2(t)$, the cross-correlation $C(\tau)$ with time shift τ can be defined in [37] by Eqn. (2.13).

$$C(\tau) = c_1(\tau) * c_2^*(-\tau) = \int_{-\infty}^{\infty} c_1(t+\tau)c_2^*(t) dt \quad (2.13)$$

Further, the cross-correlation coefficient between $c_1(t)$ and $c_2(t)$ can be represented in Eqn. (2.14).

$$\rho(\tau) = \frac{C(\tau)}{\sqrt{R_{11}(0) \times R_{22}(0)}} = \frac{\int_{-\infty}^{\infty} c_1(t+\tau)c_2^*(t) dt}{\sqrt{R_{11}(0) \times R_{22}(0)}} \quad (2.14)$$

where $R_{11}(0)$ and $R_{22}(0)$ are the autocorrelation of the signal $c_1(t)$ and $c_2(t)$ respectively. The cross-correlation indicates the degree of linear association or correlation between two signals.

2.4 The BOK Linear CSS System

Linear up-chirp and down-chirp are common choices in a practical BOK CSS system since they are the least complex. In complex baseband form, one common way of representing a linearly swept chirp signal is given in [18]:

$$\begin{cases} \text{Up:} & c_{L1} = \cos \left[2\pi \left(f_0 t + \mu \frac{t^2}{2} \right) \right] = \cos \left[(2\pi f_0 t + \pi \mu t) t \right] & -\frac{T_c}{2} \leq t \leq \frac{T_c}{2} \\ \text{Down:} & c_{L2} = \cos \left[2\pi \left(f_0 t - \mu \frac{t^2}{2} \right) \right] = \cos \left[(2\pi f_0 t - \pi \mu t) t \right] & -\frac{T_c}{2} \leq t \leq \frac{T_c}{2} \end{cases} \quad (2.15)$$

The parameter $\mu = B/T_c$ is the frequency sweep rate in Hz/s, f_0 is the center frequency in Hz, and T_c is the chirp signal duration in seconds. Both signals have a

common bandwidth B . Since almost all existing literature about linear chirps uses $-T_c/2 \leq t \leq T_c/2$ for the time period, the time period for all chirp signals in this thesis is set as $-T_c/2 \leq t \leq T_c/2$ in order to remain consistent.

The linear up-chirp signal increases its instantaneous frequency with time. Inversely, the linear down-chirp signal decreases its instantaneous frequency with time. The time-frequency characteristics of a linear up-chirp and down-chirp, along with their corresponding real parts are depicted in Figure 2.5.

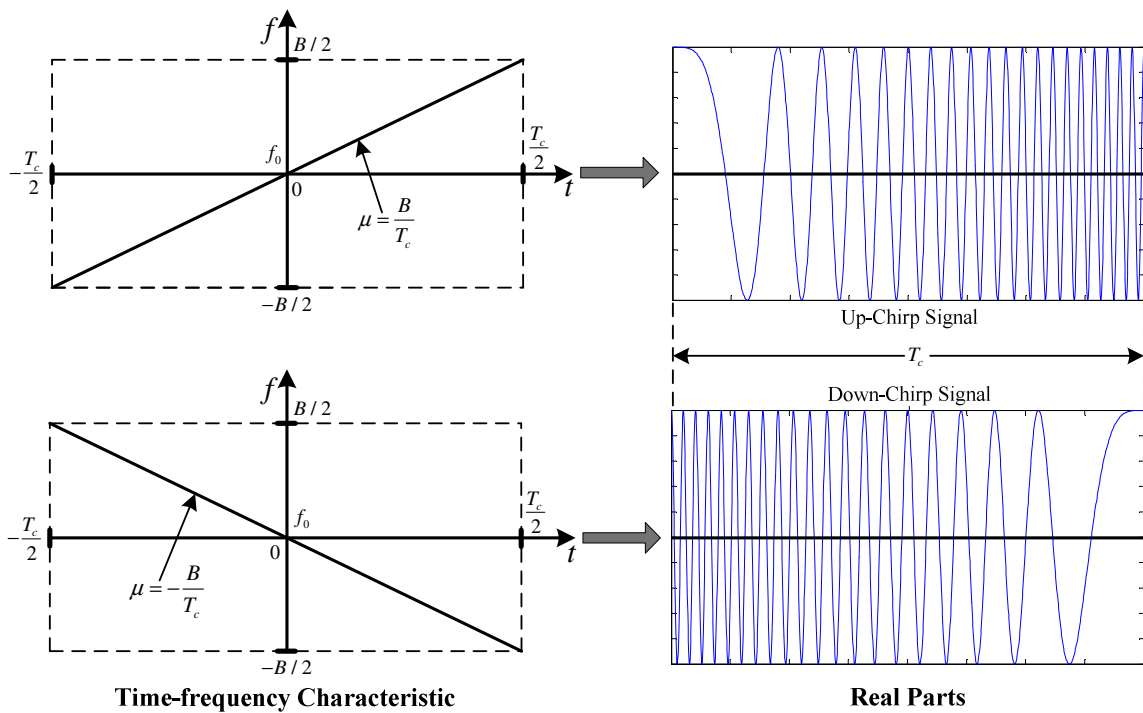


Figure 2.5: Linear chirps and their output waveforms

According to the theory of matched filter introduced in Section 2.1, by substituting Eqn. (2.15) into Eqn. (2.2), the impulse response of a matched filter for linear chirp signals can be obtained as shown in Eqn. (2.16). It is, again, a linear chirp signal but with a chirp rate of opposite sign.

$$\begin{cases} \text{Up Matched Filter:} & h_{L1}(t) = b \cos \left[2\pi \left(f_0 t - \mu \frac{t^2}{2} \right) \right] & -\frac{T_c}{2} \leq t \leq \frac{T_c}{2} \\ \text{Down Matched Filter:} & h_{L2}(t) = b \cos \left[2\pi \left(f_0 t + \mu \frac{t^2}{2} \right) \right] & -\frac{T_c}{2} \leq t \leq \frac{T_c}{2} \end{cases} \quad (2.16)$$

where b is a scaling factor for gain. In most applications of linear chirp, b is set as $\sqrt{4\mu}$ so that the gain of the matched filter at frequency f_0 is a unit [38]. If the matched filter is centered at time t , an analytical expression for the output waveform of the matched filter ($g_L^m(t)$) can be achieved by combining Eqn. (2.15) and Eqn. (2.16) into Eqn. (2.3) as given by [2]:

$$g_L^m(t) = \sqrt{\mu} \cos(2\pi f_0 t) \frac{\sin \left[\pi \mu t (T_c - |t|) \right]}{2\pi \mu t} \quad -\frac{T_c}{2} \leq t \leq \frac{T_c}{2} \quad (2.17)$$

The signal produced at the unmatched filter is also given in [18]:

$$g_L^u(t) = \frac{\cos(2\pi f_0 t)}{\sqrt{T_c B}} \left[C \left(\frac{\pi}{2} \left(\sqrt{T_c B} - |t| \sqrt{\mu} \right)^2 \right) + jS \left(\frac{\pi}{2} \left(\sqrt{T_c B} - |t| \sqrt{\mu} \right)^2 \right) \right] \quad (2.18)$$

where $C(x)$ and $S(x)$ are both Fresnel functions [39].

The matched output waveform ($g_L^m(t)$) and unmatched output waveform ($g_L^u(t)$) of a linear chirp signal are shown in Figure 2.6. As shown, the output of the matched filter is a function with most of its energy existing in the period of $-1/B \leq t \leq 1/B$. The magnitude of the centre peak is amplified up to $\sqrt{T_c B}$, and low amplitude main-lobe width of $2/B$ as its first zeroes are at $\pm B$ [3]. Therefore, if a linear chirp waveform is fed into its matched filter, the output signal typically has a narrow peak at the center frequency of linear chirp. Thus, there will be an approximate difference of $1/\sqrt{2T_c B}$ in the peak amplitude of the envelope of the matched versus unmatched output waveform [18]. The BOK linear CSS system is to use this difference to identify which output is matched or unmatched, and

can then decide which signal (c_{L1} or c_{L2}) is transmitting. The bigger this difference is, the more precise the achieved decision will be.

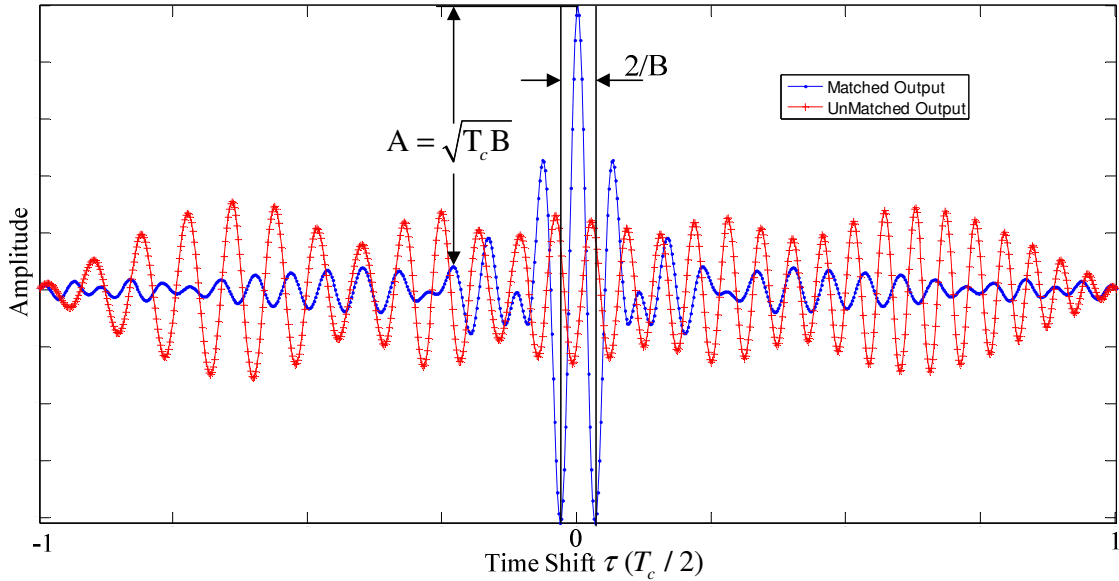


Figure 2.6: Matched and unmatched output waveforms of a linear chirp

In digital communication theory, the most frequently assumed model for a transmission channel is the additive white Gaussian noise (AWGN) channel. Bit error rate for the BOK linear CSS system in the AWGN channel (P_b^L) can be calculated by [18]:

$$P_b^L = Q_1(a_L, b_L) - \frac{1}{2} I_0(a_L b_L) e^{-\frac{[(a_L)^2 + (b_L)^2]}{2}} \quad (2.19)$$

where Q_1 is Marcum's Q function, I_0 is the modified Bessel function of the first kind with order zero [40]. The coefficients a_L and b_L are defined as:

$$\begin{cases} a_L = \sqrt{\frac{E_b(1 - \sqrt{1 - |J_0(\rho_L)|^2})}{2N_0}} \\ b_L = \sqrt{\frac{E_b(1 + \sqrt{1 - |J_0(\rho_L)|^2})}{2N_0}} \end{cases} \quad (2.20)$$

where E_b/N_0 is the energy per bit to noise power spectral density ratio [41]. ρ_L is a cross-correlation coefficient of the linear chirps, which can be obtained by substituting Eqn. (2.15) into Eqn. (2.14). The derivation process is presented in [18], and the result is given by Eqn. (2.21).

$$|\rho_L| = \frac{1}{\sqrt{T_c B}} \sqrt{\left(\int_0^{\sqrt{T_c B}} \cos \frac{\pi v^2}{2} dv\right)^2 + \left(\int_0^{\sqrt{T_c B}} \sin \frac{\pi v^2}{2} dv\right)^2} \quad (2.21)$$

From Eqn. (2.21), it can be observed that ρ_L depends on the time-bandwidth product ($T_c B$). The relationship between $T_c B$ and ρ_L is graphically shown in Figure 2.7.

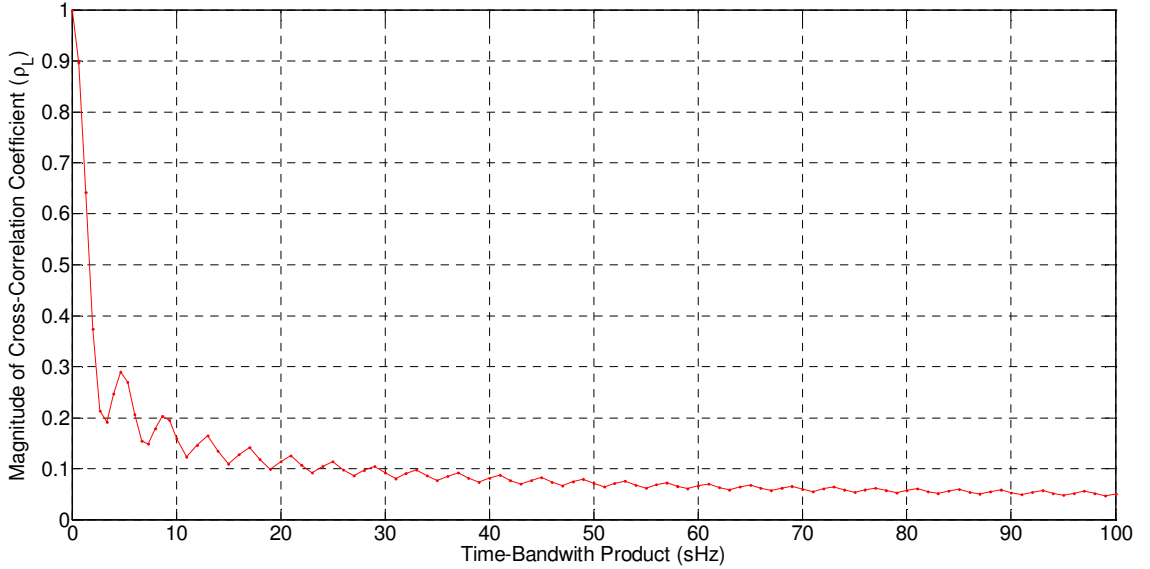


Figure 2.7: Cross-correlation coefficient vs. $T_c B$ for linear chirps

As shown, the magnitude of ρ_L decreases rapidly as $T_c B$ increases from zero to 20 shHz. However, the magnitude of ρ_L changes slightly during the period in which $T_c B$ is

from 20 sHz to 100 sHz. If $T_c B$ goes beyond 60 sHz, the magnitude of ρ_L will be less than 0.05. Even when $T_c B$ is 100 sHz, these two chirps cannot be considered as orthogonal although ρ_L is close to zero. Therefore, the linear chirps can only be considered as quasi-orthogonal [16].

The relationship between ρ_L and the BER performance of the BOK linear CSS system in the AWGN channel is depicted in Figure 2.8 [18]. It can be observed from Figure 2.8 that the value of ρ_L has significant effects on the BER performance of the BOK CSS system. The smaller the value of ρ_L is, the better BER performance will be. When ρ_L is perfectly equal to zero, which means the two chirps are orthogonal with each other, the best BER performance for the BOK CSS system will be achieved. Generally, the time-bandwidth product ($T_c B$) of the BOK linear CSS system needs to be set as 60 sHz or higher for satisfactory orthogonality. As a result, the BOK linear CSS system has to occupy wide frequency bandwidth (B) when the chirp duration (T_c) is short such as 1 μ s. Since the data rate is inversely proportional to the chirp duration, the shorter the chirp duration is, the higher data rate will be. For instance, the chirp duration in Nanotron's CSS system [28] is 1 μ s for up to 2 Mbps data rate.

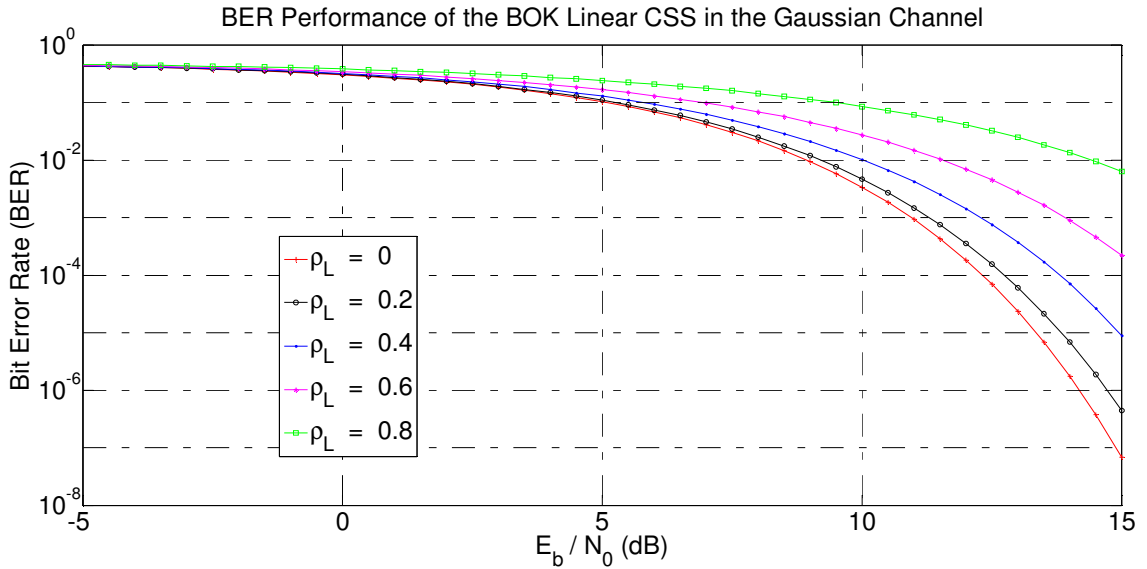


Figure 2.8: E_b/N_0 vs. BER of the BOK linear CSS system in the AWGN channel

2.5 Summary

The above introduction shows (1) orthogonality is important factor to distinguish the transmitted signals at the receiver end, and (2) the time-bandwidth product of the BOK linear CSS system is generally set as a large value (e.g. 60 sHz or over) in order to achieve good orthogonality between linear chirps. Thus, the BOK linear CSS system has to occupy a very wide bandwidth for high-speed data rate. A worthwhile question is whether there are significant benefits of using non-linear chirps to provide similar level of orthogonality, but with smaller time-bandwidth product as compared with the linear CSS system.

3. Non-Linear Chirps for the BOK CSS System

The linear chirps are the most commonly used signals in the CSS BOK system, but they have some drawbacks for the BOK mode as described in Section 2.4. A pair of non-linear chirps may be a better choice if they can outperform their linear counterpart. Therefore, this section explores some non-linear chirps in two steps. Firstly, a method is presented to briefly analyze a pair of non-linear chirps against linear chirps for the BOK CSS system. Secondly, with this method, some non-linear chirps (such as 3rd power function chirps, sine chirps, cosine chirps, and exponential chirps) are explored respectively to determine if they have potential to replace linear chirps in the BOK CSS system.

3.1 Method to Explore Non-Linear Chirps for the BOK CSS System

Although representations for linear chirps and some non-linear chirps already exist, there is no general representation to construct an arbitrary chirp waveform. Moreover, most existing non-linear chirps are considered for a radar application or the DM mode in the CSS data communication systems, in which only one chirp is required. However, at least one pair of chirps is needed for the BOK mode in the BOK CSS system. Thus, there is also no general representation to construct a pair of chirps for the BOK CSS system. Therefore, a representation of a pair of non-linear chirps for the BOK CSS system also needs to be determined before the chirps are analyzed.

3.1.1 General Representation for Arbitrary Chirps

For a given spectral bandwidth B , a chirp waveform for CSS can be generally constructed through the following steps:

(1) Determine the type of chirp signal (e.g. linear, cosine, Gaussian, etc.) to be constructed. The type can be represented by the chirp rate function $\psi(t)$. For example, when $\psi(t) = t$, which is a linear function, a linear chirp signal is going to be constructed.

(2) Calculate integral of $\psi(t)$:

$$\Theta(t) = \int_0^t \psi(t) dt \quad (3.1)$$

(3) The proposed representation needs to use a parameter ξ defined as follows:

$$\xi = \max[\psi(t)] - \min[\psi(t)] \quad t \in (-T_c/2, T_c/2) \quad (3.2)$$

where, $\max[\psi(t)]$ means the maximum value of the function $\psi(t)$ for $t \in (-T_c/2, T_c/2)$, while $\min[\psi(t)]$ is the minimum value of the function $\psi(t)$ for the same time period.

(4) Finally, this type of the chirp waveform ($c(t)$) can be represented using Eqn. (3.3):

$$c(t) = a \cos \left[\omega_0 t + 2\pi \frac{B}{\xi} \Theta(t) \right] = a \cos \left\{ 2\pi \left[f_0 t + \frac{B}{\xi} \Theta(t) \right] \right\} \quad (3.3)$$

where a is the envelope of the chirp signal, which usually uses the rectangle pulse. If a is chosen as a rectangle pulse with a value of 1, the representation of $c(t)$ can be simplified as:

$$c(t) = \cos \left[\omega_0 t + 2\pi \frac{B}{\xi} \Theta(t) \right] = \cos \left\{ 2\pi \left[f_0 t + \frac{B}{\xi} \Theta(t) \right] \right\} \quad (3.4)$$

In order to better understand this general representation of an arbitrary chirp waveform, a linear chirp signal is taken as an example. To construct a linear chirp signal, the chirp rate function is a linear function, which means $\psi_L(t) = kt$ in the simplest case. According to Eqn. (3.1), $\Theta(t)$ for linear chirp can be obtained as:

$$\Theta_L(t) = \int_0^t \psi(t) dt = \int_0^t kt dt = \frac{1}{2} kt^2 + q \quad (3.5)$$

wherein, q is a constant which can be set to 0. Therefore, Eqn. (3.5) can be simplified as:

$$\Theta_L(t) = \frac{1}{2} kt^2 \quad (3.6)$$

Similarly, the parameter ξ for linear chirp can be given by Eqn. (3.2):

$$\xi_L = k \frac{T_c}{2} - k \left(-\frac{T_c}{2} \right) = kT_c \quad \text{when } t \in (-T_c/2, T_c/2) \quad (3.7)$$

Combining Eqn. (3.6) and Eqn. (3.7) into Eqn. (3.4), the representation for a linear chirp signal can be obtained as:

$$\begin{aligned} c_L(t) &= \cos \left\{ 2\pi \left[f_0 t + \frac{B}{\xi_L} \Theta_L(t) \right] \right\} = \cos \left[2\pi \left(f_0 t + \frac{B}{kT_c} \times k \frac{t^2}{2} \right) \right] \\ &= \cos \left[2\pi \left(f_0 + \frac{B}{2T_c} t \right) t \right] \end{aligned} \quad (3.8)$$

Eqn. (3.8) is the exact same as the representation for the linear up-chirp as defined in Eqn. (2.15).

3.1.2 Representation for a Pair of Chirps for the BOK CSS System

As explained in Section 1.1, the BOK CSS system uses two different chirps with the same bandwidth and duration but opposite sweep polarity, e.g. an up-chirp and a down-chirp. Therefore, from Eqn. (3.8), a pair of chirp can be represented in the following form.

$$\begin{cases} c_1(t) = a \cos \left[\omega_0 t + 2\pi \frac{B}{\xi} \Theta(t) \right] = a \cos \left\{ 2\pi \left[f_0 t + \frac{B}{\xi} \Theta(t) \right] \right\} & -\frac{T_c}{2} \leq t \leq \frac{T_c}{2} \\ c_2(t) = a \cos \left[\omega_0 t - 2\pi \frac{B}{\xi} \Theta(t) \right] = a \cos \left\{ 2\pi \left[f_0 t - \frac{B}{\xi} \Theta(t) \right] \right\} & -\frac{T_c}{2} \leq t \leq \frac{T_c}{2} \end{cases} \quad (3.9)$$

In order to ensure that the two chirps have the same bandwidth but opposite sweep polarity, the chirp rate function $\psi(t) = d[\Theta(t)]/dt$ should be confined to either of the following cases.

(1) The chirp rate function $\psi(t)$ is an odd function, which means $\psi(-t) = -\psi(t)$ for $t \in (-T_c/2, T_c/2)$.

(2) The chirp rate function $\psi(t)$ is an even function, which means $\psi(-t) = \psi(t)$ for $t \in (-T_c/2, T_c/2)$; however, its value for $t \in (-T_c/2, T_c/2)$ contains positive and negative periods, and is symmetrically around the frequency axis. Otherwise, the frequency band occupied by the two signals defined in Eqn. (3.8) will not be the same, and, thus, will reduce the usage efficiency of the frequency spread.

3.1.3 Method to Determine Non-Linear Chirps for the BOK CSS System

As stated at the end of Section 2.4, BER performance of a BOK CSS system depends heavily on the cross-correlation coefficient of the used chirps. The smaller the value of the cross-correlation coefficient is, the better BER performance will be. Therefore, to be a good candidate to replace linear chirps in the BOK CSS systems, a pair of non-linear chirps should possess the fundamental property: they should have better orthogonal property than that of linear chirps. Thus, the comparison of cross-correlation between linear chirps and the proposed non-linear chirps can be significant to evaluate the capability of the non-linear chirps.

Moreover, it is observed that the cross-correlation of a pair of chirps normally depends on time-bandwidth product ($T_c B$). Thus, an efficient method can be used to determine a

pair of candidate chirps that have improved orthogonal property over its linear counterpart: (1) a graphical comparison of relationship between $T_c B$ and value of cross-correlation coefficient for both linear chirps and the candidate chirps can be used to observe if the candidate chirps have improved orthogonal property. (2) Based on the graphical comparison, if the magnitude of the cross-correlation coefficient of the candidate chirps is smaller than that of the linear chirps for the same $T_c B$, the candidate chirps are deemed to have an improved orthogonal property. In this case, the candidate chirps deserve more detailed investigation. More especially, if a zero crossing point exists in the curve of the candidate chirps, the candidate chirps probably can be completely orthogonal under certain condition.

3.2 Non-Linear Chirps

With the method presented in Section 3.1, some non-linear chirps are explored to determine if they have the potential to replace linear chirps in the BOK CSS system.

3.2.1 3rd Power Function Chirps

The 3rd power function is an odd function, so it can be used as the chirp rate function to construct 3rd power function chirps for BOK system. This function can be defined in the simplest case as:

$$\psi_P(t) = \left(\frac{t}{T_c}\right)^3 \quad -\frac{T_c}{2} \leq t \leq \frac{T_c}{2} \quad (3.10)$$

By substituting Eqn. (3.10) into Eqn. (3.1), the parameter $\Theta(t)$ for the 3rd power function chirp can be obtained by:

$$\Theta_P(t) = \int \left(\frac{t}{T_c}\right)^3 dt = \frac{T_c}{4} \left(\frac{t}{T_c}\right)^4 + q \quad (3.11)$$

wherein, q is a constant which can be set to 0. Therefore, Eqn. (3.11) can be simplified as:

$$\Theta_p(t) = \frac{T_c}{4} \left(\frac{t}{T_c} \right)^4 \quad (3.12)$$

The parameter ξ for the 3rd power function chirp can be obtained using Eqn. (3.2):

$$\xi_p = \max[\psi_p(t)] - \min[\psi_p(t)] = \left(\frac{T_c}{2T_c} \right)^3 - \left(-\frac{T_c}{2T_c} \right)^3 = \frac{1}{4} \quad (3.13)$$

Since $\psi_p(t) = (t/T_c)^3$ is an odd function, a pair of the 3rd power chirps for a BOK CSS can be given by combining Eqn. (3.12) and Eqn. (3.13) into Eqn. (3.9):

$$\begin{cases} \text{Up:} & c_{p1}(t) = \cos \left\{ 2\pi \left[f_0 t + BT_c \left(\frac{t}{T_c} \right)^4 \right] \right\} & -\frac{T_c}{2} \leq t \leq \frac{T_c}{2} \\ \text{Down:} & c_{p2}(t) = \cos \left\{ 2\pi \left[f_0 t - BT_c \left(\frac{t}{T_c} \right)^4 \right] \right\} & -\frac{T_c}{2} \leq t \leq \frac{T_c}{2} \end{cases} \quad (3.14)$$

The frequency spectrum of a pair of the 3rd power function chirp represented by Eqn. (3.14) is shown in Figure 3.1.

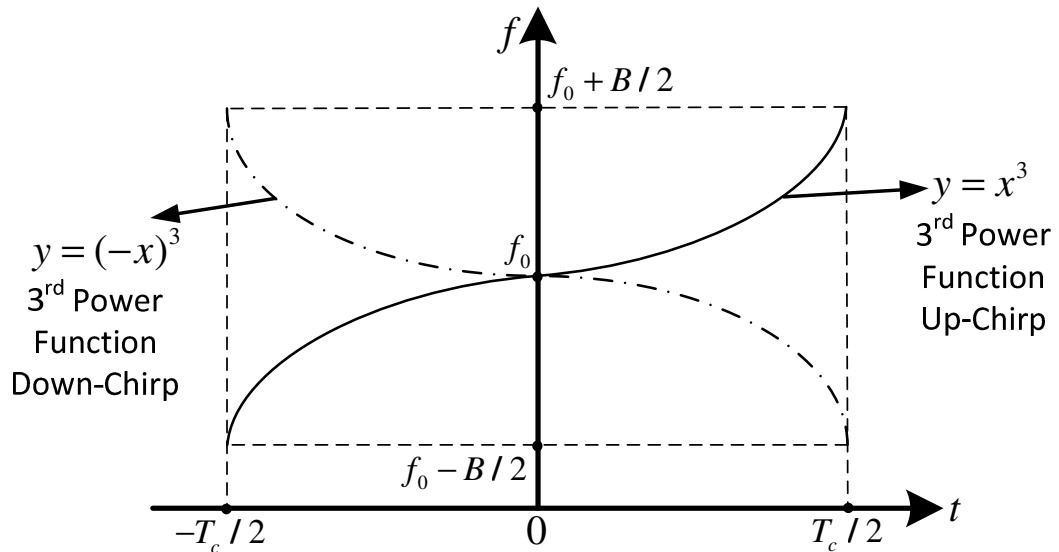


Figure 3.1: Frequency of a pair of 3rd power function chirps

The 3rd power function up-chirp signal increases its instantaneous frequency with time. Inversely, the down-chirp decreases its instantaneous frequency with time, as shown in Eqn. (3.15).

$$\left\{ \begin{array}{l} \text{Up:} \quad f_{P1} = f_0 + B \left(\frac{t}{T_c} \right)^3 \quad -\frac{T_c}{2} \leq t \leq \frac{T_c}{2} \\ \text{Down:} \quad f_{P2} = f_0 - B \left(\frac{t}{T_c} \right)^3 \quad -\frac{T_c}{2} \leq t \leq \frac{T_c}{2} \end{array} \right. \quad (3.15)$$

As stated at the beginning of this chapter, the graphical relationship between the time-bandwidth product ($T_c B$) and the cross-correlation coefficient can be an efficient method to determine a candidate non-linear chirp. Thus, the graphical relationships between $T_c B$ and the value of the cross-correlation coefficients for both linear chirps and 3rd power function chirps are shown in Figure 3.2. As depicted, the cross-correlation coefficient for 3rd power function chirps also depends on $T_c B$. Similar to that of linear chirps, the cross-correlation coefficients for 3rd power function chirps tend to decrease with the increase of $T_c B$; however, their cross-correlation coefficients are higher than that of the linear chirps under the same value of $T_c B$.

Taking $T_c B = 20$ sHz as an example, the cross-correlation coefficients of linear chirps and 3rd power function chirps are compared and the corresponding result is shown in Figure 3.3. In this figure, cross-correlation coefficient of 3rd power function chirps is higher than that of the linear chirps, especially around the area where the time shift is 0. This means that the orthogonality of 3rd power function chirps is inferior to that of linear chirps.

Therefore, based on the comparative analysis as presented in Figure 3.2 and Figure 3.3, it can be concluded that 3rd power function chirps would not outperform the linear chirp under the same $T_c B$, since 3rd power function chirps do not show improved orthogonal property over their linear chirp counterpart.

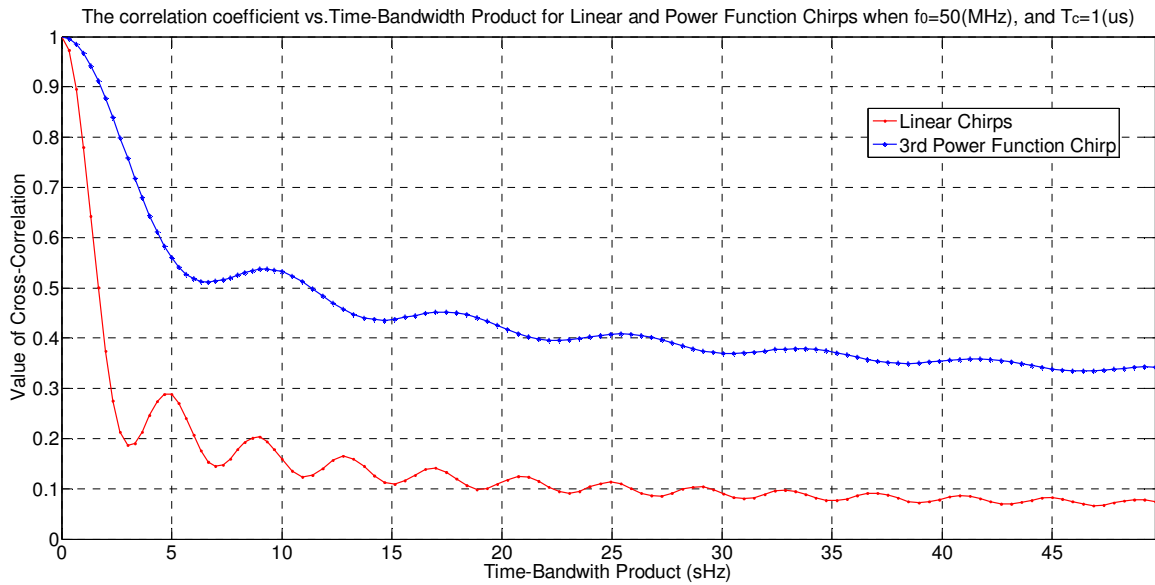


Figure 3.2: Comparison of the cross-correlation coefficient vs. $T_c B$ for linear and 3rd power function chirps

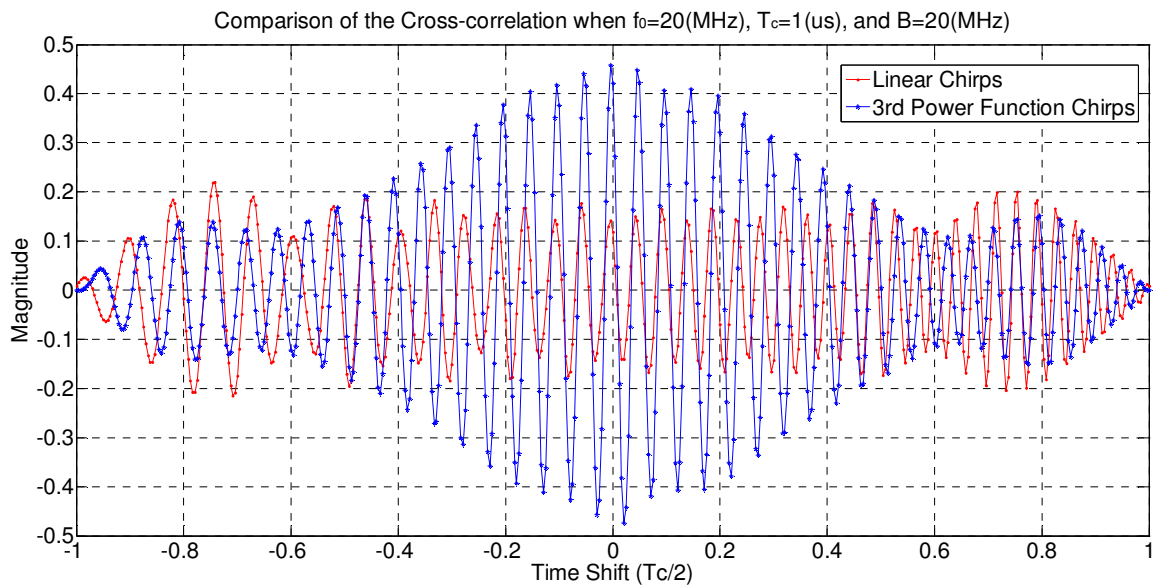


Figure 3.3: Comparison of the cross-correlation coefficient between the linear chirps and 3rd power function chirps

3.2.2 Sine Chirps

If the chirp rate function is a sine function as defined in Eqn. (3.16), a sine chirp can be generated.

$$\psi_s(t) = \sin\left(\pi\Omega\frac{t}{T_c}\right) \quad -\frac{T_c}{2} \leq t \leq \frac{T_c}{2} \quad (3.16)$$

where the parameter Ω is an integer relating to the number of sweep cycles of the sine chirp from $B/2$ to $-B/2$ during the signal time period (T_c). By substituting Eqn. (3.16) into Eqn. (3.1), the parameter $\Theta(t)$ for the sine chirp can be obtained by:

$$\Theta_s(t) = \int \sin\left(\pi\Omega\frac{t}{T_c}\right) dt = -\frac{T_c}{\pi\Omega} \cos\left(\pi\Omega\frac{t}{T_c}\right) + q \quad (3.17)$$

wherein, q is a constant which can be set to 0. Therefore, Eqn. (3.17) can be simplified as:

$$\Theta_s(t) = -\frac{T_c}{\pi\Omega} \cos\left(\pi\Omega\frac{t}{T_c}\right) \quad (3.18)$$

The parameter ξ for sine chirp can be obtained using Eqn. (3.2):

$$\xi_s = \max[\psi_s(t)] - \min[\psi_s(t)] = \sin\left(\frac{\pi\Omega}{T_c} \times \frac{T_c}{2}\right) - \sin\left(\frac{\pi\Omega}{T_c} \times -\frac{T_c}{2}\right) = 2 \quad (3.19)$$

Since the chirp rate function $\psi_s(t) = \sin(\pi\Omega t/T_c)$ is an odd function, a pair of sine chirp signals for the BOK CSS can be obtained by combining Eqn. (3.17) and Eqn. (3.19) into Eqn. (3.9):

$$\begin{cases} c_{s1}(t) = a \cos\left\{2\pi\left[f_0t - \frac{BT_c}{2\pi\Omega} \cos\left(\pi\Omega\frac{t}{T_c}\right)\right]\right\} & -\frac{T_c}{2} \leq t \leq \frac{T_c}{2} \\ c_{s2}(t) = a \cos\left\{2\pi\left[f_0t + \frac{BT_c}{2\pi\Omega} \cos\left(\pi\Omega\frac{t}{T_c}\right)\right]\right\} & -\frac{T_c}{2} \leq t \leq \frac{T_c}{2} \end{cases} \quad (3.20)$$

The Eqn. (3.20) can be simplified as:

$$\begin{cases} c_{s1}(t) = a \cos \left[2\pi f_0 t - \frac{BT_c}{\Omega} \cos \left(\pi \Omega \frac{t}{T_c} \right) \right] & -\frac{T_c}{2} \leq t \leq \frac{T_c}{2} \\ c_{s2}(t) = a \cos \left[2\pi f_0 t + \frac{BT_c}{\Omega} \cos \left(\pi \Omega \frac{t}{T_c} \right) \right] & -\frac{T_c}{2} \leq t \leq \frac{T_c}{2} \end{cases} \quad (3.21)$$

The frequency functions of the pair of sine chirps with different values of Ω are shown in Figure 3.4. When the value of Ω is set to 1, the frequency function is a half period sine curve. As a result, this kind of chirp will henceforth be referred to as a half period sine (HPS) chirp. Similarly, when the value of Ω is set at 2, it is a full period sine curve. Hence, this kind of chirp is henceforth named as full period sine (FPS) chirp. Similarly, when the value of Ω is equal to 3 and 4, the sine chirp is named triple period sine (TPS) chirp and quadruple period sine (QPS) chirp respectively.

The relationship between $T_c B$ and values of the cross-correlation coefficient for sine chirps with different Ω is described in Figure 3.5. As displayed, the value of the cross-correlation coefficient of sine chirps (ρ_s) also depends on $T_c B$. ρ_s is generally smaller than those of linear chirps for the same $T_c B$, particularly for the HPS and FPS chirps ($\Omega=1,2$), and especially when $T_c B$ is less than 6 sHz. Thus, for the same $T_c B$, sine chirps have better orthogonality than linear chirps. An interesting characteristic that can be observed is that the pair of linear chirps cannot be orthogonal ($\rho_L \neq 0$) even if $T_c B$ reaches 50 sHz, while sine chirp can result in perfect orthogonality ($\rho_s = 0$) for specific values of $T_c B$. This characteristic constitutes a fundamental difference between sine chirps and linear chirps.

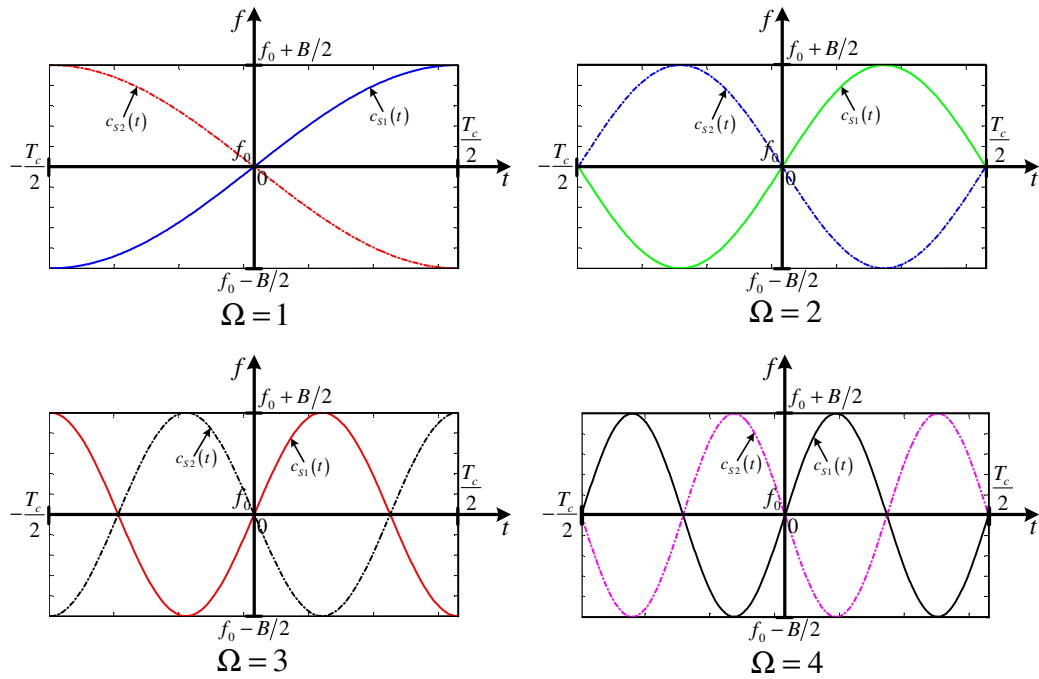


Figure 3.4: Frequency of sine chirps with different Ω

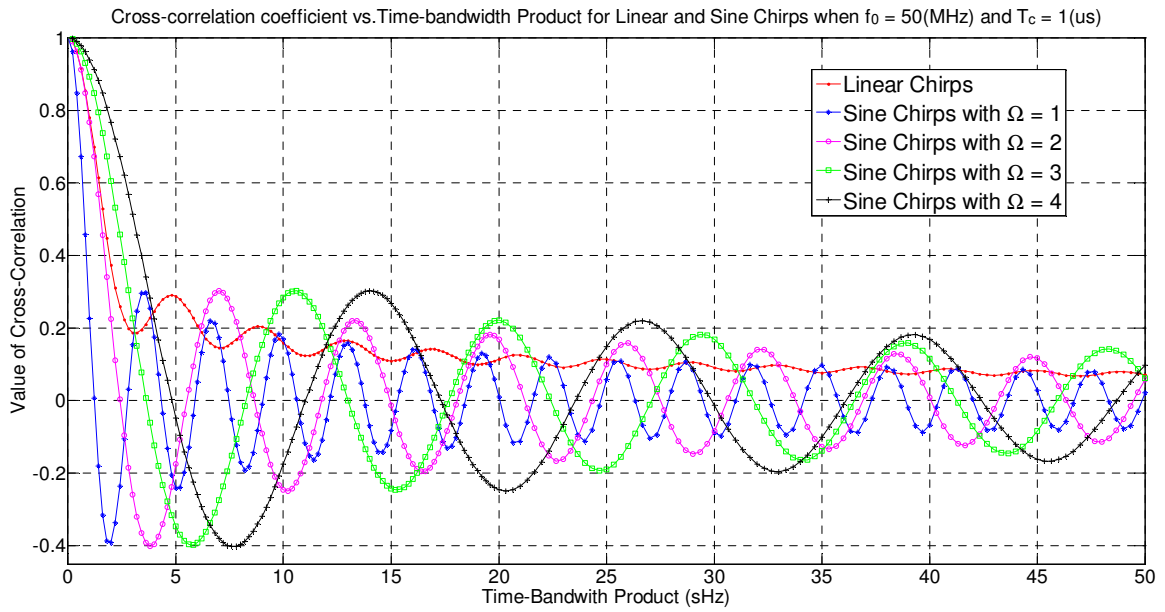


Figure 3.5: Comparison of the cross-correlation coefficient vs. $T_c B$ for linear chirps and Sine chirps for four different Ω

Moreover, another interesting characteristic of sine chirps, which can be observed from Figure 3.5, is that perfect orthogonal points of sine chirps are periodic. As shown, an orthogonal point for FPS chirps is approximately at $T_c B = 5.5$ sHz. Cross-correlation coefficient of linear chirps and HPS chirps are compared when $T_c B$ is 5.5 sHz. The comparison result is depicted in Figure 3.6. As displayed, the cross-correlation coefficient of the HPS chirps is slightly smaller than that of the linear chirps, especially when the time shift is around zero. This means that the orthogonality of sine chirps is superior to that of linear chirps.

Similarly, a comparison of the cross-correlation between linear chirps and FPS chirps when $T_c B$ is 5.5 sHz is shown in Figure 3.7. At the center of this figure, the cross-correlation coefficient of the FPS chirps is nearly equal to zero, which is much smaller than that of linear chirps. This phenomenon means FPS chirps have a much improved orthogonality over linear chirps.

Therefore, the following conclusion can be drawn from these comparative curves shown in Figure 3.5, Figure 3.6, and Figure 3.7: a pair of sine chirps has better orthogonal property than its linear counterpart under the same conditions, which means sine chirps have the potential to replace linear chirps in the BOK CSS system to achieve improved BER performance.

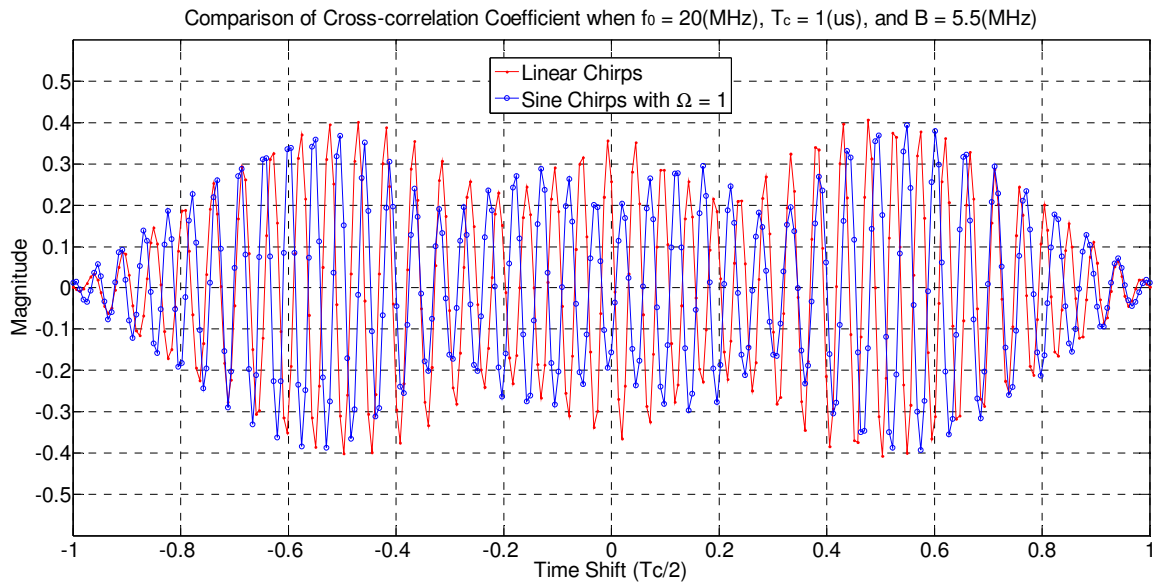


Figure 3.6: Comparison of the cross-correlation coefficient of linear chirps and HPS chirps when $T_c B = 5.5$ sHz

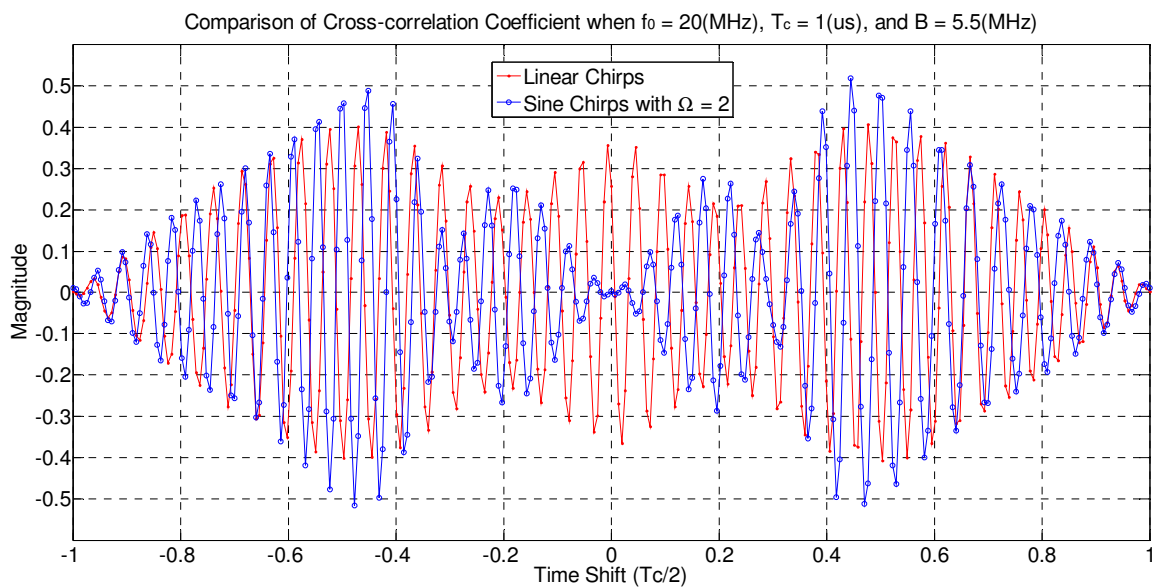


Figure 3.7: Comparison of cross-correlation coefficient of linear chirps and FPS chirps when $T_c B = 5.5$ sHz

3.2.3 Cosine Chirps

If the chirp rate function $\psi(t)$ is set as a cosine function as defined by Eqn. (3.22), a cosine chirp can be obtained as well.

$$\psi_c(t) = \cos\left(\pi\Omega \frac{t}{T_c}\right) \quad -\frac{T_c}{2} \leq t \leq \frac{T_c}{2} \quad (3.22)$$

By substituting Eqn. (3.22) into Eqn. (3.1), the parameter $\Theta(t)$ for the cosine chirp can be obtained by:

$$\Theta_c(t) = \int \cos\left(\pi\Omega \frac{t}{T_c}\right) dt = \frac{T_c}{\pi\Omega} \sin\left(\pi\Omega \frac{t}{T_c}\right) \quad (3.23)$$

When $\Omega=1$, the chirp rate function $\psi_c(t) = \sin(\pi t/T_c)$ is an even function and its value for $t \in (0, T_c/2)$ is changed from positive to negative; thus, it does not conform to the two cases stated in Section 3.1.2. Therefore, Eqn. (3.23) is not suitable to be used to represent a pair of half period cosine chirps for the BOK CSS system.

As in the cases when $\Omega \geq 2$, although the chirp rate function $\psi_c(t) = \sin(\pi\Omega t/T_c)$ is also an even function, its value for $t \in (-T_c/2, T_c/2)$ is symmetrical. Hence, Eqn. (3.23) can be used to represent a pair of cosine chirps when $\Omega \geq 2$. When $\Omega \geq 2$, the parameter ξ for the cosine chirp can be obtained using Eqn. (3.2) as follows:

$$\xi_c = \max[\psi_c(t)] - \min[\psi_c(t)] = \cos\left(\frac{2\pi}{T_c} \times 0\right) - \cos\left(\frac{2\pi}{T_c} \times \frac{T_c}{2}\right) = 2 \quad (3.24)$$

A pair of cosine chirps for the BOK CSS system can be given by combining Eqn. (3.23) and Eqn. (3.24) into Eqn. (3.9):

$$\begin{cases} c_{C1}(t) = a \cos \left\{ 2\pi \left[f_0 t + \frac{BT_c}{2\pi\Omega} \sin \left(\pi\Omega \frac{t}{T_c} \right) \right] \right\} & -\frac{T_c}{2} \leq t \leq \frac{T_c}{2} \\ c_{C2}(t) = a \cos \left\{ 2\pi \left[f_0 t - \frac{BT_c}{2\pi\Omega} \sin \left(\pi\Omega \frac{t}{T_c} \right) \right] \right\} & -\frac{T_c}{2} \leq t \leq \frac{T_c}{2} \end{cases} \quad (3.25)$$

The Eqn. (3.25) can be simplified as:

$$\begin{cases} c_{C1}(t) = a \cos \left[2\pi f_0 t + \frac{BT_c}{\Omega} \sin \left(\pi\Omega \frac{t}{T_c} \right) \right] & -\frac{T_c}{2} \leq t \leq \frac{T_c}{2} \\ c_{C2}(t) = a \cos \left[2\pi f_0 t - \frac{BT_c}{\Omega} \sin \left(\pi\Omega \frac{t}{T_c} \right) \right] & -\frac{T_c}{2} \leq t \leq \frac{T_c}{2} \end{cases} \quad (3.26)$$

The frequency functions of cosine chirps with different values of Ω are shown in Figure 3.8.

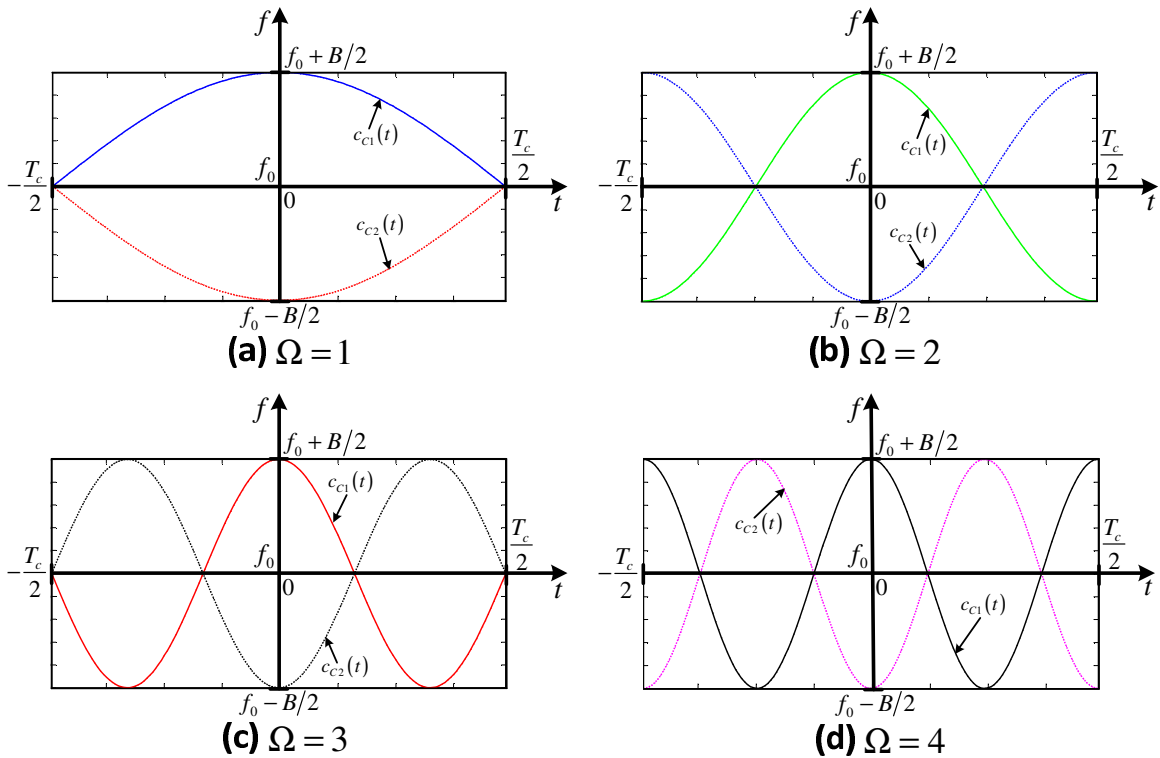


Figure 3.8: Frequency functions of cosine chirps with different Ω

As shown in Figure 3.8 (a), one cosine chirp occupies the upper half bandwidth; the other only uses the bottom half bandwidth during a frequency sweep. There is no overlap in frequency function for cosine chirps when $\Omega=1$. Thus, the usage efficiency of the frequency spread for the case where $\Omega=1$ is only half of that of other cases. Therefore, cosine chirps represented by Eqn. (3.26) for $\Omega=1$ are not a good candidate for the BOK CSS system, which is consistent with the statement at the beginning of this section: “Eqn. (3.23) is not suitable to represent a pair of half period cosine chirps for the BOK CSS system”.

The relationship between the time-bandwidth product and value of the cross-correlation coefficient for cosine chirps with different Ω ($\Omega=2,3,4$) is shown in Figure 3.9. As shown, the value of the cross-correlation coefficient of cosine chirps (ρ_C) also depends on the time-bandwidth product ($T_c B$). ρ_C is generally smaller than those of linear chirps under the same $T_c B$, especially when $T_c B$ is less than 6 sHz for the full period cosine (FPC) chirps ($\Omega=2$).

By comparing Figure 3.9 with Figure 3.5, it can be observed that the characteristics of cosine chirps in Figure 3.9 are almost same as their sine counterparts in Figure 3.5, respectively. Therefore, the orthogonal characteristics of cosine chirps are similar with that of sine chirps. As highlighted by the green circle in Figure 3.9, an orthogonal point for the FPC chirp is also approximately at $T_c B = 5.5$ sHz.

A comparison of the cross-correlation coefficient between linear chirps and FPC chirps when $T_c B$ is 5.5 sHz is shown as an example in Figure 3.10. At the centre of this figure, the cross-correlation coefficient of the FPC chirps is nearly equal to zero, which is much smaller than that of the linear chirps.

Therefore, like sine chirps, a similar conclusion can be drawn from these comparative curves shown in Figure 3.9 and Figure 3.10, i.e. a pair of cosine chirps ($\Omega=2,3,4$) can be a suitable candidate for chirp-based BOK CSS systems.

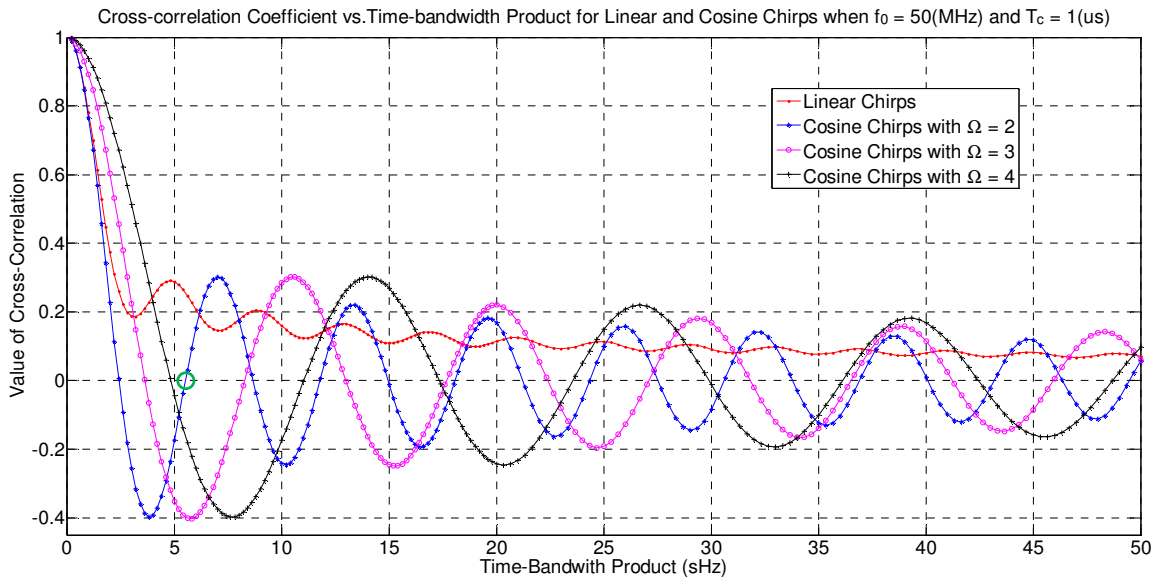


Figure 3.9: Cross-correlation coefficient vs. $T_c B$ for linear chirps and cosine chirps with different Ω

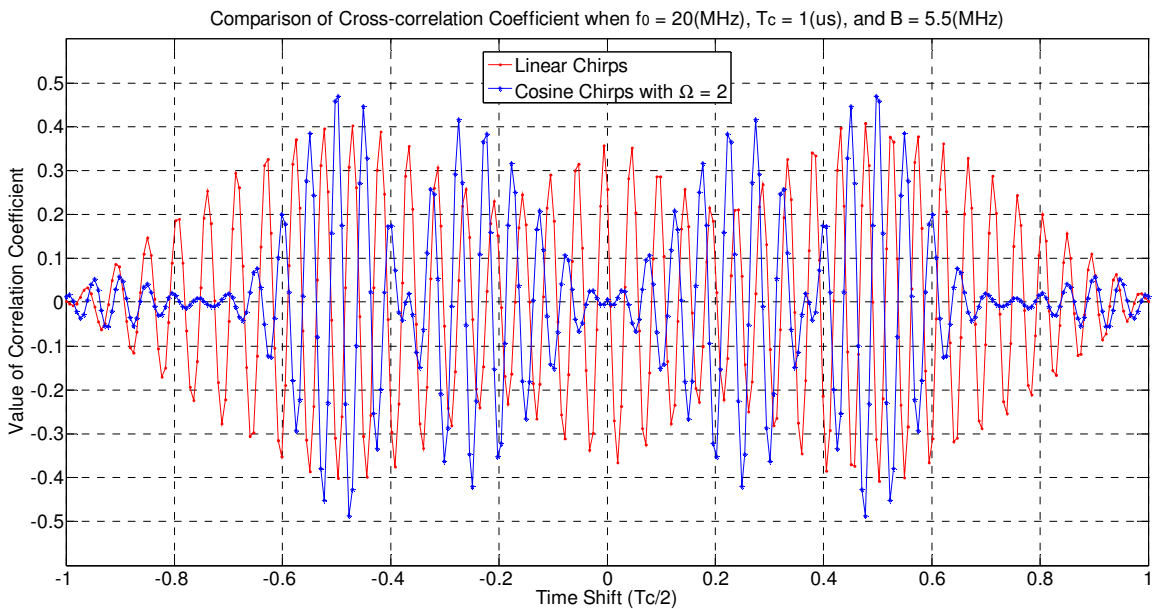


Figure 3.10: Cross-correlation coefficient of linear chirps and FPC chirps when $T_c B = 5.5$ sHz

3.2.4 Exponential and Other Non-Linear Chirps

Some other non-linear chirps such as exponential chirps have also been investigated. In order to construct a pair of exponential chirps for the BOK system, the chirp rate function can be defined as:

$$\psi_E(t) = e^{\left(\frac{t}{T_c}\right)} \quad -\frac{T_c}{2} \leq t \leq \frac{T_c}{2} \quad (3.27)$$

Since $\psi_E(t) = e^{(t/T_c)}$ is neither an even nor an odd function, and $\psi_E(t) = e^{(t/T_c)} > 0$, it does not conform to the two cases stated in Section 3.1.2. Therefore, Eqn. (3.27) is not suitable to be used to construct a pair of exponential chirps for the BOK CSS system.

Moreover, it may not be difficult to construct a non-linear chirp (such as sinh, tan, atan, Gaussian and Rayleigh chirps) according to the procedure defined in Section 3.1.1. However, since they also cannot conform to the two cases stated in Section 3.1.2, they are not suitable to be used for the BOK CSS system.

3.3 Conclusions

As stated at the end of Section 3.3 and Section 3.4, the preliminary results have shown that a significant performance improvement on orthogonality over linear chirps can be attained using the pair of cosine or sine chirps. Thus, cosine or sine chirps are chosen for further analysis in this research.

4. Properties of Sine and Cosine Chirps

4.1 Introduction

Although the numerical analysis in Section 3 have already shown that the pair of sine or cosine chirps both have some special properties, it is still necessary to perform mathematical analysis to validate these properties. Therefore, main objective of this Chapter is to validate the properties of sine or cosine chirps through mathematical analysis. Derivations of the spectral characteristics, autocorrelation and cross-correlation for both sine chirps and cosine chirps are carried out respectively. Moreover, autocorrelation and cross-correlation for a pair of sine chirps at different time period (Ω) are examined. Finally, full period sine (FPS) chirps are selected for comparison against linear chirps in terms of spectral characteristic, autocorrelation and cross-correlation.

4.2 Spectral Characteristic

Analysis of spectral characteristic is to determine the effective bandwidth of the signal, and then can determine how much bandwidth is required to transmit the signal. In theory, since a sine or cosine chirp signal contains an infinite number of side frequencies, bandwidth for transmitting such signal is also infinite. However, amplitude of some side frequencies are so small which can be practically ignored. Therefore, the bandwidth could be defined as the width over the spectrum of which has significant amplitude.

General description for a pair of sine chirps can be defined in Eqn. (4.1):

$$\begin{cases} c_{s1}(t) = a \cos \left[\omega_0 t - \frac{BT_c}{\Omega} \cos \left(\pi \Omega \frac{t}{T_c} \right) \right] & -\frac{T_c}{2} \leq t \leq \frac{T_c}{2} \\ c_{s2}(t) = a \cos \left[\omega_0 t + \frac{BT_c}{\Omega} \cos \left(\pi \Omega \frac{t}{T_c} \right) \right] & -\frac{T_c}{2} \leq t \leq \frac{T_c}{2} \end{cases} \quad (4.1)$$

General description for a pair of cosine chirps can be represented in Eqn. (4.2):

$$\begin{cases} c_{C1}(t) = a \cos \left[\omega_0 t + \frac{BT_c}{\Omega} \sin \left(\pi \Omega \frac{t}{T_c} \right) \right] & -\frac{T_c}{2} \leq t \leq \frac{T_c}{2} \\ c_{C2}(t) = a \cos \left[\omega_0 t - \frac{BT_c}{\Omega} \sin \left(\pi \Omega \frac{t}{T_c} \right) \right] & -\frac{T_c}{2} \leq t \leq \frac{T_c}{2} \end{cases} \quad (4.2)$$

where $\omega_0 = 2\pi f_0$.

4.2.1 Sine Chirps

The spectrum of sine chirps described in Eqn. (4.1) can be obtained by Fourier transform. $c_{S1}(t)$ is chosen as an example here to analyze spectral characteristic of sine chirps.

$$\begin{aligned} F_{S1}(\omega) &= \frac{1}{T_c} \int_{-T_c/2}^{T_c/2} c_{S1}(t) e^{-j\omega t} dt \\ &= \frac{a}{T_c} \int_{-T_c/2}^{T_c/2} \cos \left[\omega_0 t - \frac{BT_c}{\Omega} \sin \left(\pi \Omega \frac{t}{T_c} \right) \right] \times e^{-j\omega t} dt \end{aligned} \quad (4.3)$$

Since positive and negative parts of the spectrum are symmetrical, only the positive side is considered as example, Eqn. (4.3) can be obtained as (A detailed description of how these values were obtained is given in Appendix B.):

$$F_{S1}^P(\omega) = \frac{a}{2} \sum_{n=-\infty}^{\infty} \left\{ \left[(-1)^n J_{2n} \left(\frac{BT_c}{\Omega} \right) \right] \text{sinc} \left[\frac{(\omega_0 - \omega)T_c}{2} + n\pi\Omega \right] \right\} \quad (4.4)$$

In Eqn. (4.4), n is an integer index, $J_{2n}(x)$ is the Bessel function of the first kind of order $2n$, and $\text{sinc}(x)$ is the unnormalized sinc function defined in (4.5) [42]:

$$\text{sinc}(x) = \frac{\sin x}{x} \quad (4.5)$$

The magnitude of $\text{sinc}(x)$ at $x=0$ is defined to be $\text{sinc}(0)=1$. An important properties for the unnormalized $\text{sinc}(x)$ is that the zero crossings are at non-zero multiples of π . Therefore, when n is a non-zero integer, Eqn. (4.6) can be obtained:

$$\text{sinc}(n\pi) = \frac{\sin(n\pi)}{n\pi} = 0 \quad (4.6)$$

Magnitude Spectrum

Magnitude spectrum of sine chirp $A_{S1}(\omega)$ can be obtained from Eqn. (4.4) as:

$$\begin{aligned} A_{S1}(\omega) &= |F_{S1}^P(\omega)| \\ &= \frac{a}{2} \left| \sum_{n=-\infty}^{\infty} \left\{ \left[(-1)^n J_{2n} \left(\frac{BT_c}{\Omega} \right) \right] \text{sinc} \left[\frac{(\omega_0 - \omega)T_c}{2} + n\pi\Omega \right] \right\} \right| \end{aligned} \quad (4.7)$$

As described in Eqn. (4.6), $A_{S1}(\omega)$ will have many peaks at:

$$\frac{(\omega_0 - \omega)T_c}{2} + n\pi\Omega = 0, \quad n = 0, \pm 1, \pm 2, \pm 3, \pm 4 \dots \quad (4.8)$$

Frequencies of these peaks can be obtained from Eqn.(4.7):

$$\omega = \omega_0 + \frac{2\pi n\Omega}{T_c}, \quad n = 0, \pm 1, \pm 2, \pm 3, \pm 4 \dots \quad (4.9)$$

Since $\text{sinc}(0)=1$, the amplitude at these peaks will be:

$$A_{S1}(\omega) = \frac{a}{2} \left| J_{2n} \left(\frac{BT_c}{\Omega} \right) \right| \quad \text{when } \omega = \omega_0 + \frac{2\pi n\Omega}{T_c} \quad (4.10)$$

Phase Spectrum

Since $F_{S1}^P(\omega)$ is a real function, the phase spectrum of sine chirp $\Phi_{S1}(\omega)$ is always zero.

4.2.2 Cosine Chirps

The spectrum of cosine chirps depicted in Eqn. (4.2) can also be found by Fourier transform. $c_{C1}(t)$ is used as an example here. Taking the Fourier transforms of both sides of Eqn. (4.2):

$$\begin{aligned} F_{C1}(\omega) &= \frac{1}{T_c} \int_{-T_c/2}^{T_c/2} c_{C1}(t) e^{-j\omega t} dt \\ &= \frac{1}{T_c} \int_{-T_c/2}^{T_c/2} a \cos \left[\omega_0 t + \frac{BT_c}{\Omega} \sin \left(\pi \Omega \frac{t}{T_c} \right) \right] \times e^{-j\omega t} dt \end{aligned} \quad (4.11)$$

Since positive and negative parts of the spectrum are symmetrical, only the positive side is considered. Hence, Eqn. (4.11) can be obtained as (A detailed description of how these values were obtained is given in Appendix C.):

$$F_{C1}^P(\omega) = \frac{a}{2} \sum_{n=-\infty}^{\infty} \left\{ J_n \left(\frac{BT_c}{\Omega} \right) \text{sinc} \left[\frac{(\omega_0 - \omega)T_c + n\pi\Omega}{2} \right] \right\} \quad (4.12)$$

In Eqn. (4.12), $\text{sinc}(x)$ is the unnormalized sinc function defined in Eqn. (4.5).

Magnitude Spectrum

The magnitude spectrum of cosine chirp signal $A_{C1}(\omega)$ can be obtained from Eqn. (4.12) as:

$$\begin{aligned} A_{C1}(\omega) &= |F_{C1}^P(\omega)| \\ &= \frac{a}{2} \left| \sum_{n=-\infty}^{\infty} \left\{ J_n \left(\frac{BT_c}{\Omega} \right) \text{sinc} \left[\frac{(\omega_0 - \omega)T_c + n\pi\Omega}{2} \right] \right\} \right| \end{aligned} \quad (4.13)$$

As described in Eqn. (4.6), $A_{C1}(\omega)$ will have many peaks at:

$$\frac{(\omega_0 - \omega)T_c + n\pi\Omega}{2} = 0, \quad n = 0, \pm 1, \pm 2, \pm 3, \pm 4 \dots \quad (4.14)$$

Frequencies of these peaks can be obtained from Eqn.(4.14):

$$\omega = \omega_0 + \frac{n\pi\Omega}{T_c}, \quad n = 0, \pm 1, \pm 2, \pm 3, \pm 4 \dots \quad (4.15)$$

Since $\text{sinc}(0)=1$, the amplitude at these peaks will be:

$$A_{C1}(\omega) = \frac{a}{2} \left| J_n \left(\frac{BT_c}{\Omega} \right) \right| \quad \text{when } \omega = \omega_0 + \frac{n\pi\Omega}{T_c} \quad (4.16)$$

Phase Spectrum

Similarly, the phase spectrum of cosine chirp $\Phi_{C1}(\omega)$ is also always zero because since $F_{C1}^P(\omega)$ is a real function.

4.2.3 Summary

From Eqn. (4.10) and Eqn. (4.16), the amplitude spectrum for sine and cosine chirps are similar:

$$\begin{cases} A_{S1}(\omega) = \frac{a}{2} \left| J_{2n} \left(\frac{BT_c}{\Omega} \right) \right| & \text{when } \omega = \omega_0 + \frac{2\pi n\Omega}{T_c} \\ A_{C1}(\omega) = \frac{a}{2} \left| J_n \left(\frac{BT_c}{\Omega} \right) \right| & \text{when } \omega = \omega_0 + \frac{n\pi\Omega}{T_c} \end{cases} \quad (4.17)$$

From these results, it can be observed that the amplitude spectrums depend significantly on value of $J_{2n} \left(\frac{BT_c}{\Omega} \right)$ or $J_n \left(\frac{BT_c}{\Omega} \right)$, and are all independent on the carrier ω_0 . $J_n(x)$ is the Bessel function of the first kind of order n . Value of $J_n(x)$ versus x for different integer values of n is shown in Figure 4.1. As shown in this figure, $J_n(x)$ also depends on x , so the amplitude spectrum significantly depends on value of $\frac{BT_c}{\Omega}$.

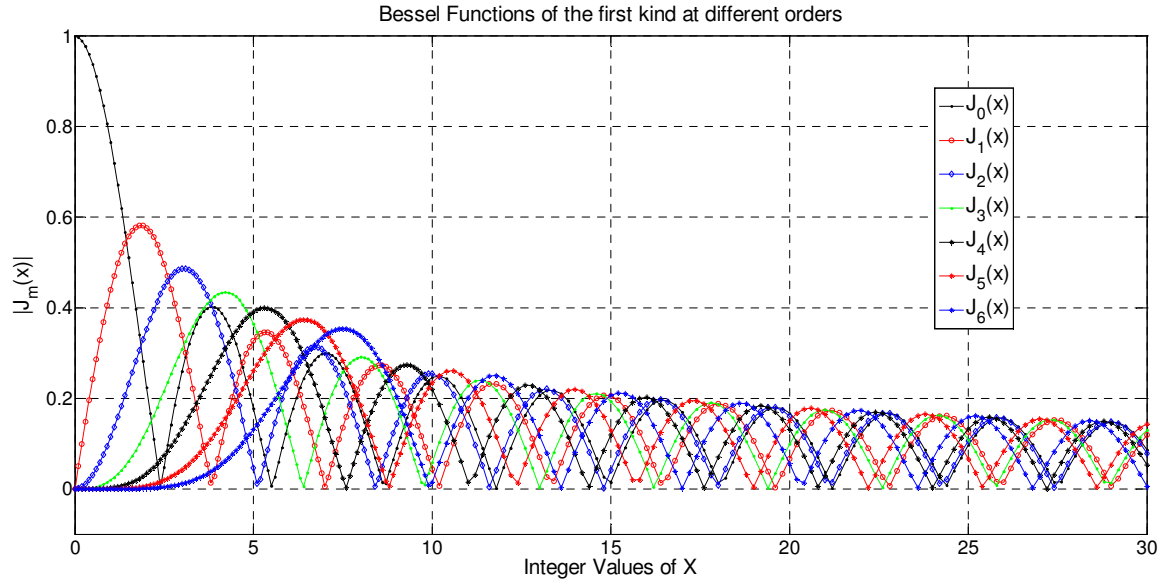


Figure 4.1: Bessel functions of the first kind at different orders

Taking sine chirp and $\frac{BT_c}{\Omega} = 10$ for an example, the magnitude spectrum of sine chirp when $\frac{BT_c}{\Omega} = 10$ is depicted in Figure 4.2. As can be seen, peaks occur at the carrier $\omega_0 = 2\pi f_0$ as well as at every $\frac{2\pi\Omega}{T_c}$ on both sides of ω_0 . In other words, the peaks are separated by $\frac{2\pi\Omega}{T_c}$ Hz.

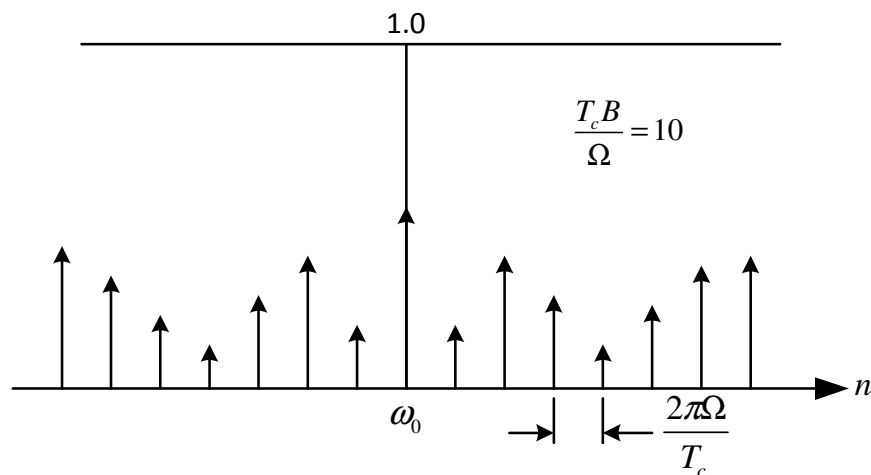


Figure 4.2: Discrete amplitude spectra of a sine chirp

4.3 Autocorrelation Properties

As stated in Section 2.3: “The output of the corresponding matched filter can be represented as the autocorrelation function of the received chirp signal”. Therefore, autocorrelation of the chirps is an important property of the BOK CSS system.

4.3.1 Sine Chirps

Theorem 4.1: If a sine chirp is represented as $c_{s1}(t) = a \cos \left[\omega_0 t + \frac{BT_c}{\Omega} \cos \left(\pi \Omega \frac{t}{T_c} \right) \right]$,

the autocorrelation coefficient of sine chirp $c_{s1}(t)$ will be:

$$\begin{aligned}
 r_s(\tau) = & \left(1 - \frac{|\tau|}{T_c} \right) \sum_{n=-\infty}^{\infty} \left\{ (-1)^n J_{2n}(k_{S1}^m) \operatorname{sinc} \left[(\omega_0 + 2n\theta)(T_c - |\tau|) \right] \right\} \\
 & + \left(1 - \frac{|\tau|}{T_c} \right) \cos(\omega_0 \tau) J_0(k_{S2}^m) \\
 & + 2 \left(1 - \frac{|\tau|}{T_c} \right) \cos(\omega_0 \tau) \sum_{n=1}^{\infty} \left\{ J_{2n}(k_{S2}^m) \operatorname{sinc} \left[2n\theta(T_c - |\tau|) \right] \right\}
 \end{aligned} \tag{4.18}$$

where

$$\theta = \frac{\pi \Omega}{2T_c}; \quad k_{S1}^m = \frac{2BT_c}{\Omega} \cos \left(\frac{\pi \Omega}{2T_c} \tau \right); \quad k_{S2}^m = \frac{2BT_c}{\Omega} \sin \left(\frac{\pi \Omega}{2T_c} \tau \right) \tag{4.19}$$

Proof. The autocorrelation coefficient of sine chirp $c_{s1}(t)$ can be obtained as by using Eqn. (2.12):

$$r_s(\tau) = \frac{\int_{-\infty}^{\infty} \left\{ \begin{aligned} & a \cos \left[\omega_0(t+\tau) - \frac{BT_c}{\Omega} \cos \left(\pi \Omega \frac{t+\tau}{T_c} \right) \right] \\ & \times a \cos \left[\omega_0 t + \frac{BT_c}{\Omega} \cos \left(\pi \Omega \frac{t}{T_c} \right) \right] \end{aligned} \right\} dt}{E(c_{s1})} \tag{4.20}$$

where $E(c_{s1})$, which is energy of $c_{s1}(t)$. Appendix D presents the detailed derivation for Eqn. (4.20).

– Q.E.D

Theorem 4.2: If a sine chirp is represented as $c_{s1}(t) = a \cos \left[\omega_0 t + \frac{BT_c}{\Omega} \cos \left(\frac{\pi \Omega}{T_c} t \right) \right]$, the autocorrelation coefficient of $c_{s1}(t)$ for analysis in the BOK CSS system can be simplified as:

$$r_s(\tau) \approx \cos(\omega_0 \tau) \left(1 - \frac{|\tau|}{T_c} \right) J_0 \left[\frac{2BT_c}{\Omega} \sin \left(\frac{\pi \Omega}{2T_c} \tau \right) \right] \quad (4.21)$$

Proof. There are three terms in the autocorrelation coefficient of sine chirp $c_{s1}(t)$ as defined in Eqn. (4.18). Taking the parameters $f_0 = 20(\text{MHz})$, $T_c = 1(\mu\text{s})$, $\Omega = 2$, and $B = 20(\text{MHz})$ as an example, values of these terms are depicted in Figure 4.3 (a) to Figure 4.3 (c) respectively, and summary of these terms is also shown in Figure 4.3 (d).

It can be observed from these figures that the second term of Eqn. (4.18) is dominant, while other two terms are so small that they can be ignored. The same conclusion can be achieved for different values of the parameters (f_0 , T_c , Ω , and B) in Eqn. (4.18). For example, value of the first term in Eqn. (4.18) with different values of Ω ($\Omega = 1, 2, \dots, 6$) is shown in Figure 4.4. As shown, absolute value of the first term in Eqn. (4.18) is always less than 0.015.

Comparisons between the corresponding value of the second term and that of all terms in Eqn. (4.18) when Ω equals 1 and 2 are depicted as an example and shown in Figure 4.5 and Figure 4.6 respectively.

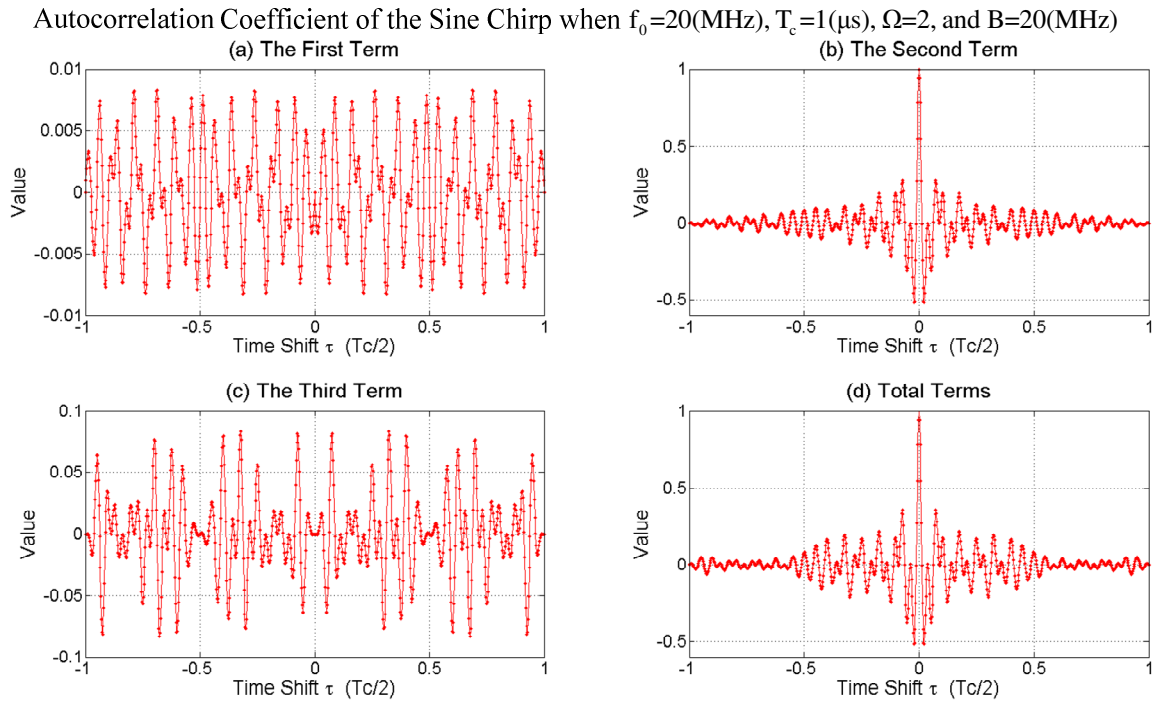


Figure 4.3: Values of the terms in Eqn. (4.18)

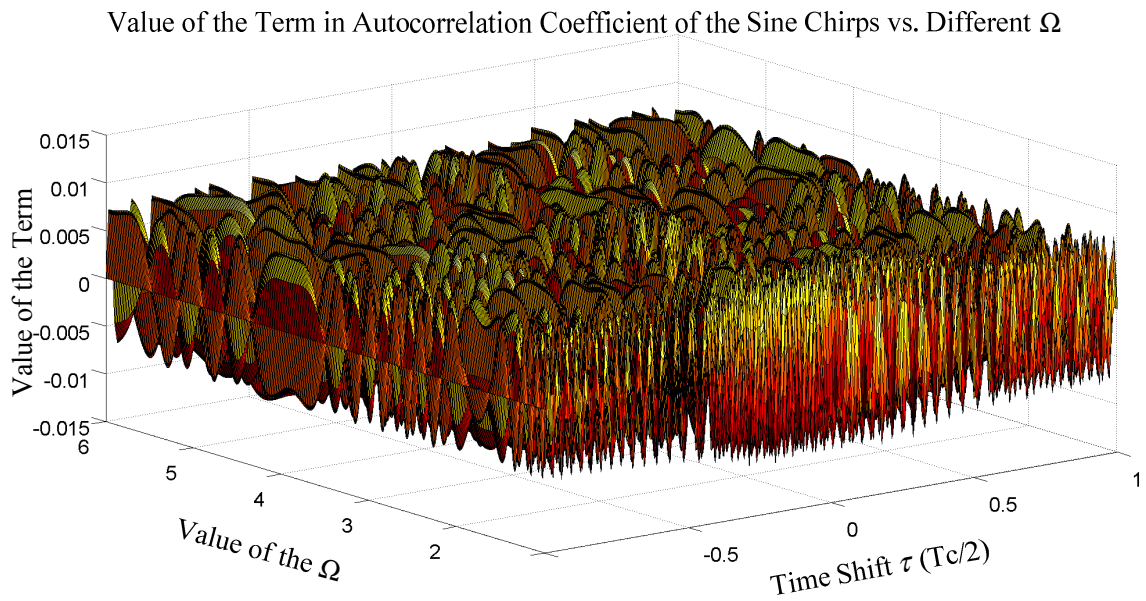


Figure 4.4: Value of the first term in Eqn. (4.18) vs. different Ω

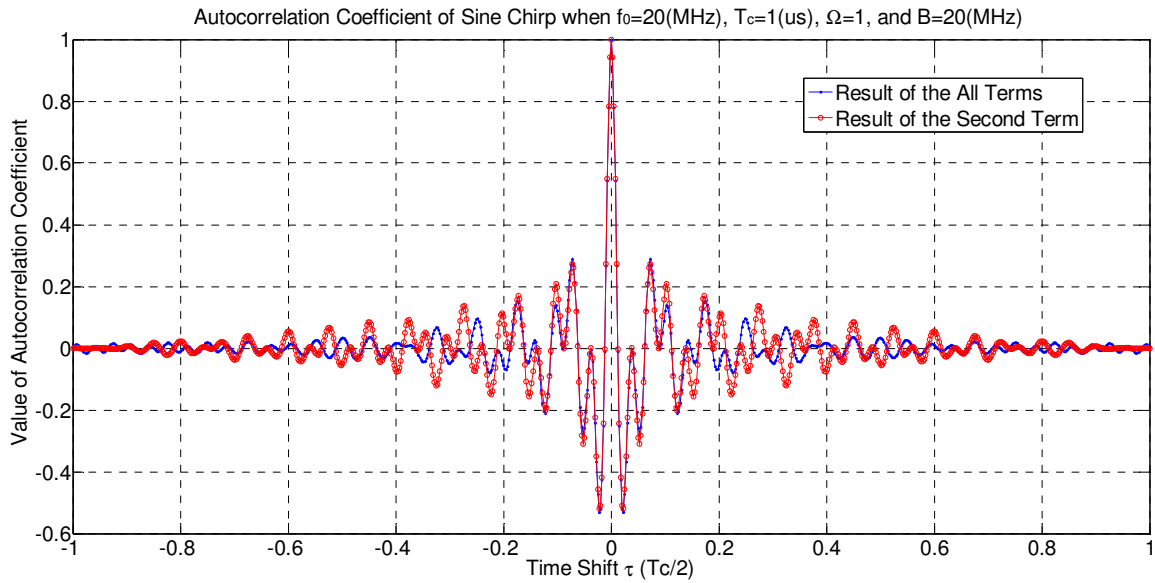


Figure 4.5: Comparison between the all terms and the second term defined in Eqn. (4.18) when $\Omega = 1$

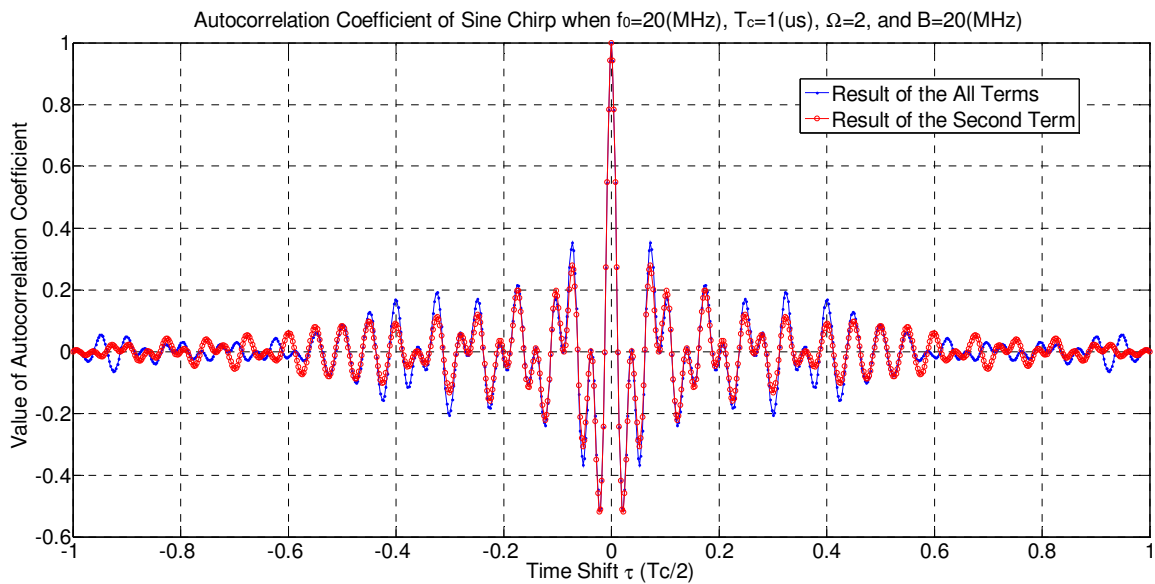


Figure 4.6: Comparison between the all terms and the second term defined in Eqn. (4.18) when $\Omega = 2$

It can be observed from Figure 4.5 and Figure 4.6 that the second term is very similar to that of all terms, which means the second term in Eqn. (4.18) is overwhelming dominant. Therefore, it can be concluded that the second term in Eqn. (4.18) can be used to represent the entire equation. Therefore, autocorrelation coefficient of sine chirp $c_{s1}(t)$ can be simplified as:

$$r_s(\tau) \approx \cos(\omega_0\tau) \left(1 - \frac{|\tau|}{T_c}\right) J_0 \left[\frac{2BT_c}{\Omega} \sin\left(\frac{\pi\Omega}{2T_c} \tau\right) \right] \quad (4.22)$$

– Q.E.D

4.3.2 Cosine Chirps

Theorem 4.3: If a cosine chirp is represented as

$$c_{c1}(t) = a \cos \left[\omega_0 t + \frac{BT_c}{\Omega} \sin \left(\pi \Omega \frac{t}{T_c} \right) \right],$$

the autocorrelation coefficient of this cosine chirp will be:

$$\begin{aligned} r_c(\tau) = & \left(1 - \frac{|\tau|}{T_c}\right) \sum_{n=-\infty}^{\infty} \left\{ J_n(k_{C1}^m) \operatorname{sinc} \left[(\omega_0 + n\theta)(T_c - |\tau|) \right] \right\} \\ & + \cos(\omega_0\tau) \left(1 - \frac{|\tau|}{T_c}\right) J_0(k_{C2}^m) \\ & + 2 \cos(\omega_0\tau) \left(1 - \frac{|\tau|}{T_c}\right) \sum_{n=1}^{\infty} \left\{ (-1)^n J_{2n}(k_{C2}^m) \operatorname{sinc} \left[2n\theta(T_c - |\tau|) \right] \right\} \\ & - 2 \sin(\omega_0\tau) \left(1 - \frac{|\tau|}{T_c}\right) \sum_{n=0}^{\infty} \left\{ (-1)^n J_{2n+1}(k_{C2}^m) \operatorname{sinc} \left[(2n+1)\theta(T_c - |\tau|) \right] \right\} \end{aligned} \quad (4.23)$$

where

$$\theta = \frac{\pi\Omega}{2T_c}; \quad k_{C1}^m = \frac{2BT_c}{\Omega} \cos\left(\frac{\pi\Omega}{2T_c} \tau\right); \quad k_{C2}^m = \frac{2BT_c}{\Omega} \sin\left(\frac{\pi\Omega}{2T_c} \tau\right) \quad (4.24)$$

Proof. The autocorrelation coefficient of cosine chirp $c_{c1}(t)$ can be obtained by using Eqn. (2.12):

$$r_c(\tau) = \frac{\int_{-\infty}^{\infty} \left\{ \begin{array}{l} a \cos \left[\omega_0(t+\tau) + \frac{BT_c}{\Omega} \sin \left(\frac{\pi\Omega}{T_c} (t+\tau) \right) \right] \\ \times a \cos \left[\omega_0 t + \frac{BT_c}{\Omega} \sin \left(\frac{\pi\Omega}{T_c} t \right) \right] \end{array} \right\} dt}{E(c_{c1})} \quad (4.25)$$

Appendix E presents the detailed derivation for Eqn. (4.25).

– Q.E.D

Theorem 4.4: If a cosine chirp is represented as $c_{c1}(t) = a \cos \left[\omega_0 t + \frac{BT_c}{\Omega} \sin \left(\frac{\pi\Omega}{T_c} t \right) \right]$,

the autocorrelation coefficient of this cosine chirp for analysis in the BOK CSS system can be simplified as:

$$r_c(\tau) \approx \cos(\omega_0 \tau) \left(1 - \frac{|\tau|}{T_c} \right) J_0 \left[\frac{2BT_c}{\Omega} \sin \left(\frac{\pi\Omega}{2T_c} \tau \right) \right] \quad (4.26)$$

Proof. There are four terms in the autocorrelation coefficient of cosine chirp $c_{c1}(t)$ as defined in Eqn. (4.23). Taking the parameters $f_0 = 20(\text{MHz})$, $T_c = 1(\mu\text{s})$, $\Omega = 2$, and $B = 20(\text{MHz})$ as an example, values of these terms are depicted in Figure 4.7 respectively.

It can be observed from Figure 4.7 that the second term of Eqn. (4.23) is overwhelming dominant, while value of the first term is so small that can be practically ignored. The same conclusion can be drawn for different values of the parameters (f_0 , T_c , Ω , and B) in Eqn. (4.23). For example, value of the first term in Eqn. (4.23) with different values of Ω ($\Omega = 1, 2, \dots, 6$) is shown in Figure 4.8. As shown in this figure, absolute value of the first term in Eqn. (4.23) is always less than 0.02, thus this term can be ignored.

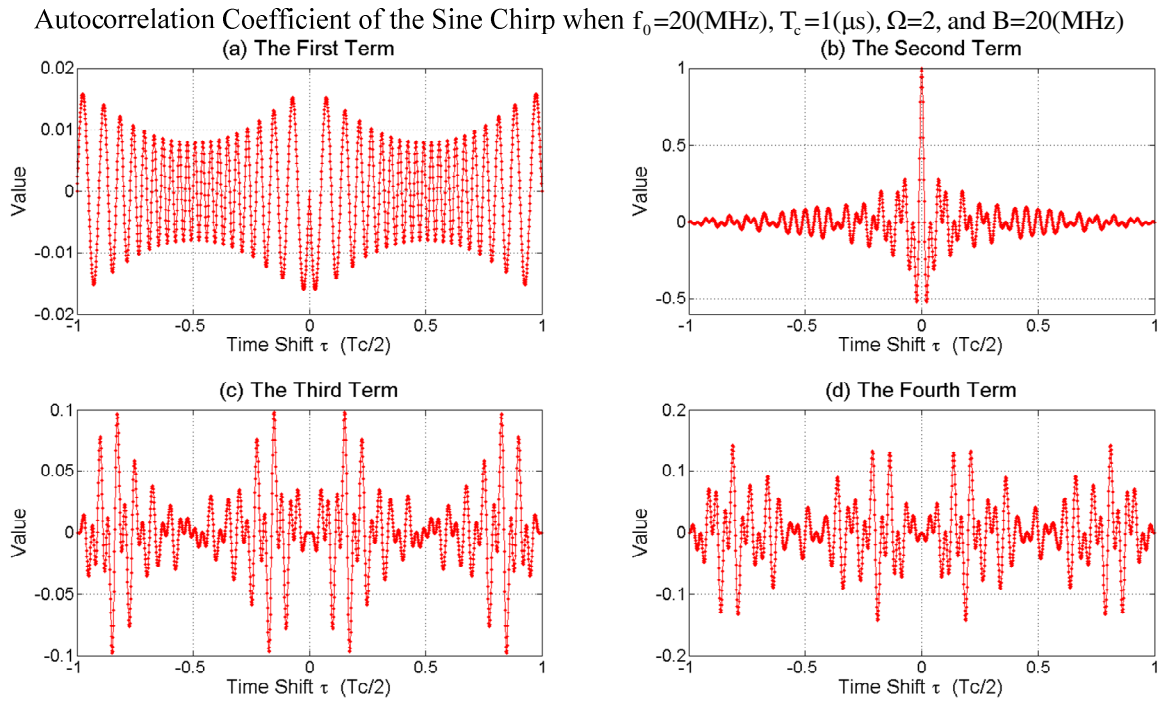


Figure 4.7: Values of the terms in Eqn. (4.23)

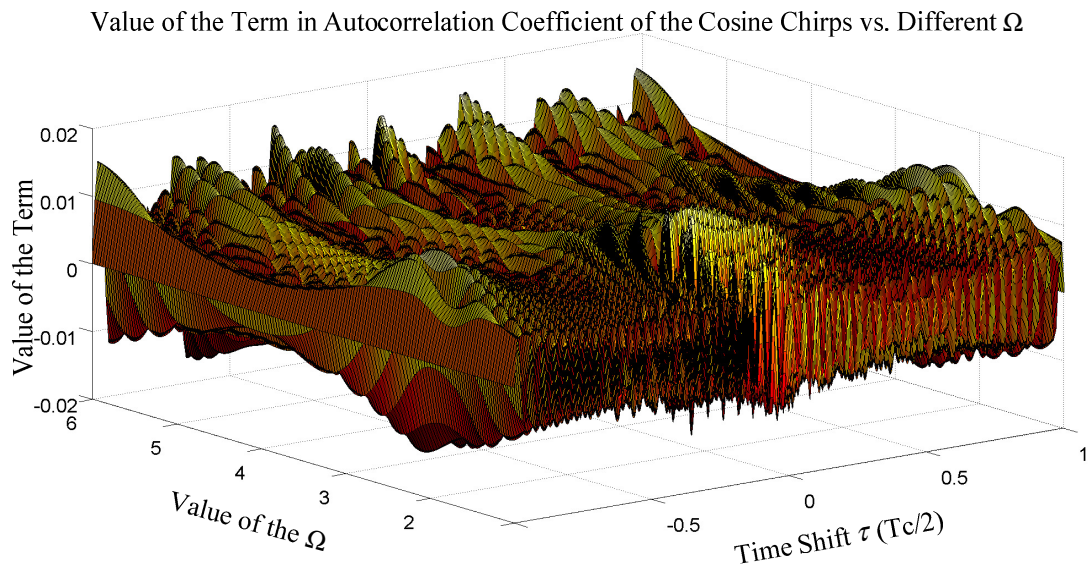


Figure 4.8: Value of the first term in Eqn. (4.23) vs. different Ω

Comparison between value of the second term and all terms defined in Eqn. (4.23) when $\Omega=2$ is shown in Figure 4.9. It can be observed that the result of Eqn. (4.23) significantly depends on the second term, except when the time shift τ is close to $\pm T_c$. As stated in Section 2.4, the narrow peak centered at $\tau = 0$ will be used by the BOK CSS system to identify the matched output, therefore, the part around the peak where the time shift $\tau = 0$ in the autocorrelation are mainly considered. The parts at the both side where the time shift τ is close to $\pm T_c/2$ is not important, since they will not be used by the BOK CSS system to identify the matched output. Thus, differences at the both sides in Figure 4.9 can also be ignored.

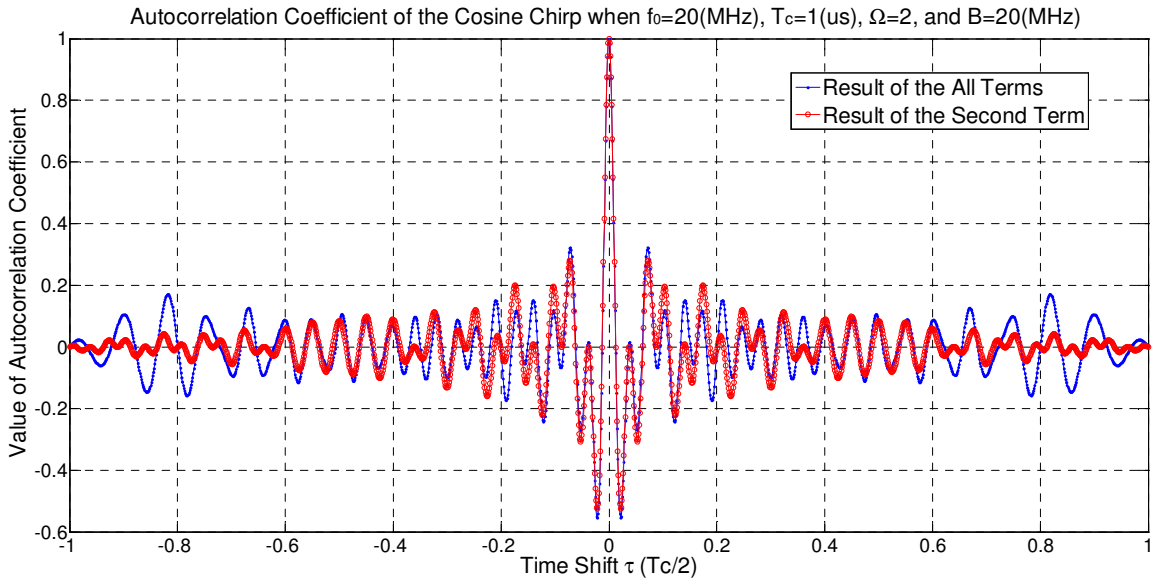


Figure 4.9: Comparison between all terms and the second term defined in Eqn. (4.23)

Therefore, the second term in Eqn. (4.23) can be used to represent the entire equation for analysis of the BOK cosine CSS system, so that autocorrelation coefficient of cosine chirps which is defined by Eqn. (4.23) can be simplified to Eqn. (4.27). Eqn. (4.27) is identical to Eqn. (4.22).

$$r_c(\tau) \approx \cos(\omega_0 \tau) \left(1 - \frac{|\tau|}{T_c} \right) J_0 \left[\frac{2BT_c}{\Omega} \sin \left(\frac{\pi\Omega}{2T_c} \tau \right) \right] \quad (4.27)$$

– Q.E.D

4.3.3 Summary

It can be seen that the results given in Eqn. (4.22) and Eqn. (4.27) are the same. Therefore, a unified equation which can represent autocorrelation coefficients of both cosine chirp and sine chirp for the BOK CSS system is:

$$r(\tau) \approx \cos(\omega_0\tau) \left(1 - \frac{|\tau|}{T_c}\right) J_0 \left[\frac{2BT_c}{\Omega} \sin\left(\frac{\pi\Omega}{2T_c}\tau\right) \right] \quad (4.28)$$

Hence, it is expected that cosine chirps and sine chirps would produce similar results in a BOK CSS system.

4.4 Cross-correlation Properties

As stated in Section 2.3: “the output of the corresponding unmatched filter can be represented as the cross-correlation function between the two chirp signals”. Therefore, cross-correlation of the chirps is another important property of the BOK CSS system.

4.4.1 Cross-correlation Coefficient

A. Sine Chirp

Theorem 4.5: If a pair of sine chirps are respectively represented as

$$c_{s1}(t) = a \cos \left[\omega_0 t + \frac{BT_c}{\Omega} \cos \left(\pi\Omega \frac{t}{T_c} \right) \right] \text{ and } c_{s2}(t) = a \cos \left[\omega_0 t - \frac{BT_c}{\Omega} \cos \left(\pi\Omega \frac{t}{T_c} \right) \right],$$

the cross-correlation coefficient between these two sine chirps will be:

$$\begin{aligned} \rho_s(\tau) = & \left(1 - \frac{|\tau|}{T_c}\right) \sum_{n=-\infty}^{\infty} \left\{ (-1)^n J_n(k_{s1}^u) \text{sinc} \left[(\omega_0 + n\theta)(T_c - |\tau|) \right] \right\} \\ & + \cos(\omega_0\tau) \left(1 - \frac{|\tau|}{T_c}\right) J_0(k_{s2}^u) \\ & + 2 \cos(\omega_0\tau) \left(1 - \frac{|\tau|}{T_c}\right) \sum_{n=1}^{\infty} \left\{ (-1)^n J_{2n}(k_{s2}^u) \text{sinc} \left[2n\theta(T_c - |\tau|) \right] \right\} \\ & - 2 \sin(\omega_0\tau) \left(1 - \frac{|\tau|}{T_c}\right) \sum_{n=0}^{\infty} \left\{ (-1)^n J_{2n+1}(k_{s2}^u) \text{sinc} \left[(2n+1)\theta(T_c - |\tau|) \right] \right\} \end{aligned} \quad (4.29)$$

where $\theta = \frac{\pi\Omega}{2T_c}$, $k_{s1}^u = \frac{2BT_c}{\Omega} \sin(\tau\theta)$, and $k_{s2}^u = \frac{2BT_c}{\Omega} \cos(\tau\theta)$

Proof. The cross-correlation coefficient between sine chirps $c_{s1}(t)$ and $c_{s2}(t)$ can be obtained by substituting Eqn. (4.1) into Eqn. (2.14):

$$\rho_s(\tau) = \frac{\int_{-\infty}^{\infty} \left\{ a \cos \left[\omega_0(t+\tau) + \frac{BT_c}{\Omega} \cos \left(\frac{\pi\Omega}{T_c} (t+\tau) \right) \right] \right.}{\sqrt{R_{11}(0) \times R_{22}(0)}} \left. \times a \cos \left[\omega_0 t - \frac{BT_c}{\Omega} \cos \left(\frac{\pi\Omega}{T_c} t \right) \right] \right\} dt}{\sqrt{R_{11}(0) \times R_{22}(0)}} \quad (4.30)$$

Detailed derivation for Eqn. (4.30) is presented in Appendix D.

– Q.E.D

Theorem 4.6: If a pair of sine chirps are respectively represented as

$$c_{s1}(t) = a \cos \left[\omega_0 t + \frac{BT_c}{\Omega} \cos \left(\frac{\pi\Omega}{T_c} t \right) \right] \text{ and } c_{s2}(t) = a \cos \left[\omega_0 t - \frac{BT_c}{\Omega} \cos \left(\frac{\pi\Omega}{T_c} t \right) \right],$$

the cross-correlation coefficient between these two sine chirps at the time shift $\tau = 0$ is

$$\rho_s(0) = J_0 \left(\frac{2T_c B}{\Omega} \right).$$

Proof. The cross-correlation coefficient of sine chirps at the time shift $\tau = 0$ can be obtained from Eqn. (4.29):

$$\begin{aligned} \rho_s(0) = & \sum_{n=-\infty}^{\infty} \left[(-1)^n J_n(0) \right] \times \text{sinc} \left[(\omega_0 + n\theta) T_c \right] \\ & + J_0 \left(\frac{2BT_c}{\Omega} \right) + 2 \sum_{n=1}^{\infty} \left[(-1)^n J_{2n} \left(\frac{2BT_c}{\Omega} \right) \right] \times \text{sinc} (2n\theta T_c) \end{aligned} \quad (4.31)$$

According to the properties of $J_n(x)$ as shown in Figure 4.1, the magnitude of $J_n(0)$ is equal to 1 when $n = 0$, and is always equal to 0 when n is other integer values [39]. So, Eqn. (4.31) can be simplified as:

$$\rho_s(0) = \text{sinc}(\omega_0 T_c) + J_0\left(\frac{2BT_c}{\Omega}\right) + 2\sum_{n=1}^{\infty} \left[(-1)^n J_{2n}\left(\frac{2BT_c}{\Omega}\right)\right] \times \text{sinc}(2n\theta T_c) \quad (4.32)$$

By substituting $\theta = \frac{\pi\Omega}{2T_c}$ and $\omega_0 = 2\pi f_0$ into Eqn. (4.32), it can be rewritten as:

$$\rho_s(0) = \text{sinc}(2\pi f_0 T_c) + J_0\left(\frac{2T_c B}{\Omega}\right) + 2\sum_{n=1}^{\infty} \left[(-1)^n J_{2n}\left(\frac{2BT_c}{\Omega}\right)\right] \times \text{sinc}(n\Omega\pi) \quad (4.33)$$

wherein $\text{sinc}(n\pi\Omega)$ is an unnormalized sinc function. As defined in Eqn. (4.6), $\text{sinc}(n\pi\Omega)$ is zero when n is a non-zero integer. Hence, $\text{sinc}(n\pi\Omega)$ is always equal to 0 because Ω is also a non-zero integer. Similarly, $\text{sinc}(2\pi f_0 T_c)$ is also equal to 0 since $f_0 T_c$ is an integer. Thus, Eqn. (4.33) can be further simplified as:

$$\rho_s(0) = J_0\left(\frac{2T_c B}{\Omega}\right) \quad (4.34)$$

– Q.E.D

B. Cosine Chirp

Theorem 4.7: If a pair of cosine chirps are respectively represented as $c_{c1}(t) = a \cos\left[\omega_0 t + \frac{BT_c}{\Omega} \sin\left(\pi\Omega \frac{t}{T_c}\right)\right]$ and $c_{c2}(t) = a \cos\left[\omega_0 t - \frac{BT_c}{\Omega} \sin\left(\pi\Omega \frac{t}{T_c}\right)\right]$, the cross-correlation coefficient between these two cosine chirps will be:

$$\begin{aligned} \rho_c(\tau) = & \left(1 - \frac{|\tau|}{T_c}\right) \sum_{n=-\infty}^{\infty} \left\{(-1)^n J_{2n}(k_{c1}^u) \text{sinc}\left[(\omega_0 + 2n\theta)(T_c - |\tau|)\right]\right\} \\ & + \cos(\omega_0 \tau) \left(1 - \frac{|\tau|}{T_c}\right) J_0(k_{c2}^u) \\ & + 2 \cos(\omega_0 \tau) \left(1 - \frac{|\tau|}{T_c}\right) \sum_{n=1}^{\infty} \left\{J_{2n}(k_{c2}^u) \text{sinc}\left[2n\theta(T_c - |\tau|)\right]\right\} \end{aligned} \quad (4.35)$$

where $\theta = \frac{\pi\Omega}{2T_c}$, $k_{c1}^u = \frac{2BT_c}{\Omega} \sin(\tau\theta)$, and $k_{c2}^u = \frac{2BT_c}{\Omega} \cos(\tau\theta)$

Proof. The cross-correlation coefficient between cosine chirps $c_{c1}(t)$ and $c_{c2}(t)$ can be obtained by substituting Eqn. (4.2) into Eqn. (2.14):

$$\rho_C(\tau) = \frac{\int_{-\infty}^{\infty} \left\{ a \cos \left[\omega_0(t+\tau) + \frac{BT_c}{\Omega} \sin \left(\pi\Omega \frac{t+\tau}{T_c} \right) \right] \right.}{\sqrt{R_{11}(0) \times R_{22}(0)}} \left. \times a \cos \left[\omega_0 t - \frac{BT_c}{\Omega} \sin \left(\pi\Omega \frac{t}{T_c} \right) \right] \right\} dt}{\sqrt{R_{11}(0) \times R_{22}(0)}} \quad (4.36)$$

Detailed derivation for Eqn. (4.36) is described in Appendix E.

– Q.E.D

Theorem 4.8: If a pair of cosine chirps are respectively represented as $c_{c1}(t) = a \cos \left[\omega_0 t + \frac{BT_c}{\Omega} \sin \left(\pi\Omega \frac{t}{T_c} \right) \right]$ and $c_{c2}(t) = a \cos \left[\omega_0 t - \frac{BT_c}{\Omega} \sin \left(\pi\Omega \frac{t}{T_c} \right) \right]$, the cross-correlation coefficient between these two cosine chirps at the time shift $\tau = 0$ will be $\rho_C(0) = J_0 \left(\frac{2T_c B}{\Omega} \right)$.

Proof. The cross-correlation coefficient of the two cosine chirps at the time shift $\tau = 0$ can be obtained from Eqn. (4.35):

$$\rho_C(\tau) = \sum_{n=-\infty}^{\infty} \left[(-1)^n J_{2n}(0) \right] \times \text{sinc} \left[(\omega_0 + 2n\theta) T_c \right] + J_0 \left(\frac{2BT_c}{\Omega} \right) + 2 \sum_{n=1}^{\infty} \left[J_{2n} \left(\frac{2BT_c}{\Omega} \right) \times \text{sinc} (2n\theta T_c) \right] \quad (4.37)$$

Since value of $J_n(0)$ is equal to 1 when $n = 0$ and is always equal to zero when n is a non-zero integer [39], Eqn. (4.37) can be simplified as:

$$\rho_C(0) = \text{sinc}(\omega_0 T_c) + J_0\left(\frac{2BT_c}{\Omega}\right) + 2\sum_{n=1}^{\infty} \left[J_{2n}\left(\frac{2BT_c}{\Omega}\right) \times \text{sinc}(2n\theta T_c) \right] \quad (4.38)$$

By substituting $\theta = \frac{\pi\Omega}{2T_c}$ and $\omega_0 = 2\pi f_0$ into Eqn. (4.38), it can be rewritten as:

$$\rho_C(0) = \text{sinc}(2\pi f_0 T_c) + J_0\left(\frac{2BT_c}{\Omega}\right) + 2\sum_{n=1}^{\infty} \left[J_{2n}\left(\frac{2BT_c}{\Omega}\right) \times \text{sinc}(n\pi\Omega) \right] \quad (4.39)$$

wherein $\text{sinc}(n\pi\Omega)$ is an unnormalized sinc function. As defined by Eqn. (4.6), $\text{sinc}(n\pi\Omega)$ is equal to zero when n is a non-zero integer. Hence, $\text{sinc}(n\pi\Omega)$ is always 0, when n is a non-zero integer because Ω is also an integer. Similarly, $\text{sinc}(2\pi f_0 T_c)$ is always 0 since $f_0 T_c$ is an integer. Thus, a finally simplified expression for $\rho_C(0)$ can be obtained as:

$$\rho_C(0) = J_0\left(\frac{2T_c B}{\Omega}\right) \quad (4.40)$$

– Q.E.D

C. Summary

From Eqn. (4.34) and Eqn. (4.40), it can be summarized that the cross-correlation coefficient for a pair of sine chirps and cosine chirps at the time shift $\tau = 0$ are identical:

$$\begin{cases} \rho_S(0) = J_0\left(\frac{2T_c B}{\Omega}\right) \\ \rho_C(0) = J_0\left(\frac{2T_c B}{\Omega}\right) \end{cases} \quad (4.41)$$

From Eqn. (4.41), it can be concluded that $\rho_S(0)$ or $\rho_C(0)$ only depends on the time-bandwidth product ($T_c B$) for a given Ω .

4.4.2 Orthogonal Characteristics

As stated in Section 3.3 and Section 3.4, two interesting characteristics for sine or cosine chirps are observed. The first one is that a pair of sine chirps or cosine chirps can be orthogonal under certain conditions. Another one is that the cross-correlation coefficient of the two sine chirps or cosine chirps shows periodic characteristics. In order to prove these two characteristics, mathematical analysis is presented in this sub-section.

A. Conditional Orthogonality

In Eqn. (4.41), $J_0(x)$ is the Bessel function of the first kind of order zero. The curve for $J_0(x)$ is depicted in Figure 4.10.

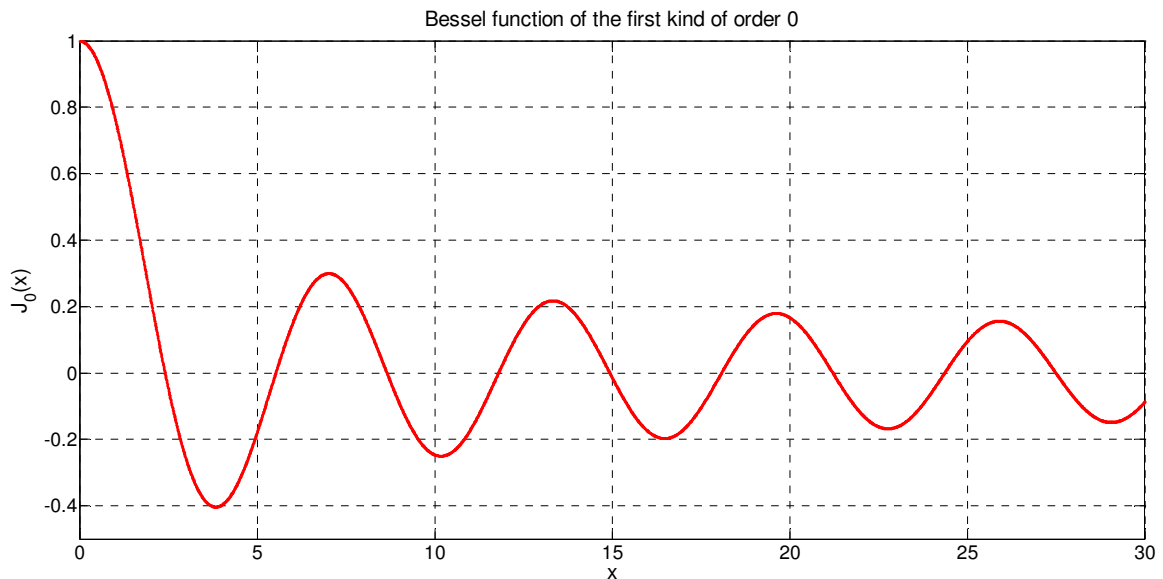


Figure 4.10: Bessel function of the first kind of order zero

The first several roots of $J_0(x)$ are and shown in Table 4.1 [39].

Table 4.1: Roots of Bessel function of the first kind of order zero

n	1	2	3	4	5	6	7	8
x	2.4048	5.5201	8.6531	11.7915	14.9309	18.0701	21.2109	24.3519

From Eqn. (4.41), it can be concluded that the cross-correlation coefficient for a pair of sine chirps or cosine chirps can be zero as long as $\frac{2T_c B}{\Omega}$ equals to the roots of $J_0(x)$:

$$\frac{2T_c B}{\Omega} = x_n \quad (4.42)$$

where x_n is a root of $J_0(x)$.

For a given Ω and T_c , the frequency spread bandwidth B , by which a pair of cosine or sine chirps can be completely orthogonal at $\tau = 0$, can be calculated by the following equation.

$$B = \frac{\Omega}{2T_c} x_n \quad (4.43)$$

B.Periodic Orthogonality

The Bessel function of the first kind of order zero $J_0(x)$ has an infinite set of positive roots:

$$x_1 < x_2 < x_3 \dots < x_n < x_{n+1} \dots \quad (4.44)$$

Hence, the number of orthogonal points for a pair of sine chirps or cosine chirps is also infinite. As n is close to ∞ , value of the period $(x_{n+1} - x_n)$ is approached to π [39]. If the product of time and bandwidth $(T_c B)$ meets the condition as defined in Eqn. (4.42), a pair of sine chirps or cosine chirps become orthogonal. Therefore, orthogonal points for a pair of sine chirps or cosine chirps are periodic. This is very different from that in the linear chirp cases. As shown in Figure 2.7, there is no orthogonal point for the linear chirps, and the linear chirps are almost closer to be orthogonal as $T_c B$ becomes bigger.

C. Validation of the Orthogonal Characteristics

Since sine chirps and cosine chirps have the same cross-correlation property, only full period sine chirps ($\Omega=2$) are chosen as an example to validate the orthogonal characteristics stated above. By using Eqn. (4.43), three different values of the frequency spread bandwidth B for a pair of orthogonal full period sine (FPS) chirps can be obtained as follows:

$$\begin{cases} B_{2-1} = \frac{\Omega}{2T_c} x_2 = \frac{2 \times 5.5201}{2 \times 10^{-6}} = 5.5201(\text{MHz}) \\ B_{2-2} = \frac{\Omega}{2T_c} x_3 = \frac{2 \times 8.6531}{2 \times 10^{-6}} = 8.6531(\text{MHz}) \\ B_{2-4} = \frac{\Omega}{2T_c} x_4 = \frac{2 \times 11.7915}{2 \times 10^{-6}} = 11.7915(\text{MHz}) \end{cases} \quad (4.45)$$

Moreover, an arbitrary bandwidth is also considered for comprising with the above three bandwidth. In this thesis, $B_{2-3} = 10$ MHz is chosen as an example. Autocorrelation and cross-correlation of a pair of FPS chirps at these bandwidths are drawn in Figure 4.11 to Figure 4.14, respectively. The red curves with circles show that values of cross-correlation coefficient are all zero not only at $\tau = 0$ but also during a short period around the center which is highlighted by the green circles. However, values of cross-correlation coefficient are not zero at $\tau = 0$ in Figure 4.13 which the frequency bandwidth is $B_{2-3} = 10$ MHz. In other words, a pair of FPS chirps at bandwidths B_{2-1} , B_{2-2} and B_{2-4} can be orthogonal, while it is not orthogonal at B_{2-3} . This is because B_{2-1} , B_{2-2} and B_{2-4} meets the condition defined in Eqn. (4.43), while B_{2-3} does not. Therefore, it is verified that a pair of sine chirps is conditional orthogonal.

As stated in previous sections, when T_c is constant, value of cross-correlation coefficient of linear chirps decreases as the bandwidth increases. However, sine chirps do not have this. From Figure 4.11 to Figure 4.14, value of cross-correlation coefficient at $\tau = 0$ for sine chirps at bandwidths B_{2-1} , B_{2-2} and B_{2-4} are all equal to zero, while that at B_{2-3} is nearly 0.3 even if B_{2-3} is bigger than both B_{2-1} and B_{2-2} . Therefore, it is validated

a pair of sine chirps is periodically orthogonal. In addition, it also shows that whether two sine chirps are orthogonal or not depends on if the condition defined in Eqn. (4.43) is met, rather than the absolute value of the product of time-bandwidth ($T_c B$).

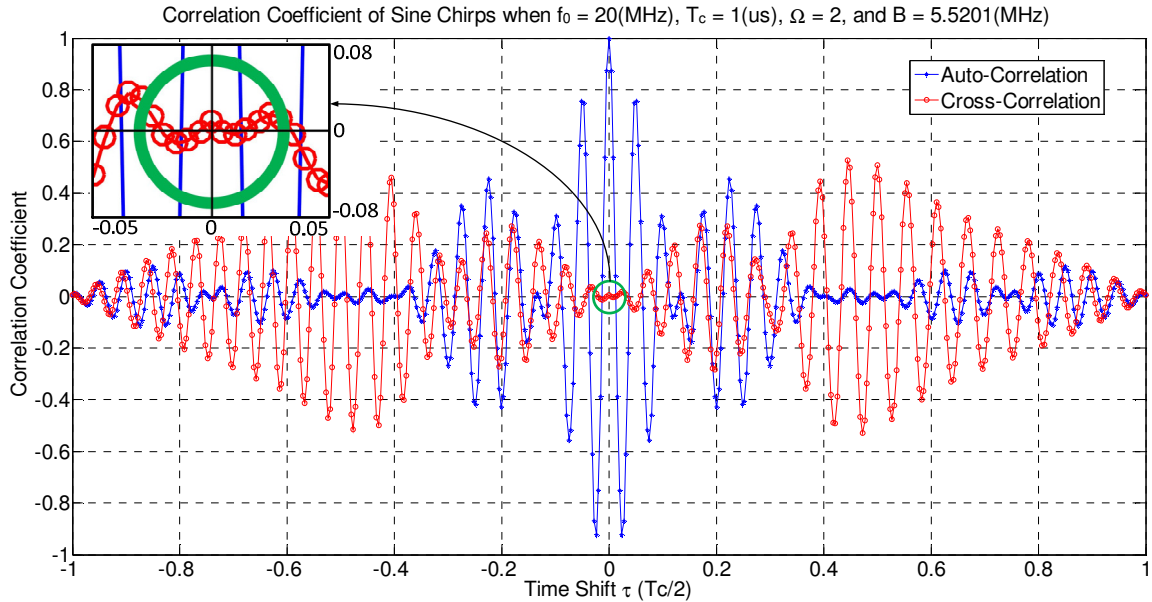


Figure 4.11: Autocorrelation & cross-correlation for FPS chirps when $B_{2-1} = 5.5201\text{MHz}$

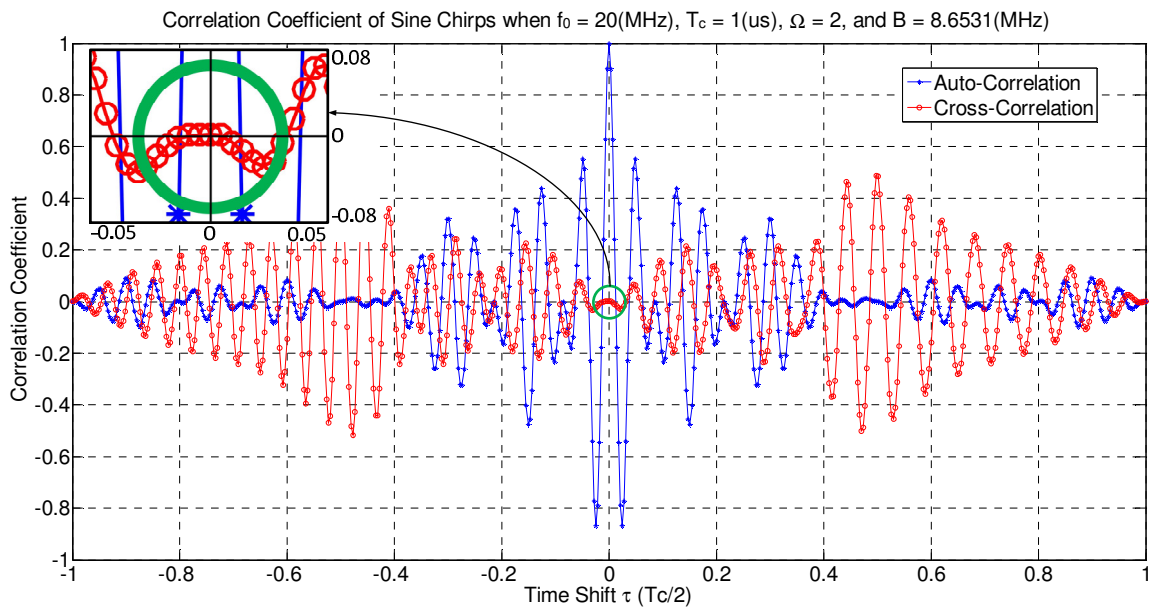


Figure 4.12: Autocorrelation & cross-correlation for FPS chirps when $B_{2-2} = 8.6531\text{MHz}$

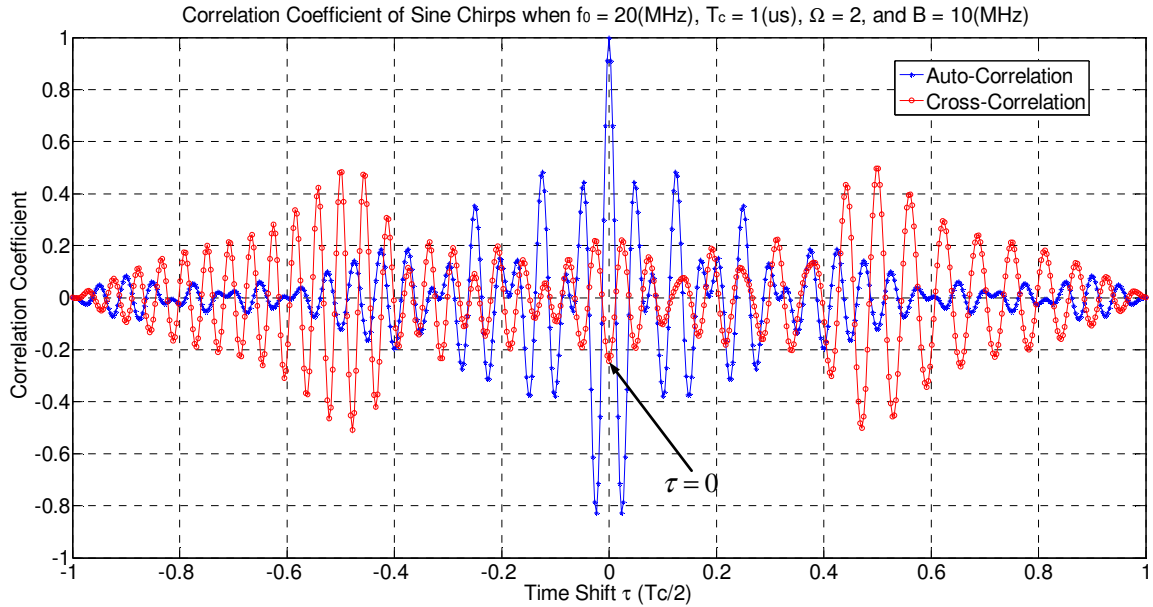


Figure 4.13: Autocorrelation & cross-correlation for FPS chirps when $B_{2-3} = 10\text{MHz}$

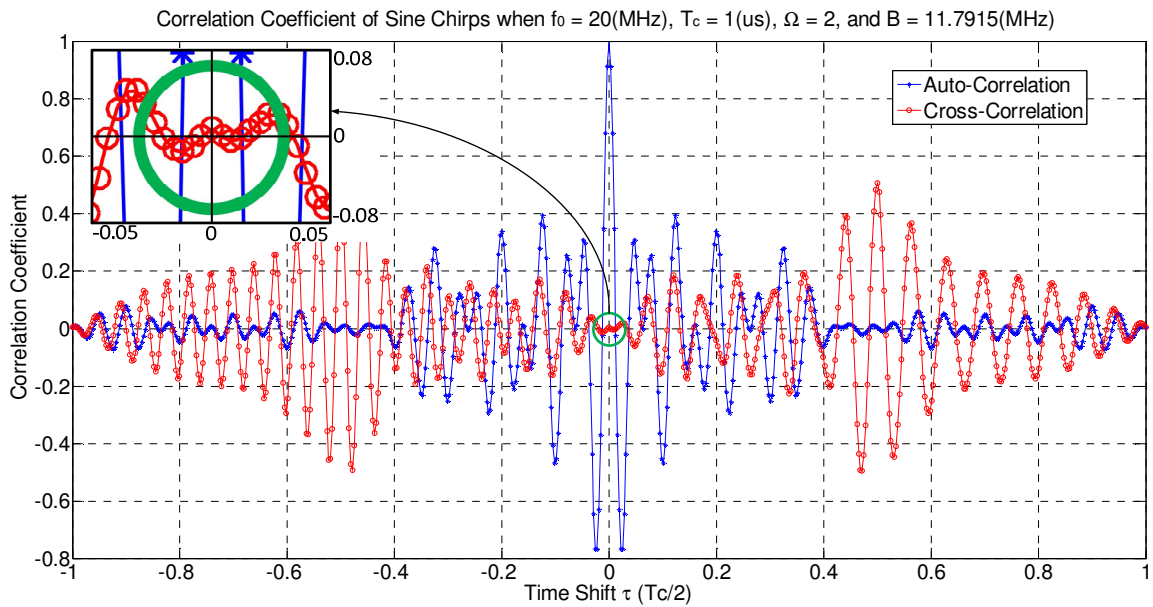


Figure 4.14: Autocorrelation & cross-correlation for FPS chirps when $B_{2-4} = 11.7915$

MHz

4.4.3 Simplification of the Cross-correlation Coefficient

A. Sine Chirp

Theorem 4.9: If a pair of sine chirps are respectively represented as

$$c_{s1}(t) = a \cos \left[\omega_0 t + \frac{BT_c}{\Omega} \cos \left(\pi \Omega \frac{t}{T_c} \right) \right] \text{ and } c_{s2}(t) = a \cos \left[\omega_0 t - \frac{BT_c}{\Omega} \cos \left(\pi \Omega \frac{t}{T_c} \right) \right],$$

the cross-correlation coefficient between these two sine chirps can be simplified as:

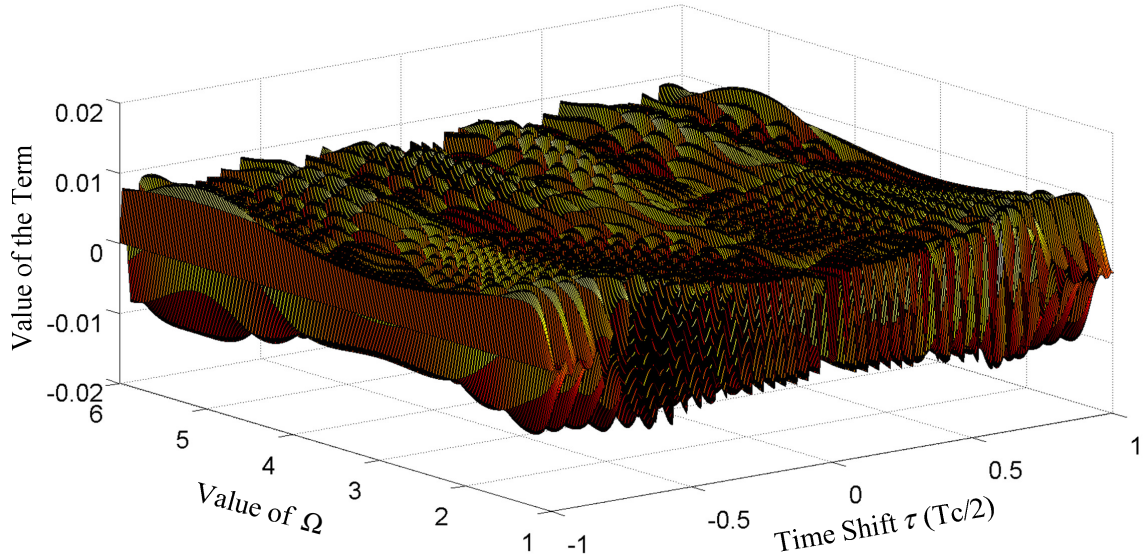
$$\begin{aligned} \rho_s(\tau) &= \cos(\omega_0 \tau) \left(1 - \frac{|\tau|}{T_c} \right) J_0(k_{s2}^u) \\ &+ 2 \cos(\omega_0 \tau) \left(1 - \frac{|\tau|}{T_c} \right) \sum_{n=1}^{\infty} \{ (-1)^n J_{2n}(k_{s2}^u) \text{sinc} [2n\theta(T_c - |\tau|)] \} \\ &- 2 \sin(\omega_0 \tau) \left(1 - \frac{|\tau|}{T_c} \right) \sum_{n=0}^{\infty} \{ (-1)^n J_{2n+1}(k_{s2}^u) \text{sinc} [(2n+1)\theta(T_c - |\tau|)] \} \end{aligned} \quad (4.46)$$

where $\theta = \frac{\pi\Omega}{2T_c}$, $k_{s1}^u = \frac{2BT_c}{\Omega} \sin(\tau\theta)$, and $k_{s2}^u = \frac{2BT_c}{\Omega} \cos(\tau\theta)$

Proof. There are three terms in the cross-correlation coefficient between the two sine chirps as defined in Eqn. (4.29). The first term is:

$$\left(1 - \frac{|\tau|}{T_c} \right) \sum_{n=-\infty}^{\infty} \{ (-1)^n J_n(k_{s1}^u) \text{sinc} [(\omega_0 + n\theta)(T_c - |\tau|)] \} \quad (4.47)$$

Value of this term with different values of Ω is shown in Figure 4.15.

Value of the Term in Cross-correlation Coefficient of the Sine Chirps vs. Different Ω Figure 4.15: Value of the first term in Eqn. (4.29) vs. different values of Ω

As shown in Figure 4.15, absolute value of the first term in Eqn. (4.29) is always less than 0.015. Value of this term is so small that it can be ignored. Therefore, Eqn. (4.29) can be simplified as:

$$\begin{aligned}
 \rho_s(\tau) &= \cos(\omega_0\tau) \left(1 - \frac{|\tau|}{T_c}\right) J_0(k_{s2}^u) \\
 &+ 2 \cos(\omega_0\tau) \left(1 - \frac{|\tau|}{T_c}\right) \sum_{n=1}^{\infty} \{(-1)^n J_{2n}(k_{s2}^u) \text{sinc}[2n\theta(T_c - |\tau|)]\} \\
 &- 2 \sin(\omega_0\tau) \left(1 - \frac{|\tau|}{T_c}\right) \sum_{n=0}^{\infty} \{(-1)^n J_{2n+1}(k_{s2}^u) \text{sinc}[(2n+1)\theta(T_c - |\tau|)]\}
 \end{aligned} \tag{4.48}$$

where $\theta = \frac{\pi\Omega}{2T_c}$, $k_{s1}^u = \frac{2BT_c}{\Omega} \sin(\tau\theta)$, and $k_{s2}^u = \frac{2BT_c}{\Omega} \cos(\tau\theta)$

– Q.E.D

B. Cosine chirp

Theorem 4.10: If a pair of cosine chirps are respectively represented as

$$c_{c1}(t) = a \cos \left[\omega_0 t + \frac{BT_c}{\Omega} \sin \left(\pi \Omega \frac{t}{T_c} \right) \right] \quad \text{and} \quad c_{c2}(t) = a \cos \left[\omega_0 t - \frac{BT_c}{\Omega} \sin \left(\pi \Omega \frac{t}{T_c} \right) \right],$$

the cross-correlation coefficient between these two cosine chirps can be simplified as:

$$\rho_c(\tau) = \cos(\omega_0 \tau) \sum_{n=-\infty}^{\infty} \left\{ J_n \left[\frac{2BT_c}{\Omega} \cos(\tau\theta) \right] \times \frac{\sin \left[n\theta(T_c - |\tau|) \right]}{n\theta T_c} \right\} \quad (4.49)$$

where $\theta = \frac{\pi\Omega}{2T_c}$, and $k_{c2}^u = \frac{2BT_c}{\Omega} \cos(\tau\theta)$

Proof. There are three terms in the cross-correlation coefficient between the two cosine chirps as defined as Eqn. (4.35). The first term is:

$$\left(1 - \frac{|\tau|}{T_c} \right) \sum_{n=-\infty}^{\infty} \left\{ (-1)^n J_{2n} \left(k_{c1}^u \right) \text{sinc} \left[(\omega_0 + 2n\theta)(T_c - |\tau|) \right] \right\} \quad (4.50)$$

Value of this term with different values of Ω is shown in Figure 4.16.

Value of the Term in Cross-correlation Coefficient of the Cosine Chirps vs. Different Ω

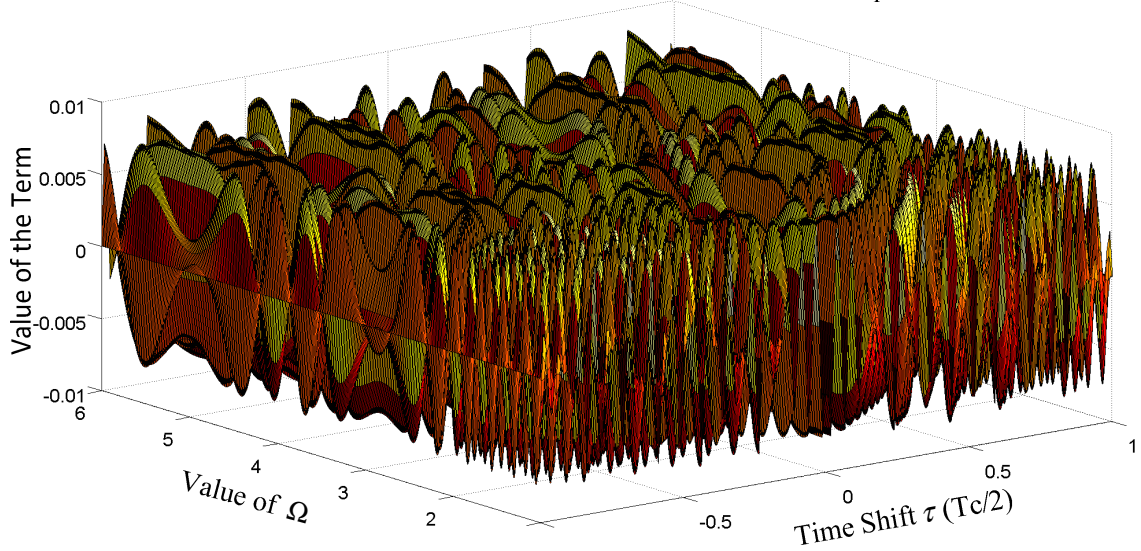


Figure 4.16: Value of the first term in Eqn. (4.35) vs. different values of Ω

As shown in Figure 4.16, absolute value of the first term in Eqn. (4.35) is always less than 0.01. Value of this term is so small that it can be ignored. Therefore, Eqn. (4.35) can be simplified as:

$$\begin{aligned} \rho_c(\tau) = & \cos(\omega_0\tau) \left(1 - \frac{|\tau|}{T_c}\right) J_0(k_{c2}^u) \\ & + 2 \cos(\omega_0\tau) \left(1 - \frac{|\tau|}{T_c}\right) \sum_{n=1}^{\infty} \left\{ J_{2n}(k_{c2}^u) \operatorname{sinc}[2n\theta(T_c - |\tau|)] \right\} \end{aligned} \quad (4.51)$$

where $\theta = \frac{\pi\Omega}{2T_c}$, and $k_{c2}^u = \frac{2BT_c}{\Omega} \cos(\tau\theta)$

Eqn. (4.51) can be written as:

$$\rho_c(\tau) = \cos(\omega_0\tau) \sum_{n=-\infty}^{\infty} \left\{ J_n \left[\frac{2BT_c}{\Omega} \cos(\tau\theta) \right] \times \frac{\sin[n\theta(T_c - |\tau|)]}{n\theta T_c} \right\} \quad (4.52)$$

– Q.E.D

C. Summary

Using these simplified representations as defined in Eqn. (4.48) and Eqn. (4.52) respectively, it is more convenient to mathematically analyze some properties of cross-correlation of sine chirps and cosine chirps, such as width of the orthogonal part, and magnitude of the maximum sidelobe.

4.5 Sine Chirps of Different Time Period

The parameter Ω (time period) in the representation of sine chirps or cosine chirps can be an arbitrary integer. For the pair of sine chirps or cosine chirps with different Ω , their autocorrelation and cross-correlation properties will be different. Since it is found that the property of a pair of sine chirps is very similar to that of a pair of cosine chirps, without loss of generality, only sine chirps are analyzed in detail. It is expected that the conclusion is also applicable to cosine chirps. Therefore, sine chirps are selected as an example for analysis in the rest of this thesis. The following subsection will explore the

properties for a pair of sine chirps with different Ω , except for $\Omega=2$ since it has been presented in subsection 4.4.2.C already.

4.5.1 Half Period

When Ω is equal to unity, the sine chirp is named as the half period sine (HPS) chirp. By using Eqn. (4.43), three different values of the frequency spread bandwidth B for a pair of orthogonal HPS chirps can be obtained:

$$\left\{ \begin{array}{l} B_{1-1} = \frac{\Omega}{2T_c} x_4 = \frac{1 \times 11.7915}{2 \times 10^{-6}} = 5.8957(\text{MHz}) \\ B_{1-2} = \frac{\Omega}{2T_c} x_6 = \frac{1 \times 18.0701}{2 \times 10^{-6}} = 9.0351(\text{MHz}) \\ B_{1-4} = \frac{\Omega}{2T_c} x_8 = \frac{1 \times 24.3519}{2 \times 10^{-6}} = 12.176(\text{MHz}) \end{array} \right. \quad (4.53)$$

Moreover, an additional $B_{1-3} = 10$ MHz, which is between the B_{1-2} and B_{1-4} , is also considered. As shown from Figure 4.17 to Figure 4.20, autocorrelation and cross-correlation of a pair of HPS chirps at these different bandwidths (5.8957 MHz, 9.0351 MHz, 10 MHz and 12.176 MHz) are drawn respectively, where the time period is set as 1 μs and the center frequency f_0 is 20 MHz. The blue curves with points represent autocorrelation coefficient of a pair of HPS chirps, while the red curves with circles are for cross-correlation coefficient between the two HPS chirps. As can be seen, value of cross-correlation coefficients are all zero when the bandwidth B is 5.8957 MHz, 9.0351 MHz, and 12.176 MHz at $\tau = 0$, while the value is almost 0.2 when the bandwidth B_{1-3} is 10 MHz. Hence, under these conditions, this pair of HPS chirps is proved to be orthogonal with each other.

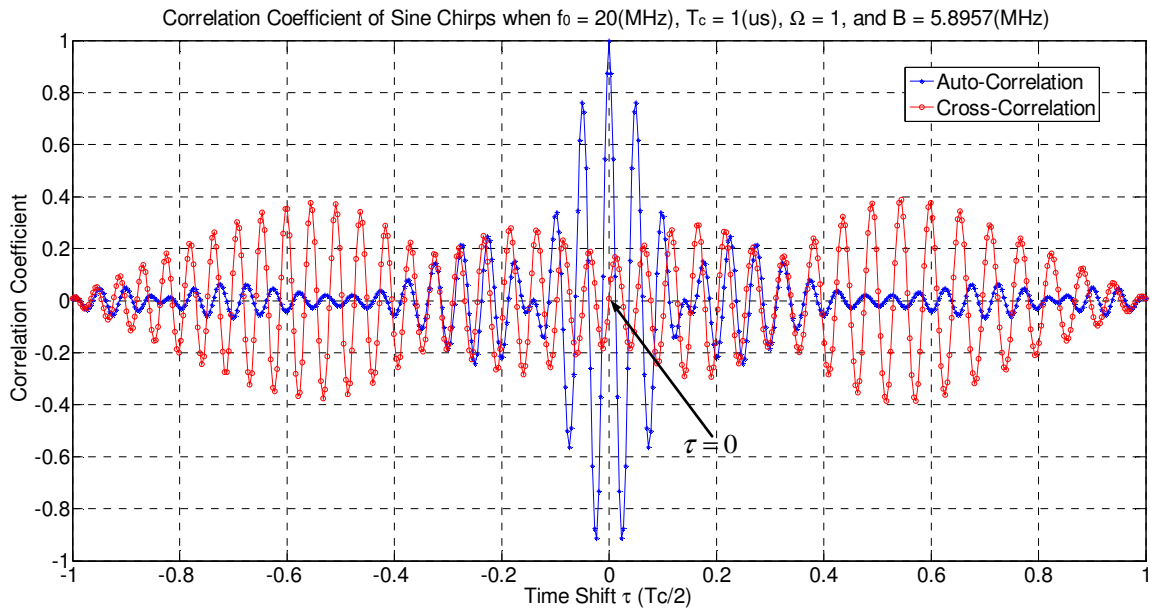


Figure 4.17: Autocorrelation & cross-correlation for HPS chirps when $B_{1-1} = 5.8957$ MHz

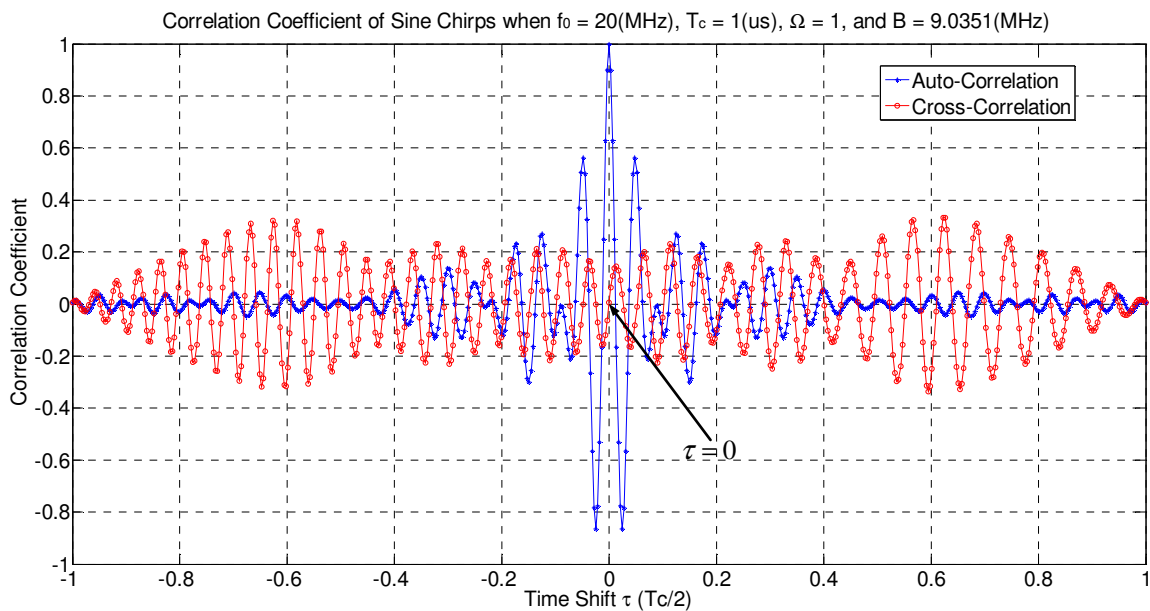


Figure 4.18: Autocorrelation & cross-correlation for HPS chirps when $B_{1-2} = 9.0351$ MHz

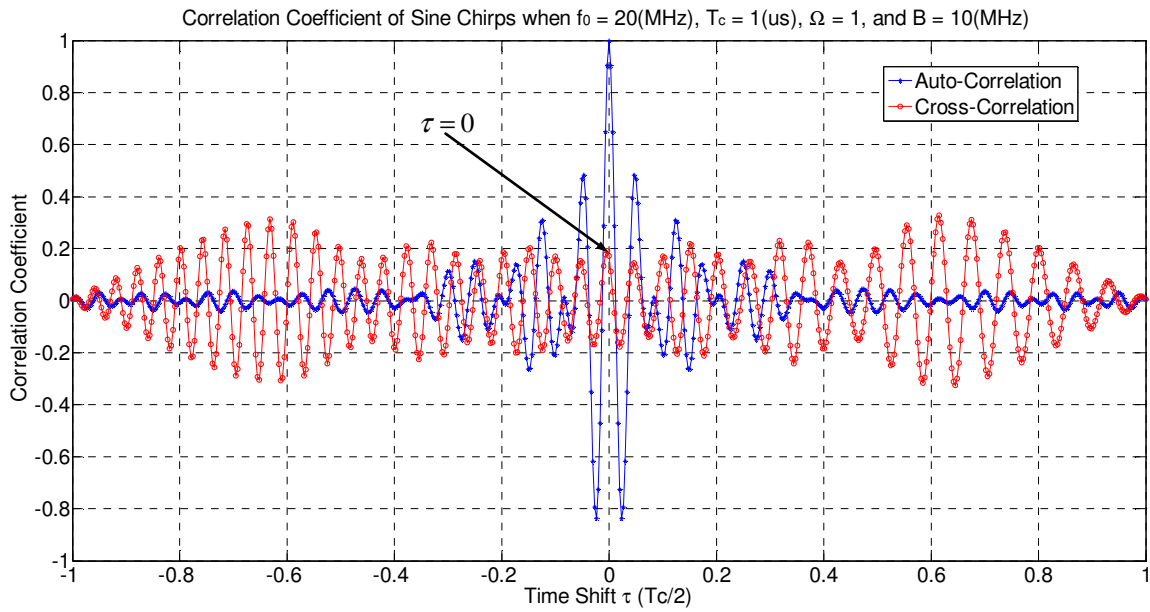


Figure 4.19: Autocorrelation & cross-correlation for HPS chirps when $B_{1-3} = 10 \text{ MHz}$

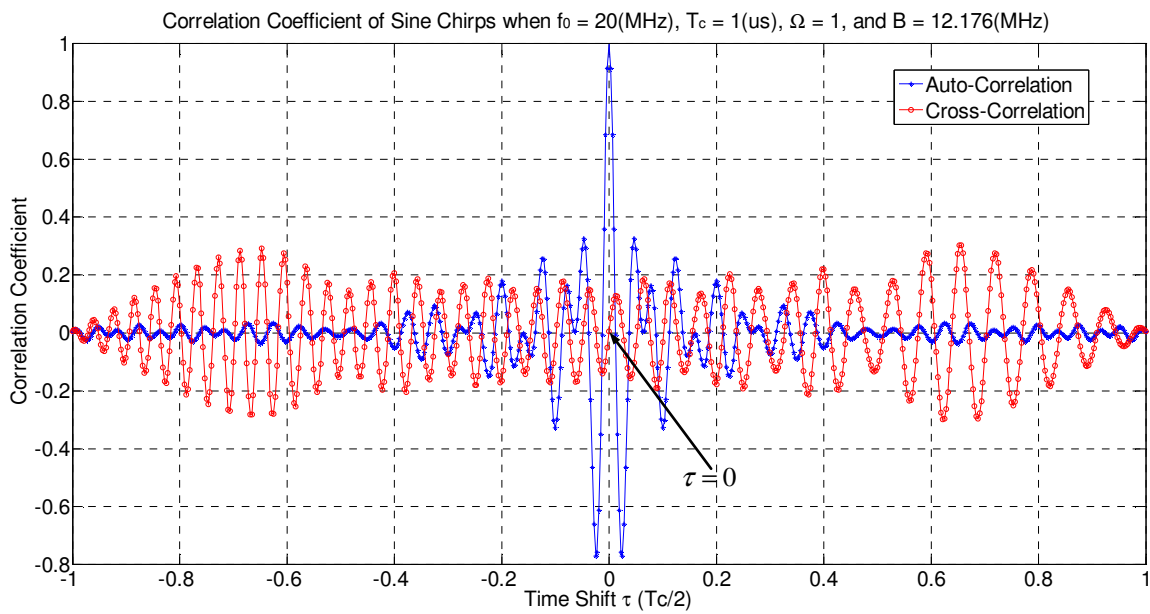


Figure 4.20: Autocorrelation & cross-correlation for HPS chirps when $B_{1-4} = 12.176$
MHz

4.5.2 Triple Period

When the value of Ω is equal to 3, the sine chirp is named as the triple period sine (TPS) chirp. Similarly, three different values of the frequency spread bandwidth B for a pair of orthogonal TPS chirps can be obtained using Eqn. (4.43):

$$\begin{cases} B_{3-1} = \frac{\Omega}{2T_c} x_2 = \frac{3 \times 5.5201}{2 \times 10^{-6}} = 8.2802(\text{MHz}) \\ B_{3-3} = \frac{\Omega}{2T_c} x_3 = \frac{3 \times 8.6531}{2 \times 10^{-6}} = 12.9796(\text{MHz}) \\ B_{3-4} = \frac{\Omega}{2T_c} x_4 = \frac{3 \times 11.7915}{2 \times 10^{-6}} = 17.6872(\text{MHz}) \end{cases} \quad (4.54)$$

Moreover, an additional $B_{3-2} = 10$ MHz, which is between the B_{3-1} and B_{3-2} , is also considered. Autocorrelation and cross-correlation of a pair of TPS chirps at these different bandwidths are drawn respectively from Figure 4.21 to Figure 4.24, where the time period is set as $1 \mu\text{s}$ and the center frequency f_0 is 20 MHz. The red curves with circles in Figure 4.21, Figure 4.23 and Figure 4.24 show that value of cross-correlation coefficients are all zero at $\tau = 0$. However, value of cross-correlation coefficients are not zero at $\tau = 0$ in Figure 4.22 which the frequency bandwidth $B_{3-2} = 10$ MHz. All of the four figures show that there exists a maximum peak valued more than 0.6 in both sides of the cross-correlation curves, which is a property of cross-correlation of the TPS chirps.

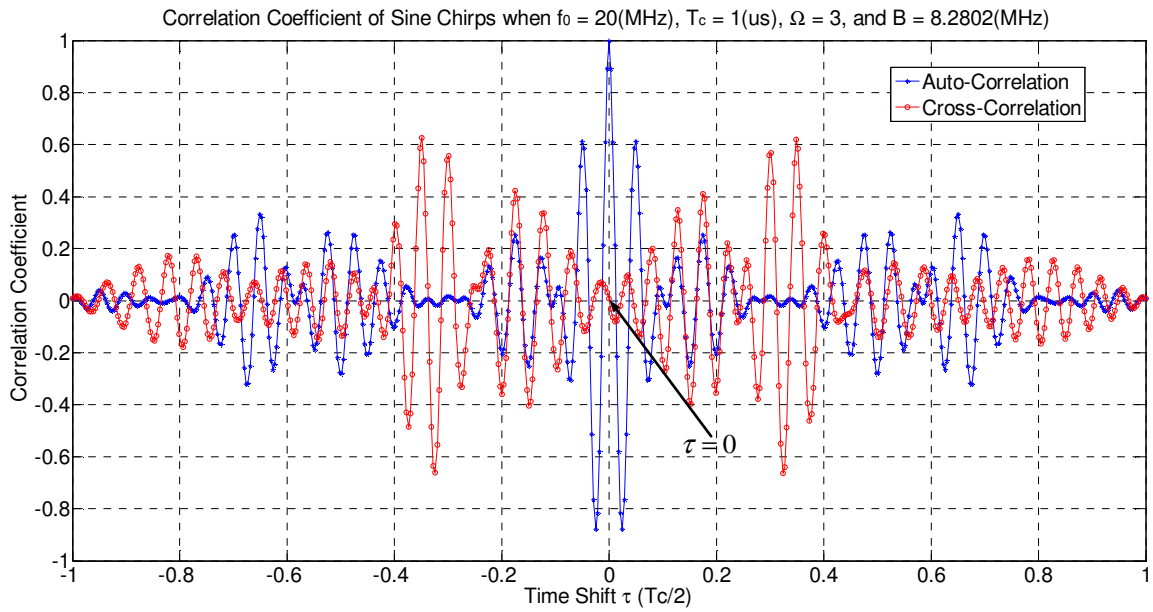


Figure 4.21: Autocorrelation & cross-correlation for TPS chirps when $B_{3-1} = 8.2802 \text{ MHz}$

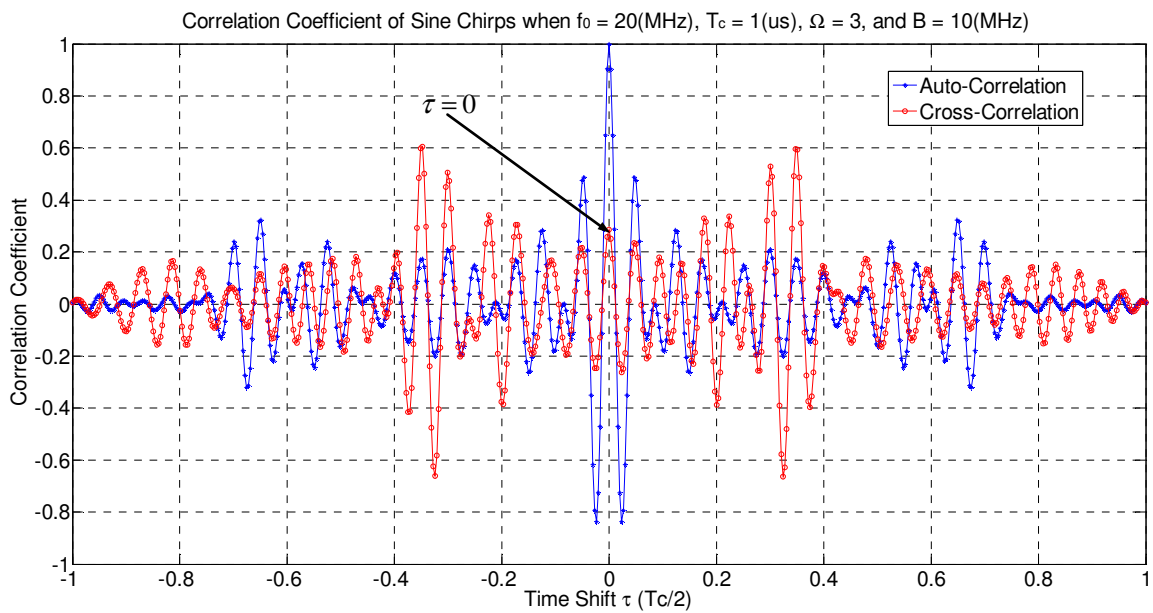


Figure 4.22: Autocorrelation & cross-correlation for TPS chirps when $B_{3-2} = 10 \text{ MHz}$

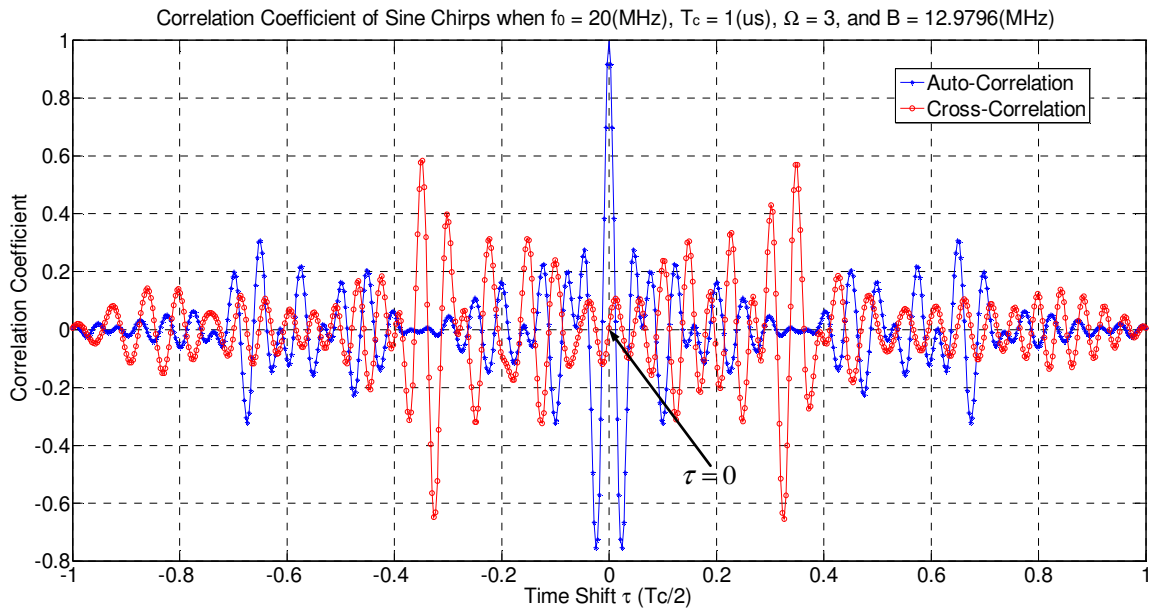


Figure 4.23: Autocorrelation & cross-correlation for TPS chirps when $B_{3-3} = 12.9796$ MHz

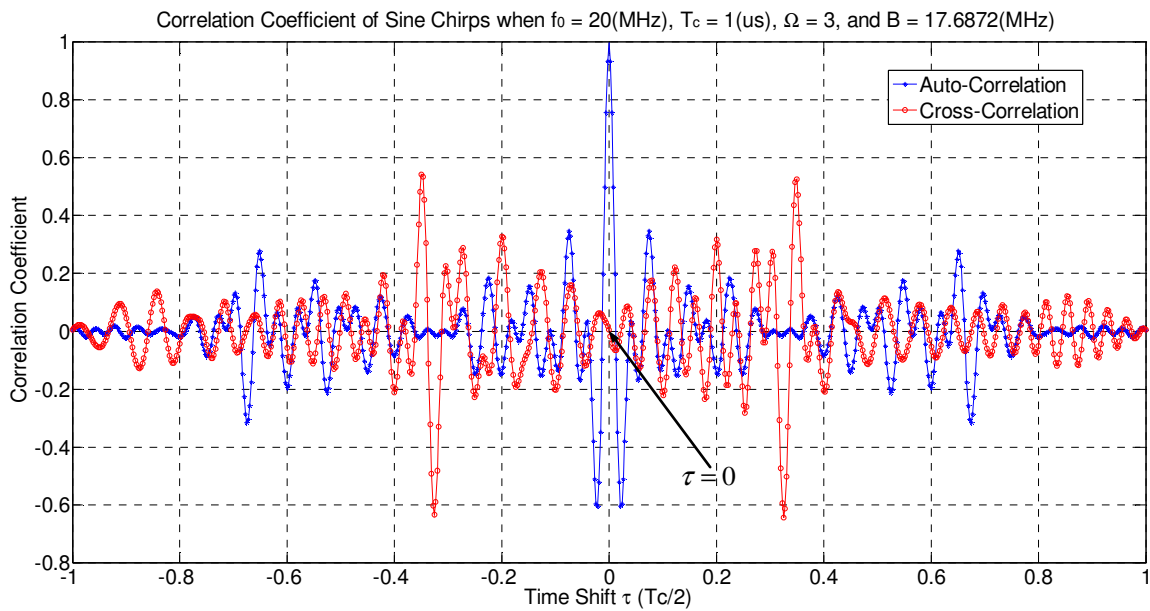


Figure 4.24: Autocorrelation & cross-correlation for TPS chirps when $B_{3-4} = 17.6872$ MHz

4.5.3 Quadruple Period

When the value of Ω is equal to 4, the sine chirp is named as the quadruple period sine (QPS) chirps. Similarly, three different values of the frequency spread bandwidth B for a pair of orthogonal QPS chirps can be obtained using Eqn. (4.43):

$$\begin{cases} B_{4-1} = \frac{\Omega}{2T_c} x_1 = \frac{4 \times 2.4048}{2 \times 10^{-6}} = 4.8096(\text{MHz}) \\ B_{4-3} = \frac{\Omega}{2T_c} x_2 = \frac{4 \times 5.5201}{2 \times 10^{-6}} = 11.0402(\text{MHz}) \\ B_{4-4} = \frac{\Omega}{2T_c} x_3 = \frac{4 \times 8.6531}{2 \times 10^{-6}} = 17.3062(\text{MHz}) \end{cases} \quad (4.55)$$

Moreover, an additional $B_{4-2} = 10$ MHz is also considered. Autocorrelation and cross-correlation of a pair of QPS chirps at these different bandwidths are drawn respectively from Figure 4.25 to Figure 4.28. Value of cross-correlation coefficients are not zero at $\tau = 0$ in Figure 4.26 which the frequency bandwidth $B_{4-2} = 10$ MHz. As shown by the zoomed inserts in Figure 4.25, Figure 4.27, and Figure 4.28, values of cross-correlation coefficients of QPS chirp are all zero not only at $\tau = 0$ but also at a short period around the centre. Thus is similar with FPS chirps. However, all of the four figures show that there exists a maximum peak valued around 0.7 in both sides of the cross-correlation curves, which is a property of cross-correlation of QPS chirps. Moreover, it worth notice that there also exists a maximum peak valued around 0.5 in both sides of the autocorrelation coefficient (blue curve with points), which is a property of autocorrelation of QPS chirps.

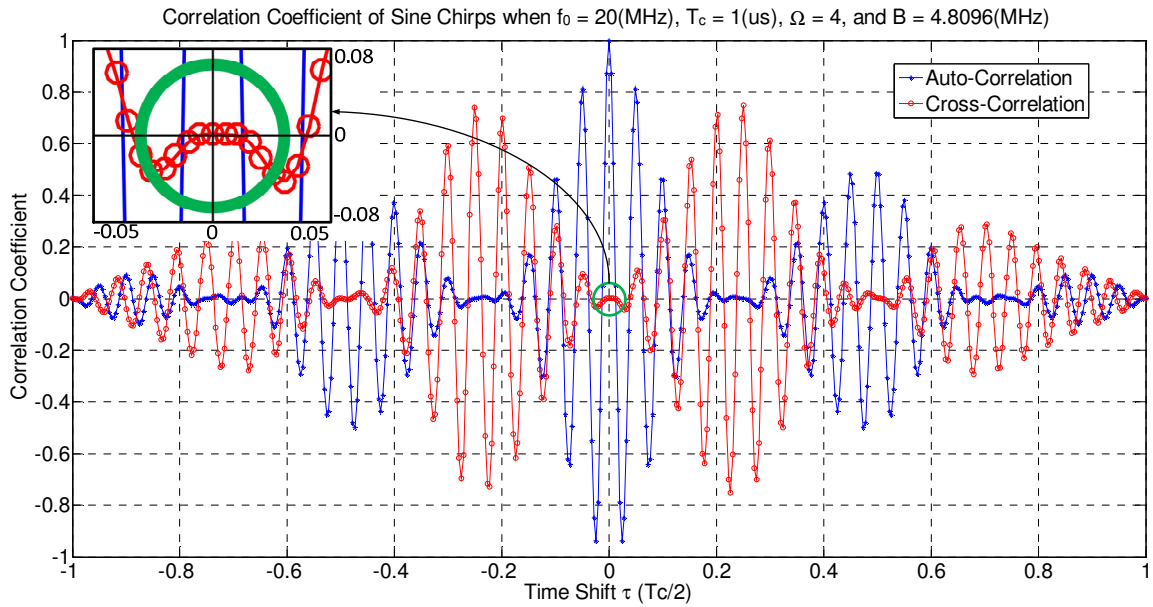


Figure 4.25: Autocorrelation & cross-correlation for QPS chirps when $B_{4-1} = 4.8096$ MHz

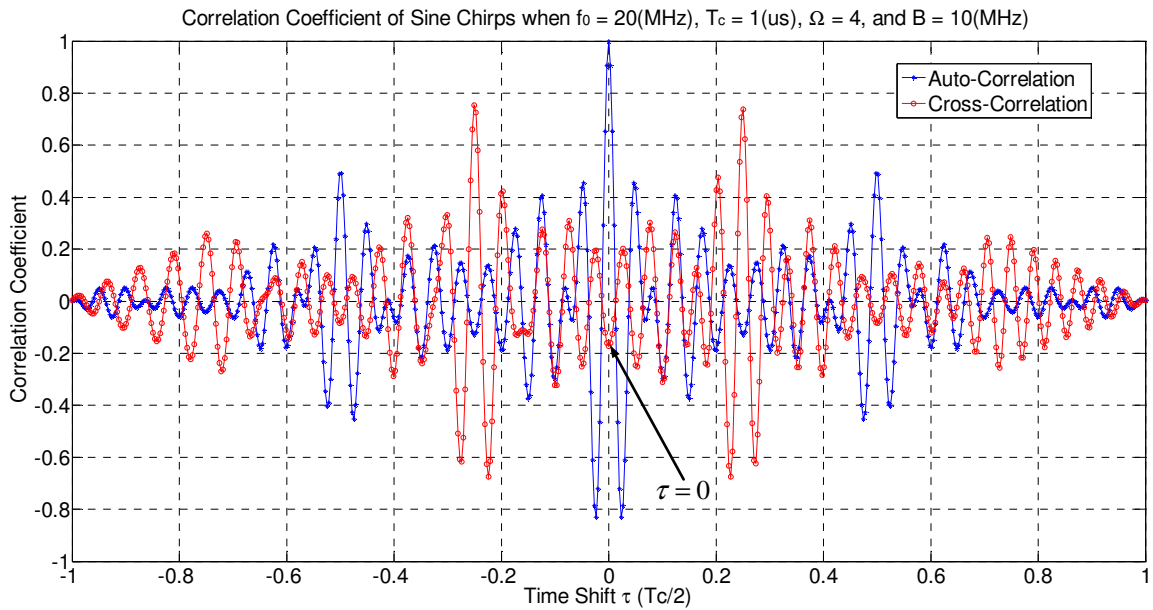


Figure 4.26: Autocorrelation & cross-correlation for QPS chirps when $B_{4-2} = 10$ MHz

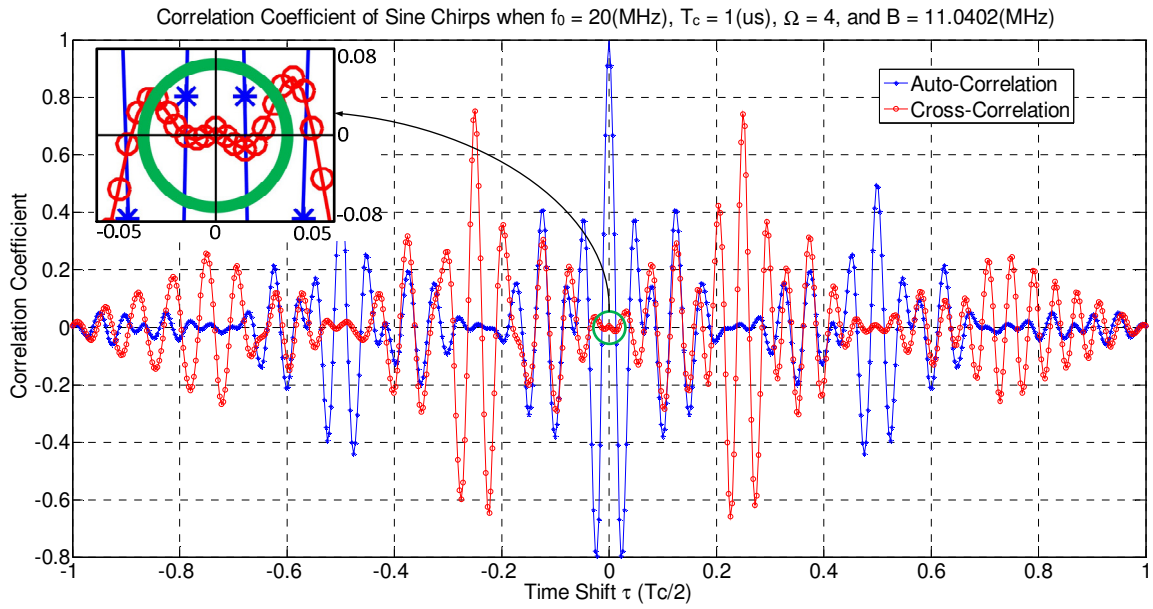


Figure 4.27: Autocorrelation & cross-correlation for QPS chirps when $B_{4-3} = 11.0402$ MHz

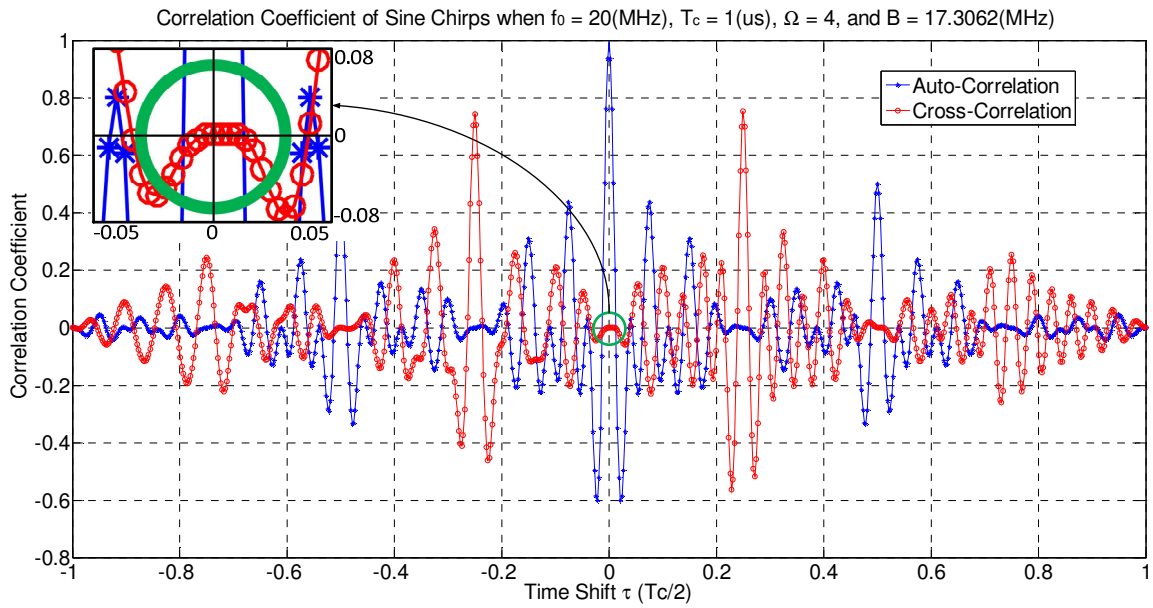


Figure 4.28: Autocorrelation & cross-correlation for QPS chirps when $B_{4-4} = 17.3062$ MHz

4.5.4 Summary

The cross-correlation coefficients of the sine chirp with different Ω at the orthogonal points presented in the above section are compared in Figure 4.29. As shown in Figure 4.29 (b) and (d), the cross-correlation coefficients for FPS chirps or QPS chirps (where $\Omega=2$ or $\Omega=4$) are all zero not only at $\tau=0$ but also at a short period around the centre highlighted by the rectangle, as long as the bandwidth meets the condition defined in Eqn. (4.43). As shown in Figure 4.29 (a) and (c), although cross-correlation coefficients for HPS chirps or TPS chirps (where $\Omega=1$ or $\Omega=3$) is zero only at $\tau=0$ highlighted by the green circle when the bandwidth meets the condition defined in Eqn. (4.43), but has no a short period around the centre. In a real BOK CSS system, it is difficult for the transmitter and receiver to be perfectly synchronized, which means it is difficult for the time shift (τ) exactly to be zero. If there is a little time synchronization error, the FPS or QPS chirps can still be orthogonal, while HPS chirps or TPS chirps can not. Therefore, FPS chirps or QPS chirps are the better choices for the BOK CSS system than HPS chirps or TPS chirps, because they are more robust with respect to time synchronization errors.

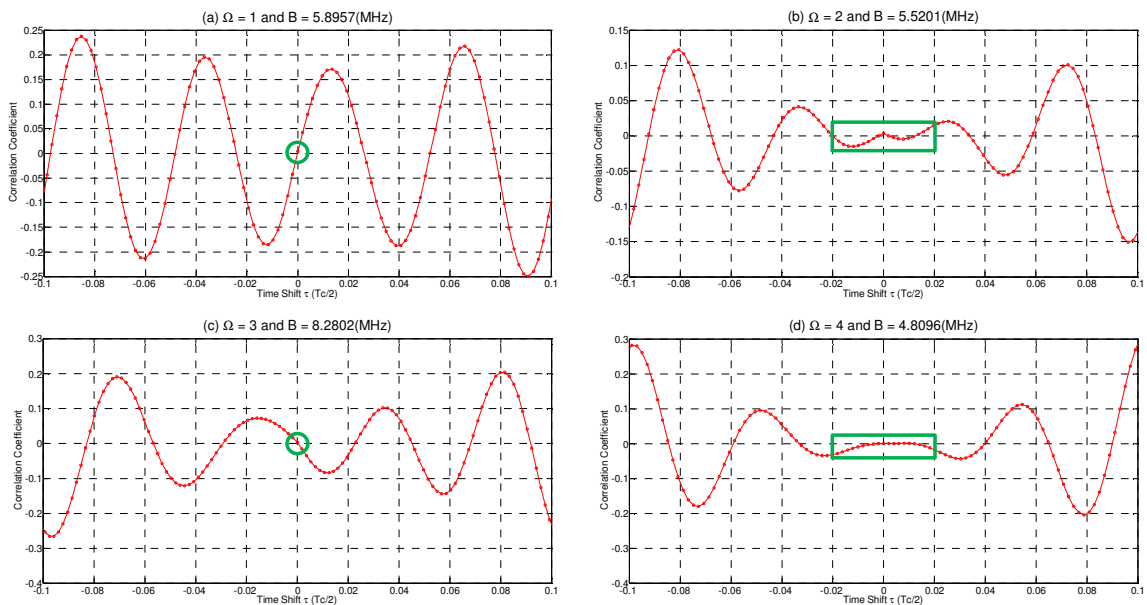


Figure 4.29: Central parts of the cross-correlation for sine chirps with different Ω

By comparing Figure 4.11 and Figure 4.25, it can be observed that the cross-correlation curve of FPS chirp has a maximum peak valued 0.5 at around $\pm 0.5(T_c/2)$, while QPS chirp has a maximum peak valued 0.7 at around $\pm 0.25(T_c/2)$. Moreover, the autocorrelation curve of QPS chirp has a maximum peak valued 0.5 at $\pm 0.5(T_c/2)$, while FPS chirp does not have. Thus, FPS chirp is better choice than QPS chirp for the BOK CSS system. Therefore, by comparing the above four kinds of sine chirps in terms of the cross-correlation and autocorrelation properties, FPS chirps are the best choice.

4.6 Comparison with the Linear Counterpart

Since sine chirps with different period exhibit similar properties, full period sine (FPS) chirps are selected for comparison with linear chirp under different parameters. The comparisons are in terms of spectral characteristics, autocorrelation and cross-correlation.

4.6.1 Spectral Characteristic

Two comparisons of spectrum between linear chirp and FPS chirp are shown respectively in Figure 4.30 and Figure 4.31 for two scenarios: $B = 30$ MHz and $B = 50$ MHz. The carrier frequency (f_0) has to be set no less than $B/2$ MHz because $f_0 - B/2$ should be positive. Therefore, f_0 is set as 50 MHz as an example in these two scenarios ($B = 30$ MHz and $B = 50$ MHz).

From Figure 4.30 and Figure 4.31, significant parts of amplitude spectrum for both linear chirp and FPS chirp are all within the effective range $(f_0 - B/2, f_0 + B/2)$. Spectrum of linear chirp outside of this range is slightly higher than that of FPS chirp. This means that FPS chirp has more energy within this effective range than their linear chirp counterpart.

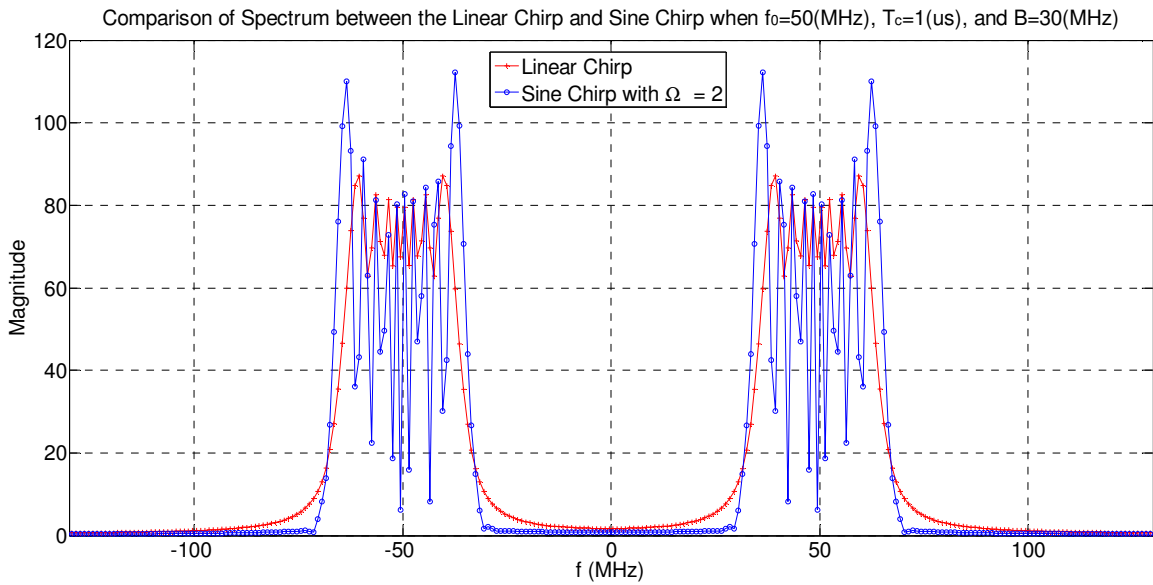


Figure 4.30: Comparison of the spectra for linear chirp and FPS chirp when $T_c B = 30 \text{ sHz}$

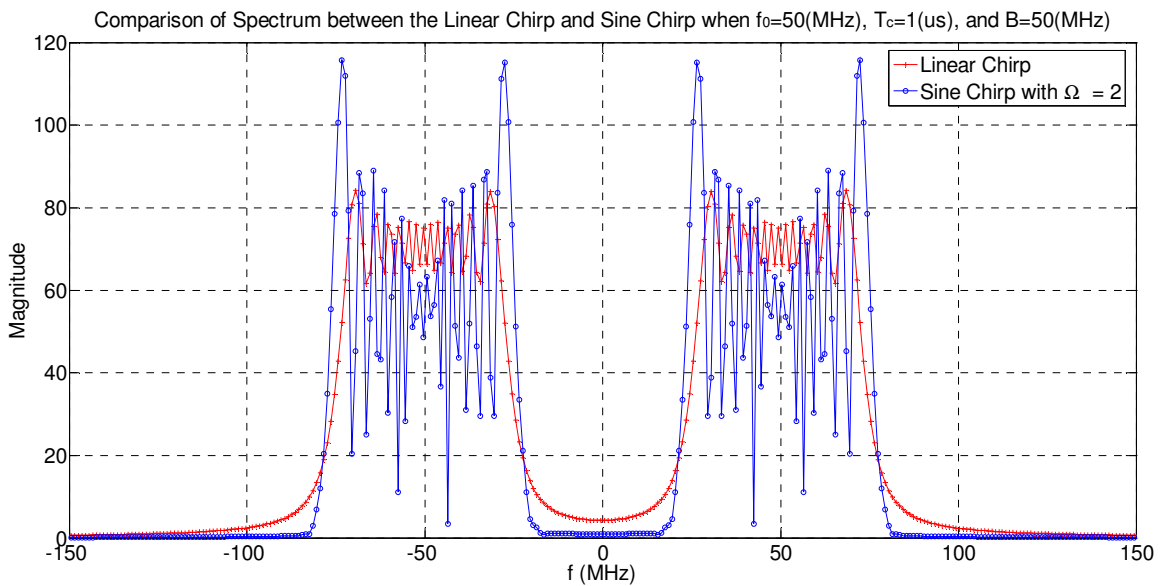


Figure 4.31: Comparison of the spectra for linear chirp and FPS chirp when $T_c B = 50 \text{ sHz}$

4.6.2 Autocorrelation Property

Autocorrelation function of a FPS chirp is compared against that of a linear chirp under the same conditions. The results are shown in Figure 4.32. As can be seen, there is a short pulse at the center for sine chirp. The width of the main-lobe is the same as that of the linear counterpart, which is $2/B$. Therefore, sine chirp can achieve similar autocorrelation properties as that of linear chirp. Although most of the sidelobes of autocorrelation for sine chirps are bigger than that of linear chirps, except for the first. Generally speaking, the higher sidelobe of the autocorrelation curve, the greater time interval between chirps is required for the same intersymbol interference [43]. Window functions and weighting techniques can be designed to reduce sidelobes [44-46].

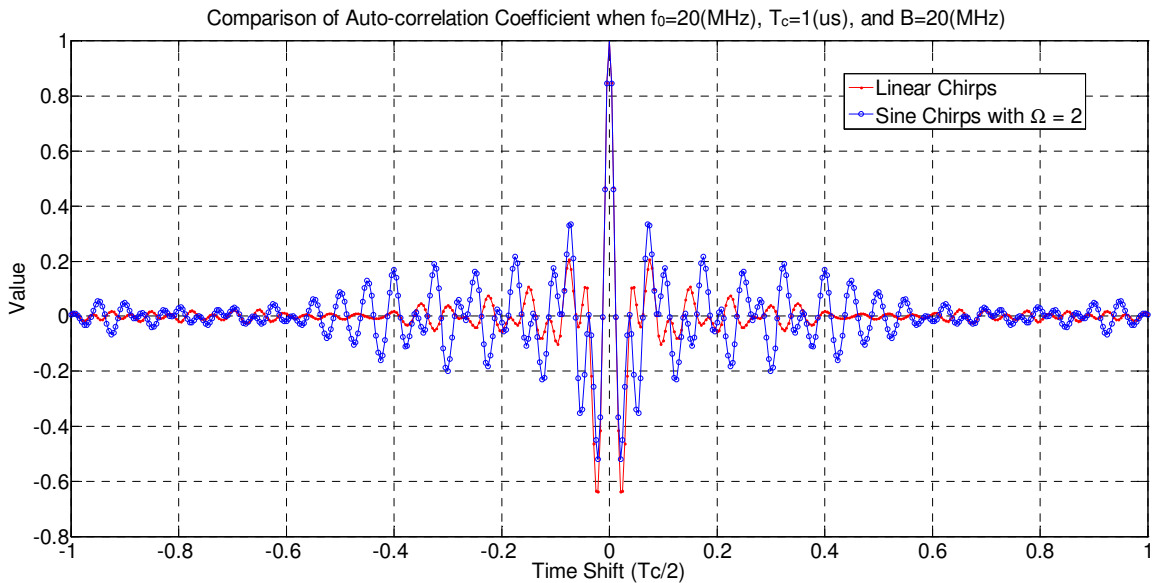


Figure 4.32: Autocorrelation coefficient of linear chirps vs. FPS chirps

4.6.3 Cross-correlation Property

The cross-correlation coefficient for linear and FPS chirps under the same condition are also comparatively shown in Figure 4.33, where $T_c B = 8.6531$ sHz. As shown, value of cross-correlation coefficient for FPS chirps is zero around the center of $\tau = 0$, while that of the linear counterpart is approximately 0.25. This result shows that FPS chirps can achieve orthogonality at $T_c B = 8.6531$ sHz since the condition of Eqn. (4.43) is met, while the linear chirp cannot be orthogonal.

The only disadvantage of FPS chirp shown in Figure 4.33 is that there is a maximum point with the value of 0.5 in both sides of its cross-correlation curve. However, in the case of BOK CSS system, a time synchronization technique can be used to eliminate their potential effects on BER caused by these maximum points. Several time synchronization techniques have been proposed in [47-49] for the BOK CSS system.

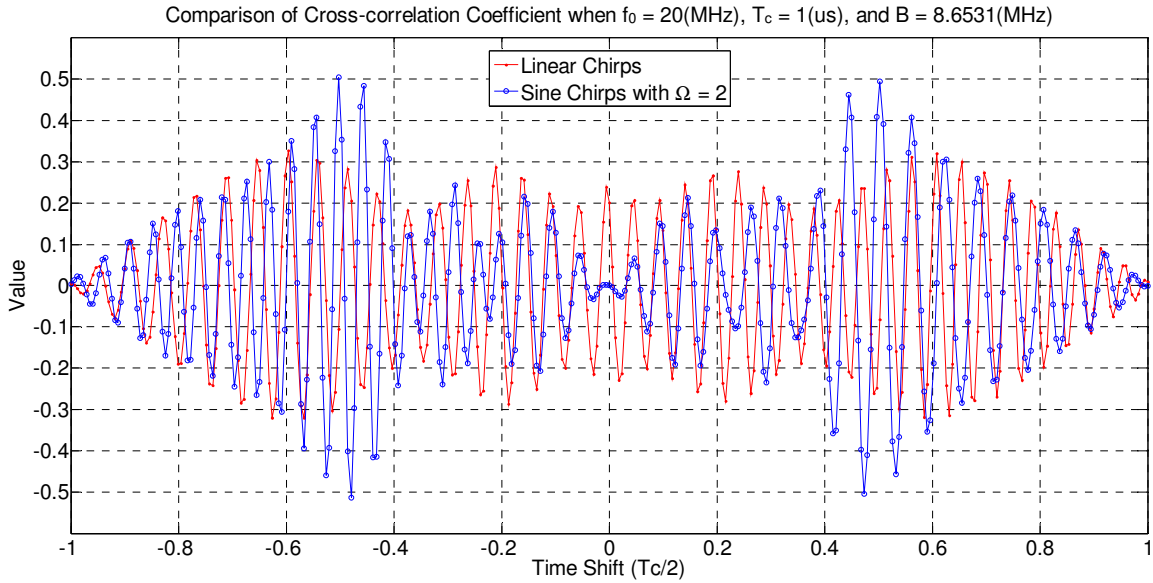


Figure 4.33: Cross-correlation coefficient of linear chirps vs. FPS chirps

4.6.4 Summary

The above analysis and comparison show that even though orthogonal characteristics of both linear and FPS chirps depend on the time-bandwidth product ($T_c B$), orthogonal characteristic of FPS chirps is not limited by the value of $T_c B$. Unlike linear chirps which have to occupy very wide frequency bandwidth (e.g. 64 MHz when $T_c = 1 \mu\text{s}$) to achieve satisfied orthogonality, FPS chirps only need very small bandwidth (e.g. 2.4048 MHz when $T_c = 1 \mu\text{s}$) as long as the condition defined in Eqn. (4.43) is met. This is less than 4% of the normally adopted bandwidth of linear chirps which indicates that FPS chirps have the potential to significantly reduce the bandwidth requirement for a BOK CSS system.

Moreover, for a BOK CSS system, shorter time period of the chirp signal (T_c) can achieve higher data rate in the system which is preferred in many wireless

communication systems. However, under a certain value of $T_c B$, shorter T_c will result in wider frequency bandwidth (B) occupancy. Thus, for the BOK linear CSS system, it is usually not a preferred approach to increase the system data rate through shortening T_c , because the frequency bandwidth occupied by a BOK linear CSS system is already very wide. On the other hand, the BOK FPS CSS system does not have this limitation since its frequency bandwidth can be very small.

Therefore, a pair of FPS chirps can be a good candidate to potentially replace the linear chirps in the BOK CSS system.

5. Performance of the BOK FPS CSS System

Although a pair of full period sine (FPS) chirps has potential to replace linear chirps in the BOK CSS system, performance of the BOK FPS CSS system deserves in-depth analysis in order to ensure that it can indeed outperform its linear counterpart. The conventional approach to study the performance is either based on analytical models or by using simulation. In this chapter, both analytical models and simulation tools are used to investigate the performance.

5.1 The BOK FPS CSS System

According to Eqn. (4.1), a general description for FPS chirps ($\Omega=2$) can be given as:

$$\begin{cases} c_{s2-1}(t) = a \cos \left[\omega_0 t + \frac{BT_c}{2} \cos \left(2\pi \frac{t}{T_c} \right) \right] & -\frac{T_c}{2} \leq t \leq \frac{T_c}{2} \\ c_{s2-2}(t) = a \cos \left[\omega_0 t - \frac{BT_c}{2} \cos \left(2\pi \frac{t}{T_c} \right) \right] & -\frac{T_c}{2} \leq t \leq \frac{T_c}{2} \end{cases} \quad (5.1)$$

where a is the maximal amplitude of the chirp signal, which usually uses the rectangle pulse. For simplification, a is chosen to be unity.

According to theory of the matched filter introduced in Section 2.2, by substituting Eqn. (5.1) into Eqn. (2.2), the impulse response of a matched filter for FPS chirps can be obtained as Eqn. (5.2).

$$\begin{cases} h_{s2-1}(t) = b \cos \left[\omega_0 t - \frac{BT_c}{2} \cos \left(2\pi \frac{t}{T_c} \right) \right] & -\frac{T_c}{2} \leq t \leq \frac{T_c}{2} \\ h_{s2-2}(t) = b \cos \left[\omega_0 t + \frac{BT_c}{2} \cos \left(2\pi \frac{t}{T_c} \right) \right] & -\frac{T_c}{2} \leq t \leq \frac{T_c}{2} \end{cases} \quad (5.2)$$

where b is a scaling factor of the filter. For simplification, b is also set to 1.

The autocorrelation coefficient of a FPS chirp can be obtained from Eqn. (4.22) by setting the parameter Ω as 2:

$$\begin{aligned} r_{s_2}(\tau) &\approx \left(1 - \frac{|\tau|}{T_c}\right) \cos(\omega_0 \tau) J_0 \left[\frac{2BT_c}{2} \sin \left(\frac{\pi \times 2}{2T_c} \tau \right) \right] \\ &= \left(1 - \frac{|\tau|}{T_c}\right) \cos(\omega_0 \tau) J_0 \left[BT_c \sin \left(\frac{\pi \tau}{T_c} \right) \right] \end{aligned} \quad (5.3)$$

By substituting $\tau = 0$ into Eqn. (5.3), it can be obtained as:

$$r_{s_2}(0) = J_0(0) = 1 \quad (5.4)$$

Similarly, the cross-correlation coefficient of FPS chirps can be achieved from Eqn. (4.29) by setting the parameter Ω as 2:

$$\begin{aligned} \rho_{s_2}(\tau) &= \left(1 - \frac{\tau}{T_c}\right) \cos(\omega_0 \tau) J_0(k_{c_2}) \\ &+ 2 \left(1 - \frac{\tau}{T_c}\right) \cos(\omega_0 \tau) \sum_{n=1}^{\infty} \left[(-1)^n J_{2n}(k_{c_2}) \right] \text{sinc} [2n\theta(T_c - \tau)] \\ &+ 2 \left(1 - \frac{\tau}{T_c}\right) \sin(\omega_0 \tau) \sum_{n=1}^{\infty} \left[(-1)^n J_{2n-1}(k_{c_2}) \right] \text{sinc} [(2n-1)\theta(T_c - \tau)] \end{aligned} \quad (5.5)$$

where $\theta = \frac{\pi}{T_c}$; $k_{c_2} = BT_c \cos \left(\frac{\pi \tau}{T_c} \right)$

By substituting $\tau = 0$ into Eqn. (5.5), it can be obtained as:

$$\rho_{s_2}(0) = J_0(BT_c) \quad (5.6)$$

The above equations in this subsection will be used by the following subsections.

5.2 Performance of the BOK FPS CSS System in an AWGN Channel

This section will examine the performance of the BOK CSS system based on a pair of FPS chirps in the AWGN channel environment. The performance will be measured in terms of BER.

4.2.1 Analysis of the BOK FPS CSS System

An illustrated diagram of a BOK FPS CSS system in the AWGN channel is depicted in Figure 5.1.

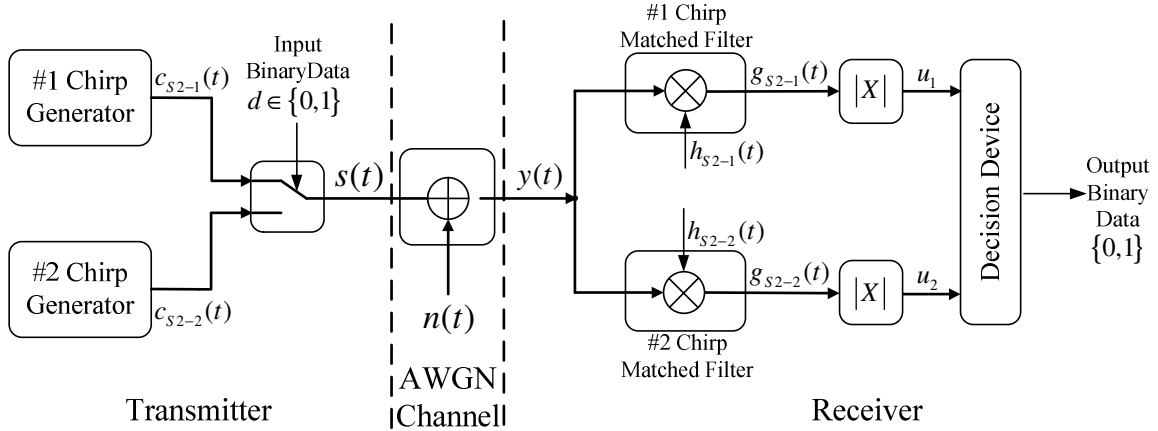


Figure 5.1: A BOK FPS CSS system in the AWGN channel

The binary data to be transmitted is denoted as $d \in \{0,1\}$. Suppose $c_{s2-1}(t)$ is to be sent out when $d = 1$, while $c_{s2-2}(t)$ is to be sent out when $d = 0$. Thus, the transmitted signal can be represented as:

$$s(t) = dc_{s2-1}(t) + (1-d)c_{s2-2}(t) \quad (5.7)$$

For an AWGN channel, a Gaussian noise sequence of zero mean and variance $\sigma_n^2 \in N_0/2$ is denoted as $n(t)$. When the transmitted signal $s(t)$ passes through the

AWGN channel, a white Gaussian noise $n(t)$ is added to the transmitted signal $s(t)$. Hence, the received signal $y(t)$ can be represented as:

$$y(t) = s(t) + n(t) \quad (5.8)$$

Substituting Eqn. (5.7) into Eqn. (5.8), the received signal becomes:

$$y(t) = dc_{s_{2-1}}(t) + (1-d)c_{s_{2-2}}(t) + n(t) \quad (5.9)$$

The signal $y(t)$ is received at the receiver end, and then is simultaneously processed by the two matched filters (#1 chirp and #2 chirp matched filters). The output of the matched filter #1 can be obtained as:

$$\begin{aligned} g_{s_{2-1}}(\tau) &= \int_{-\infty}^{+\infty} y(t)h_{s_{2-1}}(\tau-t)dt \\ &= \int_{-\infty}^{+\infty} [dc_{s_{2-1}}(t) + (1-d)c_{s_{2-2}}(t) + n(t)]h_{s_{2-1}}(\tau-t)dt \\ &= dR_{s_2}(\tau) + (1-d)C_{s_2}(\tau) + \int_{-\infty}^{+\infty} n(t)h_{s_{2-1}}(\tau-t)dt \\ &= dE_b r_{s_2}(\tau) + (1-d)E_b \rho_{s_2}(\tau) + \int_{-\infty}^{+\infty} n(t)h_{s_{2-1}}(\tau-t)dt \end{aligned} \quad (5.10)$$

where E_b is energy of the sine chirps. Similarly, the output of the matched filter #2 can be obtained as:

$$\begin{aligned} g_{s_{2-2}}(\tau) &= \int_{-\infty}^{+\infty} y(t)h_{s_{2-2}}(\tau-t)dt \\ &= \int_{-\infty}^{+\infty} [dc_{s_{2-1}}(t) + (1-d)c_{s_{2-2}}(t) + n(t)]h_{s_{2-2}}(\tau-t)dt \\ &= dE_b \rho_{s_2}(\tau) + (1-d)E_b r_{s_2}(\tau) + \int_{-\infty}^{+\infty} n(t)h_{s_{2-2}}(\tau-t)dt \end{aligned} \quad (5.11)$$

At the output of the receiver, two variables (u_1 and u_2), which are the inputs to the decision device, are produced at the outputs of the matched filters as defined by Eqn. (5.10) and Eqn. (5.11) :

$$\begin{cases} u_1 = |g_{s_{2-1}}(\tau)| = dE_b |r_{s_2}(\tau)| + (1-d)E_b |\rho_{s_2}(\tau)| + \left| \int_{-\infty}^{+\infty} n(t)h_{s_{2-1}}(\tau-t)dt \right| \\ u_2 = |g_{s_{2-2}}(\tau)| = dE_b |\rho_{s_2}(\tau)| + (1-d)E_b |r_{s_2}(\tau)| + \left| \int_{-\infty}^{+\infty} n(t)h_{s_{2-2}}(\tau-t)dt \right| \end{cases} \quad (5.12)$$

Hence, the difference between these two variables can be calculated as:

$$\begin{aligned} \Delta u &= u_1 - u_2 \\ &= (2d-1)E_b \left[|r_{s_2}(\tau)| - |\rho_{s_2}(\tau)| \right] + \int_{-\infty}^{+\infty} n(t) \left[h_{s_{2-1}}(\tau-t) - h_{s_{2-2}}(\tau-t) \right] dt \end{aligned} \quad (5.13)$$

When $d=1$, the correct result at the decision device should be $\Delta u > 0$. Similarly, when $d=0$, the correct result at the decision device should be $\Delta u < 0$. Therefore, a bit error happens in two cases: $d=1$ but $\Delta u < 0$, and $d=0$ but $\Delta u > 0$. Hence, the total probability of bit error at the decision device can be calculated as:

$$\begin{aligned} P_e^S &= P\{\Delta u < 0 | d=1\} \times P\{d=1\} + P\{\Delta u > 0 | d=0\} \times P\{d=0\} \\ &= \frac{1}{2} \left[P\{\Delta u < 0 | d=1\} + P\{\Delta u > 0 | d=0\} \right] \end{aligned} \quad (5.14)$$

Since the two cases are supposed to have the equal probability, Eqn. (5.14) can be simplified as:

$$P_e^S = P\{\Delta u < 0 | d=1\} \quad \text{or} \quad P\{\Delta u > 0 | d=0\} \quad (5.15)$$

Taking the second case as an example, the total probability of bit error can be obtained as:

$$\begin{aligned} P_e^S &= P\{\Delta u > 0 | d=0\} \\ &= P\left\{ -E_b \left[|r_{s_2}(\tau)| - |\rho_{s_2}(\tau)| \right] + \int_{-\infty}^{+\infty} n(t) \left[h_{s_{2-1}}(\tau-t) - h_{s_{2-2}}(\tau-t) \right] dt > 0 \right\} \end{aligned} \quad (5.16)$$

Let $P_{en}^S = \int_{-\infty}^{+\infty} n(t) \left[h_{s_{2-1}}(\tau-t) - h_{s_{2-2}}(\tau-t) \right] dt$, then its variance can be obtained as:

$$\begin{aligned}
\sigma_{en}^2 &= E\left[\left(P_{en}^S\right)^2\right] = E\left\{\left[\int_{-\infty}^{+\infty} n(t)\left[h_{S_{2-1}}(\tau-t)-h_{S_{2-2}}(\tau-t)\right]dt\right]^2\right\} \\
&= \int_{-\infty}^{+\infty} n^2(t)h_{S_{2-1}}^2(\tau-t)dt - 2\int_{-\infty}^{+\infty} n^2(t)h_{S_{2-1}}(\tau-t)h_{S_{2-2}}(\tau-t)dt + \int_{-\infty}^{+\infty} n^2(t)h_{S_{2-2}}^2(\tau-t)dt \quad (5.17) \\
&= E_b\sigma^2|r_{S_2}(\tau)| - 2E_b\sigma^2|\rho_{S_2}(\tau)| + E_b\sigma^2|r_{S_2}(\tau)| \\
&= E_bN_0\left(|r_{S_2}(\tau)| - |\rho_{S_2}(\tau)|\right)
\end{aligned}$$

Since $n(t)$ is a white Gaussian noise with zero mean and variance $N_0/2$, Δu is a random variable with mean $E(\Delta u) = -E_b\left[|r_{S_2}(\tau)| - |\rho_{S_2}(\tau)|\right]$ and variance $\sigma_u^2 = E\left[\left(P_e^S\right)^2\right] = E\left[\left(P_{en}^S\right)^2\right] = \left(|r_{S_2}(\tau)| - |\rho_{S_2}(\tau)|\right)E_bN_0$. Therefore, Eqn. (5.16) can be written as:

$$P_e^S = \int_0^{+\infty} \frac{1}{\sigma_u\sqrt{2\pi}} \exp\left[-\frac{(x-\Delta u)^2}{2(\sigma_u)^2}\right] dx \quad (5.18)$$

Let $\frac{x-\Delta u}{\sigma_u} = z$, Eqn. (5.16) can be represented as:

$$\begin{aligned}
P_e^S &= \int_{-\frac{\Delta u}{\sigma_u}}^{+\infty} \frac{1}{\sqrt{2\pi}} \exp\left[-\frac{z^2}{2}\right] dz \\
&= Q\left(-\frac{\Delta u}{\sigma_u}\right) \\
&= Q\left(-\frac{-E_b\left[|r_{S_2}(\tau)| - |\rho_{S_2}(\tau)|\right]}{\sqrt{\left(|r_{S_2}(\tau)| - |\rho_{S_2}(\tau)|\right)E_bN_0}}\right) \\
&= Q\left(\sqrt{\frac{E_b\left(|r_{S_2}(\tau)| - |\rho_{S_2}(\tau)|\right)}{N_0}}\right)
\end{aligned} \quad (5.19)$$

where $Q(x)$ is Q function, and is defined as in [50]:

$$Q(x) = \frac{1}{2\pi} \int_x^{\infty} e^{-t^2/2} dt \quad (5.20)$$

If time synchronization of the BOK CSS system is perfect, the time shift τ equals to zero, thus P_e^S can be achieved by substituting Eqn. (5.4) and Eqn. (5.6) into Eqn. (5.19):

$$P_e^S = Q\left(\sqrt{\frac{E_b}{N_0}[1-|J_0(T_c B)|]}\right) \quad (5.21)$$

It can be seen from (5.21) that BER performance of the BOK FPS CSS system in the AWGN channel depends on $|J_0(T_c B)|$. The BER performance vs. $T_c B$ can be shown in Figure 5.2. It can be observed that the BER performance depends on $T_c B$ and values of E_b/N_0 . As value of E_b/N_0 increases, value of BER is monotonously decreasing. As $T_c B$ increases, value of BER can fluctuate.

BER performance for different $T_c B$ at some values of E_b/N_0 (such as 0 dB, 5 dB, etc) is shown as examples in Figure 5.3. As $T_c B$ increases, the curves for the all cases fluctuate. This fluctuation is more obvious for the bigger value of E_b/N_0 . The lowest points of each curve in Figure 5.3 respectively correspond to the zero crossing points of the red curve with circles ($\Omega=2$) in Figure 3.5. Therefore, this fluctuation phenomenon is caused by the cross-correlation characteristic of sine chirps as stated in subsection 4.4.2.

Comparison of the theoretical and the simulated BER curves for the BOK FPS CSS system in the AWGN channel is shown in Figure 5.4. The theoretical result is represented by Eqn. (5.21). The simulation is carried out by implementing the system depicted by Figure 5.1. This comparison is carried out at $T_c B=5.52$ sHz, which is an orthogonal point of the pair of FPS chirps. Total data transmitted for each test case is 10^8 . It can be observed that the two curves are overlapping with each other.

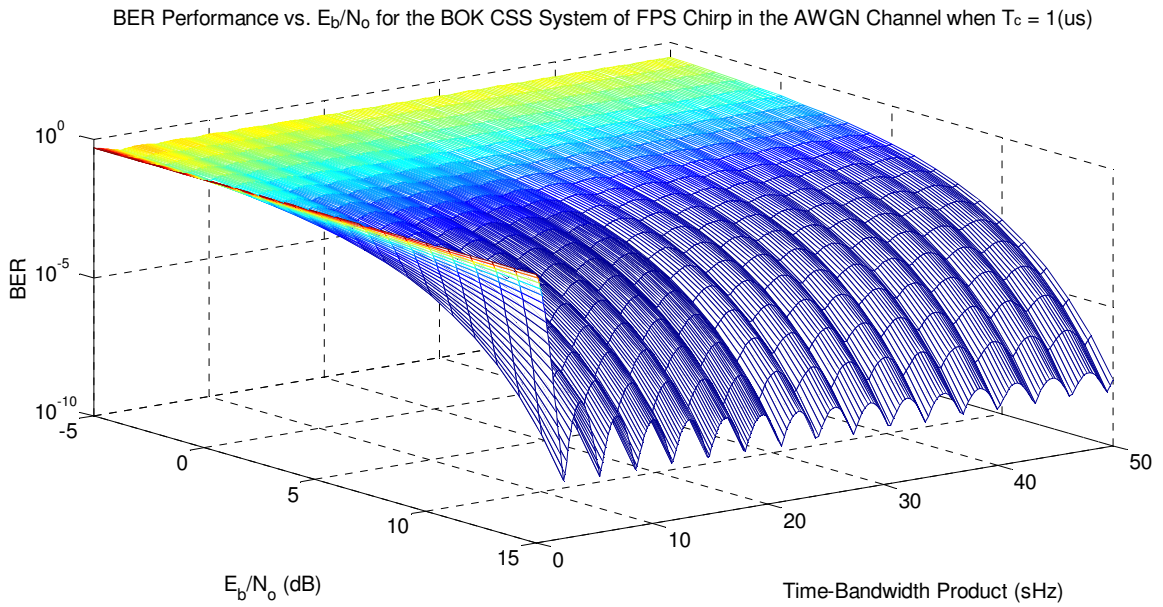


Figure 5.2: E_b/N_0 vs. BER of the BOK FPS CSS system for different $T_c B$

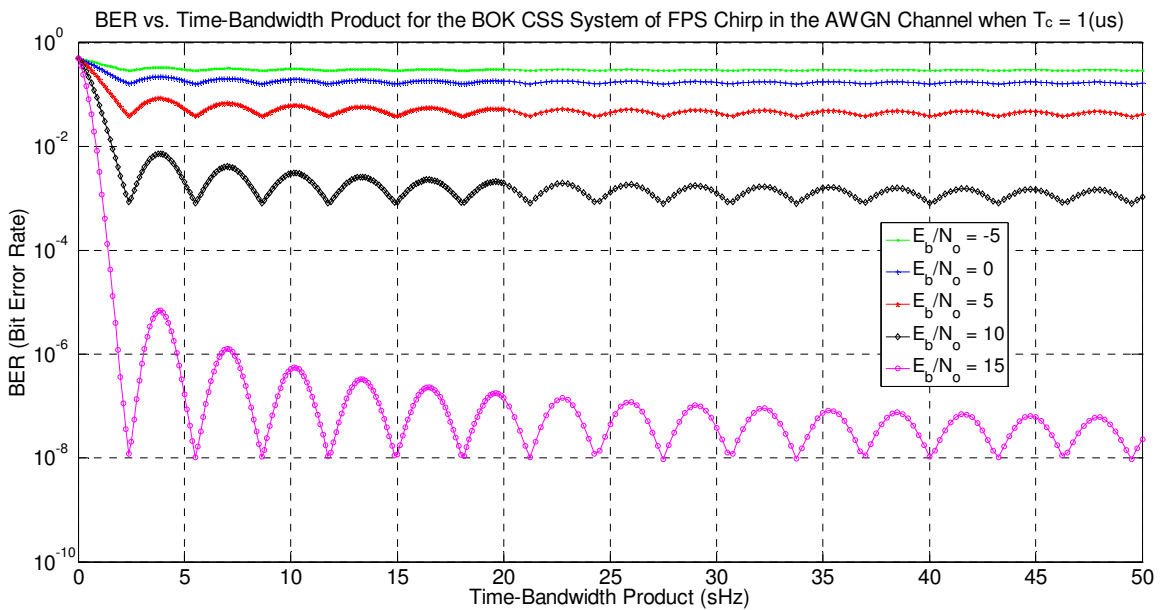


Figure 5.3: BER of the BOK FPS CSS system vs. $T_c B$ for different E_b/N_0

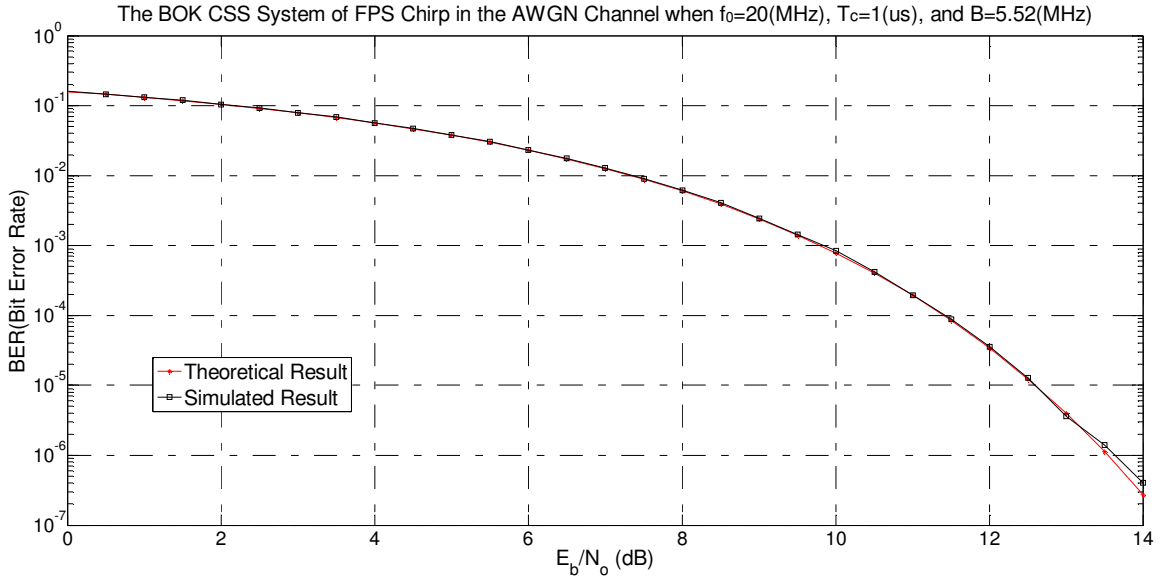


Figure 5.4: Theoretical and simulated BER for the BOK FPS CSS system

5.2.2 Performance Comparison in the AWGN Channel

BER performance vs. E_b/N_0 in AWGN channel for linear and FPS chirps is shown in Figure 5.5 with different B while T_c is $1\mu\text{s}$. As shown in this figure, the linear chirp set shows a performance improvement due to the increased B from 5.5201 MHz to 10 MHz. The BER performance of FPS chirp is better than linear chirp under the same B , such as 5.5201 MHz and 10 MHz. There are very close performance for FPS chirps with three different B (5.5201 MHz, 8.6531 MHz, and 11.7915 MHz) as defined in Eqn. (4.45). Even if the bandwidth (B) for a pair of FPS chirps is larger than another bandwidth, its performance in Gaussian channel may not be better than the latter. For example, the performance of FPS chirps with 10 MHz bandwidth is worse than that with 5.5201 MHz bandwidth. This interesting phenomenon is to be expected, since the correlation coefficient of FPS chirps shows periodic characteristic as discussed in previous sections.

As shown in Figure 5.5, when bandwidth is 5.5201 MHz and E_b/N_0 is 12 dB, the bit error rate of linear chirp is nearly 3×10^{-4} , while the bit error rate of FPS chirp is approximately 7×10^{-5} . Thus, BER of the FPS chirp is only 23.3% of that of the linear chirp. Therefore, it can be concluded that the BOK CSS system based on a pair of

orthogonal FPS chirps can achieve significant performance improvement over its linear counterpart in the AWGN channel.

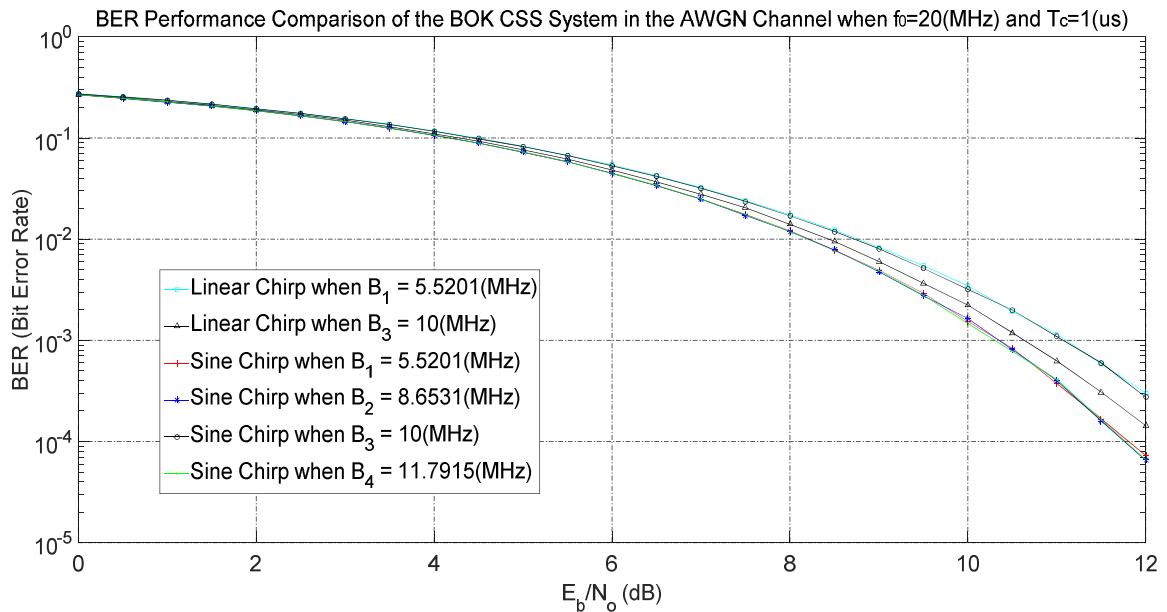


Figure 5.5: Performance of linear chirp and FPS chirp with different bandwidths in the AWGN channel

5.3 Effect of Doppler Shifts

Doppler shift (or Doppler Effect) can cause frequency offset to the transmitted waveform due to the relative movement between the transmitter and receiver. Doppler shift normally decreases the quality of communication systems using modulation schemes, such as OFDM (Orthogonal Frequency-Division Multiplexing). In a CSS system, the transmitted signal is Doppler-shifted by a moving target, while the filter at the receiver side remains matched to an unshifted signal. An important advantage of the CSS system is that it is insensitive to frequency shift [16, 44]. A chirp signal is based on change in instantaneous frequencies. Doppler shift can bring in frequency offset to a chirp signal, but it will damage its change in instantaneous frequencies. Hence, chirp signal is inherently robust to Doppler shift.

A signal $s(t)$ which is distorted with a Doppler shift f_d of a moving target is given as in [51]:

$$s_d(t) = s(t) \times e^{j2\pi f_d t} \quad (5.22)$$

wherein the Doppler frequency offset f_d is represented as:

$$f_d = \frac{v_r}{c} f_0 \quad (5.23)$$

where v_r is the relative velocity between the transmitter and the receiver, c is the velocity of light, and f_0 is the frequency of the transmitted signal.

5.3.1 Linear Chirps

5.3.1.1 Effect at the Matched Filter Output

It is widely accepted that CSS is insensitive to Doppler shift. Suppose the linear up-chirp signal (c_{L1}) as defined in Eqn. (2.15) with no Doppler shift, the output of the matched filter can be described by Eqn. (2.17) which is rewritten here for convenience:

$$g_L^m(t) = \sqrt{4\mu} \cos(2\pi f_0 t) \frac{\sin\left[\frac{\pi\mu t(T_c - |t|)}{2\pi\mu t}\right]}{2\pi\mu t} \quad -\frac{T_c}{2} \leq t \leq \frac{T_c}{2} \quad (5.24)$$

If the above linear chirp signal is received by the receiver with a certain frequency offset $\varepsilon = \omega_d / 2\pi$, then the received signal will become [52]:

$$c_{L1}^d = \cos\left[\left(\omega_0 + \omega_d\right)t + \mu \frac{t^2}{2}\right] \quad -\frac{T_c}{2} \leq t \leq \frac{T_c}{2} \quad (5.25)$$

Output of the matched filter for this signal can be represented as [52]:

$$g_L^{dm}(t, \omega_d) = \sqrt{\frac{2\mu}{\pi}} \cos \left[\left(\omega_0 + \frac{\omega_d}{2} \right) t \right] \frac{\sin \left[\frac{\omega_d + \mu t \left(\frac{T_c}{2} - |t| \right)}{2} \right]}{\omega_d + \mu t}, \quad -\frac{T_c}{2} \leq t \leq \frac{T_c}{2} \quad (5.26)$$

By comparing Eqn. (5.24) and Eqn. (5.26), one can conclude that the two outputs have the same form of a sinc function except for a time-shifted autocorrelation peak. The shift can be represented by:

$$\delta_t = -\frac{\omega_d}{\mu} = -\frac{\omega_d}{B/T_c} = -\frac{\omega_d T_c}{B} \quad (5.27)$$

Therefore, the peak exists at $t = \delta_t$. Thus, value of the output of the matched filter with Doppler shift (frequency offset) for linear chirp can be obtained as:

$$\begin{aligned} g_L^{dm}(\delta_t, \omega_d) &= \sqrt{\frac{2\mu}{\pi}} \cos \left[\left(\omega_0 + \frac{\omega_d}{2} \right) \times \left(-\frac{\omega_d T_c}{B} \right) \right] \\ &= \sqrt{\frac{2\mu}{\pi}} \cos \left[\frac{(2\omega_0 + \omega_d) \omega_d T_c}{2B} \right] \end{aligned} \quad (5.28)$$

A simulation is performed to demonstrate effect of the matched output and unmatched output of the BOK linear CSS system. The matched outputs under three different cases (no frequency offset, 1 MHz, and 3 MHz frequency offset) are comparatively shown in Figure 5.6. Time shifts exists in the both cases with Doppler shift (frequency offset). Meanwhile, magnitude of the matched output also changes. On comparison of the two simulation results, the larger the Doppler frequency offset is, the bigger the time shift will be, and the smaller magnitude of the matched output will be.

5.3.1.2 Effect of the Unmatched Filter Output

Similarly, the unmatched filter outputs under three different cases (no frequency offset, 1 MHz, and 3 MHz frequency offset) are shown in Figure 5.7. As can be seen, effects of Doppler frequency offset on time shifts and the magnitude of the unmatched output are not obvious, because the signal does not match the filter regardless whether there is a Doppler shift or not.

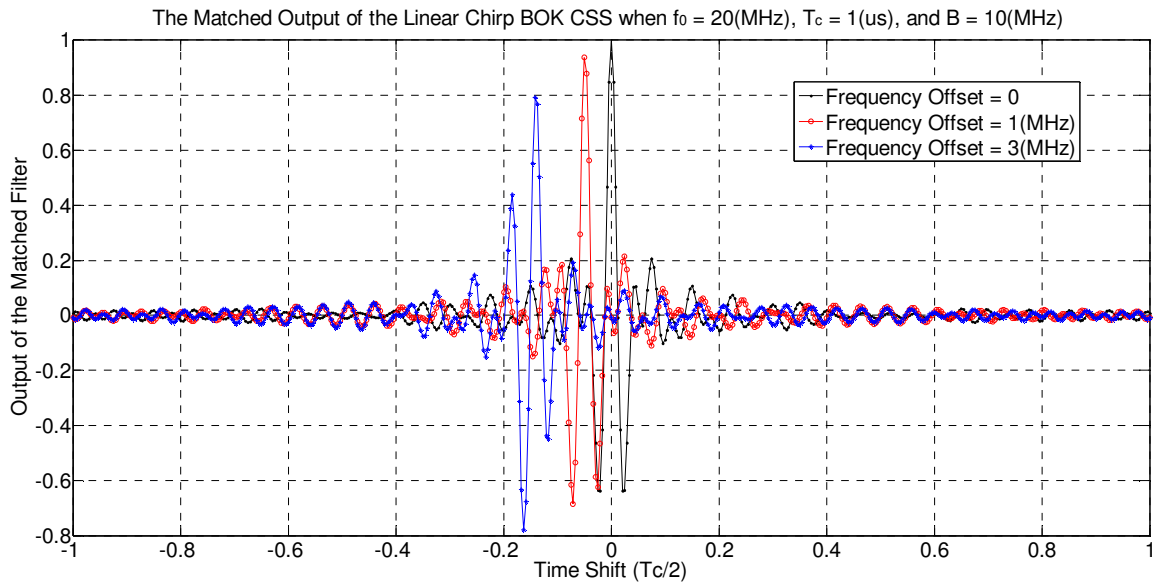


Figure 5.6: Output of the matched filter with different frequency offsets

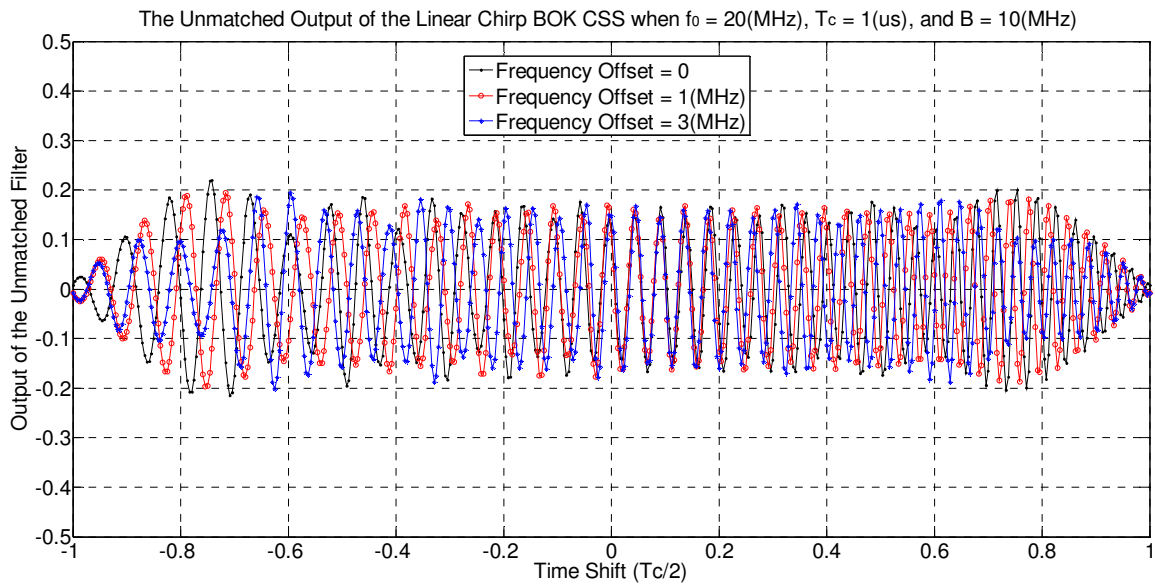


Figure 5.7: Output of the unmatched filter in the BOK linear CSS system with different frequency offsets

5.3.2 Full Period Sine Chirp

Definition 5.1: Suppose FPS chirp signal $c_{s_{2-1}}(t)$ reaches the receiver with a certain amount of frequency offset ω_d , the received signal can then be represented as:

$$c_{s_{2-1}}^d(t) = \cos \left[(\omega_0 + \omega_d)t + \frac{BT_c}{2} \cos \left(2\pi \frac{t}{T_c} \right) \right] \quad -\frac{T_c}{2} \leq t \leq \frac{T_c}{2} \quad (5.29)$$

The impulse response $h_{s_{2-1}}(t)$ of the matched filter to the FPS chirp $c_{s_{2-1}}(t)$ is:

$$h_{s_{2-1}}(t) = \cos \left[\omega_0 t - \frac{BT_c}{2} \cos \left(2\pi \frac{t}{T_c} \right) \right] \quad (5.30)$$

5.3.2.1 Effect at the Matched Filter Output

Theorem 5.1: If $c_{s_{2-1}}^d(t)$ is inputted into the matched filter $h_{s_{2-1}}(t)$, output of the matched filter will be:

$$\begin{aligned} g_{s_2}^{dm}(\tau, \omega_d) = & \left(1 - \frac{|\tau|}{T_c} \right) \cos(\pi f_d \tau) \sum_{n=-\infty}^{\infty} (-1)^n J_{2n}(k_{s_1}^{dm}) \text{sinc} \left[(2\pi f_0 + \pi f_d + 2n\theta)(T_c - |\tau|) \right] \\ & + \left(1 - \frac{|\tau|}{T_c} \right) \sin(\pi f_d \tau) \sum_{n=-\infty}^{\infty} (-1)^n J_{2n+1}(k_{s_1}^{dm}) \text{sinc} \left[(2\pi f_0 + \pi f_d + 2n\theta + \theta)(T_c - |\tau|) \right] \\ & + \left(1 - \frac{|\tau|}{T_c} \right) \cos \left[\pi \tau (f_d + 2f_0) \right] \sum_{n=-\infty}^{\infty} (-1)^n J_n(k_{s_2}^{dm}) \text{sinc} \left[(\pi f_d + n\theta)(T_c - |\tau|) \right] \end{aligned} \quad (5.31)$$

where $\theta = \pi/T_c$, $k_{s_1}^{dm} = BT_c \cos(\theta\tau)$, $k_{s_2}^{dm} = BT_c \sin(\theta\tau)$.

Proof. Output of the matched filter can be calculated by:

$$\begin{aligned}
g_{S2}^{dm}(\tau, \omega_d) &= c_{S2-1}^d(t) * h_{S2-1}(t) = \int_{-\infty}^{\infty} c_{S2-1}^d(t) h_{S2-1}(\tau - t) dt \\
&= \int_{-\infty}^{\infty} \left\{ \begin{aligned} &\cos \left[(\omega_0 + \omega_d)t + \frac{BT_c}{2} \cos \left(2\pi \frac{t}{T_c} \right) \right] \\ &\times \cos \left[\omega_0(t - \tau) + \frac{BT_c}{2} \cos \left(2\pi \frac{t - \tau}{T_c} \right) \right] \end{aligned} \right\} dt
\end{aligned} \tag{5.32}$$

Detailed derivation for the calculation is presented in Appendix H.

When ω_d is set as zero which means no Doppler shift, this equal is the same as Eqn. (5.5) which represents output of the matched filter for the FPS chirp without Doppler shift.

– Q.E.D

Theorem 5.2: If $c_{S2-1}^d(t)$ is inputted into the matched filter $h_{S2-1}(t)$, the matched filter output at $\tau = 0$ can be simplified as:

$$g_{S2}^{dm}(0, \omega_d) = \text{sinc}(\pi f_d T_c) \tag{5.33}$$

Proof. The frequency-shifted output of the matched filter at $\tau = 0$ can be obtained by substituting $\tau = 0$ to Eqn. (5.31):

$$\begin{aligned}
g_{S2}^{dm}(0, \omega_d) &= \sum_{n=-\infty}^{\infty} (-1)^n J_{2n}(BT_c) \text{sinc}[(2\pi f_0 + \pi f_d + 2n\theta)T_c] \\
&\quad + \sum_{n=-\infty}^{\infty} (-1)^n J_n(0) \text{sinc}[(\pi f_d + 2n\theta)T_c]
\end{aligned} \tag{5.34}$$

As shown in Figure 4.1, $J_n(0)$ equals to 1 when $n = 0$, while $J_n(0)$ is always zero when n is non-zero integer. Therefore, Eqn. (5.34) can be simplified as follows:

$$g_{S2}^{dm}(0, \omega_d) = \sum_{n=-\infty}^{\infty} (-1)^n J_{2n}(BT_c) \text{sinc}[(2\pi f_0 + \pi f_d + 2n\theta)T_c] + \text{sinc}(\pi f_d T_c) \tag{5.35}$$

Recall $\theta = \pi/T_c$, then Eqn. (5.35) can be obtained as:

$$g_{S2}^{dm}(0, \omega_d) = \text{sinc}(\pi f_d T_c) + \sum_{n=-\infty}^{\infty} (-1)^n J_{2n}(BT_c) \text{sinc}[\pi(2f_0 + f_d)T_c + 2n\pi] \quad (5.36)$$

Value of the second term in Eqn. (5.36) with different values of f_d and $T_c B$ is shown in Figure 5.8. As shown in this figure, absolute value of this term in Eqn. (5.36) is always less than 0.01. Comparing with the second term in Eqn. (5.36) which normally equals 1, the second term in Eqn. (5.36) is so small that it can be ignored. Thus, Eqn. (5.36) can be simplified as:

$$g_{S2}^{dm}(0, \omega_d) = \text{sinc}(\pi f_d T_c) \quad (5.37)$$

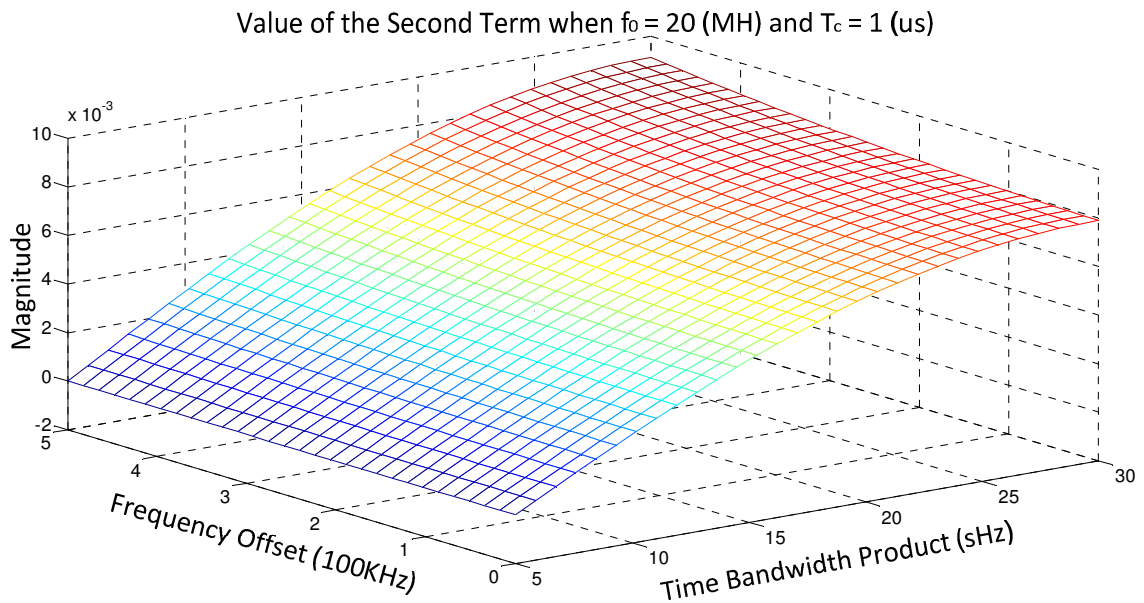


Figure 5.8: Value of the first term in Eqn. (5.36) vs. different Doppler shifts and $T_c B$

– Q.E.D

Definition 5.2: ε is an allowable error, which is $0 < \varepsilon < 1$. f_{dS}^{mt} is the tolerable frequency shift of FPS chirp to the matched output, which means effect on the matched output of sine chirp caused by this frequency shift is under the allowable error ε . sinc^{-1} is inverse function of sinc .

Theorem 5.3: Given an allowable error ε , then there exists $|f_{ds}^{mt}| \leq \frac{\text{sinc}^{-1}(1-\varepsilon)}{\pi T_c}$.

Proof. It can be observed from Theorem 5.2 that the magnitude of the peak (at $\tau = 0$) totally depends on $\text{sinc}(\pi f_d T_c)$. For a given ε , the following can be obtained from Eqn. (5.37):

$$g_{S2}^{dm}(0, \omega_d) = \text{sinc}(\pi f_d T_c) \leq 1 - \varepsilon \quad (5.38)$$

Thus, f_{ds}^{mt} can be obtained from Eqn. (5.38) as:

$$|f_{ds}^{mt}| \leq \frac{\text{sinc}^{-1}(1-\varepsilon)}{\pi T_c} \quad (5.39)$$

– Q.E.D

Example 1. Let $\varepsilon = 0.01$, then f_{ds}^{mt} can be calculated by Eqn. (5.37):

$$|f_{ds}^{mt}| \leq \frac{\text{sinc}^{-1}(1-\varepsilon)}{\pi T_c} = \frac{\text{sinc}^{-1}(1-0.01)}{\pi T_c} = \frac{\text{sinc}^{-1}(0.99)}{\pi T_c} = \frac{0.245}{\pi T_c} \quad (5.40)$$

From Eqn. (5.40), it can be observed that f_{ds}^{mt} only depend on the time period of sine chirp (T_c). The smaller T_c is, the bigger f_{ds}^{mt} will be. Given T_c is 1 μs , f_{ds}^{mt} will be:

$$|f_{ds}^{mt}| \leq \frac{0.245}{\pi} \times 10^6 \approx 78(\text{kHz}) \quad (5.41)$$

Effects with 78 kHz frequency offsets on the matched output of the FPS chirp are simulated when B is set as 5.5201 MHz as an example; the corresponding results are shown in Figure 5.9. It is worth of noting that the results remain valid for different values of B as listed in Table 4.1. As shown in Figure 5.9, the outputs with no frequency offset and 78 kHz frequency offset are almost the same, which means that the effect with a 78 kHz frequency offset can be ignored.

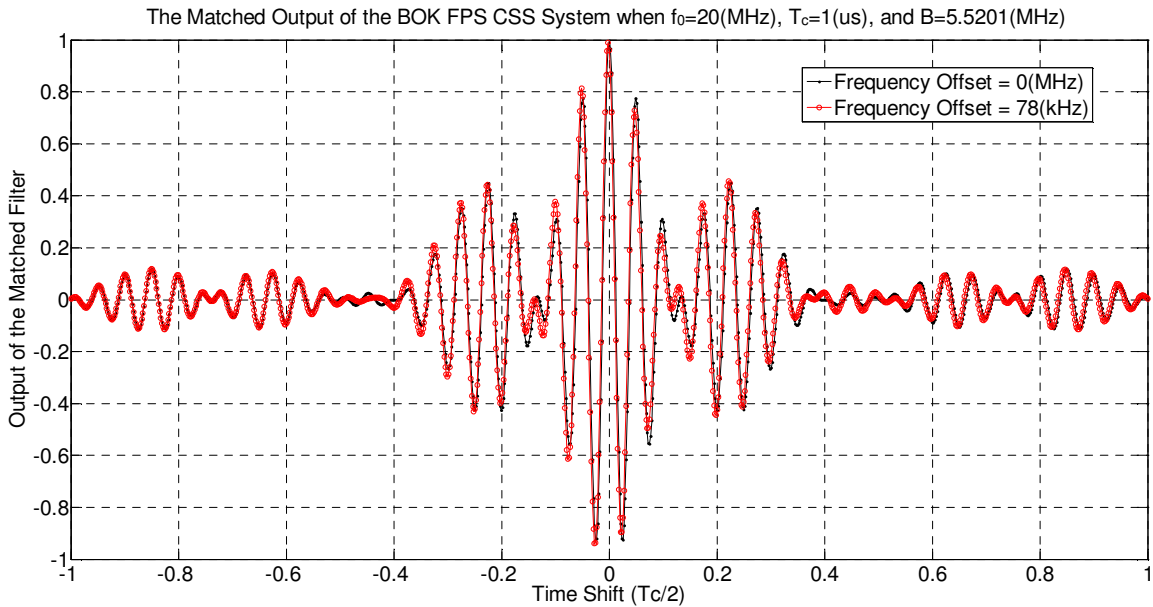


Figure 5.9: Comparison of the matched output of the BOK FPS CSS system with no frequency offset and 78 kHz frequency offset

Example 2. Let $\varepsilon = 0.1$, then f_{ds}^{mt} can be calculated by Eqn. (5.37):

$$\left| f_{ds}^{mt} \right| \leq \frac{\text{sinc}^{-1}(1-\varepsilon)}{\pi T_c} = \frac{\text{sinc}^{-1}(1-0.1)}{\pi T_c} = \frac{\text{sinc}^{-1}(0.9)}{\pi T_c} = \frac{0.787}{\pi T_c} \quad (5.42)$$

Given T_c is $1 \mu\text{s}$, f_{ds}^{mt} will be:

$$\left| f_{ds}^{mt} \right| \leq \frac{0.787}{\pi} \times 10^6 \approx 250(\text{kHz}) \quad (5.43)$$

Comparison of the matched output of FPS chirp with no frequency offsets and 250 kHz are shown in Figure 5.10. Although the two curves in Figure 5.10 are almost overlapped, magnitude of the peak at $t = 0$ for the case with 250 kHz frequency offset is smaller than that for the case without frequency offset. Moreover, peak time shift exists when frequency offsets are 250 kHz.

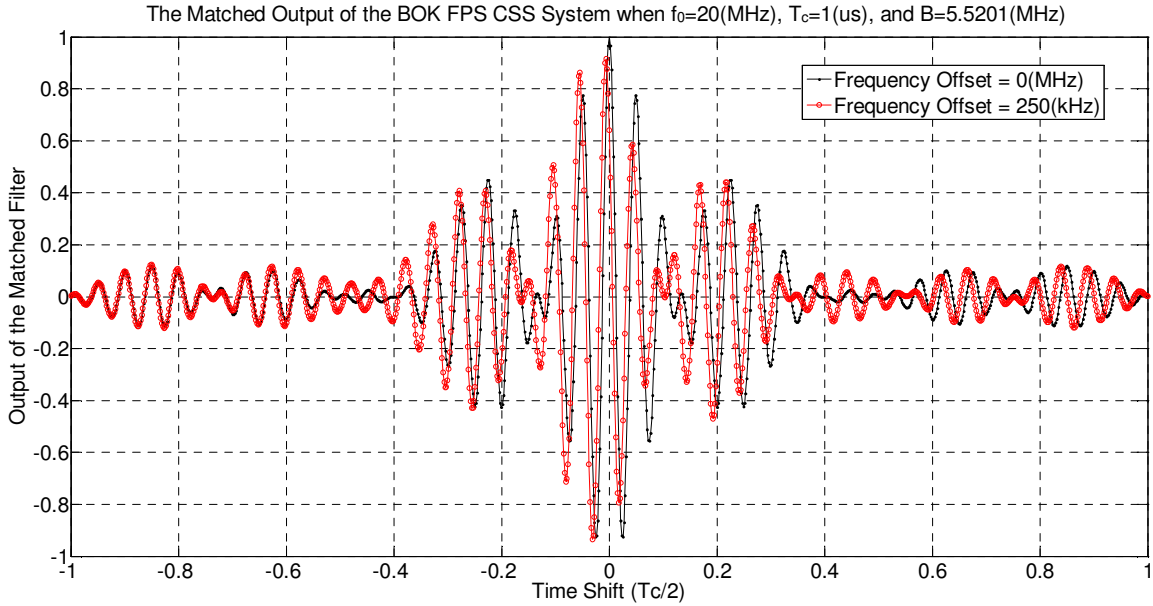


Figure 5.10: Comparison of the matched output of the BOK FPS CSS system with no frequency offset and 250 kHz frequency offset

5.3.2.2 Effect on the Unmatched Filter Output

Theorem 5.4: If $c_{S2-1}^d(t)$ is inputted into the unmatched filter $h_{S2-2}(t)$, the unmatched filter output will be:

$$\begin{aligned}
 g_{S2}^{du}(t, \omega_d) = & \left(1 - \frac{|\tau|}{T_c}\right) \cos(\pi f_d \tau) \sum_{n=-\infty}^{\infty} (-1)^n J_n(k_{S1}^{du}) \text{sinc}[(2\pi f_0 + \pi f_d + 2n\theta)(T_c - |\tau|)] \\
 & + \left(1 - \frac{|\tau|}{T_c}\right) \cos[\pi \tau (f_d + 2f_0)] \sum_{n=-\infty}^{\infty} (-1)^n J_{2n}(k_{S2}^{du}) \text{sinc}[(\pi f_d + 2n\theta)(T_c - |\tau|)] \\
 & - \left(1 - \frac{|\tau|}{T_c}\right) \sin[\pi \tau (f_d + 2f_0)] \sum_{n=-\infty}^{\infty} (-1)^n J_{2n+1}(k_{S2}^{du}) \text{sinc}[(\pi f_d + 2n\theta + \theta)(T_c - |\tau|)]
 \end{aligned}
 \tag{5.44}$$

where $\theta = \pi / T_c$; $k_{S1}^{du} = BT_c \sin(\theta\tau)$; $k_{S2}^{du} = BT_c \cos(\theta\tau)$

Proof. The unmatched filter output can be calculated by:

$$\begin{aligned}
g_{S_2}^{du}(\tau, \omega_d) &= c_{S_2-1}^d(t) * h_{S_2-1}(t) = \int_{-\infty}^{\infty} c_{S_2-1}^d(t) h_{S_2-2}(\tau-t) dt \\
&= \int_{-\infty}^{\infty} \left\{ \begin{aligned} &\cos \left[(\omega_0 + \omega_d)t + \frac{BT_c}{2} \cos \left(2\pi \frac{t}{T_c} \right) \right] \\ &\times \cos \left[\omega_0(\tau-t) + \frac{BT_c}{2} \cos \left(2\pi \frac{\tau-t}{T_c} \right) \right] \end{aligned} \right\} dt
\end{aligned} \tag{5.45}$$

Detailed derivation for the calculation is presented in Appendix I.

– Q.E.D

Theorem 5.5: If $c_{S_2-1}^d(t)$ is inputted into the unmatched filter $h_{S_2-2}(t)$, the unmatched filter output at $\tau = 0$ can be simplified as:

$$g_{S_2}^{du}(0, \omega_d) = \sum_{n=-\infty}^{\infty} \left[(-1)^n J_{2n}(BT_c) \text{sinc}(\pi f_d T_c + 2n\pi) \right] + \text{sinc}[\pi(2f_0 + f_d)T_c] \tag{5.46}$$

Proof. The frequency-shifted output of the unmatched filter at $\tau = 0$ can be obtained by substituting $\tau = 0$ to Eqn. (5.44):

$$\begin{aligned}
g_{S_2}^{du}(0, \omega_d) &= \sum_{n=-\infty}^{\infty} \left[(-1)^n J_n(0) \right] \times \text{sinc}[(2\pi f_0 + \pi f_d + 2n\theta)T_c] \\
&\quad + \sum_{n=-\infty}^{\infty} \left[(-1)^n J_{2n}(BT_c) \right] \times \text{sinc}[(\pi f_d + 2n\theta)T_c]
\end{aligned} \tag{5.47}$$

By substituting $\theta = \pi/T_c$ into Eqn. (5.47), Eqn. (5.47) can be simplified as:

$$\begin{aligned}
g_{S_2}^{du}(0, \omega_d) &= \sum_{n=-\infty}^{\infty} (-1)^n J_n(0) \times \text{sinc}[(2f_0 + f_d)\pi T_c + 2n\pi] \\
&\quad + \sum_{n=-\infty}^{\infty} (-1)^n J_{2n}(BT_c) \times \text{sinc}[\pi(f_d T_c + 2n)]
\end{aligned} \tag{5.48}$$

Since $J_n(0)$ equals to 1 when $n = 0$, while $J_n(0)$ is always zero when n is a non-zero integer. Therefore, Eqn. (5.48) can further be simplified as follows:

$$g_{S2}^{du}(0, \omega_d) = \text{sinc}[\pi(2f_0 + f_d)T_c] + \sum_{n=-\infty}^{\infty} (-1)^n J_{2n}(BT_c) \text{sinc}[\pi(f_d T_c + 2n)] \quad (5.49)$$

– Q.E.D

Definition 5.3: f_{dS}^{ut} is the tolerable frequency shift of FPS chirp to the unmatched output, which means effect on the unmatched output of sine chirp caused by this frequency shift can be ignored.

Theorem 5.6: If $c_{S2-1}^d(t)$ is inputted into the unmatched filter, then there exists

$$|f_{dS}^{ut}| \leq \frac{0.1}{T_c}.$$

Proof. From Theorem 5.5, value of $g_{S2}^{du}(0, \omega_d)$ as a function of the time-frequency offset product ($f_d T_c$) is depicted in Figure 5.11 when B is set as the values listed in Table 4.1. Since it can be observed that value of $g_{S2}^{du}(0, \omega_d)$ is less than 0.005 when $f_d T_c \leq 0.1$, value of $g_{S2}^{du}(0, \omega_d)$ can be considered as zero when $f_d T_c \leq 0.1$.

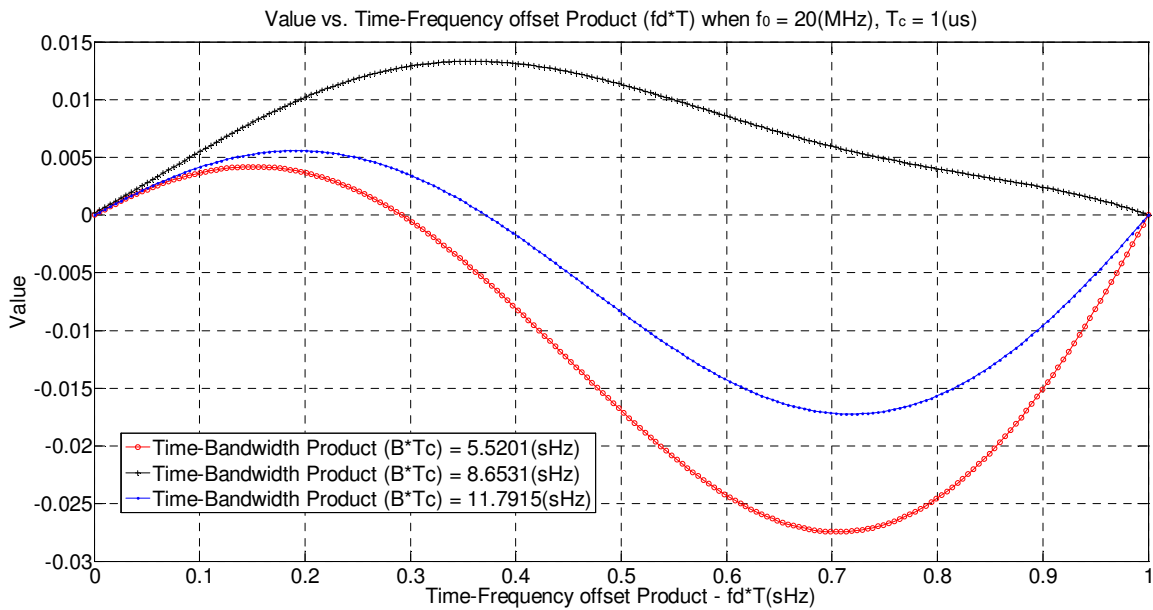


Figure 5.11: Value of Eqn. (5.49) vs. time-frequency offset product

In other words, f_{ds}^{ut} can be obtained from the following:

$$|f_{ds}^{ut}| \leq \frac{0.1}{T_c} \quad (5.50)$$

It can be observed from Eqn. (5.50) that f_{ds}^{ut} also only depends on the time period of FPS chirp (T_c). The smaller T_c is, the bigger f_{ds}^{ut} could be tolerated. Given T_c is 1 μ s, f_{ds}^{ut} will be:

$$|f_{ds}^{ut}| \leq \frac{0.1}{1} \times 10^6 = 100(\text{kHz}) \quad (5.51)$$

Comparisons of the unmatched filter output between no frequency offset and different frequency offsets (50 kHz, 100 kHz, 200 kHz, and 300 kHz) are shown from Figure 5.12 to Figure 5.15 respectively. These results are obtained under the condition that B is set as 5.5201 MHz. As shown in Figure 5.12 and Figure 5.13, the output of the unmatched filter with no frequency offset is almost the same as the output with 50 kHz and 100 kHz frequency offsets. Thus, the effect of frequency offset under 100 kHz can be effectively ignored. It can be observed from Figure 5.14 and Figure 5.15 that there is slight different for the output of the unmatched filter between with no frequency offset and 200 kHz frequency offset, while the different becomes bigger when the frequency offset is increased to 300 kHz.

– Q.E.D

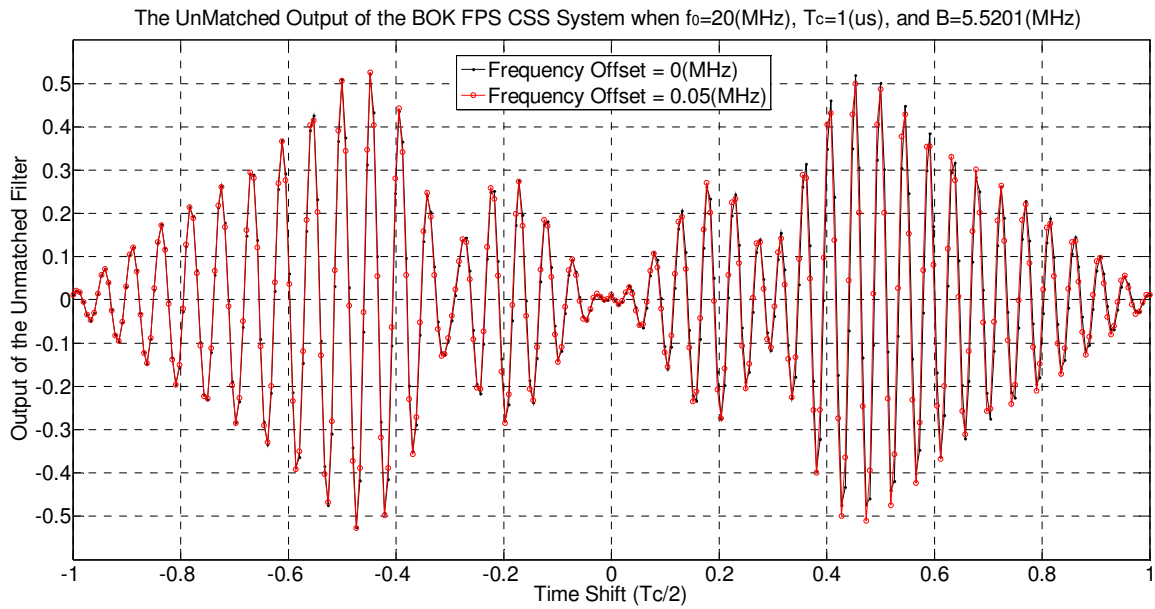


Figure 5.12: Comparison of the unmatched output of the BOK FPS CSS system between no frequency offset and 50 kHz frequency offset

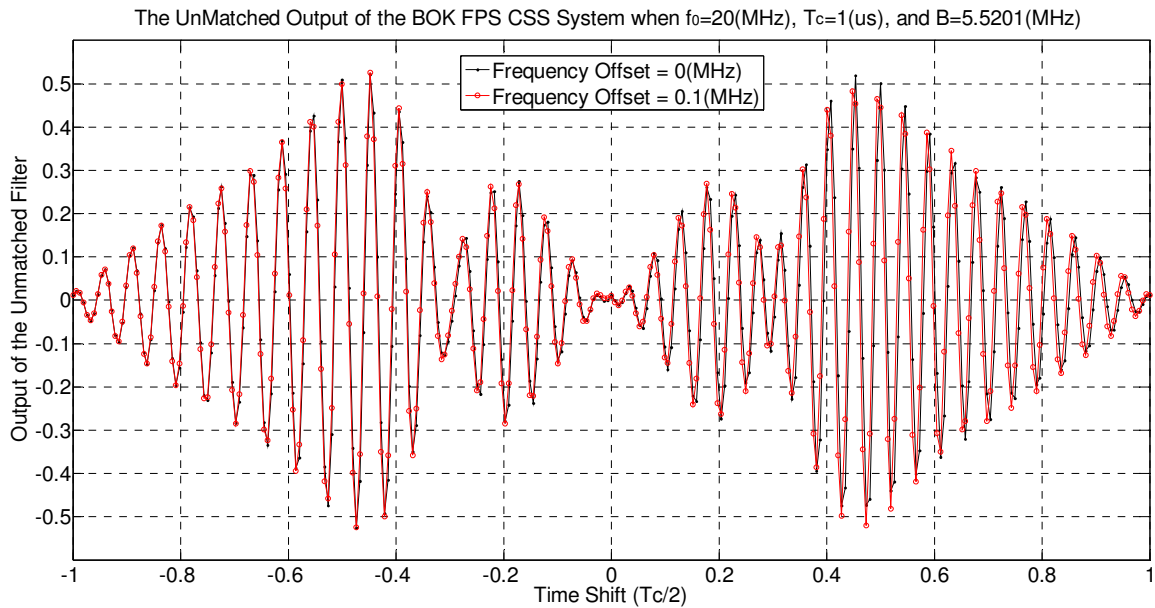


Figure 5.13: Comparison of the unmatched output of the BOK FPS CSS system between no frequency offset and 100 kHz frequency offset

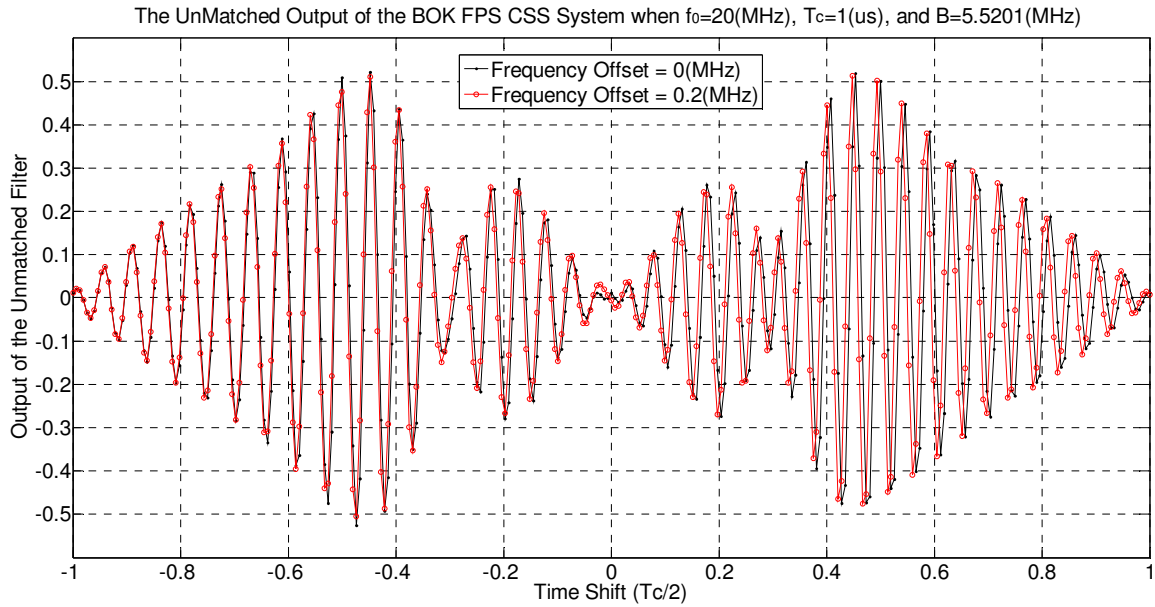


Figure 5.14: Comparison of the unmatched output of the BOK FPS between no frequency offset and 200 kHz frequency offset

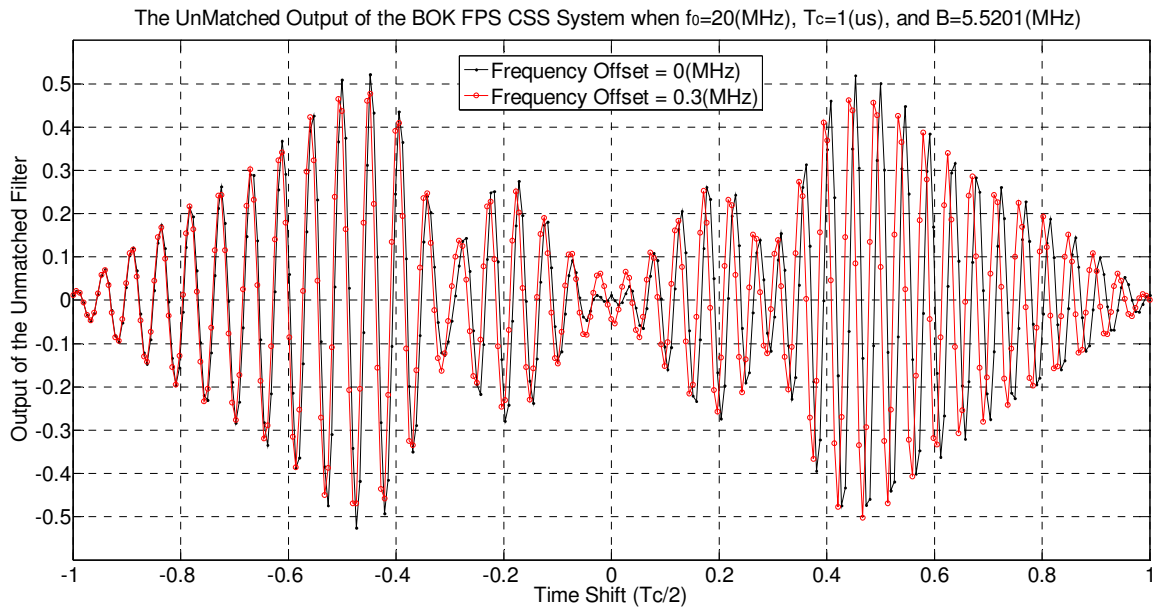


Figure 5.15: Comparison of the unmatched output of the BOK FPS CSS system between no frequency offset and 300 kHz frequency offset

5.3.2.3 Summary

In summary, the tolerable frequency shift at the matched filter output for the FPS chirps is $|f_{ds}^{mt}| \leq \frac{\text{sinc}^{-1}(1-\varepsilon)}{\pi T_c}$ for a given allowable error ε , while the tolerable frequency shift at the unmatched filter output for the FPS chirps is $|f_{ds}^{ut}| \leq \frac{0.1}{T_c}$. So, tolerable frequency shift for the BOK FPS CSS system (f_{ds}^t) should be the smaller one between f_{ds}^{mt} and f_{ds}^{ut} . Given the time period of a FPS chirp signal (T_c) is equal to 1 μ s and $\varepsilon = 0.01$, f_{ds}^{mt} and f_{ds}^{ut} are 78 kHz and 100 kHz respectively. In this case, f_{ds}^t is chosen as 78 kHz.

It should be noted that Doppler frequency offset in practice is normally less than 10 kHz [52]. For example, given the relative velocity between the transmitter and the receiver is 300 km/h and f_0 is assumed to be 2.4 GHz, the Doppler frequency offset f_d is 1.33 kHz as calculated from Eqn. (5.23). Therefore, it can be concluded that the performance of the BOK FPS CSS is insensitive to any Doppler shift in considerable practical situations.

5.3.3 Comparison of BER Performance under Different Frequency Shifts

A comparison between the BOK CSS system using linear chirp vs. FPS chirp under different frequency shifts (no offsets, 50 kHz offset, and 200 kHz offset) in the Gaussian Channel in terms of BER. The corresponding results are shown in Figure 5.16. As shown, BER performance for FPS chirp without frequency offset and 50 kHz frequency offset are almost identical. This is also true for linear chirp. When frequency offset is changed to 200 kHz, the BER performance for both kinds of chirps has degraded. For the three scenarios (no offsets, 50 kHz offset, and 200 kHz offset), BER performance of FPS chirp is always superior than that of linear chirp, especially when E_b/N_0 is greater than 8 dB. It is worthy mentioning that the FPS chirp even at 200 kHz offset outperform the linear chirp with no frequency offset.

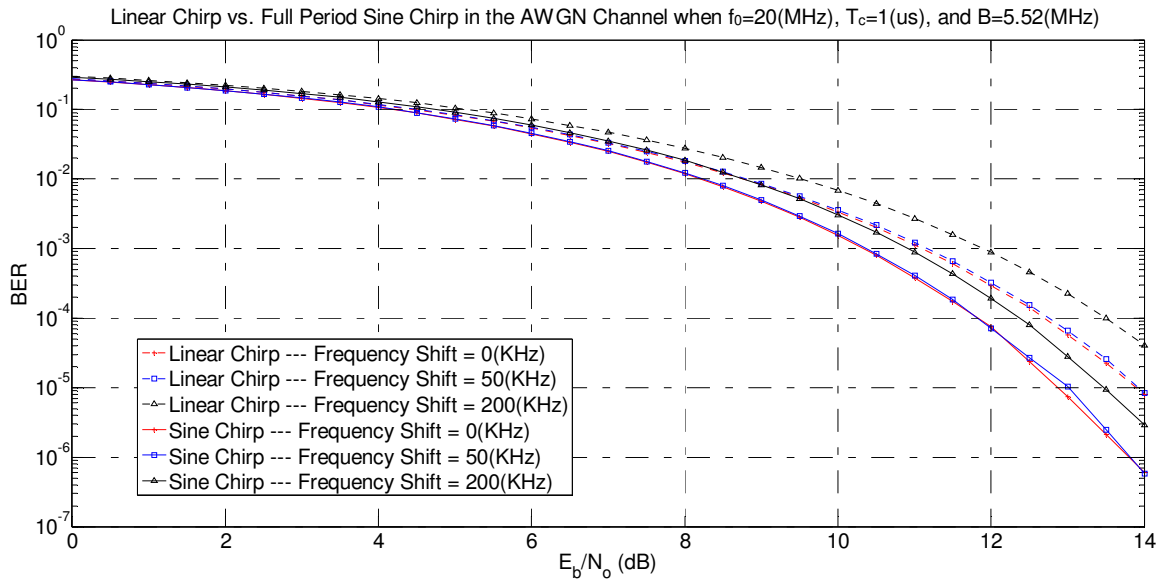


Figure 5.16: E_b/N_0 vs. BER performance in the Gaussian channel for linear and FPS chirps with different frequency shifts

In conclusion, the BOK CSS system based on a pair of orthogonal FPS chirps can achieve superior performance than that of linear chirps under the same frequency offset. In other words, the BOK CSS system based on a pair of orthogonal FPS chirps is also immunized to the frequency offset caused by Doppler effects.

5.4 Performance in a Rayleigh Fading Channel

Although the AWGN channel is a simple way to model a noisy channel, it may not capture all characteristics of a communication channel. More realistic channel models need to be considered. One commonly used non-Gaussian channel in practice is a fading channel. A typical model for such case is Rayleigh fading channel. The main difference between an AWGN channel and a Rayleigh channel resides in the fact that the fading amplitude is now a Rayleigh-distributed random variable. In a Rayleigh fading channel, there are no direct or line-of-sight (LOS) paths, and all paths fade independently.

In this section, a Rayleigh channel model is selected to evaluate the performance of FPS chirp. Comparative simulations for three different scenarios are carried out respectively using the parameters listed in Table 5.1. Since $T_c B = 5.5201$ sHz is an

orthogonal point for FPS chirps, the symbol interval (T_c) and bandwidth (B) are set as 5.52 MHz and 1 μ s respectively. The number of multipath is selected to be 2 for scenario #1 and scenario #2, and 4 for scenario #3. The multipath delay is assumed to be 10 ns, which means that the equivalent difference in transmission distance is 3 meters (the transmission speed \times the delay = 3×10^8 (m/s) \times 10(ns) = 3m).

Table 5.1: System and channel parameters

Channel Type		Rayleigh Fading+AWGN
Modulation		BOK
Chirp Signal		Linear chirp, and FPS chirp
Carrier Frequency (f_0)		20 MHz
Symbol Interval (T_c)		1 μ s
Bandwidth (B)		5.52 MHz
Total data transmitted for each test case		100,000
Scenario #1	Number of Path	2
	Maximum Doppler shift	0 Hz
	Path Delay	0, 10 (ns)
	Path Gain	0 dB, -0.9 dB
Scenario #2	Number of Path	2
	Maximum Doppler shift	50 kHz
	Path Delay	0, 10 (ns)
	Path Gain	0 dB, -0.9 dB
Scenario #3	Number of Path	4
	Maximum Doppler shift	0 Hz
	Path Delay	0, 10 (ns), 20 (ns), 30 (ns)
	Path Attenuation	0 dB, -0.9 dB, -1.7 dB, -2.6 dB

For the Rayleigh fading channel, it is practical to have a scheme to combine the signal power distributed in different paths. However, such combining scheme has not been implemented in this simulation in order to avoid its effects on the performance comparison. As a consequence, at the receiver end, the matched filter is always to be synchronized with the strongest path in the multipath fading, while the other paths in multipath fading will be considered as interferences. The corresponding results are shown in Figure 5.17.

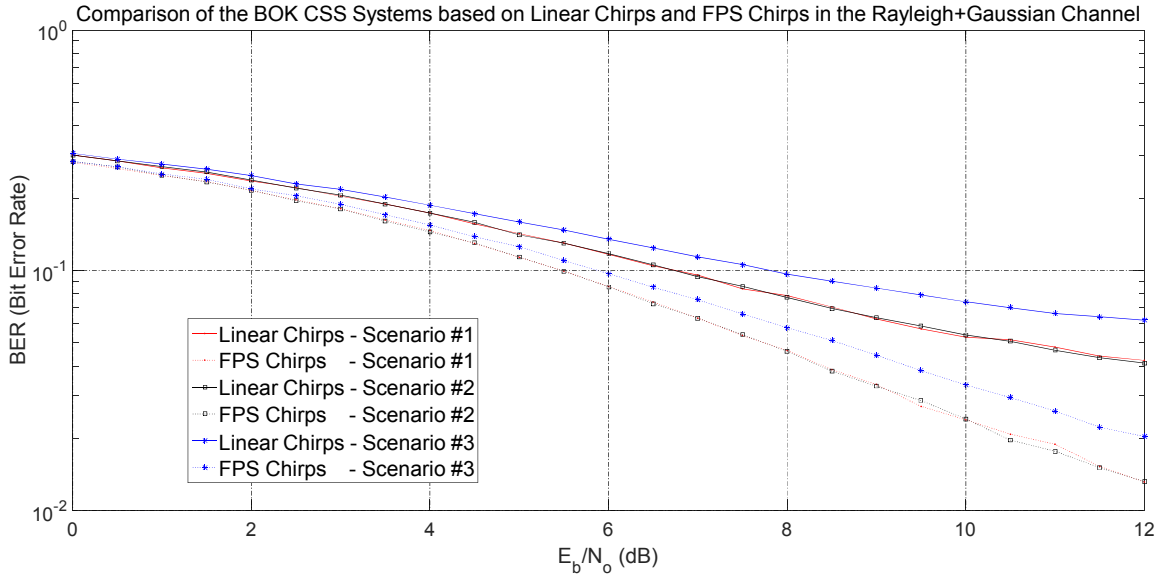


Figure 5.17: E_b/N_0 vs. BER performance for linear and FPS chirps in a Rayleigh+Gaussian channel

An important observation from the simulation results is that the BOK CSS system based on FPS chirps can achieve improved performance than linear chirps in all three scenarios. For example, as to the scenarios #3 when E_b/N_0 is 12 dB, the bit error rate of linear chirp is nearly 6.2×10^{-2} , while the bit error rate for FPS chirp is approximately 2×10^{-2} . Thus, BER of FPS chirp is only 32.3% of that of linear chirp. Therefore, the BOK CSS system based on a pair of orthogonal FPS chirps can lead to significant improvement than its linear counterpart in an AWGN+Rayleigh channel.

5.5 Summary

Using both theoretical analyses and simulations, it has been demonstrated that the BOK CSS system based on a pair of orthogonal FPS chirps can achieve improved BER performance than its linear counterpart in both AWGN and AWGN+Rayleigh channels. Moreover, the BOK CSS system based on a pair of orthogonal FPS chirp is also immunized to the frequency offset.

6. Conclusions

This chapter concludes the dissertation by summarizing major contributions. Future research relevant to this topic is also outlined.

Through rigorous mathematical analysis and simulation studies, this thesis has proved that a pair of sine or cosine chirps can be completely orthogonal under some conditions. The results have far-reaching implications in BOK CSS system in terms of reduced time-bandwidth product.

6.1 Summary of Specific Contributions

1. Two general representations are developed respectively to construct an arbitrary kind of chirps for a given spectral bandwidth B , and to construct a pair of chirps for the BOK CSS system. With these two general representations, many kinds of non-linear chirps can be constructed for the BOK CSS system before they are analyzed.
2. An efficient method is proposed to determine a pair of candidate chirps which have improved orthogonal property over its linear counterpart. (1) A comparison of relationship between the time-bandwidth product ($T_c B$) and value of cross-correlation coefficient for both linear chirps and the candidate chirps can be used to observe if the candidate chirps have improved orthogonal property. (2) Based on the graphical comparison, if the magnitude of cross-correlation coefficient of the candidate chirps is smaller than that of the linear chirps for same $T_c B$, the candidate chirps are deemed to have improved orthogonal property. More especially, if a zero crossing point exists in the curve of the candidate chirps, the candidate chirps probably can be completely orthogonal under a certain condition. This proposed method can be used by other researchers to quickly evaluate if a pair of candidate chirps has improved orthogonal property over its linear counterpart.

3. Preliminary results have shown that a significant performance advantage on orthogonality over linear chirps can be attained using the pair of cosine or sine chirps. Thus, the properties of sine or cosine chirps are analyzed in detail. The derivations of the spectral characteristics, autocorrelation and cross-correlation for sine chirps are carried out. Similarly, the derivations of the spectral characteristics, autocorrelation and cross-correlation for cosine chirps are also carried out. This significant discovery is validated by mathematical derivation and simulation: a pair of sine or cosine chirps is orthogonal as long as $\frac{2BT_c}{\Omega}$ is equal to the roots of the Bessel function of the first kind of order zero ($J_0(x)$). A significant of this discovery is that a pair of orthogonal sine or cosine chirps can be determined.
4. The effect of Doppler shift on the BOK FPS CSS system has been investigated, and then validated by simulation. The tolerable frequency shift to the matched filter output of sine chirp (f_{ds}^{mt}) is $f_{ds}^{mt} \leq \frac{\text{sinc}^{-1}(1-\varepsilon)}{\pi T_c}$ for a given allowable error ε , while the tolerable frequency shift to the unmatched filter output of sine chirp (f_{ds}^{ut}) is $|f_{ds}^{ut}| \leq \frac{0.1}{T_c}$. Therefore, tolerable frequency shift for the BOK FPS CSS system (f_{ds}^t) should be the smaller one between f_{ds}^{mt} and f_{ds}^{ut} . It is proven that the BOK CSS system based on a pair of orthogonal sine chirp is immuned to frequency offsets in considerable practical situations. This means the BOK FPS CSS system can be used in some applications which have serious Doppler or frequency offsets, such as high speed train wireless communication.
5. BER performance of the BOK CSS system based on FPS chirps in an additive white Gaussian noise (AWGN) channel is derived and then validated. The results prove that a pair of orthogonal FPS chirps can outperform its linear counterpart in the AWGN channel. Furthermore, the performance comparison between linear chirps and FPS chirps for the BOK CSS system in an AWGN+Rayleigh channel has been analyzed. The corresponding result also shows that a pair of orthogonal

FPS chirps can achieve superior BER performance than its linear counterpart in the AWGN+Rayleigh channel. From a communication system point of view, this means a pair of orthogonal FPS chirps are much quantified to replace linear chirps for the BOK CSS system.

6.2 Suggestions for Future Research

1. In this thesis, some properties of the BOK CSS system based on FPS chirp are analyzed analytically and by simulations. However, practical design and implementation techniques for the BOK CSS system based on FPS chirp are not considered in this thesis, and, thus, could be a future research topic.
2. Though FPS chirps are shown to be robustness in a fading environment, it is possible some enhancement can be done to obtain improved performance. The performance degradation caused by multipath fading can be reduced using different techniques, such as a RAKE receiver [53]. In this way, chirp energy distributed along multipath can be collected and the performance of the system will be further improved. The method used to collect chirp multipath signals is an interesting research topic.
3. An open topic for future research is to develop a method to increase the data rate for the BOK CSS system based on sine chirps. In this thesis, only a BOK CSS system is considered. One of the possibilities is to use M-ary sine chirps, and to increase the speed of the chirp system up to \log_2^M .

References

- [1] R.C.Dixon, *Spread spectrum systems*. New York: Wiley, 1976.
- [2] M. Kowatsch and J. T. Lafferl, "A spread-spectrum concept combining chirp modulation and pseudonoise coding," *IEEE Transactions on Communications*, vol. 31, pp. 1133-1142, 1983.
- [3] A. Springer, W. Gugler, M. Huemer, R. Koller, and R. Weigel, "A wireless spread-spectrum communication system using SAW chirped delay lines," *IEEE Transactions on Microwave Theory and Techniques*, vol. 49, pp. 754-760, 2001.
- [4] A. Kadri, "Low-power chirp signals for wireless data communication in industrial environments," Ph.D Thesis, Department of Electrical and Computer Engineering, University of Western Ontario, London, Ontario, Canada, 2009.
- [5] M. Winkler, "Chirp signals for communications," *Wescon Convention Record*, vol. Pt.7, 1962.
- [6] J. Q. Pinkney, A. B. Sesay, S. Nichols, and R. Behin, "Robust high speed indoor wireless communications system using chirp spread spectrum," in *1999 IEEE Canadian Conference on Electrical and Computer Engineering 'Engineering Solutions for the Next Millennium'*, Edmonton, Alberta, Can, May 9-12, 1999, pp. 84-89.
- [7] "IEEE Standard for Information Technology - Telecommunications and Information Exchange Between Systems - Local and Metropolitan Area Networks - Specific Requirement Part 15.4: Wireless Medium Access Control (MAC) and Physical Layer (PHY) Specifications for Low-Rate Wireless Personal Area Networks (WPANs)," *IEEE Std 802.15.4a-2007 (Amendment to IEEE Std 802.15.4-2006)*, pp. 1-203, 2007.
- [8] S. Lee, H. Shin, R. Ha, and H. Cha, "IEEE 802.15.4a CSS-based mobile object locating system using sequential monte carlo method," *Computer Communications*, vol. 38, pp. 13-25, Jan. 2014.
- [9] A. Kadri, "Performance of IEEE 802.15.4-based wireless sensors in harsh environments," in *8th International Wireless Communications and Mobile Computing Conference (IWCMC)*, 2012, pp. 526-530.
- [10] Y. D. Kim, S. Kwon, J. W. Son, and D. Kim, "Design and performance verification of dynamic load aware geographic routing protocol in IEEE 802.15.4a networks," *International Journal of Distributed Sensor Networks*, 2014.

- [11] J. Pinkney and A. Sesay, "Performance of N-ary chirp spread spectrum modulation in the AWGN and broadband multipath channels," presented at the 2004 Wireless proceedings, Calgary, Alberta, 2004.
- [12] A. J. Berni and W. D. Gregg, "On the utility of chirp modulation for digital signaling," *IEEE Transactions on Communications*, vol. 21, pp. 748-751, 1973.
- [13] Y. R. Tsai and J. F. Chang, "The feasibility of combating multipath interference by chirp spread spectrum techniques over Rayleigh and Rician fading channels," in *IEEE 3rd International Symposium on Spread Spectrum Techniques and Applications (IEEE ISSSTA)*, 1994, pp. 282-286.
- [14] D. Penunuri, "Recent progress in SAW filters at GHz frequencies," in *1997 IEEE MTT-S International Microwave Symposium Digest*, 1997, pp. 169-172 vol.1.
- [15] M. Hikita, N. Shibagaki, A. Isobe, K. Asai, and K. Sakiyama, "Recent and future RF SAW technology for mobile communications," in *1997 IEEE MTT-S International Microwave Symposium Digest*, 1997, pp. 173-176 vol.1.
- [16] A. Springer, M. Huemer, L. Reindl, C. C. W. Ruppel, A. Pohl, F. Seifert, *et al.*, "A robust ultra-broad-band wireless communication system using SAW chirped delay lines," *IEEE Transactions on Microwave Theory and Techniques*, vol. 46, pp. 2213-2219, 1998.
- [17] S. Hengstler, D. P. Kasilingam, and A. H. Costa, "A novel chirp modulation spread spectrum technique for multiple access," in *7th IEEE International Symposium on Spread Spectrum Techniques and Applications*, 2002, pp. 73-77 vol.1.
- [18] J. Pinkney, "Low complexity indoor wireless data links using chirp spread spectrum," Ph.D Thesis, Department of Electrical and Computer Engineering, University of Calgary, Calgary, Canada, 2003.
- [19] S. Hanbing, Z. Weihua, and K. Kyung-Sup, "Using non-linear chirp waveform to suppress narrowband interference in UWB system," in *International Symposium on Communications and Information Technologies (ISCIT)*, 2006, pp. 1212-1215.
- [20] E. Fowle, "The design of FM pulse compression signals," *IEEE Transactions on Information Theory*, vol. 10, pp. 61-67, 1964.
- [21] C. E. Cook, "A class of nonlinear FM pulse compression signals," *Proceedings of the IEEE*, vol. 52, pp. 1369-1371, 1964.
- [22] T. Collins, "Active sonar pulse designs," University of Birmingham, 1996.
- [23] L. Xiaotong, B. Zhiquan, and K. Kyungsup, "NBI suppression UWB system based on novel nonlinear chirp pulses," in *9th International Symposium on Communications and Information Technology (ISCIT 2009)*, 2009, pp. 1167-1170.

- [24] S. Hanbing, Z. Weihua, and K. Kyung-Sup, "Modified chirp waveforms in cognitive UWB system," in *2008 IEEE International Conference on Communications Workshops (ICC Workshops '08)*, 2008, pp. 504-507.
- [25] B. L. Prakash and K. R. Rajeswari, "Performance comparison between Gaussian NLFM, Rayleigh NLFM signals," *International Journal of Engineering Science and Technology (IJEST)*, vol. 3, pp. 5905-5911, July 2011.
- [26] M. A. Khan, R. K. Rao, and W. Xianbin, "Performance of quadratic and exponential multiuser chirp spread spectrum communication systems," in *2013 International Symposium on Performance Evaluation of Computer and Telecommunication Systems (SPECTS)*, 2013, pp. 58-63.
- [27] I. Dotlic and R. Kohno, "Low complexity chirp pulsed Ultra-Wideband system with near-optimum multipath performance," *IEEE Transactions on Wireless Communications*, vol. 10, pp. 208-218, 2011.
- [28] N. Technologies. Technical description of nanoPAN 5360 RF module. [Online]. Available: http://www.gaw.ru/pdf/Nanotron/nanoPAN5360_Preliminary_Technical_Description_V100_2005-07-18.pdf
- [29] C. E. Cook and M. Bernfeld, *Radar signals - an introduction to theory and application*. New York: Academic Press, 1967.
- [30] Y. K. Chan, M. Y. Chua, and V. C. Koo, "Sidelobes reduction using simple two and tri-stages non linear frequency modulation (NLFM)," *Progress in Electromagnetics Research*, vol. 98, pp. 33-52, 2009.
- [31] J. R. Klauder, *The theory and design of chirp radars*: Bell Telephone Laboratories, 1960.
- [32] M. Pollakowski and H. Ermert, "Chirp signal matching and signal power optimization in pulse-echo mode ultrasonic nondestructive testing," *IEEE Transactions on Ultrasonics, Ferroelectrics and Frequency Control*, vol. 41, pp. 655-659, 1994.
- [33] C. J. Bouras, *Trends in Telecommunications Technologies*: InTech, 2010.
- [34] C. E. Cook and M. Bernfeld, "CHAPTER 1 - The Basic Elements of Matched Filtering and Pulse Compression," in *Radar Signals*, C. E. C. Bernfeld, Ed., ed: Academic Press, 1967, pp. 1-17.
- [35] Y. F. Chang, "A software controlled pulse compression technique applied to ultrasonic non - destructive testing," *Journal of the Chinese Institute of Engineers*, vol. 26, pp. 147-153, 2003/03/01 2003.

- [36] C. D. Rawat and A. D. Sarate, "High Resolution Low Power Radar Pulse Compression Techniques," *International Journal of Advanced Research in Electrical, Electronics and Instrumentation Engineering*, vol. 3, 2014.
- [37] P. F. Dunn, *Measurement and Data Analysis for Engineering and Science, Third Edition*: Taylor & Francis, 2014.
- [38] C. E. Cook, "Pulse compression-key to more efficient Radar transmission," *Proceedings of the IRE*, vol. 48, pp. 310-316, 1960.
- [39] G. N. Watson, *A treatise on the theory of Bessel functions*: Cambridge University Press, 1995.
- [40] M. Abramowitz and I. A. Stegun, *Handbook of Mathematical Functions: With Formulas, Graphs, and Mathematical Tables*: Dover Publications, 1964.
- [41] A. P. Clark, *Principles of digital data transmission*: Pentech, 1983.
- [42] F. W. Olver, D. W. Lozier, R. F. Boisvert, and C. W. Clark, *NIST handbook of mathematical functions*: Cambridge University Press, 2010.
- [43] J. Pinkney, "Low Complexity Indoor Wireless Data Links Using Chirp Spread Spectrum," Ph.D, Department of Electrical Computer Engineering, The University of Calgary, Calgary, Alberta, Canada, 2003.
- [44] J. A. Johnston and A. C. Fairhead, "Waveform design and doppler sensitivity analysis for nonlinear FM chirp pulses," *IEE Proceedings F (Communications, Radar and Signal Processing)*, vol. 133, pp. 163-175, 1986.
- [45] T. Collins and P. Atkins, "Nonlinear frequency modulation chirps for active sonar," *IEE Proceedings: Radar, Sonar and Navigation*, vol. 146, pp. 312-316, 1999.
- [46] T. H. Powell and A. I. Sinsky, "A Time sidelobe reduction technique for small time-bandwidth chirp," *IEEE Transactions on Aerospace and Electronic Systems*, vol. AES-10, pp. 390-392, 1974.
- [47] K. Dostert and M. Pandit, "Synchronization of spread spectrum binary orthogonal keyed (BOK) burst transmission systems," in *IEEE Military Communications Conference (MILCOM)*, New York, NY, USA, 1982, pp. 20-5.
- [48] S. Jia and L. Hao, "An Improved synchronization method of chirp UWB," in *2008 ISECS International Colloquium on Computing, Communication, Control, and Management (CCCM)*, Piscataway, NJ, USA, 2008, pp. 654-8.
- [49] H. Liu, "Novel synchronization method for chirp communication system," *Journal of University of Electronic Science and Technology of China*, vol. 38, pp. 913-15, Nov. 2009.

- [50] G. K. Karagiannidis and A. S. Lioumpas, "An Improved Approximation for the Gaussian Q-Function," *IEEE Communications Letters*, vol. 11, pp. 644-646, 2007.
- [51] F. Hofele, "Overview of the present state of the art in pulse compression," in *1st International Workshop on Compressed Sensing applied to Radar*, Bonn, Germany, 2012.
- [52] P. Zhang and H. Liu, "An Ultra-Wide Band system with chirp spread spectrum transmission technique," *6th International Conference on ITS Telecommunications Proceedings*, pp. 294-297, 2006.
- [53] C. Kyungwhoon, "Performance of direct-sequence spread-spectrum RAKE receivers with random spreading sequences," *IEEE Transactions on Communications*, vol. 45, pp. 1130-1143, 1997.

Appendix A: Formulas Used

The Jacobi's expansions in series of Bessel coefficient is defined by [39]:

$$\left\{ \begin{array}{l} \cos[\beta \cos(\theta)] = J_0(\beta) + 2 \sum_{n=1}^{\infty} [(-1)^n J_{2n}(\beta) \cos(2n\theta)] \\ \sin[\beta \cos(\theta)] = 2 \sum_{n=0}^{\infty} [(-1)^n J_{2n+1}(\beta) \cos[(2n+1)\theta]] \\ \cos[\beta \sin(\theta)] = J_0(\beta) + 2 \sum_{n=1}^{\infty} [J_{2n}(\beta) \cos(2n\theta)] \\ \sin[\beta \sin(\theta)] = 2 \sum_{n=0}^{\infty} [J_{2n+1}(\beta) \sin[(2n+1)\theta]] \end{array} \right. \quad (\text{A.1})$$

In this equation, $J_n(x)$ is the Bessel function of the first kind of order n [42]. As to Bessel functions of the first kind, for integer order n , the following relationship is valid [42]:

$$J_{-n}(x) = (-1)^n J_n(x) \quad (\text{A.2})$$

When n in Eqn. (A.2) is even, the following equation for $J_n(x)$ can be obtained:

$$J_{-n}(x) = J_n(x) \quad (\text{A.3})$$

When n in Eqn. (A.2) is odd, the following equation for $J_n(x)$ can be obtained:

$$J_n(x) = (-1) J_{-n}(x) \quad (\text{A.4})$$

A.1 Cosine Extension in term of Cosine Jacobi's expansion

A.1.1 Cosine extension

The following equation can be achieved from Eqn. (A.1):

$$\begin{aligned}
\cos(\alpha) \cos[\beta \cos(\theta)] &= \cos(\alpha) \left\{ J_0(\beta) + 2 \sum_{n=1}^{\infty} [(-1)^n J_{2n}(\beta) \cos(2n\theta)] \right\} \\
&= \cos(\alpha) J_0(\beta) + \sum_{n=1}^{\infty} \left\{ (-1)^n J_{2n}(\beta) [\cos(\alpha + 2n\theta) + \cos(\alpha - 2n\theta)] \right\} \\
&= \cos(\alpha) J_0(\beta) + \sum_{n=1}^{\infty} [(-1)^n J_{2n}(\beta) \cos(\alpha + 2n\theta)] \\
&\quad + \sum_{n=-\infty}^{-1} [(-1)^n J_{-2n}(\beta) \cos(\alpha + 2n\theta)]
\end{aligned} \tag{A.5}$$

Since $2n$ is even in Eqn. (A.5), Eqn. (A.5) can become by recalling Eqn. (A.3):

$$\cos(\alpha) \cos[\beta \cos(\theta)] = \sum_{n=-\infty}^{\infty} [(-1)^n J_{2n}(\beta) \cos(\alpha + 2n\theta)] \tag{A.6}$$

A.1.2 Sine extension

The following equation can be achieved from Eqn. (A.1):

$$\begin{aligned}
\sin(\alpha) \sin[\beta \cos(\theta)] &= \sin(\alpha) \left\{ 2 \sum_{n=0}^{\infty} [(-1)^n J_{2n+1}(\beta) \cos[(2n+1)\theta]] \right\} \\
&= \sum_{n=0}^{\infty} \left\{ (-1)^n J_{2n+1}(\beta) [\sin[\alpha + (2n+1)\theta] + \sin[\alpha - (2n+1)\theta]] \right\} \\
&= \sum_{n=0}^{\infty} \left\{ (-1)^n J_{2n+1}(\beta) \sin[\alpha + (2n+1)\theta] \right\} \\
&\quad + \sum_{n=-\infty}^{-1} \left\{ (-1)^n J_{(2n+1)}(\beta) \sin[\alpha + (2n+1)\theta] \right\}
\end{aligned} \tag{A.7}$$

Since $2n+1$ is odd in Eqn. (A.7), Eqn. (A.7) can become by recalling Eqn. (A.4):

$$\sin(\alpha) \sin[\beta \cos(\theta)] = \sum_{n=-\infty}^{\infty} \left\{ (-1)^n J_{2n+1}(\beta) \sin[\alpha + (2n+1)\theta] \right\} \tag{A.8}$$

A.1.3 Summary

The following equation can be achieved as:

$$\cos[\alpha \pm \beta \cos(\theta)] = \cos(\alpha) \cos[\beta \cos(\theta)] \mp \sin(\alpha) \sin[\beta \cos(\theta)] \tag{A.9}$$

By combining Eqn. (A.6) and Eqn. (A.8) into Eqn. (A.9), then Eqn. (A.9) becomes as:

$$\begin{aligned} \cos[\alpha \pm \beta \cos(\theta)] &= \sum_{n=-\infty}^{\infty} \left[(-1)^n J_{2n}(\beta) \cos(\alpha + 2n\theta) \right] \\ &\mp \sum_{n=-\infty}^{\infty} \left\{ (-1)^n J_{2n+1}(\beta) \sin[\alpha + (2n+1)\theta] \right\} \end{aligned} \quad (\text{A.10})$$

A.2 Sine extension in term of Cosine Jacobi's expansion

A.2.1 Sine & Cosine extension

The following equation can be achieved from Eqn. (A.1):

$$\begin{aligned} \sin(\alpha) \cos[\beta \cos(\theta)] &= \sin(\alpha) \left\{ J_0(\beta) + 2 \sum_{n=1}^{\infty} \left[(-1)^n J_{2n}(\beta) \cos(2n\theta) \right] \right\} \\ &= \sin(\alpha) J_0(\beta) + \sum_{n=1}^{\infty} \left\{ (-1)^n J_{2n}(\beta) \left[\sin(\alpha + 2n\theta) + \sin(\alpha - 2n\theta) \right] \right\} \\ &= \sin(\alpha) J_0(\beta) + \sum_{n=1}^{\infty} \left[(-1)^n J_{2n}(\beta) \sin(\alpha + 2n\theta) \right] \\ &\quad + \sum_{n=-\infty}^{-1} \left[(-1)^n J_{-2n}(\beta) \sin(\alpha + 2n\theta) \right] \end{aligned} \quad (\text{A.11})$$

Since $2n$ is even in Eqn. (A.11), Eqn. (A.11) can become by recalling Eqn. (A.4):

$$\sin(\alpha) \cos[\beta \cos(\theta)] = \sum_{n=-\infty}^{\infty} \left[(-1)^n J_{2n}(\beta) \sin(\alpha + 2n\theta) \right] \quad (\text{A.12})$$

A.2.2 Cosine & Sine extension

The following equation can be achieved from Eqn. (A.1):

$$\begin{aligned}
\cos(\alpha) \sin[\beta \cos(\theta)] &= \cos(\alpha) \left\{ 2 \sum_{n=0}^{\infty} [(-1)^n J_{2n+1}(\beta) \cos[(2n+1)\theta]] \right\} \\
&= \sum_{n=0}^{\infty} (-1)^n J_{2n+1}(\beta) \left\{ \sin[\alpha + (2n+1)\theta] - \sin[\alpha - (2n+1)\theta] \right\} \\
&= \sum_{n=0}^{\infty} \left\{ (-1)^n J_{2n+1}(\beta) \sin[\alpha + (2n+1)\theta] \right\} \\
&\quad - \sum_{n=-\infty}^{-1} \left\{ (-1)^n J_{-(2n+1)}(\beta) \sin[\alpha + (2n+1)\theta] \right\}
\end{aligned} \tag{A.13}$$

Since $2n+1$ is odd in Eqn. (A.13), Eqn. (A.13) can become by recalling Eqn. (A.4):

$$\begin{aligned}
\cos(\alpha) \sin[\beta \cos(\theta)] &= \sum_{n=0}^{\infty} \left\{ (-1)^n J_{2n+1}(\beta) \sin[\alpha + (2n+1)\theta] \right\} \\
&\quad - \sum_{n=-\infty}^{-1} \left\{ (-1)^n \times (-1) J_{(2n+1)}(\beta) \sin[\alpha + (2n+1)\theta] \right\}
\end{aligned} \tag{A.14}$$

Eqn. (A.14) can be simplified as:

$$\cos(\alpha) \sin[\beta \cos(\theta)] = \sum_{n=-\infty}^{\infty} \left\{ (-1)^n J_{2n+1}(\beta) \sin[\alpha + (2n+1)\theta] \right\} \tag{A.15}$$

A.2.3 Summary

The following equation can be achieved as:

$$\sin[\alpha \pm \beta \cos(\theta)] = \sin(\alpha) \cos[\beta \cos(\theta)] \pm \cos(\alpha) \sin[\beta \cos(\theta)] \tag{A.16}$$

By combining Eqn. (A.12) and Eqn. (A.14) into Eqn. (A.16), then Eqn. (A.16) becomes as:

$$\begin{aligned}
\sin[\alpha \pm \beta \cos(\theta)] &= \sum_{n=-\infty}^{\infty} \left[(-1)^n J_{2n}(\beta) \sin(\alpha + 2n\theta) \right] \\
&\quad \pm \sum_{n=-\infty}^{\infty} \left\{ (-1)^n J_{2n+1}(\beta) \sin[\alpha + (2n+1)\theta] \right\}
\end{aligned} \tag{A.17}$$

A.3 Cosine extension in term of Sine Jacobi's expansion

A.3.1 Cosine extension

The following equation can be achieved from Eqn. (A.1):

$$\begin{aligned}\cos(\alpha) \cos[\beta \sin(\theta)] &= \cos(\alpha) \left\{ J_0(\beta) + 2 \sum_{n=1}^{\infty} [J_{2n}(\beta) \cos(2n\theta)] \right\} \\ &= \cos(\alpha) J_0(\beta) + \sum_{n=1}^{\infty} \left\{ J_{2n}(\beta) [\cos(\alpha + 2n\theta) + \cos(\alpha - 2n\theta)] \right\}\end{aligned}\quad (\text{A.18})$$

Since $2n$ is even in Eqn. (A.18), Eqn. (A.18) can become by recalling Eqn. (A.3):

$$\cos(\alpha) \cos[\beta \sin(\theta)] = \sum_{n=-\infty}^{\infty} [J_{2n}(\beta) \cos(\alpha + 2n\theta)] \quad (\text{A.19})$$

A.3.2 Sine extension

The following equation can be achieved from Eqn. (A.1):

$$\begin{aligned}\sin(\alpha) \sin[\beta \sin(\theta)] &= \sin(\alpha) \left\{ 2 \sum_{n=0}^{\infty} [J_{2n+1}(\beta) \sin[(2n+1)\theta]] \right\} \\ &= - \sum_{n=0}^{\infty} \left\{ J_{2n+1}(\beta) [\cos[\alpha + (2n+1)\theta] - \cos[\alpha - (2n+1)\theta]] \right\} \\ &= - \left\{ \begin{aligned} &\sum_{n=0}^{\infty} \{ J_{2n+1}(\beta) \cos[\alpha + (2n+1)\theta] \} \\ &- \sum_{n=-1}^{-\infty} \{ J_{-(2n+1)}(\beta) \cos[\alpha + (2n+1)\theta] \} \end{aligned} \right\}\end{aligned}\quad (\text{A.20})$$

Since $2n+1$ is even in Eqn. (A.20), Eqn. (A.20) can become by recalling Eqn. (A.4):

$$\sin(\alpha) \sin[\beta \sin(\theta)] = - \sum_{n=-\infty}^{\infty} \{ J_{2n+1}(\beta) \cos[\alpha + (2n+1)\theta] \} \quad (\text{A.21})$$

A.3.3 Summary

The following equation can be achieved as:

$$\cos[\alpha + \beta \sin(\theta)] = \cos(\alpha) \cos[\beta \sin(\theta)] - \sin(\alpha) \sin[\beta \sin(\theta)] \quad (\text{A.22})$$

By combining Eqn. (A.19) and Eqn. (A.21) into Eqn. (A.22), then Eqn. (A.22) becomes as:

$$\begin{aligned}\cos[\alpha + \beta \sin(\theta)] &= \sum_{n=-\infty}^{\infty} [J_{2n}(\beta) \cos(\alpha + 2n\theta)] \\ &\quad + \sum_{n=-\infty}^{\infty} \{J_{2n+1}(\beta) \cos[\alpha + (2n+1)\theta]\} \\ &= \sum_{n=-\infty}^{\infty} [J_n(\beta) \cos(\alpha + n\theta)]\end{aligned}\quad (\text{A.23})$$

The following equation can be achieved as:

$$\cos[\alpha - \beta \sin(\theta)] = \cos(\alpha) \cos[\beta \sin(\theta)] + \sin(\alpha) \sin[\beta \sin(\theta)] \quad (\text{A.24})$$

By combining Eqn. (A.19) and Eqn. (A.21) into Eqn. (A.24), then Eqn. (A.24) becomes as:

$$\begin{aligned}\cos[\alpha - \beta \sin(\theta)] &= \sum_{n=-\infty}^{\infty} [J_{2n}(\beta) \cos(\alpha + 2n\theta)] \\ &\quad - \sum_{n=-\infty}^{\infty} \{J_{2n+1}(\beta) \cos[\alpha + (2n+1)\theta]\} \\ &= \sum_{n=-\infty}^{\infty} [(-1)^n J_n(\beta) \cos(\alpha + n\theta)]\end{aligned}\quad (\text{A.25})$$

Finally, Eqn. (A.23) and Eqn. (A.25) can be summarized as:

$$\begin{cases} \cos[\alpha + \beta \sin(\theta)] = \sum_{n=-\infty}^{\infty} [J_n(\beta) \cos(\alpha + n\theta)] \\ \cos[\alpha - \beta \sin(\theta)] = \sum_{n=-\infty}^{\infty} [(-1)^n J_n(\beta) \cos(\alpha + n\theta)] \end{cases} \quad (\text{A.26})$$

A.4 Sine extension in term of Sine Jacobi's expansion

A.4.1 Sine & Cosine extension

The following equation can be achieved from Eqn. (A.1):

$$\begin{aligned}
\sin(\alpha) \cos[\beta \sin(\theta)] &= \sin(\alpha) \left\{ J_0(\beta) + 2 \sum_{n=1}^{\infty} [J_{2n}(\beta) \cos(2n\theta)] \right\} \\
&= \sin(\alpha) J_0(\beta) + \sum_{n=1}^{\infty} \{ J_{2n}(\beta) [\sin(\alpha + 2n\theta) + \sin(\alpha - 2n\theta)] \} \\
&= \sin(\alpha) J_0(\beta) + \sum_{n=1}^{\infty} [J_{2n}(\beta) \sin(\alpha + 2n\theta)] + \sum_{n=-\infty}^{-1} [J_{-2n}(\beta) \sin(\alpha + 2n\theta)]
\end{aligned} \tag{A.27}$$

Since $2n$ is even in Eqn. (A.27), Eqn. (A.27) can become by recalling Eqn. (A.3):

$$\cos(\alpha) \cos[\beta \sin(\theta)] = \sum_{n=-\infty}^{\infty} [J_{2n}(\beta) \sin(\alpha + 2n\theta)] \tag{A.28}$$

A.4.2 Cosine & Sine extension

The following equation can be achieved from Eqn. (A.1):

$$\begin{aligned}
\cos(\alpha) \sin[\beta \sin(\theta)] &= \cos(\alpha) \left\{ 2 \sum_{n=0}^{\infty} [J_{2n+1}(\beta) \sin[(2n+1)\theta]] \right\} \\
&= \sum_{n=0}^{\infty} J_{2n+1}(\beta) \{ \sin[\alpha + (2n+1)\theta] - \sin[\alpha - (2n+1)\theta] \} \\
&= \sum_{n=0}^{\infty} \{ J_{2n+1}(\beta) \sin[\alpha + (2n+1)\theta] \} - \sum_{n=-\infty}^{-1} \{ J_{-(2n+1)}(\beta) \sin[\alpha + (2n+1)\theta] \}
\end{aligned} \tag{A.29}$$

Since $2n+1$ is odd in Eqn. (A.29), Eqn. (A.29) can become by recalling Eqn. (A.4):

$$\begin{aligned}
\cos(\alpha) \sin[\beta \sin(\theta)] &= \sum_{n=0}^{\infty} \{ J_{2n+1}(\beta) \sin[\alpha + (2n+1)\theta] \} \\
&\quad + \sum_{n=-\infty}^{-1} \{ J_{(2n+1)}(\beta) \sin[\alpha + (2n+1)\theta] \} \\
&= \sum_{n=-\infty}^{\infty} \{ J_{2n+1}(\beta) \sin[\alpha + (2n+1)\theta] \}
\end{aligned} \tag{A.30}$$

A.4.3 Summary

The following equation can be achieved as:

$$\sin[\alpha + \beta \sin(\theta)] = \sin(\alpha) \cos[\beta \sin(\theta)] + \cos(\alpha) \sin[\beta \sin(\theta)] \quad (\text{A.31})$$

By combining Eqn. (A.28) and Eqn. (A.30) into Eqn. (A.31), then Eqn. (A.31) becomes as:

$$\begin{aligned} \sin[\alpha + \beta \sin(\theta)] &= \sum_{n=-\infty}^{\infty} [J_{2n}(\beta) \sin(\alpha + 2n\theta)] + \sum_{n=-\infty}^{\infty} \{J_{2n+1}(\beta) \sin[\alpha + (2n+1)\theta]\} \\ &= \sum_{n=-\infty}^{\infty} [J_n(\beta) \sin(\alpha + n\theta)] \end{aligned} \quad (\text{A.32})$$

The following equation can be achieved as:

$$\sin[\alpha - \beta \sin(\theta)] = \sin(\alpha) \cos[\beta \sin(\theta)] - \cos(\alpha) \sin[\beta \sin(\theta)] \quad (\text{A.33})$$

By combining Eqn. (A.28) and Eqn. (A.30) into Eqn. (A.33), then Eqn. (A.33) becomes as:

$$\begin{aligned} \sin[\alpha - \beta \sin(\theta)] &= \sum_{n=-\infty}^{\infty} [J_{2n}(\beta) \sin(\alpha + 2n\theta)] - \sum_{n=-\infty}^{\infty} \{J_{2n+1}(\beta) \sin[\alpha + (2n+1)\theta]\} \\ &= \sum_{n=-\infty}^{\infty} [(-1)^n J_n(\beta) \sin(\alpha + n\theta)] \end{aligned} \quad (\text{A.34})$$

Finally, Eqn. (A.32) and Eqn. (A.34) can be summarized as:

$$\begin{cases} \sin[\alpha + \beta \sin(\theta)] = \sum_{n=-\infty}^{\infty} [J_n(\beta) \sin(\alpha + n\theta)] \\ \sin[\alpha - \beta \sin(\theta)] = \sum_{n=-\infty}^{\infty} [(-1)^n J_n(\beta) \sin(\alpha + n\theta)] \end{cases} \quad (\text{A.35})$$

A.5 Some Frequently Used Equations

A.5.1 #1 Equation

One equation frequently used in the following appendices is:

$$\sum_{n=-\infty}^{\infty} [(-1)^n J_n(x)] = J_0(x) + \sum_{n=1}^{\infty} [(-1)^n J_n(x)] + \sum_{n=-\infty}^{-1} [(-1)^n J_n(x)] \quad (\text{A.36})$$

Recalling Eqn. (A.2), the following results can obtained:

$$\begin{aligned} \sum_{n=-\infty}^{\infty} [(-1)^n J_n(x)] &= J_0(x) + \sum_{n=1}^{\infty} [(-1)^n J_n(x)] + \sum_{n=-\infty}^{-1} [(-1)^n \times (-1)^{-n} J_{-n}(x)] \\ &= J_0(x) + \sum_{n=1}^{\infty} [(-1)^n J_n(x)] + \sum_{n=1}^{\infty} [J_n(x)] \\ &= J_0(x) + 2 \sum_{n=1}^{\infty} [J_{2n}(x)] \end{aligned} \quad (\text{A.37})$$

A.5.2 #2 Equation

Another equation frequently used in the following appendies is:

$$\sum_{n=-\infty}^{\infty} [(-1)^n J_{2n}(x)] = J_0(x) + \sum_{n=1}^{\infty} [(-1)^n J_{2n}(x)] + \sum_{n=-\infty}^{-1} [(-1)^n J_{2n}(x)] \quad (\text{A.38})$$

Recalling Eqn. (A.2), the following results can obtained:

$$\begin{aligned} \sum_{n=-\infty}^{\infty} [(-1)^n J_{2n}(x)] &= J_0(x) + \sum_{n=1}^{\infty} [(-1)^n J_{2n}(x)] + \sum_{n=-\infty}^{-1} [(-1)^n J_{-2n}(x)] \\ &= J_0(x) + 2 \sum_{n=1}^{\infty} [(-1)^n J_{2n}(x)] \end{aligned} \quad (\text{A.39})$$

A.5.3 #3 Equation

Another equation frequently used in the following appendies is:

$$\sum_{n=-\infty}^{\infty} [(-1)^n J_{2n+1}(x)] = \sum_{n=0}^{\infty} [(-1)^n J_{2n+1}(x)] + \sum_{n=-\infty}^{-1} [(-1)^n J_{2n+1}(x)] \quad (\text{A.40})$$

Recalling Eqn. (A.2), the following results can obtained:

$$\begin{aligned}
\sum_{n=-\infty}^{\infty} \left[(-1)^n J_{2n+1}(x) \right] &= \sum_{n=0}^{\infty} (-1)^n J_{2n+1}(x) + \sum_{n=-\infty}^{-1} \left[(-1)^n \times (-1)^{-(2n+1)} J_{-(2n+1)}(x) \right] \\
&= \sum_{n=0}^{\infty} (-1)^n J_{2n+1}(x) + \sum_{n=-\infty}^{-1} \left[(-1)^{-(n+1)} J_{-(2n+1)}(x) \right] \quad (\text{A.41}) \\
&= 2 \sum_{n=0}^{\infty} (-1)^n J_{2n+1}(x)
\end{aligned}$$

Appendix B: Spectrum of Sine Chirps

In this appendix, spectrum of sine chirp is derived. In general, a pair of sine chirp can be represented as:

$$\begin{cases} c_{S1}(t) = a \cos \left[\omega_0 t + \frac{BT_c}{\Omega} \cos \left(\frac{\pi \Omega}{T_c} t \right) \right] & -\frac{T_c}{2} \leq t \leq \frac{T_c}{2} \\ c_{S2}(t) = a \cos \left[\omega_0 t - \frac{BT_c}{\Omega} \cos \left(\frac{\pi \Omega}{T_c} t \right) \right] & -\frac{T_c}{2} \leq t \leq \frac{T_c}{2} \end{cases} \quad (\text{B.1})$$

The spectrum of sine chirp Signals depicted in Eqn. (B.1) can be obtained by taking the Fourier transform of itself. $c_{S1}(t)$ is taking as an example here for analyze spectral characteristic of sine chirps.

$$\begin{aligned} F_{S1}(\omega) &= \frac{1}{T_c} \int_{-T_c/2}^{T_c/2} f_{S1}(t) e^{-j\omega t} dt \\ &= \frac{1}{T_c} \int_{-T_c/2}^{T_c/2} a \cos \left[\omega_0 t + \frac{BT_c}{\Omega} \cos \left(\frac{\pi \Omega}{T_c} t \right) \right] \times e^{-j\omega t} dt \end{aligned} \quad (\text{B.2})$$

Let

$$z = \frac{BT_c}{\Omega} \quad \text{and} \quad \vartheta = \frac{\pi \Omega}{T_c} \quad (\text{B.3})$$

Recalling the Euler's formula $e^{-j\omega t} = \cos(\omega t) - j \sin(\omega t)$, Eqn. (B.2) becomes:

$$\begin{aligned} F_{S1}(\omega) &= \frac{1}{T_c} \int_{-T_c/2}^{T_c/2} \left\{ a \cos \left[\omega_0 t + z \cos(\vartheta t) \right] \times \left[\cos(\omega t) - j \sin(\omega t) \right] \right\} dt \\ &= \frac{a}{2T_c} \int_{-T_c/2}^{T_c/2} \left\{ \cos \left[(\omega_0 + \omega) t + z \cos(\vartheta t) \right] + \cos \left[(\omega_0 - \omega) t + z \cos(\vartheta t) \right] \right\} dt \\ &\quad - j \times \frac{a}{2T_c} \int_{-T_c/2}^{T_c/2} \left\{ \sin \left[(\omega_0 + \omega) t + z \cos(\vartheta t) \right] - \sin \left[(\omega_0 - \omega) t + z \cos(\vartheta t) \right] \right\} dt \end{aligned} \quad (\text{B.4})$$

Let $\omega^+ = \omega_0 + \omega$, $\omega^- = \omega_0 - \omega$, then:

$$\begin{aligned}
F_{S1}(\omega) &= \frac{a}{2T_c} \int_{-T_c/2}^{T_c/2} \cos[\omega^+ t + z \cos(\vartheta t)] dt + \frac{a}{2T_c} \int_{-T_c/2}^{T_c/2} \cos[\omega^- t + z \cos(\vartheta t)] dt \\
&\quad - \frac{a}{2T_c} j \left\{ \int_{-T_c/2}^{T_c/2} \sin[\omega^+ t + z \cos(\vartheta t)] dt - \int_{-T_c/2}^{T_c/2} \sin[\omega^- t + z \cos(\vartheta t)] dt \right\} \\
&= \frac{a}{2T_c} \left\{ \int_{-T_c/2}^{T_c/2} \cos[\omega^+ t + z \cos(\vartheta t)] dt - j \int_{-T_c/2}^{T_c/2} \sin[\omega^+ t + z \cos(\vartheta t)] dt \right\} \quad (\text{B.5}) \\
&\quad + \frac{a}{2T_c} \left\{ \int_{-T_c/2}^{T_c/2} \cos[\omega^- t + z \cos(\vartheta t)] dt + j \int_{-T_c/2}^{T_c/2} \sin[\omega^- t + z \cos(\vartheta t)] dt \right\} \\
&= F_{S1}^N(\omega) + F_{S1}^P(\omega)
\end{aligned}$$

where $F_{S1}^P(\omega)$ and $F_{S1}^N(\omega)$ are positive and negative sides of the spectrum respectively.

$$F_{S1}^P(\omega) = \frac{a}{2T_c} \left\{ \int_{-T_c/2}^{T_c/2} \cos[\omega^- t + z \cos(\vartheta t)] dt - j \int_{-T_c/2}^{T_c/2} \sin[\omega^- t + z \cos(\vartheta t)] dt \right\} \quad (\text{B.6})$$

and

$$F_{S1}^N(\omega) = \frac{a}{2T_c} \left\{ \int_{-T_c/2}^{T_c/2} \cos[\omega^+ t + z \cos(\vartheta t)] dt + j \int_{-T_c/2}^{T_c/2} \sin[\omega^+ t + z \cos(\vartheta t)] dt \right\} \quad (\text{B.7})$$

B.1 Calculation of the positive side

Only positive side of the spectrum is considered as example, so Eqn. (B.6) can be simplified as:

$$F_{S1}^P(\omega) = \frac{a}{2} \{ F_{S1}^{PR} - jF_{S1}^{PI} \} \quad (\text{B.8})$$

where F_{S1}^{PR} is the real part:

$$F_{S1}^{PR} = \frac{1}{T_c} \int_{-T_c/2}^{T_c/2} \cos[\omega^- t + z \cos(\vartheta t)] dt \quad (\text{B.9})$$

and F_{S1}^{PI} is the image part:

$$F_{S1}^{PI} = \frac{1}{T_c} \int_{-T_c/2}^{T_c/2} \sin[\omega^- t + z \cos(\vartheta t)] dt \quad (\text{B.10})$$

B.1.1 Calculation of the real part

Substituting Eqn. (A.10) into Eqn. (B.9), the real part F_{S1}^{PR} can be obtained as:

$$F_{S1}^{PR} = \frac{1}{T_c} \int_{-T_c/2}^{T_c/2} \left\{ \begin{aligned} &\sum_{n=-\infty}^{\infty} [(-1)^n J_{2n}(z) \cos(\omega^- t + 2n\vartheta t)] \\ & - \sum_{n=-\infty}^{\infty} \{(-1)^n J_{|2n+1|}(z) \sin[\omega^- t + (2n+1)\vartheta t]\} \end{aligned} \right\} dt \quad (\text{B.11})$$

Eqn. (B.11) can be simplified as:

$$\begin{aligned} F_{S1}^{PR} &= \frac{1}{T_c} \sum_{n=-\infty}^{\infty} [(-1)^n J_{2n}(z)] \times \int_{-T_c/2}^{T_c/2} \cos(\omega^- t + 2n\vartheta t) dt \\ &\quad - \frac{1}{T_c} \sum_{n=-\infty}^{\infty} [(-1)^n J_{|2n+1|}(z)] \times \int_{-T_c/2}^{T_c/2} \sin[\omega^- t + (2n+1)\vartheta t] dt \\ &= \frac{1}{T_c} \sum_{n=-\infty}^{\infty} [(-1)^n J_{2n}(z)] \times \frac{2}{(\omega^- + 2n\vartheta)} \sin\left[(\omega^- + 2n\vartheta) \frac{T_c}{2}\right] - 0 \\ &= \sum_{n=-\infty}^{\infty} \left\{ [(-1)^n J_{2n}(z)] \operatorname{sinc}\left[(\omega^- + 2n\vartheta) \frac{T_c}{2}\right] \right\} \end{aligned} \quad (\text{B.12})$$

B.2.2 Calculation of the image part

Substituting Eqn. (A.17) into Eqn. (B.10), the image part F_{S1}^{PI} can be obtained as:

$$F_{S1}^{PI} = \frac{1}{T_c} \int_{-T_c/2}^{T_c/2} \left\{ \begin{aligned} &\sum_{n=-\infty}^{\infty} [(-1)^n J_{2n}(z) \sin(\omega^- t + 2n\vartheta t)] \\ & + \sum_{n=-\infty}^{\infty} \{(-1)^n J_{2n+1}(z) \sin[\omega^- t + (2n+1)\vartheta t]\} \end{aligned} \right\} dt = 0 \quad (\text{B.13})$$

B.2.3 Summary

By substituting Eqn. (B.10) and Eqn. (B.13) into Eqn. (B.8), positive side of the spectrum can be obtained as:

$$F_{s1}^P(\omega) = \frac{a}{2} \sum_{n=-\infty}^{\infty} \left\{ \left[(-1)^n J_{2n}(z) \right] \text{sinc} \left[(\omega + 2n\vartheta) \frac{T_c}{2} \right] \right\} \quad (\text{B.14})$$

By substituting Eqn. (B.3) into Eqn. (B.14), finally, positive side of the spectrum is:

$$F_{s1}^P(\omega) = \frac{a}{2} \sum_{n=-\infty}^{\infty} \left\{ \left[(-1)^n J_{2n} \left(\frac{BT_c}{\Omega} \right) \right] \text{sinc} \left[\frac{(\omega_0 - \omega)T_c}{2} + n\pi\Omega \right] \right\} \quad (\text{B.15})$$

Appendix C: Spectrum of Cosine Chirps

In this appendix, spectrum of cosine chirp is derived. In general, a pair of cosine chirp can be represented as:

$$\begin{cases} c_{C1}(t) = a \cos \left[\omega_0 t + \frac{BT_c}{\Omega} \sin \left(\pi \Omega \frac{t}{T_c} \right) \right] & -\frac{T_c}{2} \leq t \leq \frac{T_c}{2} \\ c_{C2}(t) = a \cos \left[\omega_0 t - \frac{BT_c}{\Omega} \sin \left(\pi \Omega \frac{t}{T_c} \right) \right] & -\frac{T_c}{2} \leq t \leq \frac{T_c}{2} \end{cases} \quad (\text{C.1})$$

The spectrum of cosine chirp signals depicted in Eqn. (C.1) can be obtained by taking the Fourier transform of itself. $c_{C1}(t)$ is taking as an example here for analyze spectral characteristic of cosine chirps.

$$\begin{aligned} F_{C1}(\omega) &= \frac{1}{T_c} \int_{-T_c/2}^{T_c/2} c_{C1}(t) e^{-j\omega t} dt \\ &= \frac{1}{T_c} \int_{-T_c/2}^{T_c/2} a \cos \left[\omega_0 t + \frac{BT_c}{\Omega} \sin \left(\pi \Omega \frac{t}{T_c} \right) \right] \times e^{-j\omega t} dt \end{aligned} \quad (\text{C.2})$$

Let

$$z = \frac{BT_c}{\Omega} \quad \text{and} \quad \vartheta = \frac{\pi \Omega}{T_c} \quad (\text{C.3})$$

Recalling the Euler's formula $e^{-j\omega t} = \cos(\omega t) - j \sin(\omega t)$, Eqn. (C.2) becomes:

$$\begin{aligned} F_{C1}(\omega) &= \frac{1}{T_c} \int_{-T_c/2}^{T_c/2} \left\{ a \cos \left[\omega_0 t + z \sin(\vartheta t) \right] \times \left[\cos(\omega t) - j \sin(\omega t) \right] \right\} dt \\ &= \frac{a}{2T_c} \int_{-T_c/2}^{T_c/2} \left\{ \cos \left[(\omega_0 + \omega) t + z \sin(\vartheta t) \right] + \cos \left[(\omega_0 - \omega) t + z \sin(\vartheta t) \right] \right\} dt \\ &\quad - j \times \frac{a}{2T_c} \int_{-T_c/2}^{T_c/2} \left\{ \sin \left[(\omega_0 + \omega) t + z \sin(\vartheta t) \right] - \sin \left[(\omega_0 - \omega) t + z \sin(\vartheta t) \right] \right\} dt \end{aligned} \quad (\text{C.4})$$

Let

$$\begin{cases} \omega^+ = \omega_0 + \omega \\ \omega^- = \omega_0 - \omega \end{cases} \quad (\text{C.5})$$

then Eqn. (C.4) can be simplified as:

$$\begin{aligned} F_{C1}(\omega) &= \frac{a}{2T_c} \int_{-T_c/2}^{T_c/2} \cos[\omega^+ t + z \sin(\vartheta t)] dt + \frac{a}{2T_c} \int_{-T_c/2}^{T_c/2} \cos[\omega^- t + z \sin(\vartheta t)] dt \\ &\quad - \frac{a}{2T_c} j \left\{ \int_{-T_c/2}^{T_c/2} \sin[\omega^+ t + z \sin(\vartheta t)] dt - \int_{-T_c/2}^{T_c/2} \sin[\omega^- t + z \sin(\vartheta t)] dt \right\} \\ &= \frac{a}{2T_c} \left\{ \int_{-T_c/2}^{T_c/2} \cos[\omega^+ t + z \sin(\vartheta t)] dt - j \int_{-T_c/2}^{T_c/2} \sin[\omega^+ t + z \sin(\vartheta t)] dt \right\} \\ &\quad + \frac{a}{2T_c} \left\{ \int_{-T_c/2}^{T_c/2} \cos[\omega^- t + z \sin(\vartheta t)] dt + j \int_{-T_c/2}^{T_c/2} \sin[\omega^- t + z \sin(\vartheta t)] dt \right\} \\ &= F_{C1}^N(\omega) + F_{C1}^P(\omega) \end{aligned} \quad (\text{C.6})$$

where $F_{C1}^N(\omega)$ is negative side of the spectrum of cosine chirp:

$$F_{C1}^N(\omega) = \frac{a}{2T_c} \left\{ \int_{-T_c/2}^{T_c/2} \cos[\omega^+ t + z \sin(\vartheta t)] dt + j \int_{-T_c/2}^{T_c/2} \sin[\omega^+ t + z \sin(\vartheta t)] dt \right\} \quad (\text{C.7})$$

$F_{C1}^P(\omega)$ is positive side of the spectrum of cosine chirp:

$$F_{C1}^P(\omega) = \frac{a}{2T_c} \left\{ \int_{-T_c/2}^{T_c/2} \cos[\omega^- t + z \sin(\vartheta t)] dt - j \int_{-T_c/2}^{T_c/2} \sin[\omega^- t + z \sin(\vartheta t)] dt \right\} \quad (\text{C.8})$$

C.1 Calculation of the positive side

Only positive side of the spectrum is considered as example, so Eqn. (C.8) can be simplified as:

$$F_{C1}^P(\omega) = \frac{a}{2} \{ F_{C1}^{PR} - j F_{C1}^{PI} \} \quad (\text{C.9})$$

where F_{C1}^{PR} is the real part:

$$F_{C1}^{PR} = \frac{1}{T_c} \int_{-T_c/2}^{T_c/2} \cos[\omega^- t + z \sin(\vartheta t)] dt \quad (C.10)$$

and F_{C1}^{PI} is the image part:

$$F_{C1}^{PI} = \frac{1}{T_c} \int_{-T_c/2}^{T_c/2} \sin[\omega^- t + z \sin(\vartheta t)] dt \quad (C.11)$$

C.1.1 Calculation of the real part

Substituting Eqn. (A.26) into Eqn. (C.10), the real part F_{C1}^{PR} can be obtained as:

$$\begin{aligned} F_{C1}^{PR} &= \frac{1}{T_c} \int_{-T_c/2}^{T_c/2} \sum_{n=-\infty}^{\infty} [J_n(z) \cos(\omega^- t + n\vartheta t)] dt \\ &= \frac{1}{T_c} \sum_{n=-\infty}^{\infty} J_n(z) \times \int_{-T_c/2}^{T_c/2} \cos[(\omega^- + n\vartheta)t] dt \\ &= \frac{1}{T_c} \sum_{n=-\infty}^{\infty} J_n(z) \times \frac{2}{(\omega^- + n\vartheta)} \sin\left[(\omega^- + n\vartheta) \frac{T_c}{2}\right] \\ &= \sum_{n=-\infty}^{\infty} \left\{ J_n(z) \sin\left[(\omega^- + n\vartheta) \frac{T_c}{2}\right] \right\} \end{aligned} \quad (C.12)$$

C.1.2 Calculation of the image part

Substituting Eqn. (A.35) into Eqn. (C.11), the real part F_{C1}^{PI} can be obtained as:

$$\begin{aligned} F_{C1}^{PI} &= \frac{1}{T_c} \int_{-T_c/2}^{T_c/2} \sum_{n=-\infty}^{\infty} [J_n(z) \sin(\omega^- t + n\vartheta t)] dt \\ &= \frac{1}{T_c} \sum_{n=-\infty}^{\infty} J_n(z) \int_{-T_c/2}^{T_c/2} \sin(\omega^- t + n\vartheta t) dt \\ &= 0 \end{aligned} \quad (C.13)$$

C.1.3 Summary

Substituting Eqn. (C.12) and Eqn. (C.13) into Eqn. (C.9), positive side of the spectrum of cosine chirp can be obtained as:

$$F_{Cl}^P(\omega) = \frac{a}{2} \sum_{n=-\infty}^{\infty} \left\{ J_n(z) \sin \left[\left(\omega^- + n\nu \right) \frac{T_c}{2} \right] \right\} \quad (\text{C.14})$$

Again, substituting Eqn. (C.3) and Eqn. (C.5) into Eqn. (C.14), Eqn. (C.14) can be represented as:

$$F_{Cl}^P(\omega) = \frac{a}{2} \sum_{n=-\infty}^{\infty} \left\{ J_n \left(\frac{BT_c}{\Omega} \right) \sin \left[\frac{(\omega_0 - \omega)T_c + n\pi\Omega}{2} \right] \right\} \quad (\text{C.15})$$

Appendix D: Autocorrelation of Sine Chirps

The sine chirp $c_{s1}(t)$ is defined as:

$$c_{s1}(t) = a \cos \left[\omega_0 t + \frac{BT_c}{\Omega} \cos \left(\pi \Omega \frac{t}{T_c} \right) \right] \quad -\frac{T_c}{2} \leq t \leq \frac{T_c}{2} \quad (\text{D.1})$$

Autocorrelation coefficient of $c_{s1}(t)$ can be obtained as:

$$r_s(\tau) = \frac{\int_{-\infty}^{\infty} c_{s1}(t) c_{s1}(t-\tau) dt}{E(c_{s1})} = \frac{R_s(\tau)}{E(c_{s1})} \quad (\text{D.2})$$

where $E(c_{s1})$, which is energy of $c_{s1}(t)$, can be obtained as:

$$E(c_{s1}) = \int_{-T_c/2}^{T_c/2} c_{s1}^2(t) dt = \frac{a^2}{2T_c} \quad (\text{D.3})$$

and

$$R_s(\tau) = a^2 \int_{-\infty}^{\infty} \left\{ \begin{array}{l} \cos \left[\omega_0 t + \frac{BT_c}{\Omega} \cos \left(\pi \Omega \frac{t}{T_c} \right) \right] \\ \times \cos \left[\omega_0 (t-\tau) + \frac{BT_c}{\Omega} \cos \left(\pi \Omega \frac{(t-\tau)}{T_c} \right) \right] \end{array} \right\} dt \quad (\text{D.4})$$

Let

$$z = \frac{BT_c}{\Omega} \quad \text{and} \quad \theta = \frac{\pi \Omega}{2T_c} \quad (\text{D.5})$$

Then Eqn. (D.4) can be represented as:

$$\begin{aligned}
R_s(\tau) &= \int_{-\infty}^{\infty} \left\{ a \cos[\omega_0 t + 2z \cos(2\theta t)] \times a \cos[\omega_0(t-\tau) + z \cos[2\theta(t-\tau)]] \right\} dt \\
&= \frac{1}{2} a^2 \int_{-\infty}^{\infty} \left\{ \begin{aligned} &\cos[2\omega_0 t - \omega_0 \tau + z \cos(2\theta t) + z \cos[2\theta(t-\tau)]] \\ &+ \cos[\omega_0 \tau + z \cos(2\theta t) - z \cos[2\theta(t-\tau)]] \end{aligned} \right\} dt \quad (D.6) \\
&= \frac{1}{2} a^2 \left(\int_{-\infty}^{\infty} \left\{ \begin{aligned} &\cos[2\omega_0 t - \omega_0 \tau + 2z \cos[(2t-\tau)\theta] \cos(\theta\tau)] \\ &+ \cos[\omega_0 \tau - 2z \sin[(2t-\tau)\theta] \sin(\theta\tau)] \end{aligned} \right\} dt \right)
\end{aligned}$$

Let,

$$\begin{cases} k_{S1}^m = 2z \cos(\tau\theta) \\ k_{S2}^m = 2z \sin(\tau\theta) \\ k = (2t - \tau)\theta \end{cases} \quad (D.7)$$

By substituting Eqn. (D.3) and Eqn. (D.6) into Eqn. (D.2), then autocorrelation coefficient of $c_{S1}(t)$ can be obtained as:

$$r_s(\tau) = \frac{1}{T_c} \left(\int_{-\infty}^{\infty} \left\{ \begin{aligned} &\cos[2\omega_0 t - \omega_0 \tau + k_{S1}^m \cos(k)] \\ &+ \cos[\omega_0 \tau - k_{S2}^m \sin(k)] \end{aligned} \right\} dt \right) \quad (D.8)$$

By recalling Eqn. (A.10) and Eqn. (A.26), then Eqn. (D.8) can be rewritten as:

$$\begin{aligned}
r_s(\tau) &= \frac{1}{T_c} \left(\int_{-\infty}^{\infty} \left\{ \begin{aligned} &\sum_{n=-\infty}^{\infty} [(-1)^n J_{2n}(k_{S1}^m) \cos(2\omega_0 t - \omega_0 \tau + 2nk)] \\ &- \sum_{n=-\infty}^{\infty} \{(-1)^n J_{2n+1}(k_{S1}^m) \sin[2\omega_0 t - \omega_0 \tau + (2n+1)k]\} \end{aligned} \right\} dt \\ &\quad + \int_{-\infty}^{\infty} \sum_{n=-\infty}^{\infty} [(-1)^n J_n(k_{S2}^m) \cos(\omega_0 \tau + nk)] dt \end{aligned} \right) \quad (D.9) \\
&= \frac{1}{T_c} \left\{ \begin{aligned} &\sum_{n=-\infty}^{\infty} [(-1)^n J_{2n}(k_{S1}^m)] \times K_{S1}^m \\ &- \sum_{n=-\infty}^{\infty} [(-1)^n J_{2n+1}(k_{S1}^m)] \times K_{S2}^m + \sum_{n=-\infty}^{\infty} [(-1)^n J_n(k_{S2}^m)] \times K_{S3}^m \end{aligned} \right\}
\end{aligned}$$

where

$$\begin{cases} \mathbf{K}_{S1}^m = \int_{-\infty}^{\infty} \cos(2\omega_0 t - \omega_0 \tau + 2nk) dt \\ \mathbf{K}_{S2}^m = \int_{-\infty}^{\infty} \sin[2\omega_0 t - \omega_0 \tau + (2n+1)k] dt \\ \mathbf{K}_{S3}^m = \int_{-\infty}^{\infty} \cos(\omega_0 \tau + nk) dt \end{cases} \quad (\text{D.10})$$

Substituting $k = (2t + \tau)\theta$ defined in Eqn. (D.7) into Eqn. (D.10), Eqn. (D.10) can be rewritten as:

$$\begin{cases} \mathbf{K}_{S1}^m = \int_{-\infty}^{\infty} \cos[2\omega_0 t - \omega_0 \tau + 2n(2t - \tau)\theta] dt \\ \mathbf{K}_{S2}^m = \int_{-\infty}^{\infty} \sin[2\omega_0 t - \omega_0 \tau + (2n+1)(2t - \tau)\theta] dt \\ \mathbf{K}_{S3}^m = \int_{-\infty}^{\infty} \cos[\omega_0 \tau + n(2t - \tau)\theta] dt \end{cases} \quad (\text{D.11})$$

Eqn. (D.11) can be simplified as:

$$\begin{cases} \mathbf{K}_{S1}^m = \int_{-\infty}^{\infty} \cos[(\omega_0 + 2n\theta)(2t - \tau)] dt \\ \mathbf{K}_{S2}^m = \int_{-\infty}^{\infty} \sin[(\omega_0 + 2n\theta + \theta)(2t - \tau)] dt \\ \mathbf{K}_{S3}^m = \int_{-\infty}^{\infty} \cos[2n\theta t + (\omega_0 - n\theta)\tau] dt \end{cases} \quad (\text{D.12})$$

D.1 When $\tau \geq 0$

Since the chirp duration is $-T_c/2 \leq t \leq T_c/2$ shown in Eqn. (D.3), value of $c_{S1}(t)$ when t is out of the duration is zero. Similarly, value of $c_{S1}(t - \tau)$ when $t + \tau$ is out of the duration is also zero. So, the integral range for (D.12) when $\tau \geq 0$ can be calculated as:

$$\begin{cases} -\frac{T_c}{2} \leq t \leq \frac{T_c}{2} \\ -\frac{T_c}{2} \leq (t - \tau) \leq \frac{T_c}{2} \Rightarrow -\frac{T_c}{2} + \tau \leq t \leq \frac{T_c}{2} + \tau \end{cases} \Rightarrow -\frac{T_c}{2} + \tau \leq t \leq \frac{T_c}{2} \quad (\text{D.13})$$

Eqn. (D.12) in the case of $\tau \geq 0$ can be achieved by substituting Eqn. (D.13):

$$\begin{cases} \mathbf{K}_{S1}^{m+} = \int_{-T_c/2+\tau}^{T_c/2} \cos[(\omega_0 + 2n\theta)(2t - \tau)] dt \\ \mathbf{K}_{S2}^{m+} = \int_{-T_c/2+\tau}^{T_c/2-\tau} \sin[(\omega_0 + 2n\theta + \theta)(2t - \tau)] dt \\ \mathbf{K}_{S3}^{m+} = \int_{-T_c/2+\tau}^{T_c/2-\tau} \cos[2n\theta t + (\omega_0 - n\theta)\tau] dt \end{cases} \quad (\text{D.14})$$

Result of the first term in Eqn. (D.14) can be obtained as:

$$\begin{aligned} \mathbf{K}_{S1}^{m+} &= \int_{-T_c/2+\tau}^{T_c/2} \cos[(\omega_0 + 2n\theta)(2t - \tau)] dt \\ &= \frac{1}{2(\omega_0 + 2n\theta)} \sin[(\omega_0 + 2n\theta)(2t - \tau)] \Big|_{-T_c/2+\tau}^{T_c/2} \\ &= \frac{\{\sin[(\omega_0 + 2n\theta)(T_c - \tau)] - \sin[(\omega_0 + 2n\theta)(-T_c + \tau)]\}}{2(\omega_0 + 2n\theta)} \\ &= \frac{\sin[(\omega_0 + 2n\theta)(T_c - \tau)]}{(\omega_0 + 2n\theta)} \end{aligned} \quad (\text{D.15})$$

Result of the second term in Eqn. (D.14) can be obtained as:

$$\begin{aligned} \mathbf{K}_{S2}^{m+} &= \int_{-T_c/2+\tau}^{T_c/2} \sin[(\omega_0 + 2n\theta + \theta)(2t - \tau)] dt \\ &= \frac{-1}{2(\omega_0 + 2n\theta + \theta)} \cos[(\omega_0 + 2n\theta + \theta)(2t - \tau)] \Big|_{-T_c/2+\tau}^{T_c/2} \\ &= \frac{1}{2(\omega_0 + 2n\theta + \theta)} \left\{ \cos[(\omega_0 + 2n\theta + \theta)(T_c - \tau)] \right. \\ &\quad \left. - \cos[(\omega_0 + 2n\theta + \theta)(-T_c + \tau)] \right\} \\ &= 0 \end{aligned} \quad (\text{D.16})$$

Result of the third term in Eqn. (D.14) can be obtained as:

$$\begin{aligned}
\mathbf{K}_{S3}^{m+} &= \int_{-T_c/2+\tau}^{T_c/2} \cos[2n\theta t + (\omega_0 - n\theta)\tau] dt \\
&= \frac{1}{2n\theta} \sin[2n\theta t + (\omega_0 - n\theta)\tau] \Big|_{-T_c/2+\tau}^{T_c/2} \\
&= \frac{1}{2n\theta} \left\{ \begin{array}{l} \sin[n\theta T_c + (\omega_0 - n\theta)\tau] \\ -\sin[n\theta(-T_c + 2\tau) + (\omega_0 - n\theta)\tau] \end{array} \right\} \\
&= \frac{1}{2n\theta} \left\{ 2 \cos(\omega_0\tau) \sin[n\theta(T_c - \tau)] \right\} \\
&= \frac{\cos(\omega_0\tau) \sin[n\theta(T_c - \tau)]}{n\theta}
\end{aligned} \tag{D.17}$$

Then Eqn. (D.14) for $\tau \geq 0$ can be updated by recalling the results shown in Eqn. (D.15), Eqn. (D.16) and Eqn. (D.17):

$$\left\{ \begin{array}{l} \mathbf{K}_{S1}^{m+} = \frac{\sin[(\omega_0 + 2n\theta)(T_c - \tau)]}{(\omega_0 + 2n\theta)} \\ \mathbf{K}_{S2}^{m+} = 0 \\ \mathbf{K}_{S3}^{m+} = \frac{\cos(\omega_0\tau) \sin[n\theta(T_c - \tau)]}{n\theta} \end{array} \right. \tag{D.18}$$

D.2 When $\tau \leq 0$

Since the chirp duration is $-T_c/2 \leq t \leq T_c/2$ shown in Eqn. (D.3), value of $c_{s1}(t)$ when t is out of the duration is zero. Similarly, value of $c_{s1}(t-\tau)$ when $t-\tau$ is out of the duration is also zero. So, the integral range for (D.12) when $\tau \leq 0$ can be calculated as:

$$\left\{ \begin{array}{l} -\frac{T_c}{2} \leq t \leq \frac{T_c}{2} \\ -\frac{T_c}{2} \leq (t-\tau) \leq \frac{T_c}{2} \Rightarrow -\frac{T_c}{2} + \tau \leq t \leq \frac{T_c}{2} + \tau \end{array} \right. \Rightarrow -\frac{T_c}{2} \leq t \leq \frac{T_c}{2} + \tau \tag{D.19}$$

Eqn. (D.12) in the case of $\tau \leq 0$ can be achieved by substituting Eqn. (D.19):

$$\begin{cases} \mathbf{K}_{S1}^{m-} = \int_{-T_c/2}^{T_c/2+\tau} \cos[(\omega_0 + 2n\theta)(2t + \tau)] dt \\ \mathbf{K}_{S2}^{m-} = \int_{-T_c/2}^{T_c/2+\tau} \sin[(\omega_0 + 2n\theta + \theta)(2t + \tau)] dt \\ \mathbf{K}_{S3}^{m-} = \int_{-T_c/2}^{T_c/2+\tau} \cos[2n\theta t + (\omega_0 + n\theta)\tau] dt \end{cases} \quad (\text{D.20})$$

Result of the first term in Eqn. (D.20) can be obtained as:

$$\begin{aligned} \mathbf{K}_{S1}^{m-} &= \int_{-T_c/2}^{T_c/2+\tau} \cos[(\omega_0 + 2n\theta)(2t - \tau)] dt \\ &= \frac{1}{2(\omega_0 + 2n\theta)} \sin[(\omega_0 + 2n\theta)(2t - \tau)] \Big|_{-T_c/2}^{T_c/2+\tau} \\ &= \frac{1}{2(\omega_0 + 2n\theta)} \left\{ \begin{array}{l} \sin[(\omega_0 + 2n\theta)(T_c + \tau)] \\ -\sin[(\omega_0 + 2n\theta)(-T_c - \tau)] \end{array} \right\} \\ &= \frac{\sin[(\omega_0 + 2n\theta)(T_c + \tau)]}{(\omega_0 + 2n\theta)} \end{aligned} \quad (\text{D.21})$$

Result of the second term in Eqn. (D.20) can be obtained as:

$$\begin{aligned} \mathbf{K}_{S2}^{m-} &= \int_{-T_c/2}^{T_c/2+\tau} \sin[(\omega_0 + 2n\theta + \theta)(2t - \tau)] dt \\ &= \frac{-1}{2(\omega_0 + 2n\theta + \theta)} \cos[(\omega_0 + 2n\theta + \theta)(2t - \tau)] \Big|_{-T_c/2}^{T_c/2+\tau} \\ &= \frac{1}{2(\omega_0 + 2n\theta + \theta)} \left\{ \begin{array}{l} \cos[(\omega_0 + 2n\theta + \theta)(T_c + \tau)] \\ -\cos[(\omega_0 + 2n\theta + \theta)(-T_c - \tau)] \end{array} \right\} \\ &= 0 \end{aligned} \quad (\text{D.22})$$

Result of the third term in Eqn. (D.20) can be obtained as:

$$\begin{aligned}
\mathbf{K}_{S3}^{m-} &= \int_{-T_c/2+\tau}^{T_c/2} \cos[2n\theta t + (\omega_0 - n\theta)\tau] dt \\
&= \frac{1}{2n\theta} \sin[2n\theta t + (\omega_0 - n\theta)\tau] \Big|_{-T_c/2}^{T_c/2+\tau} \\
&= \frac{1}{2n\theta} \left\{ \begin{array}{l} \sin[n\theta(T_c + 2\tau) + (\omega_0 - n\theta)\tau] \\ -\sin[-n\theta T_c + (\omega_0 - n\theta)\tau] \end{array} \right\} \\
&= \frac{1}{2n\theta} \{2\cos(\omega_0\tau)\sin[n\theta(T_c + \tau)]\} \\
&= \frac{\cos(\omega_0\tau)\sin[n\theta(T_c + \tau)]}{n\theta}
\end{aligned} \tag{D.23}$$

Then Eqn. (D.14) for $\tau \leq 0$ can be updated by substituting the results shown in Eqn. (D.21), Eqn. (D.22) and Eqn. (D.23):

$$\left\{ \begin{array}{l} \mathbf{K}_{S1}^{m-} = \frac{\sin[(\omega_0 + 2n\theta)(T_c + \tau)]}{(\omega_0 + 2n\theta)} \\ \mathbf{K}_{S2}^{m-} = 0 \\ \mathbf{K}_{S3}^{m-} = \frac{\cos(\omega_0\tau)\sin[n\theta(T_c + \tau)]}{n\theta} \end{array} \right. \tag{D.24}$$

Combing Eqn. (D.18) and Eqn. (D.24), a uniform representation for Eqn. (D.12) when $\tau \geq 0$ or $\tau \leq 0$ can be given:

$$\left\{ \begin{array}{l} \mathbf{K}_{S1}^m = \frac{\sin[(\omega_0 + 2n\theta)(T_c - |\tau|)]}{(\omega_0 + 2n\theta)} \\ \mathbf{K}_{S2}^m = 0 \\ \mathbf{K}_{S3}^m = \frac{\cos(\omega_0\tau)\sin[n\theta(T_c - |\tau|)]}{n\theta} \end{array} \right. \tag{D.25}$$

D.3 Summary

Substituting Eqn. (D.25) into Eqn. (D.9), autocorrelation coefficient of sine chirp $r_s(\tau)$ can be represented as:

$$\begin{aligned}
r_s(\tau) &= \frac{1}{T_c} \left\{ \sum_{n=-\infty}^{\infty} [(-1)^n J_{2n}(k_{S1}^m)] \times \mathbf{K}_{S1}^m - \sum_{n=-\infty}^{\infty} [(-1)^n J_{2n+1}(k_{S1}^m)] \times \mathbf{K}_{S2}^m \right. \\
&\quad \left. + \sum_{n=-\infty}^{\infty} [(-1)^n J_n(k_{S2}^m)] \times \mathbf{K}_{S3}^m \right\} \\
&= \sum_{n=-\infty}^{\infty} [(-1)^n J_{2n}(k_{S1}^m)] \frac{\sin[(\omega_0 + 2n\theta)(T_c - |\tau|)]}{(\omega_0 + 2n\theta)T_c} \\
&\quad + \cos(\omega_0\tau) \sum_{n=-\infty}^{\infty} [(-1)^n J_n(k_{S2}^m)] \frac{\sin[n\theta(T_c - |\tau|)]}{n\theta T_c}
\end{aligned} \tag{D.26}$$

Eqn. (D.26) can be rewritten in form of sinc function as follows:

$$\begin{aligned}
r_s(\tau) &= \left(1 - \frac{|\tau|}{T_c}\right) \sum_{n=-\infty}^{\infty} [(-1)^n J_{2n}(k_{S1}^m)] \text{sinc}[(\omega_0 + 2n\theta)(T_c - |\tau|)] \\
&\quad + \left(1 - \frac{|\tau|}{T_c}\right) \cos(\omega_0\tau) \sum_{n=-\infty}^{\infty} [(-1)^n J_n(k_{S2}^m)] \text{sinc}[n\theta(T_c - |\tau|)]
\end{aligned} \tag{D.27}$$

Recalling Eqn. (A.37), autocorrelation coefficient of sine chirp $r_s(\tau)$ can be achieved as:

$$\begin{aligned}
r_s(\tau) &= \left(1 - \frac{|\tau|}{T_c}\right) \sum_{n=-\infty}^{\infty} \left\{ (-1)^n J_{2n}(k_{S1}^m) \text{sinc}[(\omega_0 + 2n\theta)(T_c - |\tau|)] \right\} \\
&\quad + \left(1 - \frac{|\tau|}{T_c}\right) \cos(\omega_0\tau) J_0(k_{S2}^m) \\
&\quad + 2 \left(1 - \frac{|\tau|}{T_c}\right) \cos(\omega_0\tau) \sum_{n=1}^{\infty} \left\{ J_{2n}(k_{S2}^m) \text{sinc}[2n\theta(T_c - |\tau|)] \right\}
\end{aligned} \tag{D.28}$$

$$\text{where } \theta = \frac{\pi\Omega}{2T_c}; \quad k_{S1}^m = \frac{2BT_c}{\Omega} \cos\left(\frac{\pi\Omega}{2T_c} \tau\right); \quad k_{S2}^m = \frac{2BT_c}{\Omega} \sin\left(\frac{\pi\Omega}{2T_c} \tau\right).$$

Appendix E: Autocorrelation of Cosine Chirps

The cosine chirp $c_{c1}(t)$ is defined as:

$$c_{c1}(t) = a \cos \left[\omega_0 t + \frac{BT_c}{\Omega} \sin \left(\pi \Omega \frac{t}{T_c} \right) \right] \quad -\frac{T_c}{2} \leq t \leq \frac{T_c}{2} \quad (\text{E.1})$$

Autocorrelation coefficient of $c_{c1}(t)$ can be obtained as:

$$r_c(\tau) = \frac{\int_{-\infty}^{\infty} c_{c1}(t)c_{c1}(t-\tau) dt}{E(c_{c1})} = \frac{R_c(\tau)}{E(c_{c1})} \quad (\text{E.2})$$

where $E(c_{c1})$, which is energy of $c_{c1}(t)$, can be obtained as:

$$E(c_{c1}) = \int_{-T_c/2}^{T_c/2} c_{c1}^2(t) dt = \frac{a^2}{2T_c} \quad (\text{E.3})$$

and

$$R_c(\tau) = a^2 \int_{-\infty}^{\infty} \left\{ \begin{array}{l} \cos \left[\omega_0 t + \frac{BT_c}{\Omega} \sin \left(\pi \Omega \frac{t}{T_c} \right) \right] \\ \times \cos \left[\omega_0 (t-\tau) + \frac{BT_c}{\Omega} \sin \left(\pi \Omega \frac{(t-\tau)}{T_c} \right) \right] \end{array} \right\} dt \quad (\text{E.4})$$

Let

$$z = \frac{BT_c}{\Omega} \quad \text{and} \quad \theta = \frac{\pi \Omega}{2T_c} \quad (\text{E.5})$$

Then Eqn. (E.5) can be represented as:

$$\begin{aligned}
R_c(\tau) &= \int_{-\infty}^{\infty} \left\{ a \cos[\omega_0 t + 2z \sin(2\theta t)] \times a \cos[\omega_0(t-\tau) + z \sin[2\theta(t-\tau)]] \right\} dt \\
&= \frac{1}{2} a^2 \int_{-\infty}^{\infty} \left\{ \cos[2\omega_0 t - \omega_0 \tau + z \sin(2\theta t) + z \sin[2\theta(t-\tau)]] \right. \\
&\quad \left. + \cos[\omega_0 \tau + z \sin(2\theta t) - z \sin[2\theta(t-\tau)]] \right\} dt \tag{E.6} \\
&= \frac{1}{2} a^2 \left(\int_{-\infty}^{\infty} \left\{ \cos[2\omega_0 t - \omega_0 \tau + 2z \sin[(2t-\tau)\theta] \cos(\theta\tau)] \right\} dt \right. \\
&\quad \left. + \int_{-\infty}^{\infty} \left\{ \cos[\omega_0 \tau + 2z \cos[(2t-\tau)\theta] \sin(\theta\tau)] \right\} dt \right)
\end{aligned}$$

Let,

$$\begin{cases} k_{C1}^m = 2z \cos(\theta\tau) = \frac{2BT_c}{\Omega} \cos\left(\frac{\pi\Omega}{2T_c} \tau\right) \\ k_{C2}^m = 2z \sin(\theta\tau) = \frac{2BT_c}{\Omega} \cos\left(\frac{\pi\Omega}{2T_c} \tau\right) \\ k = (2t - \tau)\theta \end{cases} \tag{E.7}$$

Then Eqn. (E.7) can be represented as:

$$R_c(\tau) = \frac{1}{2} a^2 \left(\int_{-\infty}^{\infty} \left\{ \cos[2\omega_0 t - \omega_0 \tau + k_{C1}^m \sin(k)] \right\} dt \right. \tag{E.8} \\
\left. + \int_{-\infty}^{\infty} \left\{ \cos[\omega_0 \tau + k_{C2}^m \cos(k)] \right\} dt \right)$$

By substituting Eqn. (E.3) and Eqn. (E.8) into Eqn. (E.2), then autocorrelation coefficient of $c_{C1}(t)$ can be obtained as:

$$r_c(\tau) = \frac{1}{T_c} \left(\int_{-\infty}^{\infty} \left\{ \cos[2\omega_0 t - \omega_0 \tau + k_{C1}^m \sin(k)] \right\} dt \right. \tag{E.9} \\
\left. + \int_{-\infty}^{\infty} \left\{ \cos[\omega_0 \tau + k_{C2}^m \cos(k)] \right\} dt \right)$$

By recalling Eqn. (A.26) and Eqn. (A.10), then Eqn. (E.9) can be rewritten as:

$$\begin{aligned}
r_c(\tau) &= \frac{1}{T_c} \left(\int_{-\infty}^{\infty} \left\{ \sum_{n=-\infty}^{\infty} \left[J_n(k_{C1}^m) \cos(2\omega_0 t - \omega_0 \tau + nk) \right] \right\} dt \right. \\
&\quad \left. + \int_{-\infty}^{\infty} \left\{ \begin{aligned} &\sum_{n=-\infty}^{\infty} \left[(-1)^n J_{2n}(k_{C2}^m) \cos(\omega_0 \tau + 2nk) \right] \\ &- \sum_{n=-\infty}^{\infty} \left\{ (-1)^n J_{2n+1}(k_{C2}^m) \sin[\omega_0 \tau + (2n+1)k] \right\} \end{aligned} \right\} dt \right) \quad (E.10) \\
&= \frac{1}{T_c} \left\{ \begin{aligned} &\sum_{n=-\infty}^{\infty} J_n(k_{C1}^m) \times \mathbf{K}_{C1}^m \\ &+ \sum_{n=-\infty}^{\infty} \left[(-1)^n J_{2n}(k_{C2}^m) \right] \times \mathbf{K}_{C2}^m + \sum_{n=-\infty}^{\infty} \left[(-1)^n J_{2n+1}(k_{C2}^m) \right] \times \mathbf{K}_{C3}^m \end{aligned} \right\}
\end{aligned}$$

where

$$\begin{cases} \mathbf{K}_{C1}^m = \int_{-\infty}^{\infty} \cos(2\omega_0 t - \omega_0 \tau + nk) dt \\ \mathbf{K}_{C2}^m = \int_{-\infty}^{\infty} \cos(\omega_0 \tau + 2nk) dt \\ \mathbf{K}_{C3}^m = - \int_{-\infty}^{\infty} \sin[\omega_0 \tau + (2n+1)k] dt \end{cases} \quad (E.11)$$

Substituting $k = (2t + \tau)\theta$ defined in Eqn. (E.7) into Eqn. (E.11), Eqn. (E.11) can be rewritten as:

$$\begin{cases} \mathbf{K}_{C1}^m = \int_{-\infty}^{\infty} \cos[2\omega_0 t + \omega_0 \tau + n(2t - \tau)\theta] dt \\ \mathbf{K}_{C2}^m = \int_{-\infty}^{\infty} \cos[\omega_0 \tau + 2n(2t - \tau)\theta] dt \\ \mathbf{K}_{C3}^m = - \int_{-\infty}^{\infty} \sin[\omega_0 \tau + (2n+1)(2t - \tau)\theta] dt \end{cases} \quad (E.12)$$

Eqn. (E.12) can be simplified as:

$$\begin{cases} \mathbf{K}_{C1}^m = \int_{-\infty}^{\infty} \cos[(\omega_0 + n\theta)(2t - \tau)] dt \\ \mathbf{K}_{C2}^m = \int_{-\infty}^{\infty} \cos[4n\theta t + (\omega_0 - 2n\theta)\tau] dt \\ \mathbf{K}_{C3}^m = - \int_{-\infty}^{\infty} \sin[2(2n+1)\theta t + (\omega_0 - 2n\theta - \theta)\tau] dt \end{cases} \quad (E.13)$$

E.1 When $\tau \geq 0$

Since the chirp duration is $-T_c/2 \leq t \leq T_c/2$ shown in Eqn. (E.1), value of $c_{C1}(t)$ when t is out of the duration is zero. Similarly, value of $c_{C1}(t-\tau)$ when $t-\tau$ is out of the duration is also zero. So, the integral range for Eqn. (E.13) when $\tau \geq 0$ can be calculated as:

$$\begin{cases} -\frac{T_c}{2} \leq t \leq \frac{T_c}{2} \\ -\frac{T_c}{2} \leq (t-\tau) \leq \frac{T_c}{2} \Rightarrow -\frac{T_c}{2} + \tau \leq t \leq \frac{T_c}{2} + \tau \end{cases} \Rightarrow -\frac{T_c}{2} + \tau \leq t \leq \frac{T_c}{2} \quad (\text{E.14})$$

Eqn. (E.13) in the case of $\tau \geq 0$ can be achieved by substituting Eqn. (E.14):

$$\begin{cases} \mathbf{K}_{C1}^{m+} = \int_{-T_c/2+\tau}^{T_c/2} \cos[(\omega_0 + n\theta)(2t - \tau)] dt \\ \mathbf{K}_{C2}^{m+} = \int_{-T_c/2+\tau}^{T_c/2} \cos[4n\theta t + (\omega_0 - 2n\theta)\tau] dt \\ \mathbf{K}_{C3}^{m+} = -\int_{-T_c/2+\tau}^{T_c/2} \sin[2(2n+1)\theta t + (\omega_0 - 2n\theta - \theta)\tau] dt \end{cases} \quad (\text{E.15})$$

Result of the first term in Eqn. (E.15) can be obtained as:

$$\begin{aligned} \mathbf{K}_{C1}^{m+} &= \int_{-T_c/2+\tau}^{T_c/2} \cos[(\omega_0 + n\theta)(2t - \tau)] dt \\ &= \frac{1}{2(\omega_c + n\theta)} \sin[(\omega_0 + n\theta)(2t - \tau)] \Big|_{-T_c/2+\tau}^{T_c/2} \\ &= \frac{1}{2(\omega_c + n\theta)} \left\{ \sin[(\omega_0 + n\theta)(T_c - \tau)] - \sin[(\omega_0 + n\theta)(-T_c + \tau)] \right\} \\ &= \frac{\sin[(\omega_0 + n\theta)(T_c - \tau)]}{(\omega_0 + n\theta)} \end{aligned} \quad (\text{E.16})$$

Result of the second term in Eqn. (E.15) can be obtained as:

$$\begin{aligned}
\mathbf{K}_{C2}^{m+} &= \int_{-T_c/2+\tau}^{T_c/2} \cos[4n\theta t + (\omega_0 - 2n\theta)\tau] dt \\
&= \frac{1}{4n\theta} \sin[4n\theta t + (\omega_0 - 2n\theta)\tau] \Big|_{-T_c/2+\tau}^{T_c/2} \\
&= \frac{1}{4n\theta} \left\{ \begin{aligned} &\sin[2n\theta T_c + (\omega_0 - 2n\theta)\tau] \\ &-\sin[2n\theta(-T_c + 2\tau) + (\omega_0 - 2n\theta)\tau] \end{aligned} \right\} \\
&= \frac{\cos(\omega_0\tau) \sin[2n\theta(T_c - \tau)]}{2n\theta}
\end{aligned} \tag{E.17}$$

Result of the third term in Eqn. (E.15) can be obtained as:

$$\begin{aligned}
\mathbf{K}_{C3}^{m+} &= - \int_{-T_c+\tau}^{T_c/2} \sin[2(2n+1)\theta t + (\omega_0 - 2n\theta - \theta)\tau] dt \\
&= \frac{1}{2(2n+1)\theta} \cos[2(2n+1)\theta t + (\omega_0 - 2n\theta - \theta)\tau] \Big|_{-T_c+\tau}^{T_c/2} \\
&= \frac{1}{2(2n+1)\theta} \left\{ \begin{aligned} &\cos[(2n+1)\theta T_c + (\omega_0 - 2n\theta - \theta)\tau] \\ &-\cos[(2n+1)\theta(-T_c + 2\tau) + (\omega_0 - 2n\theta - \theta)\tau] \end{aligned} \right\} \\
&= \frac{1}{2(2n+1)\theta} \{-2\sin(\omega_0\tau) \sin[(2n+1)\theta(T_c - \tau)]\} \\
&= - \frac{\sin(\omega_0\tau) \sin[(2n+1)\theta(T_c - \tau)]}{(2n+1)\theta}
\end{aligned} \tag{E.18}$$

Then Eqn. (E.15) for $\tau \geq 0$ can be updated by recalling the results shown in Eqn. (E.16), Eqn. (E.17) and Eqn. (E.18):

$$\left\{ \begin{aligned} \mathbf{K}_{C1}^{m+} &= \frac{\sin[(\omega_0 + n\theta)(T_c - \tau)]}{(\omega_c + n\theta)} \\ \mathbf{K}_{C2}^{m+} &= \frac{\cos(\omega_0\tau) \sin[2n\theta(T_c - \tau)]}{2n\theta} \\ \mathbf{K}_{C3}^{m+} &= - \frac{\sin(\omega_0\tau) \sin[(2n+1)\theta(T_c - \tau)]}{(2n+1)\theta} \end{aligned} \right. \tag{E.19}$$

E.2 When $\tau \leq 0$

Since the chirp duration is $-T_c/2 \leq t \leq T_c/2$ shown in Eqn. (E.1), value of $c_{C1}(t)$ when t is out of the duration is zero. Similarly, value of $c_{C1}(t-\tau)$ when $t-\tau$ is out of the duration is also zero. So, the integral range for Eqn. (E.13) when $\tau \leq 0$ can be calculated as:

$$\begin{cases} -\frac{T_c}{2} \leq t \leq \frac{T_c}{2} \\ -\frac{T_c}{2} \leq (t-\tau) \leq \frac{T_c}{2} \Rightarrow -\frac{T_c}{2} + \tau \leq t \leq \frac{T_c}{2} + \tau \end{cases} \Rightarrow -\frac{T_c}{2} \leq t \leq \frac{T_c}{2} + \tau \quad (\text{E.20})$$

Eqn. (E.13) in the case of $\tau \leq 0$ can be achieved by substituting Eqn. (E.20):

$$\begin{cases} \mathbf{K}_{C1}^{m-} = \int_{-T_c/2}^{T_c/2+\tau} \cos[(\omega_0 + n\theta)(2t - \tau)] dt \\ \mathbf{K}_{C2}^{m-} = \int_{-T_c/2}^{T_c/2+\tau} \cos[4n\theta t + (\omega_0 - 2n\theta)\tau] dt \\ \mathbf{K}_{C3}^{m-} = -\int_{-T_c/2}^{T_c/2+\tau} \sin[2(2n+1)\theta t + (\omega_0 - 2n\theta - \theta)\tau] dt \end{cases} \quad (\text{E.21})$$

Result of the first term in Eqn. (E.21) can be obtained as:

$$\begin{aligned} \mathbf{K}_{C1}^{m-} &= \int_{-T_c/2}^{T_c/2+\tau} \cos[(\omega_0 + n\theta)(2t - \tau)] dt \\ &= \frac{1}{2(\omega_0 + n\theta)} \sin[(\omega_0 + n\theta)(2t - \tau)] \Big|_{-T_c/2}^{T_c/2+\tau} \\ &= \frac{1}{2(\omega_0 + n\theta)} \left\{ \sin[(\omega_0 + n\theta)(T_c + \tau)] - \sin[(\omega_0 + n\theta)(-T_c - \tau)] \right\} \\ &= \frac{\sin[(\omega_0 + n\theta)(T_c + \tau)]}{(\omega_0 + n\theta)} \end{aligned} \quad (\text{E.22})$$

Result of the second term in Eqn. (E.21) can be obtained as:

$$\begin{aligned}
\mathbf{K}_{C2}^{m-} &= \int_{-T_c/2}^{T_c/2+\tau} \cos[4n\theta t + (\omega_0 - 2n\theta)\tau] dt \\
&= \frac{1}{4n\theta} \sin[4n\theta t + (\omega_0 - 2n\theta)\tau] \Big|_{-T_c/2}^{T_c/2+\tau} \\
&= \frac{1}{4n\theta} \left\{ \begin{array}{l} \sin[2n\theta(T_c + 2\tau) + (\omega_0 - 2n\theta)\tau] \\ -\sin[-2n\theta T_c + (\omega_0 - 2n\theta)\tau] \end{array} \right\} \\
&= \frac{\cos(\omega_0\tau) \sin[2n\theta(T_c + \tau)]}{2n\theta}
\end{aligned} \tag{E.23}$$

Result of the third term in Eqn. (E.21) can be obtained as:

$$\begin{aligned}
\mathbf{K}_{C3}^{m-} &= - \int_{-T_c/2}^{T_c/2+\tau} \sin[2(2n+1)\theta t + (\omega_0 - 2n\theta - \theta)\tau] dt \\
&= \frac{1}{2(2n+1)\theta} \cos[2(2n+1)\theta t + (\omega_0 - 2n\theta - \theta)\tau] \Big|_{-T_c/2}^{T_c/2+\tau} \\
&= \frac{1}{2(2n+1)\theta} \left\{ \begin{array}{l} \cos[(2n+1)\theta(T_c + 2\tau) + (\omega_0 - 2n\theta - \theta)\tau] \\ -\cos[-(2n+1)\theta T_c + (\omega_0 - 2n\theta - \theta)\tau] \end{array} \right\} \\
&= \frac{1}{2(2n+1)\theta} \left\{ -2 \sin(\omega_0\tau) \sin[(2n+1)\theta(T_c + \tau)] \right\} \\
&= - \frac{\sin(\omega_0\tau) \sin[(2n+1)\theta(T_c + \tau)]}{(2n+1)\theta}
\end{aligned} \tag{E.24}$$

Then Eqn. (E.15) for $\tau \leq 0$ can be updated by substituting the results shown in Eqn. (E.22), Eqn. (E.23) and Eqn. (E.24):

$$\left\{ \begin{array}{l} \mathbf{K}_{C1}^{m-} = \frac{\sin[(\omega_0 + n\theta)(T_c + \tau)]}{(\omega_0 + n\theta)} \\ \mathbf{K}_{C2}^{m-} = \frac{\cos(\omega_0\tau) \sin[2n\theta(T_c + \tau)]}{2n\theta} \\ \mathbf{K}_{C3}^{m-} = - \frac{\sin(\omega_0\tau) \sin[(2n+1)\theta(T_c + \tau)]}{(2n+1)\theta} \end{array} \right. \tag{E.25}$$

Combing Eqn. (E.19) and Eqn. (E.25), a uniform representation for Eqn. (E.13) when $\tau \geq 0$ or $\tau \leq 0$ can be given:

$$\left\{ \begin{array}{l} \mathbf{K}_{C1}^m = \frac{\sin[(\omega_0 + n\theta)(T_c - |\tau|)]}{(\omega_0 + n\theta)} \\ \mathbf{K}_{C2}^m = \frac{\cos(\omega_0\tau) \sin[2n\theta(T_c - |\tau|)]}{2n\theta} \\ \mathbf{K}_{C3}^m = -\frac{\sin(\omega_0\tau) \sin[(2n+1)\theta(T_c - |\tau|)]}{(2n+1)\theta} \end{array} \right. \quad (\text{E.26})$$

E.3 Summary

Substituting Eqn. (E.26) into Eqn. (E.10), autocorrelation coefficient of cosine chirp $c_{C1}(t)$ can be represented as:

$$\begin{aligned} r_c(\tau) &= \sum_{n=-\infty}^{\infty} J_n(k_{C1}^m) \frac{\sin[(\omega_0 + n\theta)(T_c - |\tau|)]}{(\omega_0 + n\theta)T_c} \\ &+ \sum_{n=-\infty}^{\infty} [(-1)^n J_{2n}(k_{C2}^m)] \frac{\cos(\omega_0\tau) \sin[2n\theta(T_c - |\tau|)]}{2n\theta T_c} \\ &- \sum_{n=-\infty}^{\infty} [(-1)^n J_{2n+1}(k_{C2}^m)] \frac{\sin(\omega_0\tau) \sin[(2n+1)\theta(T_c - |\tau|)]}{(2n+1)\theta T_c} \end{aligned} \quad (\text{E.27})$$

$$\text{where } \theta = \frac{\pi\Omega}{2T_c}; k_{C1}^m = \frac{2BT_c}{\Omega} \cos\left(\frac{\pi\Omega}{2T_c}\tau\right); k_{C2}^m = \frac{2BT_c}{\Omega} \sin\left(\frac{\pi\Omega}{2T_c}\tau\right).$$

Eqn. (E.27) can be rewritten in form of sinc function as follows:

$$\begin{aligned} r_c(\tau) &= \left(1 - \frac{|\tau|}{T_c}\right) \sum_{n=-\infty}^{\infty} J_n(k_{C1}^m) \text{sinc}[(\omega_0 + n\theta)(T_c - |\tau|)] \\ &+ \cos(\omega_0\tau) \left(1 - \frac{|\tau|}{T_c}\right) \sum_{n=-\infty}^{\infty} [(-1)^n J_{2n}(k_{C2}^m)] \text{sinc}[2n\theta(T_c - |\tau|)] \\ &- \sin(\omega_0\tau) \left(1 - \frac{|\tau|}{T_c}\right) \sum_{n=-\infty}^{\infty} [(-1)^n J_{2n+1}(k_{C2}^m)] \text{sinc}[(2n+1)\theta(T_c - |\tau|)] \end{aligned} \quad (\text{E.28})$$

Recalling Eqn. (A.39) and Eqn. (A.41), autocorrelation coefficient of sine chirp $r_c(\tau)$ can be achieved as:

$$\begin{aligned}
 r_c(\tau) = & \left(1 - \frac{|\tau|}{T_c}\right) \sum_{n=-\infty}^{\infty} \left\{ J_n(k_{C1}^m) \operatorname{sinc}[(\omega_0 + n\theta)(T_c - |\tau|)] \right\} \\
 & + \cos(\omega_0\tau) \left(1 - \frac{|\tau|}{T_c}\right) J_0(k_{C2}^m) \\
 & + 2\cos(\omega_0\tau) \left(1 - \frac{|\tau|}{T_c}\right) \sum_{n=1}^{\infty} \left\{ (-1)^n J_{2n}(k_{C2}^m) \operatorname{sinc}[2n\theta(T_c - |\tau|)] \right\} \\
 & - 2\sin(\omega_0\tau) \left(1 - \frac{|\tau|}{T_c}\right) \sum_{n=0}^{\infty} \left\{ (-1)^n J_{2n+1}(k_{C2}^m) \operatorname{sinc}[(2n+1)\theta(T_c - |\tau|)] \right\}
 \end{aligned} \tag{E.29}$$

$$\text{where } \theta = \frac{\pi\Omega}{2T_c}; k_{C1}^m = \frac{2BT_c}{\Omega} \cos\left(\frac{\pi\Omega}{2T_c}\tau\right); k_{C2}^m = \frac{2BT_c}{\Omega} \sin\left(\frac{\pi\Omega}{2T_c}\tau\right).$$

Appendix F: Cross-correlation of Sine Chirps

Cross-correlation coefficient of sine chirps can be obtained as:

$$\rho_s(\tau) = \frac{\int_{-\infty}^{\infty} c_{s1}(t)c_{s2}(t-\tau) dt}{\sqrt{R_{11}(0) \times R_{22}(0)}} = \frac{C_s(\tau)}{\sqrt{R_{11}(0) \times R_{22}(0)}} \quad (\text{F.1})$$

In Eqn. (F.1), $R_{11}(0)$, which is autocorrelation of sine chirp $c_{s1}(t)$ when the time shift equals zero, can be given as:

$$R_{11}(0) = \frac{a^2}{2T_c} \quad (\text{F.2})$$

In Eqn. (F.1), $R_{22}(0)$, which is autocorrelation of sine chirp $c_{s2}(t)$ when the time shift equals zero, can be similarly obtained as:

$$R_{22}(0) = \frac{a^2}{2T_c} \quad (\text{F.3})$$

In Eqn. (F.1), $C_s(\tau)$, which is cross-correlation between $c_{s1}(t)$ and $c_{s2}(t)$, can be represented as:

$$C_s(\tau) = \int_{-\infty}^{\infty} \left\{ \begin{array}{l} a \cos \left[\omega_0 t + \frac{BT_c}{\Omega} \cos \left(\pi \Omega \frac{t}{T_c} \right) \right] \\ \times a \cos \left[\omega_0 (t-\tau) - \frac{BT_c}{\Omega} \cos \left(\pi \Omega \frac{(t-\tau)}{T_c} \right) \right] \end{array} \right\} dt \quad (\text{F.4})$$

Let

$$z = \frac{BT_c}{\Omega} \quad \text{and} \quad \theta = \frac{\pi \Omega}{2T_c} \quad (\text{F.5})$$

Then Eqn. (F.4) becomes:

$$\begin{aligned}
C_s(\tau) &= \int_{-\infty}^{\infty} \left\{ a \cos[\omega_0 t + z \cos(2\theta t)] \times a \cos[\omega_0(t-\tau) - z \cos(2\theta(t-\tau))] \right\} dt \\
&= \frac{1}{2} a^2 \int_{-\infty}^{\infty} \left\{ \cos[2\omega_0 t - \omega_0 \tau + z \cos(2\theta t) - z \cos(2\theta(t-\tau))] \right. \\
&\quad \left. + \cos[\omega_0 \tau + z \cos(2\theta t) + z \cos(2\theta(t-\tau))] \right\} dt \quad (F.6) \\
&= \frac{1}{2} a^2 \int_{-\infty}^{\infty} \left\{ \cos[2\omega_0 t - \omega_0 \tau - 2z \sin(\theta(2t-\tau)) \sin(\theta\tau)] \right. \\
&\quad \left. + \cos[\omega_0 \tau + 2z \cos(\theta(2t-\tau)) \cos(\theta\tau)] \right\} dt
\end{aligned}$$

Let,

$$\begin{cases}
k_{s1}'' = 2z \sin(\tau\theta) = \frac{2BT_c}{\Omega(s)} \sin(\tau\theta) \\
k_{s2}'' = 2z \cos(\tau\theta) = \frac{2BT_c}{\Omega(s)} \cos(\tau\theta) \\
k = (2t - \tau)\theta
\end{cases} \quad (F.7)$$

Then Eqn. (F.6) becomes:

$$C_s(\tau) = \frac{1}{2} a^2 \int_{-\infty}^{\infty} \left\{ \cos[2\omega_0 t - \omega_0 \tau - k_{s1}'' \sin(k)] + \cos[\omega_0 \tau + k_{s2}'' \cos(k)] \right\} dt \quad (F.8)$$

By substituting Eqn. (F.2), Eqn. (F.3), and Eqn. (F.8), then cross-correlation coefficient of sine chirps defined in Eqn. (F.1) can be written as:

$$\rho_s(\tau) = \frac{1}{T_c} \int_{-\infty}^{\infty} \left\{ \cos[2\omega_0 t - \omega_0 \tau - k_{s1}'' \sin(k)] + \cos[\omega_0 \tau + k_{s2}'' \cos(k)] \right\} dt \quad (F.9)$$

By recalling Eqn. (A.35), then Eqn. (F.9) can be obtained as:

$$\begin{aligned}
\rho_s(\tau) &= \frac{1}{T_c} \left(\int_{-\infty}^{\infty} \sum_{n=-\infty}^{\infty} \left[(-1)^n J_n(k_{S1}^u) \cos(2\omega_0 t - \omega_c \tau + nk) \right] dt \right. \\
&\quad \left. + \int_{-\infty}^{\infty} \left\{ \sum_{n=-\infty}^{\infty} \left[(-1)^n J_{2n}(k_{S2}^u) \cos(\omega_0 \tau + 2nk) \right] \right. \right. \\
&\quad \left. \left. - \sum_{n=-\infty}^{\infty} \left\{ (-1)^n J_{2n+1}(k_{S2}^u) \sin[\omega_0 \tau + (2n+1)k] \right\} \right\} dt \right) \quad (F.10) \\
&= \frac{1}{T_c} \left\{ \sum_{n=-\infty}^{\infty} \left[(-1)^n J_n(k_{S1}^u) \right] \times K_{S1}^u \right. \\
&\quad \left. + \sum_{n=-\infty}^{\infty} \left[(-1)^n J_{2n}(k_{S2}^u) \right] \times K_{S2}^u - \sum_{n=-\infty}^{\infty} \left[(-1)^n J_{2n+1}(k_{S2}^u) \right] \times K_{S3}^u \right\}
\end{aligned}$$

where

$$\begin{cases}
K_{S1}^u = \int_{-\infty}^{\infty} \cos(2\omega_0 t - \omega_c \tau + nk) dt \\
K_{S2}^u = \int_{-\infty}^{\infty} \cos(\omega_0 \tau + 2nk) dt \\
K_{S3}^u = \int_{-\infty}^{\infty} \sin[\omega_0 \tau + (2n+1)k] dt
\end{cases} \quad (F.11)$$

By substituting $k = (2t + \tau)\theta$ defined in Eqn. (F.7), then Eqn. (F.11) can be rewritten

as:

$$\begin{cases}
K_{S1}^u = \int_{-\infty}^{\infty} \cos[2\omega_0 t - \omega_0 \tau + n(2t - \tau)\theta] dt \\
K_{S2}^u = \int_{-\infty}^{\infty} \cos[\omega_0 \tau + 2n(2t - \tau)\theta] dt \\
K_{S3}^u = \int_{-\infty}^{\infty} \sin[\omega_0 \tau + (2n+1)(2t - \tau)\theta] dt
\end{cases} \quad (F.12)$$

Eqn. (F.12) can be simplified as:

$$\begin{cases}
K_{S1}^u = \int_{-\infty}^{\infty} \cos[(\omega_0 + n\theta)(2t - \tau)] dt \\
K_{S2}^u = \int_{-\infty}^{\infty} \cos[4n\theta t + (\omega_0 - 2n\theta)\tau] dt \\
K_{S3}^u = \int_{-\infty}^{\infty} \sin[2\theta(2n+1)t + (\omega_0 \tau - 2n\theta - \theta)\tau] dt
\end{cases} \quad (F.13)$$

F.1 When $\tau \geq 0$

Since the chirp duration shown in Eqn. (F.4) is $-T_c/2 \leq t \leq T_c/2$, the integral range for (F.13) when $\tau \geq 0$ can be calculated as:

$$\begin{cases} -\frac{T_c}{2} \leq t \leq \frac{T_c}{2} \\ -\frac{T_c}{2} \leq (t-\tau) \leq \frac{T_c}{2} \Rightarrow -\frac{T_c}{2} + \tau \leq t \leq \frac{T_c}{2} + \tau \end{cases} \Rightarrow -\frac{T_c}{2} + \tau \leq t \leq \frac{T_c}{2} \quad (\text{F.14})$$

Eqn. (F.13) in the case of $\tau \geq 0$ can be achieved by recalling Eqn. (F.14):

$$\begin{cases} \mathbf{K}_{S1}^u = \int_{-T_c/2+\tau}^{T_c/2} \cos[(\omega_0 + n\theta)(2t - \tau)] dt \\ \mathbf{K}_{S2}^u = \int_{-T_c/2+\tau}^{T_c/2} \cos[4n\theta t + (\omega_0 - 2n\theta)\tau] dt \\ \mathbf{K}_{S3}^u = \int_{-T_c/2+\tau}^{T_c/2} \sin[2\theta(2n+1)t + (\omega_0\tau - 2n\theta - \theta)\tau] dt \end{cases} \quad (\text{F.15})$$

Result of the first term in Eqn. (F.15) can be obtained as:

$$\begin{aligned} \mathbf{K}_{S1}^u &= \int_{-T_c/2+\tau}^{T_c/2} \cos[(\omega_0 + n\theta)(2t - \tau)] dt \\ &= \frac{1}{2(\omega_0 + n\theta)} \sin[(\omega_0 + n\theta)(2t - \tau)] \Big|_{-T_c/2+\tau}^{T_c/2} \\ &= \frac{1}{2(\omega_0 + n\theta)} \left\{ \sin[(\omega_0 + n\theta)(T_c - \tau)] - \sin[-(\omega_0 + n\theta)(T_c - \tau)] \right\} \\ &= \frac{1}{2(\omega_0 + n\theta)} \left\{ 2 \sin[(\omega_0 + n\theta)(T_c - \tau)] \right\} = \frac{\sin[(\omega_0 + n\theta)(T_c - \tau)]}{(\omega_0 + n\theta)} \end{aligned} \quad (\text{F.16})$$

Result of the second term in Eqn. (F.15) can be obtained as:

$$\begin{aligned}
K_{S2}^u &= \int_{-T_c/2+\tau}^{T_c/2} \cos[4n\theta t + (\omega_0 - 2n\theta)\tau] dt \\
&= \frac{1}{4n\theta} \sin[4n\theta t + (\omega_0 - 2n\theta)\tau] \Big|_{-T_c/2+\tau}^{T_c/2} \\
&= \frac{\{\sin[2n\theta T_c + (\omega_0 - 2n\theta)\tau] - \sin[2n\theta(-T_c + 2\tau) + (\omega_0 - 2n\theta)\tau]\}}{4n\theta} \\
&= \frac{[\sin(2n\theta T_c + \omega_0\tau - 2n\theta\tau) - \sin(-2n\theta T_c + \omega_0\tau + 2n\theta\tau)]}{4n\theta} \\
&= \frac{\cos(\omega_0\tau) \sin[2n\theta(T_c - \tau)]}{2n\theta}
\end{aligned} \tag{F.17}$$

Result of the third term in Eqn. (F.15) can be obtained as:

$$\begin{aligned}
K_{S3}^u &= \int_{-T_c/2+\tau}^{T_c/2} \sin[2\theta(2n+1)t + (\omega_0 - 2n\theta - \theta)\tau] dt \\
&= \frac{-1}{2\theta(2n+1)} \cos[2\theta(2n+1)t + (\omega_0 - 2n\theta - \theta)\tau] \Big|_{-T_c/2+\tau}^{T_c/2} \\
&= \frac{-\{\cos[\theta(2n+1)(T_c - \tau) + \omega_0\tau] - \cos[\theta(2n+1)(-T_c + \tau) + \omega_0\tau]\}}{2\theta(2n+1)} \\
&= \frac{-[-2\sin(\omega_0\tau) \sin[\theta(2n+1)(T_c - \tau)]]}{2\theta(2n+1)} \\
&= \frac{\sin(\omega_0\tau) \sin[(2n+1)\theta(T_c - \tau)]}{(2n+1)\theta}
\end{aligned} \tag{F.18}$$

Then Eqn. (F.15) can be updated by recalling Eqn. (F.16) , Eqn. (F.17) and Eqn. (F.18):

$$\left\{ \begin{aligned}
K_{S1}^u &= \frac{\sin[(\omega_0 + n\theta)(T_c - \tau)]}{(\omega_0 + n\theta)} \\
K_{S2}^u &= \frac{\cos(\omega_0\tau) \sin[2n\theta(T_c - \tau)]}{2n\theta} \\
K_{S3}^u &= \frac{\sin(\omega_0\tau) \sin[(2n+1)\theta(T_c - \tau)]}{(2n+1)\theta}
\end{aligned} \right. \tag{F.19}$$

F.2 When $\tau \leq 0$

Since the chirp duration is $-T_c/2 \leq t \leq T_c/2$ shown in Eqn. (F.4), the integral range for Eqn. (F.13) when $\tau \leq 0$ can be calculated as:

$$\begin{cases} -\frac{T_c}{2} \leq t \leq \frac{T_c}{2} \\ -\frac{T_c}{2} \leq (t-\tau) \leq \frac{T_c}{2} \Rightarrow -\frac{T_c}{2} + \tau \leq t \leq \frac{T_c}{2} + \tau \end{cases} \Rightarrow -\frac{T_c}{2} \leq t \leq \frac{T_c}{2} + \tau \quad (\text{F.20})$$

By recalling (F.20), then Eqn. (F.13) for $\tau \leq 0$ becomes:

$$\begin{cases} \mathbf{K}_{S1}^u = \int_{-T_c/2}^{T_c/2+\tau} \cos[(\omega_0 + n\theta)(2t - \tau)] dt \\ \mathbf{K}_{S2}^u = \int_{-T_c/2}^{T_c/2+\tau} \cos[4n\theta t + (\omega_0 - 2n\theta)\tau] dt \\ \mathbf{K}_{S3}^u = \int_{-T_c/2}^{T_c/2+\tau} \sin[2\theta(2n+1)t + (\omega_0\tau - 2n\theta - \theta)\tau] dt \end{cases} \quad (\text{F.21})$$

Result of the first term in Eqn. (F.21) can be obtained as:

$$\begin{aligned} \mathbf{K}_{S1}^u &= \int_{-T_c/2}^{T_c/2+\tau} \cos[(\omega_0 + n\theta)(2t - \tau)] dt \\ &= \frac{1}{2(\omega_0 + n\theta)} \sin[(\omega_0 + n\theta)(2t - \tau)] \Big|_{-T_c/2}^{T_c/2+\tau} \\ &= \frac{\{\sin[(\omega_0 + n\theta)(T_c + \tau)] - \sin[(\omega_0 + n\theta)(-T_c - \tau)]\}}{2(\omega_0 + n\theta)} \\ &= \frac{\sin[(\omega_0 + n\theta)(T_c + \tau)]}{(\omega_0 + n\theta)} \end{aligned} \quad (\text{F.22})$$

Result of the second term in Eqn. (F.21) can be obtained as:

$$\begin{aligned}
K_{S2}^u &= \int_{-T_c/2}^{T_c/2+\tau} \cos[4n\theta t + (\omega_0 - 2n\theta)\tau] dt \\
&= \frac{1}{4n\theta} \sin[4n\theta t + (\omega_0 - 2n\theta)\tau] \Big|_{-T_c/2}^{T_c/2+\tau} \\
&= \frac{\{\sin[2n\theta(T_c + 2\tau) + (\omega_0 - 2n\theta)\tau] - \sin[-2n\theta T_c + (\omega_0 - 2n\theta)\tau]\}}{4n\theta} \\
&= \frac{\{\sin[2n\theta(T_c + \tau) + \omega_0\tau] - \sin[-2n\theta(T_c + \tau) + \omega_0\tau]\}}{4n\theta} \\
&= \frac{\cos(\omega_0\tau) \sin[2n\theta(T_c + \tau)]}{2n\theta}
\end{aligned} \tag{F.23}$$

Result of the third term in Eqn. (F.21) can be obtained as:

$$\begin{aligned}
K_{S3}^u &= \int_{-T_c/2}^{T_c/2+\tau} \sin[2\theta(2n+1)t + (\omega_0 - 2n\theta - \theta)\tau] dt \\
&= \frac{-1}{2\theta(2n+1)} \cos[2\theta(2n+1)t + (\omega_0 - 2n\theta - \theta)\tau] \Big|_{-T_c/2}^{T_c/2+\tau} \\
&= \frac{-\{\cos[\theta(2n+1)(T_c + \tau) + \omega_0\tau] - \cos[-\theta(2n+1)T_c + (\omega_0 - 2n\theta - \theta)\tau]\}}{2\theta(2n+1)} \\
&= \frac{-1}{2\theta(2n+1)} \{-2 \sin(\omega_0\tau) \sin[\theta(2n+1)(T_c + \tau)]\} \\
&= \frac{\sin(\omega_0\tau) \sin[(2n+1)\theta(T_c + \tau)]}{(2n+1)\theta}
\end{aligned} \tag{F.24}$$

Then Eqn. (F.15) can be updated by recalling Eqn. (F.16) , Eqn. (F.17) and Eqn. (F.18):

$$\left\{ \begin{aligned}
K_{S1}^u &= \frac{\sin[(\omega_0 + n\theta)(T_c + \tau)]}{(\omega_0 + n\theta)} \\
K_{S2}^u &= \frac{\cos(\omega_0\tau) \sin[2n\theta(T_c + \tau)]}{2n\theta} \\
K_{S3}^u &= \frac{\sin(\omega_0\tau) \sin[(2n+1)\theta(T_c + \tau)]}{(2n+1)\theta}
\end{aligned} \right. \tag{F.25}$$

F.3 Summary

Combing Eqn. (F.19) and Eqn. (F.25), a uniform representation for Eqn. (F.13) for both $\tau \geq 0$ or $\tau \leq 0$ can be given:

$$\left\{ \begin{array}{l} \mathbf{K}_{S1}^u = \frac{\sin[(\omega_0 + n\theta)(T_c - |\tau|)]}{(\omega_0 + n\theta)} \\ \mathbf{K}_{S2}^u = \frac{\cos(\omega_0\tau) \sin[2n\theta(T_c - |\tau|)]}{2n\theta} \\ \mathbf{K}_{S3}^u = \frac{\sin(\omega_0\tau) \sin[(2n+1)\theta(T_c - |\tau|)]}{(2n+1)\theta} \end{array} \right. \quad (\text{F.26})$$

After substitution of Eqn. (F.26) into Eqn. (F.10), cross-correlation coefficient of sine chirps can be finally represented as:

$$\begin{aligned} \rho_S(\tau) &= \left\{ \begin{array}{l} \sum_{n=-\infty}^{\infty} [(-1)^n J_n(k_{S1}^u)] \times \mathbf{K}_{S1}^u + \sum_{n=-\infty}^{\infty} [(-1)^n J_{2n}(k_{S2}^u)] \times \mathbf{K}_{S2}^u \\ - \sum_{n=-\infty}^{\infty} [(-1)^n J_{2n+1}(k_{S2}^u)] \times \mathbf{K}_{S3}^u \end{array} \right\} / T_c \\ &= \sum_{n=-\infty}^{\infty} [(-1)^n J_n(k_{S1}^u)] \times \frac{\sin[(\omega_0 + n\theta)(T_c - |\tau|)]}{(\omega_0 + n\theta)T_c} \\ &\quad + \cos(\omega_0\tau) \sum_{n=-\infty}^{\infty} [(-1)^n J_{2n}(k_{S2}^u)] \times \frac{\sin[2n\theta(T_c - |\tau|)]}{2n\theta T_c} \\ &\quad - \sin(\omega_0\tau) \sum_{n=-\infty}^{\infty} [(-1)^n J_{2n+1}(k_{S2}^u)] \times \frac{\sin[(2n+1)\theta(T_c - |\tau|)]}{(2n+1)\theta T_c} \end{aligned} \quad (\text{F.27})$$

Eqn. (F.27) can be rewritten in form of sinc function as follows:

$$\begin{aligned} \rho_S(\tau) &= \left(1 - \frac{|\tau|}{T_c}\right) \sum_{n=-\infty}^{\infty} \left\{ (-1)^n J_n(k_{S1}^u) \text{sinc}[(\omega_0 + n\theta)(T_c - |\tau|)] \right\} \\ &\quad + \cos(\omega_0\tau) \left(1 - \frac{|\tau|}{T_c}\right) \sum_{n=-\infty}^{\infty} \left\{ (-1)^n J_{2n}(k_{S2}^u) \text{sinc}[2n\theta(T_c - |\tau|)] \right\} \\ &\quad - \sin(\omega_0\tau) \left(1 - \frac{|\tau|}{T_c}\right) \sum_{n=-\infty}^{\infty} \left\{ (-1)^n J_{2n+1}(k_{S2}^u) \text{sinc}[(2n+1)\theta(T_c - |\tau|)] \right\} \end{aligned} \quad (\text{F.28})$$

Recalling Eqn. (A.39) and Eqn. (A.41), cross-correlation coefficient of sine chirp $\rho_s(\tau)$ can be achieved as:

$$\begin{aligned}
\rho_s(\tau) = & \left(1 - \frac{|\tau|}{T_c}\right) \sum_{n=-\infty}^{\infty} \left\{ (-1)^n J_n(k_{S1}^u) \operatorname{sinc}[(\omega_0 + n\theta)(T_c - |\tau|)] \right\} \\
& + \cos(\omega_0\tau) \left(1 - \frac{|\tau|}{T_c}\right) J_0(k_{S2}^u) \\
& + 2 \cos(\omega_0\tau) \left(1 - \frac{|\tau|}{T_c}\right) \sum_{n=1}^{\infty} \left\{ (-1)^n J_{2n}(k_{S2}^u) \operatorname{sinc}[2n\theta(T_c - |\tau|)] \right\} \\
& - 2 \sin(\omega_0\tau) \left(1 - \frac{|\tau|}{T_c}\right) \sum_{n=0}^{\infty} \left\{ (-1)^n J_{2n+1}(k_{S2}^u) \operatorname{sinc}[(2n+1)\theta(T_c - |\tau|)] \right\}
\end{aligned} \tag{F.29}$$

where $\theta = \frac{\pi\Omega}{2T_c}$, $k_{S1}^u = \frac{2BT_c}{\Omega} \sin(\tau\theta)$, $k_{S2}^u = \frac{2BT_c}{\Omega} \cos(\tau\theta)$

Appendix G: Cross-correlation of Cosine Chirps

Cross-correlation coefficient of cosine chirps can be obtained as:

$$\rho_c(\tau) = \frac{\int_{-\infty}^{\infty} c_{c_1}(t)c_{c_2}(t-\tau) dt}{\sqrt{R_{11}(0) \times R_{22}(0)}} = \frac{C_c(\tau)}{\sqrt{R_{11}(0) \times R_{22}(0)}} \quad (\text{G.1})$$

In Eqn. (G.1), $R_{11}(0)$, which is autocorrelation of cosine chirp $c_{c_1}(t)$ when the time shift equals zero, can be given as:

$$R_{11}(0) = \frac{a^2}{2T_c} \quad (\text{G.2})$$

In Eqn. (G.1), $R_{22}(0)$, which is autocorrelation of cosine chirp $c_{c_2}(t)$ when the time shift equals zero, can be given as:

$$R_{22}(0) = \frac{a^2}{2T_c} \quad (\text{G.3})$$

In Eqn. (G.1), $C_c(\tau)$, which is cross-correlation between $c_{c_1}(t)$ and $c_{c_2}(t)$, can be represented as:

$$C_c(\tau) = \int_{-\infty}^{\infty} \left\{ \begin{array}{l} a \cos \left[\omega_0 t + \frac{BT_c}{\Omega} \sin \left(\pi \Omega \frac{t}{T_c} \right) \right] \\ \times a \cos \left[\omega_0 (t-\tau) - \frac{BT_c}{\Omega} \sin \left(\pi \Omega \frac{(t-\tau)}{T_c} \right) \right] \end{array} \right\} dt \quad (\text{G.4})$$

Let

$$z = \frac{BT_c}{\Omega} \quad \text{and} \quad \theta = \frac{\pi \Omega}{2T_c} \quad (\text{G.5})$$

Then Eqn. (G.4) becomes:

$$\begin{aligned}
C_c(\tau) &= \int_{-\infty}^{\infty} \left\{ a \cos[\omega_0 t + z \sin(2\theta t)] \times a \cos[\omega_0(t-\tau) - z \sin(2\theta(t-\tau))] \right\} dt \\
&= \frac{1}{2} a^2 \int_{-\infty}^{\infty} \left\{ \begin{aligned} &\cos[2\omega_0 t - \omega_c \tau + z \sin(2\theta t) - z \sin(2\theta(t-\tau))] \\ &+ \cos[\omega_0 \tau + z \sin(\theta t) + z \sin(2\theta(t+\tau))] \end{aligned} \right\} dt \quad (G.6) \\
&= \frac{1}{2} a^2 \int_{-\infty}^{\infty} \left\{ \begin{aligned} &\cos[2\omega_0 t - \omega_0 \tau + 2z \cos(\theta(2t-\tau)) \sin(\theta\tau)] \\ &+ \cos[\omega_0 \tau + 2z \sin(\theta(2t-\tau)) \cos(\theta\tau)] \end{aligned} \right\} dt
\end{aligned}$$

Let,

$$\begin{cases} k_{c1}^u = 2z \sin(\tau\theta) = \frac{2BT_c}{\Omega} \sin(\tau\theta) \\ k_{c2}^u = 2z \cos(\tau\theta) = \frac{2BT_c}{\Omega} \cos(\tau\theta) \\ k = (2t - \tau)\theta \end{cases} \quad (G.7)$$

Then Eqn. (G.7) becomes:

$$C_c(\tau) = \frac{1}{2} a^2 \int_{-\infty}^{\infty} \left\{ \cos[2\omega_0 t - \omega_0 \tau + k_{c1}^u \cos(k)] + \cos[\omega_0 \tau + k_{c2}^u \sin(k)] \right\} dt \quad (G.8)$$

By substituting Eqn. (G.2), Eqn. (G.3), and Eqn. (G.8), then cross-correlation coefficient of sine chirps defined in Eqn. (G.1) can be written as:

$$\rho_c(\tau) = \frac{1}{T_c} \int_{-\infty}^{\infty} \left\{ \cos[2\omega_0 t - \omega_0 \tau + k_{c1}^u \cos(k)] + \cos[\omega_0 \tau + k_{c2}^u \sin(k)] \right\} dt \quad (G.9)$$

By recalling Eqn. (A.10) and Eqn. (A.26), then Eqn. (G.9) can be obtained as:

$$\begin{aligned}
\rho_C(\tau) &= \frac{1}{T_c} \left(\int_{-\infty}^{\infty} \left\{ \begin{aligned} &\sum_{n=-\infty}^{\infty} [(-1)^n J_{2n}(k_{C1}^u) \cos(2\omega_0 t - \omega_0 \tau + 2nk)] \\ & - \sum_{n=-\infty}^{\infty} \{(-1)^n J_{2n+1}(k_{C1}^u) \sin[2\omega_0 t + \omega_0 \tau + (2n+1)k]\} \end{aligned} \right\} dt \right. \\
&\quad \left. + \int_{-\infty}^{\infty} \sum_{n=-\infty}^{\infty} [J_n(k_{C2}^u) \cos(\omega_0 \tau + nk)] dt \right) \quad (G.10) \\
&= \frac{1}{T_c} \left\{ \begin{aligned} &\sum_{n=-\infty}^{\infty} [(-1)^n J_{2n}(k_{C1}^u)] \times K_{C1}^u \\ & - \sum_{n=-\infty}^{\infty} [(-1)^n J_{2n+1}(k_{C1}^u)] \times K_{C1}^u + \sum_{n=-\infty}^{\infty} [J_n(k_{C2}^u)] \times K_{C3}^u \end{aligned} \right\}
\end{aligned}$$

where

$$\begin{cases} K_{C1}^u = \int_{-\infty}^{\infty} \cos(2\omega_0 t - \omega_0 \tau + 2nk) dt \\ K_{C2}^u = \int_{-\infty}^{\infty} \sin[2\omega_0 t + \omega_0 \tau + (2n+1)k] dt \\ K_{C3}^u = \int_{-\infty}^{\infty} \cos(\omega_0 \tau + nk) dt \end{cases} \quad (G.11)$$

By substituting $k = (2t + \tau)\theta$ defined in Eqn. (G.7), then Eqn. (G.11) can be rewritten

as:

$$\begin{cases} K_{C1}^u = \int_{-\infty}^{\infty} \cos[2\omega_0 t - \omega_0 \tau + 2n(2t - \tau)\theta] dt \\ K_{C2}^u = \int_{-\infty}^{\infty} \sin[2\omega_0 t + \omega_0 \tau + (2n+1)(2t - \tau)\theta] dt \\ K_{C3}^u = \int_{-\infty}^{\infty} \cos[\omega_0 \tau + n(2t - \tau)\theta] dt \end{cases} \quad (G.12)$$

Eqn. (G.12) can be simplified as:

$$\begin{cases} K_{C1}^u = \int_{-\infty}^{\infty} \cos[(\omega_0 + 2n\theta)(2t - \tau)] dt \\ K_{C2}^u = \int_{-\infty}^{\infty} \sin[(\omega_0 + 2n\theta + \theta)(2t - \tau)] dt \\ K_{C3}^u = \int_{-\infty}^{\infty} \cos[2n\theta t + (\omega_0 - n\theta)\tau] dt \end{cases} \quad (G.13)$$

G.1 When $\tau \geq 0$

Since the chirp duration is $-T_c/2 \leq t \leq T_c/2$ shown in Eqn. (G.4), the integral range for Eqn. (G.13) when $\tau \geq 0$ can be calculated as:

$$\begin{cases} -\frac{T_c}{2} \leq t \leq \frac{T_c}{2} \\ -\frac{T_c}{2} \leq (t-\tau) \leq \frac{T_c}{2} \Rightarrow -\frac{T_c}{2} + \tau \leq t \leq \frac{T_c}{2} + \tau \end{cases} \Rightarrow -\frac{T_c}{2} + \tau \leq t \leq \frac{T_c}{2} \quad (\text{G.14})$$

Eqn. (G.13) in the case of $\tau \geq 0$ can be achieved by recalling Eqn. (G.14):

$$\begin{cases} \mathbf{K}_{C1}^u = \int_{-T_c/2+\tau}^{T_c/2} \cos[(\omega_0 + 2n\theta)(2t - \tau)] dt \\ \mathbf{K}_{C2}^u = \int_{-T_c/2+\tau}^{T_c/2} \sin[(\omega_0 + 2n\theta + \theta)(2t - \tau)] dt \\ \mathbf{K}_{C3}^u = \int_{-T_c/2+\tau}^{T_c/2} \cos[2n\theta t + (\omega_0 - n\theta)\tau] dt \end{cases} \quad (\text{G.15})$$

Result of the first term in Eqn. (G.15) can be obtained as:

$$\begin{aligned} \mathbf{K}_{C1}^u &= \int_{-T_c/2+\tau}^{T_c/2} \cos[(\omega_0 + 2n\theta)(2t - \tau)] dt \\ &= \frac{1}{2(\omega_0 + 2n\theta)} \sin[(\omega_0 + 2n\theta)(2t - \tau)] \Big|_{-T_c/2+\tau}^{T_c/2} \\ &= \frac{1}{2(\omega_0 + n\theta)} \left\{ \sin[(\omega_0 + 2n\theta)(T_c - \tau)] - \sin[(\omega_0 + 2n\theta)(-T_c + \tau)] \right\} \\ &= \frac{1}{2(\omega_0 + 2n\theta)} \left\{ 2 \sin[(\omega_0 + 2n\theta)(T_c - \tau)] \right\} = \frac{\sin[(\omega_0 + 2n\theta)(T_c - \tau)]}{(\omega_0 + 2n\theta)} \end{aligned} \quad (\text{G.16})$$

Result of the second term in Eqn. (G.15) can be obtained as:

$$\begin{aligned}
K_{C2}^u &= \int_{-T_c/2+\tau}^{T_c/2} \sin[(\omega_0 + 2n\theta + \theta)(2t + \tau)] dt \\
&= \frac{-1}{(\omega_c + 2n\theta + \theta)} \cos[(\omega_0 + 2n\theta + \theta)(2t + \tau)] \Big|_{-T_c/2+\tau}^{T_c/2} \\
&= 0
\end{aligned} \tag{G.17}$$

Result of the third term in Eqn. (G.15) can be obtained as:

$$\begin{aligned}
K_{C3}^u &= \int_{-T_c/2+\tau}^{T_c/2} \cos[2n\theta t + (\omega_0 - n\theta)\tau] dt \\
&= \frac{1}{2n\theta} \sin[2n\theta t + (\omega_0 - n\theta)\tau] \Big|_{-T_c/2+\tau}^{T_c/2} \\
&= \frac{1}{2n\theta} \left\{ \sin[n\theta(T_c - \tau) + \omega_0\tau] - \sin[n\theta(-T_c + \tau) + \omega_0\tau] \right\} \\
&= \frac{1}{2n\theta} \left[2\cos(\omega_0\tau) \sin[n\theta(T_c - \tau)] \right] \\
&= \frac{\cos(\omega_0\tau) \sin[n\theta(T_c - \tau)]}{n\theta}
\end{aligned} \tag{G.18}$$

Then Eqn. (G.15) can be updated by recalling Eqn. (G.16) , Eqn. (G.17) and Eqn. (G.18):

$$\left\{ \begin{aligned}
K_{C1}^u &= \frac{\sin[(\omega_0 + 2n\theta)(T_c - \tau)]}{(\omega_0 + 2n\theta)} \\
K_{C2}^u &= 0 \\
K_{C3}^u &= \frac{\cos(\omega_0\tau) \sin[n\theta(T_c - \tau)]}{n\theta}
\end{aligned} \right. \tag{G.19}$$

G.2 When $\tau \leq 0$

Since the chirp duration is $-T_c/2 \leq t \leq T_c/2$ shown in Eqn. (G.4), the integral range for Eqn. (G.13) when $\tau \leq 0$ can be calculated as:

$$\left\{ \begin{array}{l} -\frac{T_c}{2} \leq t \leq \frac{T_c}{2} \\ -\frac{T_c}{2} \leq (t-\tau) \leq \frac{T_c}{2} \Rightarrow -\frac{T_c}{2} + \tau \leq t \leq \frac{T_c}{2} + \tau \end{array} \right. \Rightarrow -\frac{T_c}{2} \leq t \leq \frac{T_c}{2} + \tau \quad (\text{G.20})$$

By recalling (G.20), then Eqn. (G.13) for $\tau \leq 0$ becomes:

$$\left\{ \begin{array}{l} \mathbf{K}_{C1}^u = \int_{-T_c/2}^{T_c/2+\tau} \cos[(\omega_0 + 2n\theta)(2t + \tau)] dt \\ \mathbf{K}_{C2}^u = \int_{-T_c/2}^{T_c/2+\tau} \sin[(\omega_0 + 2n\theta + \theta)(2t + \tau)] dt \\ \mathbf{K}_{C3}^u = \int_{-T_c/2}^{T_c/2+\tau} \cos[2n\theta t + (\omega_0 + n\theta)\tau] dt \end{array} \right. \quad (\text{G.21})$$

Result of the first term in Eqn. (G.21) can be obtained as:

$$\begin{aligned} \mathbf{K}_{C1}^u &= \int_{-T_c/2}^{T_c/2+\tau} \cos[(\omega_0 + 2n\theta)(2t - \tau)] dt \\ &= \frac{1}{2(\omega_0 + 2n\theta)} \sin[(\omega_0 + 2n\theta)(2t - \tau)] \Big|_{-T_c/2}^{T_c/2+\tau} \\ &= \frac{1}{2(\omega_0 + 2n\theta)} \left\{ \sin[(\omega_0 + 2n\theta)(T_c + \tau)] - \sin[-(\omega_0 + 2n\theta)(T_c + \tau)] \right\} \\ &= \frac{1}{2(\omega_0 + 2n\theta)} \left\{ 2 \sin[(\omega_0 + 2n\theta)(T_c + \tau)] \right\} = \frac{\sin[(\omega_0 + 2n\theta)(T_c + \tau)]}{(\omega_0 + 2n\theta)} \end{aligned} \quad (\text{G.22})$$

Result of the second term in Eqn. (G.21) can be obtained as:

$$\begin{aligned} \mathbf{K}_{C2}^u &= \int_{-T_c/2}^{T_c/2+\tau} \sin[(\omega_0 + 2n\theta + \theta)(2t - \tau)] dt \\ &= \frac{-1}{(\omega_0 + 2n\theta + \theta)} \cos[(\omega_0 + 2n\theta + \theta)(2t - \tau)] \Big|_{-T_c/2}^{T_c/2+\tau} \\ &= 0 \end{aligned} \quad (\text{G.23})$$

Result of the third term in Eqn. (G.21) can be obtained as:

$$\begin{aligned}
\mathbf{K}_{C3}^u &= \int_{-T_c/2}^{T_c/2+\tau} \cos[2n\theta t + (\omega_0 - n\theta)\tau] dt \\
&= \frac{1}{2n\theta} \sin[2n\theta t + (\omega_0 - n\theta)\tau] \Big|_{-T_c/2}^{T_c/2+\tau} \\
&= \frac{1}{2n\theta} \{ \sin(n\theta T_c + \omega_0\tau + n\theta\tau) - \sin(-n\theta T_c - n\theta\tau + \omega_0\tau) \} \\
&= \frac{1}{2n\theta} [2 \cos(\omega_0\tau) \sin[n\theta(T_c + \tau)]] \\
&= \frac{\cos(\omega_0\tau) \sin[n\theta(T_c + \tau)]}{n\theta}
\end{aligned} \tag{G.24}$$

Then Eqn. (G.21) can be updated by recalling Eqn. (G.22) , Eqn. (G.23) and Eqn. (G.24):

$$\left\{ \begin{array}{l} \mathbf{K}_{C1}^u = \frac{\sin[(\omega_0 + 2n\theta)(T_c + \tau)]}{(\omega_0 + 2n\theta)} \\ \mathbf{K}_{C2}^u = 0 \\ \mathbf{K}_{C3}^u = \frac{\cos(\omega_0\tau) \sin[n\theta(T_c + \tau)]}{n\theta} \end{array} \right. \tag{G.25}$$

Combing Eqn. (G.19) and Eqn. (G.25), a uniform representation for Eqn. (G.13) for both $\tau \geq 0$ or $\tau \leq 0$ can be given:

$$\left\{ \begin{array}{l} \mathbf{K}_{C1}^u = \frac{\sin[(\omega_0 + 2n\theta)(T_c - |\tau|)]}{(\omega_0 + 2n\theta)} \\ \mathbf{K}_{C2}^u = 0 \\ \mathbf{K}_{C3}^u = \frac{\cos(\omega_0\tau) \sin[n\theta(T_c - |\tau|)]}{n\theta} \end{array} \right. \tag{G.26}$$

G.3 Summary

After substitution of Eqn. (G.26) into Eqn. (G.10), cross-correlation coefficient of sine chirps can be represented as:

$$\begin{aligned}
\rho_C(\tau) &= \left\{ \begin{aligned} &\sum_{n=-\infty}^{\infty} [(-1)^n J_{2n}(k_{C1}^u)] \times K_{C1}^u \\ &+ \sum_{n=-\infty}^{\infty} [(-1)^n J_{2n+1}(k_{C1}^u)] \times K_{C1}^u + \sum_{n=-\infty}^{\infty} [J_n(k_{C2}^u)] \times K_{C3}^u \end{aligned} \right\} / T_c \\
&= \sum_{n=-\infty}^{\infty} [(-1)^n J_{2n}(k_{C1}^u)] \times \frac{\sin[(\omega_0 + 2n\theta)(T_c - |\tau|)]}{(\omega_0 + 2n\theta)T_c} \\
&\quad + \sum_{n=-\infty}^{\infty} [(-1)^n J_{2n+1}(k_{C1}^u)] \times 0 \\
&\quad + \sum_{n=-\infty}^{\infty} [J_n(k_{C2}^u)] \times \frac{\cos(\omega_0\tau) \sin[n\theta(T_c - |\tau|)]}{n\theta T_c}
\end{aligned} \tag{G.27}$$

Eqn. (G.27) can be rewritten in form of sinc function as follows:

$$\begin{aligned}
\rho_C(\tau) &= \left(1 - \frac{|\tau|}{T_c}\right) \sum_{n=-\infty}^{\infty} \{(-1)^n J_{2n}(k_{C1}^u) \text{sinc}[(\omega_0 + 2n\theta)(T_c - |\tau|)]\} \\
&\quad + \cos(\omega_0\tau) \left(1 - \frac{|\tau|}{T_c}\right) \sum_{n=-\infty}^{\infty} \{J_n(k_{C2}^u) \text{sinc}[n\theta(T_c - |\tau|)]\}
\end{aligned} \tag{G.28}$$

Recalling Eqn. (A.2), the following results can be obtained:

$$\sum_{n=-\infty}^{\infty} [J_n(k_{C2}^u)] = J_0(k_{C2}^u) + 2 \sum_{n=1}^{\infty} [J_{2n}(k_{C2}^u)] \tag{G.29}$$

Eqn. (G.28) can be simplified by substituting Eqn. (G.29) as:

$$\begin{aligned}
\rho_C(\tau) &= \left(1 - \frac{|\tau|}{T_c}\right) \sum_{n=-\infty}^{\infty} \{(-1)^n J_{2n}(k_{C1}^u) \text{sinc}[(\omega_0 + 2n\theta)(T_c - |\tau|)]\} \\
&\quad + \cos(\omega_0\tau) \left(1 - \frac{|\tau|}{T_c}\right) J_0(k_{C2}^u) \\
&\quad + 2 \cos(\omega_0\tau) \left(1 - \frac{|\tau|}{T_c}\right) \sum_{n=1}^{\infty} \{J_{2n}(k_{C2}^u) \text{sinc}[2n\theta(T_c - |\tau|)]\}
\end{aligned} \tag{G.30}$$

Where $\theta = \frac{\pi\Omega}{2T_c}$, $k_{C1}^u = \frac{2BT_c}{\Omega} \sin(\tau\theta)$, $k_{C2}^u = \frac{2BT_c}{\Omega} \cos(\tau\theta)$

Appendix H: Doppler Effect on Matched Output of Sine Chirps

A pair of sine chirps can be represented as:

$$\begin{cases} c_{S1}(t) = a \cos \left[\omega_0 t + \frac{BT_c}{\Omega} \cos \left(\pi \Omega \frac{t}{T_c} \right) \right] & -\frac{T_c}{2} \leq t \leq \frac{T_c}{2} \\ c_{S2}(t) = a \cos \left[\omega_0 t - \frac{BT_c}{\Omega} \cos \left(\pi \Omega \frac{t}{T_c} \right) \right] & -\frac{T_c}{2} \leq t \leq \frac{T_c}{2} \end{cases} \quad (\text{H.1})$$

Suppose $c_{S1}(t)$ has reached the receiver with a certain frequency offset ω_d , then the received signal can be represented as:

$$c_{S1}^d(t) = a \cos \left[(\omega_0 + \omega_d)t + \frac{BT_c}{\Omega} \cos \left(\pi \Omega \frac{t}{T_c} \right) \right] \quad -\frac{T_c}{2} \leq t \leq \frac{T_c}{2} \quad (\text{H.2})$$

According to the definition of a matched filter in Eqn. (2.7), the impulse response $h_{S1}(t)$ of a filter matched to the signal $c_{S1}(t)$ is:

$$h_{S1}(t) = c_{S1}^*(-t) = a \cos \left[\omega_0 t - \frac{BT_c}{\Omega} \cos \left(\pi \Omega \frac{t}{T_c} \right) \right] \quad (\text{H.3})$$

Output of the matched filter is:

$$\begin{aligned} g_S^{dm}(\tau, \omega_d) &= c_{S1}^d(t) * h_{S1}(t) = \int_{-\infty}^{\infty} c_{S1}^d(t) h_{S1}(\tau - t) dt \\ &= \int_{-\infty}^{\infty} \left\{ \begin{aligned} &a \cos \left[(\omega_0 + \omega_d)t + \frac{BT_c}{\Omega} \cos \left(\pi \Omega \frac{t}{T_c} \right) \right] \\ &\times a \cos \left[\omega_0(t - \tau) + \frac{BT_c}{\Omega} \cos \left(\pi \Omega \frac{t - \tau}{T_c} \right) \right] \end{aligned} \right\} dt \end{aligned} \quad (\text{H.4})$$

Let

$$z = \frac{BT_c}{\Omega} \quad \text{and} \quad \theta = \frac{\pi\Omega}{2T_c} \quad (\text{H.5})$$

Then Eqn. (H.4) can be represented as:

$$\begin{aligned} g_s^{dm}(\tau, \omega_d) &= a^2 \int_{-\infty}^{\infty} \left\{ \cos[(\omega_0 + \omega_d)t + z \cos(2\theta t)] \right. \\ &\quad \left. \times \cos[\omega_0(t - \tau) + z \cos(2\theta(t - \tau))] \right\} dt \\ &= \frac{1}{2} a^2 \int_{-\infty}^{\infty} \left\{ \cos[(2\omega_0 + \omega_d)t - \omega_0\tau + z \cos(2\theta t) + z \cos(2\theta(t - \tau))] \right. \\ &\quad \left. + \cos[\omega_d t + \omega_0\tau + z \cos(2\theta t) - z \cos(2\theta(t - \tau))] \right\} dt \end{aligned} \quad (\text{H.6})$$

Eqn. (H.6) can be rearranged as:

$$g_s^{dm}(\tau, \omega_d) = \frac{1}{2} a^2 \int_{-\infty}^{\infty} \left\{ \cos[(2\omega_0 + \omega_d)t - \omega_0\tau + 2z \cos(\theta\tau) \cos[\theta(2t - \tau)]] \right. \\ \left. + \cos[\omega_d t + \omega_0\tau - 2z \sin(\theta\tau) \sin[\theta(2t - \tau)]] \right\} dt \quad (\text{H.7})$$

Let

$$\begin{cases} k_{s1}^{dm} = 2z \cos(\theta\tau) = \frac{2BT_c}{\Omega} \cos\left(\frac{\pi\Omega}{2T_c} \tau\right) \\ k_{s2}^{dm} = 2z \sin(\theta\tau) = \frac{2BT_c}{\Omega} \sin\left(\frac{\pi\Omega}{2T_c} \tau\right) \\ k = (2t - \tau)\theta = (2t - \tau) \frac{\pi\Omega}{2T_c}; \end{cases} \quad (\text{H.8})$$

Eqn. (H.7) can be represented as:

$$g_s^{dm}(\tau, \omega_d) = \frac{1}{2} a^2 \int_{-\infty}^{\infty} \left\{ \cos[(2\omega_0 + \omega_d)t - \omega_0\tau + k_{s1}^{dm} \cos(k)] \right. \\ \left. + \cos[\omega_d t + \omega_0\tau - k_{s2}^{dm} \sin(k)] \right\} dt \quad (\text{H.9})$$

By recalling Eqn. (A.10) and Eqn. (A.26), then Eqn. (H.9) can be obtained as:

$$\begin{aligned}
g_s^{dm}(\tau, \omega_d) &= \frac{1}{2} a^2 \left(\begin{aligned} &\int_{-\infty}^{\infty} \sum_{n=-\infty}^{\infty} \left[(-1)^n J_{2n}(k_{S1}^{dm}) \cos[(2\omega_0 + \omega_d)t - \omega_0\tau + 2nk] \right] dt \\ &- \int_{-\infty}^{\infty} \sum_{n=-\infty}^{\infty} \left\{ (-1)^n J_{2n+1}(k_{S1}^{dm}) \sin[(2\omega_0 + \omega_d)t - \omega_0\tau + (2n+1)k] \right\} dt \\ &+ \int_{-\infty}^{\infty} \sum_{n=-\infty}^{\infty} \left\{ (-1)^n J_n(k_{S1}^{dm}) \cos(\omega_d t + \omega_0\tau + nk) \right\} dt \end{aligned} \right) \quad (\text{H.10}) \\
&= \frac{1}{2} a^2 \left\{ \begin{aligned} &\sum_{n=-\infty}^{\infty} \left[(-1)^n J_{2n}(k_{S1}^{dm}) \right] \times M_{S1}^{dm} + \sum_{n=-\infty}^{\infty} \left[(-1)^n J_{2n+1}(k_{S1}^{dm}) \right] \times M_{S2}^{dm} \\ &+ \sum_{n=-\infty}^{\infty} \left[(-1)^n J_n(k_{S2}^{dm}) \right] \times M_{S3}^{dm} \end{aligned} \right\}
\end{aligned}$$

where:

$$\begin{cases} M_{S1}^{dm} = \int_{-\infty}^{\infty} \cos[(2\omega_0 + \omega_d)t - \omega_0\tau + 2nk] dt \\ M_{S2}^{dm} = -\int_{-\infty}^{\infty} \sin[(2\omega_0 + \omega_d)t - \omega_0\tau + (2n+1)k] dt \\ M_{S3}^{dm} = \int_{-\infty}^{\infty} \cos(\omega_d t + \omega_0\tau + nk) dt \end{cases} \quad (\text{H.11})$$

Recall $k = (2t - \tau)\theta$, Eqn. (H.11) can be represented as:

$$\begin{cases} M_{S1}^{dm} = \int_{-\infty}^{\infty} \cos[(2\omega_0 + \omega_d)t - \omega_0\tau + 2n(2t - \tau)\theta] dt \\ M_{S2}^{dm} = -\int_{-\infty}^{\infty} \sin[(2\omega_0 + \omega_d)t - \omega_0\tau + (2n+1)(2t - \tau)\theta] dt \\ M_{S3}^{dm} = \int_{-\infty}^{\infty} \cos[\omega_d t + \omega_0\tau + n(2t - \tau)\theta] dt \end{cases} \quad (\text{H.12})$$

Eqn. (H.12) can be rearranged as:

$$\begin{cases} M_{S1}^{dm} = \int_{-\infty}^{\infty} \cos[(2\omega_0 + \omega_d + 4n\theta)t - (\omega_0 + 2n\theta)\tau] dt \\ M_{S2}^{dm} = -\int_{-\infty}^{\infty} \sin[(2\omega_0 + \omega_d + 4n\theta + 2\theta)t - (\omega_0 + 2n\theta + \theta)\tau] dt \\ M_{S3}^{dm} = \int_{-\infty}^{\infty} \cos[(\omega_d + 2n\theta)t + (\omega_0 - n\theta)\tau] dt \end{cases} \quad (\text{H.13})$$

H.1 When $\tau \geq 0$

Since the chirp duration is $-T_c/2 \leq t \leq T_c/2$ shown in Eqn. (H.2), the integral range for (H.13) when $\tau \geq 0$ can be calculated as:

$$\begin{cases} -\frac{T_c}{2} \leq t \leq \frac{T_c}{2} \\ -\frac{T_c}{2} \leq (t-\tau) \leq \frac{T_c}{2} \Rightarrow -\frac{T_c}{2} + \tau \leq t \leq \frac{T_c}{2} + \tau \end{cases} \Rightarrow -\frac{T_c}{2} + \tau \leq t \leq \frac{T_c}{2} \quad (\text{H.14})$$

Eqn. (H.13) in the case of $\tau \geq 0$ can be achieved by recalling Eqn. (H.14):

$$\begin{cases} M_{S1}^{dm+} = \int_{-T_c/2+\tau}^{T_c/2} \cos[(2\omega_0 + \omega_d + 4n\theta)t - (\omega_0 + 2n\theta)\tau] dt \\ M_{S2}^{dm+} = -\int_{-T_c/2+\tau}^{T_c/2} \sin[(2\omega_0 + \omega_d + 4n\theta + 2\theta)t - (\omega_0 + 2n\theta + \theta)\tau] dt \\ M_{S3}^{dm+} = \int_{-T_c/2+\tau}^{T_c/2} \cos[(\omega_d + 2n\theta)t + (\omega_0 - n\theta)\tau] dt \end{cases} \quad (\text{H.15})$$

Result of the first term in Eqn. (H.15) can be obtained as:

$$\begin{aligned} M_{S1}^{dm+} &= \int_{-T_c/2+\tau}^{T_c/2} \cos[(2\omega_0 + \omega_d + 4n\theta)t - (\omega_0 + 2n\theta)\tau] dt \\ &= \frac{\sin[(2\omega_0 + \omega_d + 4n\theta)t - (\omega_0 + 2n\theta)\tau] \Big|_{-T_c/2+\tau}^{T_c/2}}{(2\omega_0 + \omega_d + 4n\theta)} \\ &= \frac{1}{(2\omega_0 + \omega_d + 4n\theta)} \left\{ \begin{aligned} &\sin[(2\omega_0 + \omega_d + 4n\theta)(T_c/2) - (\omega_0 + 2n\theta)\tau] \\ &- \sin[(2\omega_0 + \omega_d + 4n\theta)(-T_c/2 + \tau) - (\omega_0 + 2n\theta)\tau] \end{aligned} \right\} \quad (\text{H.16}) \\ &= \frac{2}{(2\omega_0 + \omega_d + 4n\theta)} \cos\left(\frac{\omega_d}{2}\tau\right) \sin\left[\frac{(2\omega_0 + \omega_d + 4n\theta)(T_c - \tau)}{2}\right] \end{aligned}$$

Result of the second term in Eqn. (H.15) can be obtained as:

$$\begin{aligned}
M_{S2}^{dm+} &= -\int_{-T_c/2+\tau}^{T_c/2} \sin\left[(2\omega_0 + \omega_d + 4n\theta + 2\theta)t - (\omega_0 + 2n\theta + \theta)\tau\right] dt \\
&= \frac{\cos\left[(2\omega_0 + \omega_d + 4n\theta + 2\theta)t - (\omega_0 + 2n\theta + \theta)\tau\right]_{-T_c/2+\tau}^{T_c/2}}{(2\omega_0 + \omega_d + 4n\theta + 2\theta)} \\
&= \frac{\left\{ \begin{aligned} &\cos\left[(2\omega_0 + \omega_d + 4n\theta + 2\theta)\left(\frac{T_c}{2}\right) - (\omega_0 + 2n\theta + \theta)\tau\right] \\ &-\cos\left[(2\omega_0 + \omega_d + 4n\theta + 2\theta)\left(-\frac{T_c}{2} + \tau\right) - (\omega_0 + 2n\theta + \theta)\tau\right] \end{aligned} \right\}}{(2\omega_0 + \omega_d + 4n\theta + 2\theta)} \\
&= \frac{2}{(2\omega_0 + \omega_d + 4n\theta + 2\theta)} \sin\left(\frac{\omega_d}{2}\tau\right) \sin\left[\frac{(2\omega_0 + \omega_d + 4n\theta + 2\theta)(T_c - \tau)}{2}\right]
\end{aligned} \tag{H.17}$$

Result of the final term in Eqn. (H.15) can be obtained as:

$$\begin{aligned}
M_{S3}^{dm+} &= \int_{-T_c/2+\tau}^{T_c/2} \cos\left[(\omega_d + 2n\theta)t + (\omega_0 - n\theta)\tau\right] dt \\
&= \frac{\sin\left[(\omega_d + 2n\theta)t + (\omega_0 - n\theta)\tau\right]_{-T_c/2+\tau}^{T_c/2}}{(2\omega_0 + \omega_d + 2n\theta)} \\
&= \frac{1}{(\omega_d + 2n\theta)} \left\{ \begin{aligned} &\sin\left[(\omega_d + 2n\theta)(T_c/2) + (\omega_0 - n\theta)\tau\right] \\ &-\sin\left[(\omega_d + 2n\theta)(-T_c/2 + \tau) + (\omega_0 - n\theta)\tau\right] \end{aligned} \right\} \\
&= \frac{2}{(\omega_d + 2n\theta)} \cos\left(\frac{\omega_d + 2\omega_0}{2}\tau\right) \sin\left[\frac{(\omega_d + 2n\theta)(T_c - \tau)}{2}\right]
\end{aligned} \tag{H.18}$$

Then Eqn. (H.15) can be updated by recalling Eqn. (H.16) , Eqn. (H.17) and Eqn. (H.18):

$$\left\{ \begin{aligned} M_{S1}^{dm+} &= \frac{2}{(2\omega_0 + \omega_d + 4n\theta)} \cos\left(\frac{\omega_d}{2}\tau\right) \sin\left[\frac{(2\omega_0 + \omega_d + 4n\theta)(T_c - \tau)}{2}\right] \\ M_{S2}^{dm+} &= \frac{2}{(2\omega_0 + \omega_d + 4n\theta + 2\theta)} \sin\left(\frac{\omega_d}{2}\tau\right) \sin\left[\frac{(2\omega_0 + \omega_d + 4n\theta + 2\theta)(T_c - \tau)}{2}\right] \\ M_{S3}^{dm+} &= \frac{2}{(\omega_d + 2n\theta)} \cos\left(\frac{\omega_d + 2\omega_0}{2}\tau\right) \sin\left[\frac{(\omega_d + 2n\theta)(T_c - \tau)}{2}\right] \end{aligned} \right. \tag{H.19}$$

H.2 When $\tau \leq 0$

Since the chirp duration is $-T_c/2 \leq t \leq T_c/2$ shown in Eqn. (H.2), the integral range for (H.13) when $\tau \leq 0$ can be calculated as:

$$\begin{cases} -\frac{T_c}{2} \leq t \leq \frac{T_c}{2} \\ -\frac{T_c}{2} \leq (t-\tau) \leq \frac{T_c}{2} \Rightarrow -\frac{T_c}{2} + \tau \leq t \leq \frac{T_c}{2} + \tau \end{cases} \Rightarrow -\frac{T_c}{2} \leq t \leq \frac{T_c}{2} + \tau \quad (\text{H.20})$$

Eqn. (H.13) in the case of $\tau \leq 0$ can be achieved by recalling Eqn. (H.20):

$$\begin{cases} M_{S1}^{dm-} = \int_{-T_c/2}^{T_c/2+\tau} \cos[(2\omega_0 + \omega_d + 4n\theta)t - (\omega_0 + 2n\theta)\tau] dt \\ M_{S2}^{dm-} = -\int_{-T_c/2}^{T_c/2+\tau} \sin[(2\omega_0 + \omega_d + 4n\theta + 2\theta)t - (\omega_0 + 2n\theta + \theta)\tau] dt \\ M_{S3}^{dm-} = \int_{-T_c/2}^{T_c/2+\tau} \cos[(\omega_d + 2n\theta)t + (\omega_0 - n\theta)\tau] dt \end{cases} \quad (\text{H.21})$$

Result of the first term in Eqn. (H.21) can be obtained as:

$$\begin{aligned} M_{S1}^{dm-} &= \int_{-T_c/2}^{T_c/2+\tau} \cos[(2\omega_0 + \omega_d + 4n\theta)t - (\omega_0 + 2n\theta)\tau] dt \\ &= \frac{\sin[(2\omega_0 + \omega_d + 4n\theta)t - (\omega_0 + 2n\theta)\tau] \Big|_{-T_c/2}^{T_c/2+\tau}}{(2\omega_0 + \omega_d + 4n\theta)} \\ &= \frac{1}{(2\omega_0 + \omega_d + 4n\theta)} \left\{ \begin{aligned} &\sin[(2\omega_0 + \omega_d + 4n\theta)(T_c/2 + \tau) - (\omega_0 + 2n\theta)\tau] \\ &- \sin[(2\omega_0 + \omega_d + 4n\theta)(-T_c/2) - (\omega_0 + 2n\theta)\tau] \end{aligned} \right\} \quad (\text{H.22}) \\ &= \frac{2}{(2\omega_0 + \omega_d + 4n\theta)} \cos\left(\frac{\omega_d}{2}\tau\right) \sin\left[\frac{(2\omega_0 + \omega_d + 4n\theta)(T_c + \tau)}{2}\right] \end{aligned}$$

Result of the second term in Eqn. (H.21) can be obtained as:

$$\begin{aligned}
M_{S2}^{dm-} &= -\int_{-T_c/2}^{T_c/2+\tau} \sin \left[(2\omega_0 + \omega_d + 4n\theta + 2\theta)t - (\omega_0 + 2n\theta + \theta)\tau \right] dt \\
&= \frac{\cos \left[(2\omega_0 + \omega_d + 4n\theta + 2\theta)t - (\omega_0 + 2n\theta + \theta)\tau \right] \Big|_{-T_c/2}^{T_c/2+\tau}}{(2\omega_0 + \omega_d + 4n\theta + 2\theta)} \\
&= \frac{\left\{ \cos \left[(2\omega_0 + \omega_d + 4n\theta + 2\theta) \left(\frac{T_c}{2} + \tau \right) - (\omega_0 + 2n\theta + \theta)\tau \right] \right.}{(2\omega_c + \omega_d + 4n\theta + 2\theta)} \\
&\quad \left. - \cos \left[(2\omega_0 + \omega_d + 4n\theta + 2\theta) \left(-\frac{T_c}{2} \right) - (\omega_0 + 2n\theta + \theta)\tau \right] \right\}}{(2\omega_c + \omega_d + 4n\theta + 2\theta)} \\
&= \frac{2}{(2\omega_0 + \omega_d + 4n\theta + 2\theta)} \sin \left(\frac{\omega_d}{2} \tau \right) \sin \left[\frac{(2\omega_0 + \omega_d + 4n\theta + 2\theta)(T_c + \tau)}{2} \right]
\end{aligned} \tag{H.23}$$

Result of the final term in Eqn. (H.21) can be obtained as:

$$\begin{aligned}
M_{S3}^{dm-} &= \int_{-T_c/2}^{T_c/2+\tau} \cos \left[(\omega_d + 2n\theta)t + (\omega_0 - n\theta)\tau \right] dt \\
&= \frac{\sin \left[(\omega_d + 2n\theta)t + (\omega_0 - n\theta)\tau \right] \Big|_{-T_c/2}^{T_c/2+\tau}}{(2\omega_0 + \omega_d + 2n\theta)} \\
&= \frac{1}{(\omega_d + 2n\theta)} \left\{ \sin \left[(\omega_d + 2n\theta)(T_c/2 + \tau) + (\omega_0 - n\theta)\tau \right] \right. \\
&\quad \left. - \sin \left[(\omega_d + 2n\theta)(-T_c/2) + (\omega_0 - n\theta)\tau \right] \right\} \\
&= \frac{2}{(\omega_d + 2n\theta)} \cos \left(\frac{\omega_d + 2\omega_0}{2} \tau \right) \sin \left[\frac{(\omega_d + 2n\theta)(T_c + \tau)}{2} \right]
\end{aligned} \tag{H.24}$$

Then Eqn. (H.15) can be updated by recalling Eqn. (H.22) , Eqn. (H.23) and Eqn. (H.24):

$$\left\{ \begin{aligned}
M_{S1}^{dm-} &= \frac{2}{(2\omega_0 + \omega_d + 4n\theta)} \cos \left(\frac{\omega_d}{2} \tau \right) \sin \left[\frac{(2\omega_0 + \omega_d + 4n\theta)(T_c + \tau)}{2} \right] \\
M_{S2}^{dm-} &= \frac{2}{(2\omega_0 + \omega_d + 4n\theta + 2\theta)} \sin \left(\frac{\omega_d}{2} \tau \right) \sin \left[\frac{(2\omega_0 + \omega_d + 4n\theta + 2\theta)(T_c + \tau)}{2} \right] \\
M_{S3}^{dm-} &= \frac{2}{(\omega_d + 2n\theta)} \cos \left(\frac{\omega_d + 2\omega_0}{2} \tau \right) \sin \left[\frac{(\omega_d + 2n\theta)(T_c + \tau)}{2} \right]
\end{aligned} \right. \tag{H.25}$$

H.3 Summary

Combing Eqn. (H.19) and Eqn. (H.25), a uniform representation for Eqn. (H.13) for both $\tau \geq 0$ or $\tau \leq 0$ can be given:

$$\begin{cases} M_{S1}^{dm} = \frac{2}{(2\omega_0 + \omega_d + 4n\theta)} \cos\left(\frac{\omega_d}{2}\tau\right) \sin\left[\frac{(2\omega_0 + \omega_d + 4n\theta)(T_c - |\tau|)}{2}\right] \\ M_{S2}^{dm} = \frac{2}{(2\omega_0 + \omega_d + 4n\theta + 2\theta)} \sin\left(\frac{\omega_d}{2}\tau\right) \sin\left[\frac{(2\omega_0 + \omega_d + 4n\theta + 2\theta)(T_c - |\tau|)}{2}\right] \\ M_{S3}^{dm} = \frac{2}{(\omega_d + 2n\theta)} \cos\left(\frac{\omega_d + 2\omega_0}{2}\tau\right) \sin\left[\frac{(\omega_d + 2n\theta)(T_c - |\tau|)}{2}\right] \end{cases} \quad (\text{H.26})$$

After substitution of Eqn. (H.26) into Eqn. (H.10), finally, Doppler Effect on the matched output of sine chirp signals can be represented as:

$$\begin{aligned} g_s^{dm}(\tau, \omega_d) = & \cos\left(\frac{\omega_d \tau}{2}\right) \sum_{n=-\infty}^{\infty} (-1)^n J_{2n}(k_{S1}^{dm}) \frac{2 \sin\left[\frac{(2\omega_0 + \omega_d + 4n\theta)(T_c - |\tau|)}{2}\right]}{(2\omega_0 + \omega_d + 4n\theta)} \\ & + \sin\left(\frac{\omega_d \tau}{2}\right) \sum_{n=-\infty}^{\infty} (-1)^n J_{2n+1}(k_{S1}^{dm}) \frac{2 \sin\left[\frac{(2\omega_0 + \omega_d + 4n\theta + 2\theta)(T_c - |\tau|)}{2}\right]}{(2\omega_0 + \omega_d + 4n\theta + 2\theta)} \\ & + \cos\left(\frac{\omega_d + 2\omega_0}{2}\tau\right) \sum_{n=-\infty}^{\infty} (-1)^n J_n(k_{S2}^{dm}) \frac{2 \sin\left[\frac{(\omega_d + 2n\theta)(T_c - |\tau|)}{2}\right]}{(\omega_d + 2n\theta)} \end{aligned} \quad (\text{H.27})$$

Eqn. (H.27) can be written in form of sinc function as:

$$\begin{aligned} g_s^{dm}(\tau, \omega_d) = & \left(1 - \frac{|\tau|}{T_c}\right) \cos\left(\frac{\omega_d \tau}{2}\right) \sum_{n=-\infty}^{\infty} (-1)^n J_{2n}(k_{S1}^{dm}) \text{sinc}\left[\frac{(2\omega_0 + \omega_d + 4n\theta)(T_c - |\tau|)}{2}\right] \\ & + \left(1 - \frac{|\tau|}{T_c}\right) \sin\left(\frac{\omega_d \tau}{2}\right) \sum_{n=-\infty}^{\infty} (-1)^n J_{2n+1}(k_{S1}^{dm}) \text{sinc}\left[\frac{(2\omega_0 + \omega_d + 4n\theta + 2\theta)(T_c - |\tau|)}{2}\right] \\ & + \left(1 - \frac{|\tau|}{T_c}\right) \cos\left(\frac{\omega_d + 2\omega_0}{2}\tau\right) \sum_{n=-\infty}^{\infty} (-1)^n J_n(k_{S2}^{dm}) \text{sinc}\left[\frac{(\omega_d + 2n\theta)(T_c - |\tau|)}{2}\right] \end{aligned} \quad (\text{H.28})$$

Recalling $\omega_0 = 2\pi f_0$ and $\omega_d = 2\pi f_d$, then Eqn. (H.28) can be:

$$\begin{aligned}
g_S^{dm}(\tau, \omega_d) = & \left(1 - \frac{|\tau|}{T_c}\right) \cos(\pi f_d \tau) \sum_{n=-\infty}^{\infty} (-1)^n J_{2n}(k_{S1}^{dm}) \text{sinc}[(2\pi f_0 + \pi f_d + 2n\theta)(T_c - |\tau|)] \\
& + \left(1 - \frac{|\tau|}{T_c}\right) \sin(\pi f_d \tau) \sum_{n=-\infty}^{\infty} (-1)^n J_{2n+1}(k_{S1}^{dm}) \text{sinc}[(2\pi f_0 + \pi f_d + 2n\theta + \theta)(T_c - |\tau|)] \quad (\text{H.29}) \\
& + \left(1 - \frac{|\tau|}{T_c}\right) \cos[\pi\tau(f_d + 2f_0)] \sum_{n=-\infty}^{\infty} (-1)^n J_n(k_{S2}^{dm}) \text{sinc}[(\pi f_d + n\theta)(T_c - |\tau|)]
\end{aligned}$$

where $\theta = \frac{\pi\Omega}{2T_c}$, $k_{S1}^{dm} = \frac{2BT_c}{\Omega} \cos(\theta\tau)$, $k_{S2}^{dm} = \frac{2BT_c}{\Omega} \sin(\theta\tau)$

Appendix I: Doppler Effect on Unmatched Output of Sine Chirps

A pair of sine chirps can be represented as:

$$\begin{cases} c_{S1}(t) = a \cos \left[\omega_0 t + \frac{BT_c}{\Omega} \cos \left(\pi \Omega \frac{t}{T_c} \right) \right] & -\frac{T_c}{2} \leq t \leq \frac{T_c}{2} \\ c_{S2}(t) = a \cos \left[\omega_0 t - \frac{BT_c}{\Omega} \cos \left(\pi \Omega \frac{t}{T_c} \right) \right] & -\frac{T_c}{2} \leq t \leq \frac{T_c}{2} \end{cases} \quad (\text{I.1})$$

Suppose $c_{S1}(t)$ has reached the receiver with a certain frequency offset ω_d , then the received signal can be represented as:

$$c_{S1}^d(t) = a \cos \left[(\omega_0 + \omega_d)t + \frac{BT_c}{\Omega} \cos \left(\pi \Omega \frac{t}{T_c} \right) \right] \quad -\frac{T_c}{2} \leq t \leq \frac{T_c}{2} \quad (\text{I.2})$$

According to the definition of an unmatched filter in Eqn. (2.7), the impulse response $h_{S2}(t)$ of a filter unmatched to the signal $c_{S1}(t)$ is:

$$h_{S2}(t) = b \cos \left[\omega_0 t + \frac{BT_c}{\Omega} \cos \left(\pi \Omega \frac{t}{T_c} \right) \right] \quad (\text{I.3})$$

Output of the unmatched filter is:

$$\begin{aligned} g_S^{du}(\tau, \omega_d) &= c_{S1}^d(t) * h_{S2}(t) = \int_{-\infty}^{\infty} c_{S1}^d(t) h_{S2}(\tau - t) dt \\ &= ab \int_{-\infty}^{\infty} \left\{ \begin{aligned} &\cos \left[(\omega_0 + \omega_d)t + \frac{BT_c}{\Omega} \cos \left(\pi \Omega \frac{t}{T_c} \right) \right] \\ &\times \cos \left[\omega_0 (t - \tau) - \frac{BT_c}{\Omega} \cos \left(\pi \Omega \frac{t - \tau}{T_c} \right) \right] \end{aligned} \right\} dt \end{aligned} \quad (\text{I.4})$$

Let

$$z = \frac{BT_c}{\Omega} \quad \text{and} \quad \theta = \frac{\pi\Omega}{2T_c} \quad (\text{I.5})$$

Then Eqn. (I.4) can be represented as:

$$\begin{aligned} g_s^{du}(\tau, \omega_d) &= ab \int_{-\infty}^{\infty} \left\{ \begin{aligned} &\cos[(\omega_0 + \omega_d)t + z \cos(2\theta t)] \\ &\times \cos[\omega_0(t - \tau) - z \cos(2\theta(t - \tau))] \end{aligned} \right\} dt \\ &= \frac{1}{2} ab \int_{-\infty}^{\infty} \left\{ \begin{aligned} &\cos[(2\omega_0 + \omega_d)t - \omega_0\tau + z \cos(2\theta t) - z \cos(2\theta(t - \tau))] \\ &+ \cos[\omega_d t + \omega_0\tau + z \cos(2\theta t) + z \cos(2\theta(t - \tau))] \end{aligned} \right\} dt \end{aligned} \quad (\text{I.6})$$

Eqn. (I.6) can be rearranged as:

$$g_s^{du}(\tau, \omega_d) = \frac{1}{2} ab \int_{-\infty}^{\infty} \left\{ \begin{aligned} &\cos[(2\omega_0 + \omega_d)t - \omega_0\tau - 2z \sin(\theta\tau) \sin(\theta(2t - \tau))] \\ &+ \cos[\omega_d t + \omega_0\tau + 2z \cos(\theta\tau) \cos(\theta(2t - \tau))] \end{aligned} \right\} dt \quad (\text{I.7})$$

Let

$$\begin{cases} k_{s1}^{du} = 2z \sin(\theta\tau) = \frac{2BT_c}{\Omega} \sin\left(\frac{\pi\Omega}{2T_c} \tau\right) \\ k_{s2}^{du} = 2z \cos(\theta\tau) = \frac{2BT_c}{\Omega} \cos\left(\frac{\pi\Omega}{2T_c} \tau\right) \\ k = (2t - \tau)\theta = (2t - \tau) \frac{\pi\Omega}{2T_c}; \end{cases} \quad (\text{I.8})$$

Then Eqn. (I.7) can be represented as:

$$g_s^{du}(\tau, \omega_d) = \frac{1}{2} ab \int_{-\infty}^{\infty} \left\{ \begin{aligned} &\cos[(2\omega_0 + \omega_d)t - \omega_0\tau - k_{s1}^{du} \sin(k)] \\ &+ \cos[\omega_d t + \omega_0\tau + k_{s2}^{du} \cos(k)] \end{aligned} \right\} dt \quad (\text{I.9})$$

By recalling Eqn. (A.26) and Eqn. (A.10), then Eqn. (I.9) can be obtained as:

$$\begin{aligned}
g_S^{du}(\tau, \omega_d) &= \frac{1}{2} ab \left(\int_{-\infty}^{\infty} \left\{ \sum_{n=-\infty}^{\infty} (-1)^n J_n(k_{S1}^{du}) \cos[(2\omega_0 + \omega_d)t - \omega_0\tau + nk] \right\} dt \right. \\
&\quad \left. + \int_{-\infty}^{\infty} \sum_{n=-\infty}^{\infty} \left\{ (-1)^n J_{2n}(k_{S2}^{du}) \cos(\omega_d t + \omega_0\tau + 2nk) \right\} dt \right. \\
&\quad \left. - \int_{-\infty}^{\infty} \sum_{n=-\infty}^{\infty} \left\{ (-1)^n J_{2n+1}(k_{S2}^{du}) \sin[\omega_d t + \omega_0\tau + (2n+1)k] \right\} dt \right) \quad (I.10) \\
&= \frac{1}{2} ab \left\{ \sum_{n=-\infty}^{\infty} [(-1)^n J_n(k_{S1}^{du})] \times M_{S1}^{du} + \sum_{n=-\infty}^{\infty} [(-1)^n J_{2n}(k_{S2}^{du})] \times M_{S2}^{du} \right. \\
&\quad \left. - \sum_{n=-\infty}^{\infty} [(-1)^n J_{2n+1}(k_{S2}^{du})] \times M_{S3}^{du} \right\}
\end{aligned}$$

where:

$$\begin{cases}
M_{S1}^{du} = \int_{-\infty}^{\infty} \cos[(2\omega_0 + \omega_d)t - \omega_0\tau + nk] dt \\
M_{S2}^{du} = \int_{-\infty}^{\infty} \cos(\omega_d t + \omega_0\tau + 2nk) dt \\
M_{S3}^{du} = \int_{-\infty}^{\infty} \sin[\omega_d t + \omega_0\tau + (2n+1)k] dt
\end{cases} \quad (I.11)$$

Recall $k = (2t - \tau)\theta$, Eqn. (I.11) can be represented as:

$$\begin{cases}
M_{S1}^{du} = \int_{-\infty}^{\infty} \cos[(2\omega_0 + \omega_d)t - \omega_0\tau + n(2t - \tau)\theta] dt \\
M_{S2}^{du} = \int_{-\infty}^{\infty} \cos[(\omega_d t + \omega_0\tau + 2n(2t - \tau)\theta)] dt \\
M_{S3}^{du} = \int_{-\infty}^{\infty} \sin[\omega_d t + \omega_0\tau + (2n+1)(2t - \tau)\theta] dt
\end{cases} \quad (I.12)$$

Eqn. (I.12) can be rearranged as:

$$\begin{cases}
M_{S1}^{du} = \int_{-\infty}^{\infty} \cos[(2\omega_0 + \omega_d + 2n\theta)t - (\omega_0 + n\theta)\tau] dt \\
M_{S2}^{du} = \int_{-\infty}^{\infty} \cos[(\omega_d + 4n\theta)t + (\omega_0 - 2n\theta)\tau] dt \\
M_{S3}^{du} = \int_{-\infty}^{\infty} \sin[(\omega_d + 4n\theta + 2\theta)t + (\omega_0 - 2n\theta - \theta)\tau] dt
\end{cases} \quad (I.13)$$

I.1 When $\tau \geq 0$

Since the chirp duration is $-T_c/2 \leq t \leq T_c/2$ shown in Eqn. (I.2), the integral range for (I.13) when $\tau \geq 0$ can be calculated as:

$$\begin{cases} -\frac{T_c}{2} \leq t \leq \frac{T_c}{2} \\ -\frac{T_c}{2} \leq (t-\tau) \leq \frac{T_c}{2} \Rightarrow -\frac{T_c}{2} + \tau \leq t \leq \frac{T_c}{2} + \tau \end{cases} \Rightarrow -\frac{T_c}{2} + \tau \leq t \leq \frac{T_c}{2} \quad (\text{I.14})$$

Eqn. (I.13) in the case of $\tau \geq 0$ can be achieved by recalling Eqn. (I.14):

$$\begin{cases} M_{S1}^{du+} = \int_{-T_c/2+\tau}^{T_c/2} \cos[(2\omega_0 + \omega_d + 2n\theta)t - (\omega_0 + n\theta)\tau] dt \\ M_{S2}^{du+} = \int_{-T_c/2+\tau}^{T_c/2} \cos[(\omega_d + 4n\theta)t + (\omega_0 - 2n\theta)\tau] dt \\ M_{S3}^{du+} = \int_{-T_c/2+\tau}^{T_c/2} \sin[(\omega_d + 4n\theta + 2\theta)t + (\omega_0 - 2n\theta - \theta)\tau] dt \end{cases} \quad (\text{I.15})$$

Result of the first term in Eqn. (I.15) can be obtained as:

$$\begin{aligned} M_{S1}^{du+} &= \int_{-T_c/2+\tau}^{T_c/2} \cos[(2\omega_0 + \omega_d + 2n\theta)t - (\omega_0 + n\theta)\tau] dt \\ &= \frac{1}{(2\omega_0 + \omega_d + 2n\theta)} \sin[(2\omega_0 + \omega_d + 2n\theta)t - (\omega_0 + n\theta)\tau] \Big|_{-T_c/2+\tau}^{T_c/2} \\ &= \frac{1}{(2\omega_0 + \omega_d + 2n\theta)} \left\{ \begin{aligned} &\sin\left[(2\omega_0 + \omega_d + 2n\theta)\left(\frac{T_c}{2}\right) - (\omega_0 + n\theta)\tau\right] \\ &-\sin\left[(2\omega_0 + \omega_d + 2n\theta)\left(-\frac{T_c}{2} + \tau\right) - (\omega_0 + n\theta)\tau\right] \end{aligned} \right\} \quad (\text{I.16}) \\ &= \frac{2}{(2\omega_0 + \omega_d + 2n\theta)} \cos\left(\frac{\omega_d \tau}{2}\right) \sin\left[\frac{(2\omega_0 + \omega_d + 2n\theta)(T_c - \tau)}{2}\right] \end{aligned}$$

Result of the second term in Eqn. (I.15) can be obtained as:

$$M_{S2}^{du+} = \frac{2}{(\omega_d + 4n\theta)} \cos\left(\frac{\omega_d + 2\omega_0}{2} \tau\right) \sin\left[\frac{(\omega_d + 4n\theta)(T_c - \tau)}{2}\right] \quad (\text{I.17})$$

Result of the final term in Eqn. (I.15) can be obtained as:

$$\begin{aligned}
M_{S2}^{du+} &= \int_{-T_c/2+\tau}^{T_c/2} \sin [(\omega_d + 4n\theta + 2\theta)t + (\omega_0 - 2n\theta - \theta)\tau] dt \\
&= -\frac{\cos [(\omega_d + 4n\theta + 2\theta)t + (\omega_0 - 2n\theta - \theta)\tau] \Big|_{-T_c/2+\tau}^{T_c/2}}{(\omega_d + 4n\theta + 2\theta)} \\
&= -\frac{\left\{ \begin{aligned} &\cos [(\omega_d + 4n\theta + 2\theta)(T_c/2) + (\omega_0 - 2n\theta - \theta)\tau] \\ &-\cos [(\omega_d + 4n\theta + 2\theta)(-T_c/2 + \tau) + (\omega_0 - 2n\theta - \theta)\tau] \end{aligned} \right\}}{(\omega_d + 4n\theta + 2\theta)} \quad (I.18) \\
&= \frac{2}{(\omega_d + 4n\theta + 2\theta)} \sin \left(\frac{\omega_d + 2\omega_0}{2} \tau \right) \sin \left[\frac{(\omega_d + 4n\theta + 2\theta)(T_c - \tau)}{2} \right]
\end{aligned}$$

Then Eqn. (I.15) can be updated by recalling Eqn. (I.16), Eqn. (I.17) and Eqn. (I.18):

$$\left\{ \begin{aligned} M_{S1}^{du+} &= \frac{2}{(2\omega_0 + \omega_d + 2n\theta)} \cos \left(\frac{\omega_d \tau}{2} \right) \sin \left[\frac{(2\omega_0 + \omega_d + 2n\theta)(T_c - \tau)}{2} \right] \\ M_{S2}^{du+} &= \frac{2}{(\omega_d + 4n\theta)} \cos \left(\frac{\omega_d + 2\omega_0}{2} \tau \right) \sin \left[\frac{(\omega_d + 4n\theta)(T_c - \tau)}{2} \right] \\ M_{S3}^{du+} &= \frac{2}{(\omega_d + 4n\theta + 2\theta)} \sin \left(\frac{\omega_d + 2\omega_0}{2} \tau \right) \sin \left[\frac{(\omega_d + 4n\theta + 2\theta)(T_c - \tau)}{2} \right] \end{aligned} \right. \quad (I.19)$$

I.2 When $\tau \leq 0$

Since the chirp duration is $-T_c/2 \leq t \leq T_c/2$ shown in Eqn. (I.2), the integral range for (I.13) when $\tau \leq 0$ can be calculated as:

$$\left\{ \begin{aligned} &-\frac{T_c}{2} \leq t \leq \frac{T_c}{2} \\ &-\frac{T_c}{2} \leq (t - \tau) \leq \frac{T_c}{2} \Rightarrow -\frac{T_c}{2} + \tau \leq t \leq \frac{T_c}{2} + \tau \end{aligned} \right. \Rightarrow -\frac{T_c}{2} \leq t \leq \frac{T_c}{2} + \tau \quad (I.20)$$

Eqn. (I.13) in the case of $\tau \leq 0$ can be achieved by recalling Eqn. (I.20):

$$\begin{cases} M_{S1}^{du-} = \int_{-T_c/2}^{T_c/2+\tau} \cos[(2\omega_0 + \omega_d + 2n\theta)t - (\omega_0 + n\theta)\tau] dt \\ M_{S2}^{du-} = \int_{-T_c/2}^{T_c/2+\tau} \cos[(\omega_d + 4n\theta)t + (\omega_0 - 2n\theta)\tau] dt \\ M_{S3}^{du-} = \int_{-T_c/2}^{T_c/2+\tau} \sin[(\omega_d + 4n\theta + 2\theta)t + (\omega_0 - 2n\theta - \theta)\tau] dt \end{cases} \quad (\text{I.21})$$

Result of the first term in Eqn. (I.21) can be obtained as:

$$\begin{aligned} M_{S1}^{du-} &= \int_{-T_c/2}^{T_c/2+\tau} \cos[(2\omega_0 + \omega_d + 2n\theta)t - (\omega_0 + n\theta)\tau] dt \\ &= \frac{1}{(2\omega_0 + \omega_d + 2n\theta)} \sin[(2\omega_0 + \omega_d + 2n\theta)t - (\omega_0 + n\theta)\tau] \Big|_{-T_c/2}^{T_c/2+\tau} \\ &= \frac{1}{(2\omega_0 + \omega_d + 2n\theta)} \left\{ \begin{aligned} &\sin\left[(2\omega_0 + \omega_d + 2n\theta)\left(\frac{T_c}{2} + \tau\right) - (\omega_0 + n\theta)\tau\right] \\ &-\sin\left[(2\omega_0 + \omega_d + 2n\theta)\left(-\frac{T_c}{2}\right) - (\omega_0 + n\theta)\tau\right] \end{aligned} \right\} \\ &= \frac{2}{(2\omega_0 + \omega_d + 2n\theta)} \cos\left(\frac{\omega_d \tau}{2}\right) \sin\left[\frac{(2\omega_0 + \omega_d + 2n\theta)(T_c + \tau)}{2}\right] \end{aligned} \quad (\text{I.22})$$

Result of the second term in Eqn. (I.22) can be obtained as:

$$M_{S2}^{du-} = \frac{2}{(\omega_d + 4n\theta)} \cos\left(\frac{\omega_d + 2\omega_0}{2} \tau\right) \sin\left[\frac{(\omega_d + 4n\theta)(T_c + \tau)}{2}\right] \quad (\text{I.23})$$

Result of the final term in Eqn. (I.22) can be obtained as:

$$\begin{aligned} M_{S3}^{du-} &= \int_{-T_c/2}^{T_c/2+\tau} \sin[(\omega_d + 4n\theta + 2\theta)t + (\omega_0 - 2n\theta - \theta)\tau] dt \\ &= -\frac{\cos[(\omega_d + 4n\theta + 2\theta)t + (\omega_0 - 2n\theta - \theta)\tau] \Big|_{-T_c/2}^{T_c/2+\tau}}{(\omega_d + 4n\theta + 2\theta)} \\ &= \frac{-1}{(\omega_d + 4n\theta + 2\theta)} \left\{ \begin{aligned} &\cos[(\omega_d + 4n\theta + 2\theta)(T_c/2 + \tau) + (\omega_0 - 2n\theta - \theta)\tau] \\ &-\cos[(\omega_d + 4n\theta + 2\theta)(-T_c/2) + (\omega_0 - 2n\theta - \theta)\tau] \end{aligned} \right\} \\ &= \frac{2}{(\omega_d + 4n\theta + 2\theta)} \sin\left(\frac{\omega_d + 2\omega_0}{2} \tau\right) \sin\left[\frac{(\omega_d + 4n\theta + 2\theta)(T_c + \tau)}{2}\right] \end{aligned} \quad (\text{I.24})$$

Then Eqn. (I.21) can be updated by recalling Eqn. (I.22), Eqn. (I.23) and Eqn. (I.24):

$$\begin{cases} M_{S1}^{du-} = \frac{2}{(2\omega_0 + \omega_d + 2n\theta)} \cos\left(\frac{\omega_d \tau}{2}\right) \sin\left[\frac{(2\omega_0 + \omega_d + 2n\theta)(T_c + \tau)}{2}\right] \\ M_{S2}^{du-} = \frac{2}{(\omega_d + 4n\theta)} \cos\left(\frac{\omega_d + 2\omega_0}{2} \tau\right) \sin\left[\frac{(\omega_d + 4n\theta)(T_c + \tau)}{2}\right] \\ M_{S3}^{du-} = \frac{2}{(\omega_d + 4n\theta + 2\theta)} \sin\left(\frac{\omega_d + 2\omega_0}{2} \tau\right) \sin\left[\frac{(\omega_d + 4n\theta + 2\theta)(T_c + \tau)}{2}\right] \end{cases} \quad (\text{I.25})$$

I.3 Summary

Combing Eqn. (I.19) and Eqn. (I.25), a uniform representation for Eqn. (I.13) for both $\tau \geq 0$ or $\tau \leq 0$ can be given:

$$\begin{cases} M_{S1}^{du} = \frac{2}{(2\omega_0 + \omega_d + 2n\theta)} \cos\left(\frac{\omega_d \tau}{2}\right) \sin\left[\frac{(2\omega_0 + \omega_d + 2n\theta)(T_c - |\tau|)}{2}\right] \\ M_{S2}^{du} = \frac{2}{(\omega_d + 4n\theta)} \cos\left(\frac{\omega_d + 2\omega_0}{2} \tau\right) \sin\left[\frac{(\omega_d + 4n\theta)(T_c - |\tau|)}{2}\right] \\ M_{S3}^{du} = \frac{2}{(\omega_d + 4n\theta + 2\theta)} \sin\left(\frac{\omega_d + 2\omega_0}{2} \tau\right) \sin\left[\frac{(\omega_d + 4n\theta + 2\theta)(T_c - |\tau|)}{2}\right] \end{cases} \quad (\text{I.26})$$

After substitution of Eqn. (I.26) into Eqn. (I.10), finally, Doppler Effect on the unmatched output of sine chirp signals can be represented as:

$$\begin{aligned} g_S^{du}(t, \omega_d) = & \cos\left(\frac{\omega_d \tau}{2}\right) \sum_{n=-\infty}^{\infty} (-1)^n J_n(k_{S1}^{du}) \frac{2 \sin\left[\frac{(2\omega_0 + \omega_d + 2n\theta)(T_c - |\tau|)}{2}\right]}{(2\omega_0 + \omega_d + 2n\theta)T_c} \\ & + \cos\left(\frac{\omega_d + 2\omega_0}{2} \tau\right) \sum_{n=-\infty}^{\infty} (-1)^n J_{2n}(k_{S2}^{du}) \frac{2 \sin\left[\frac{(\omega_d + 4n\theta)(T_c - |\tau|)}{2}\right]}{(\omega_d + 4n\theta)T_c} \\ & - \sin\left(\frac{\omega_d + 2\omega_0}{2} \tau\right) \sum_{n=-\infty}^{\infty} (-1)^n J_{2n+1}(k_{S2}^{du}) \frac{2 \sin\left[\frac{(\omega_d + 4n\theta + 2\theta)(T_c - |\tau|)}{2}\right]}{(\omega_d + 4n\theta + 2\theta)T_c} \end{aligned} \quad (\text{I.27})$$

Eqn. (I.27) can be written in form of sinc function as:

$$\begin{aligned}
g_S^{du}(t, \omega_d) = & \left(1 - \frac{|\tau|}{T_c}\right) \cos\left(\frac{\omega_d \tau}{2}\right) \sum_{n=-\infty}^{\infty} (-1)^n J_n(k_{S1}^{du}) \operatorname{sinc}\left[\frac{(2\omega_0 + \omega_d + 2n\theta)(T_c - |\tau|)}{2}\right] \\
& + \left(1 - \frac{|\tau|}{T_c}\right) \cos\left(\frac{\omega_d + 2\omega_0}{2} \tau\right) \sum_{n=-\infty}^{\infty} (-1)^n J_{2n}(k_{S2}^{du}) \operatorname{sinc}\left[\frac{(\omega_d + 4n\theta)(T_c - |\tau|)}{2}\right] \\
& - \left(1 - \frac{|\tau|}{T_c}\right) \sin\left(\frac{\omega_d + 2\omega_0}{2} \tau\right) \sum_{n=-\infty}^{\infty} (-1)^n J_{2n+1}(k_{S2}^{du}) \operatorname{sinc}\left[\frac{(\omega_d + 4n\theta + 2\theta)(T_c - |\tau|)}{2}\right]
\end{aligned} \quad (\text{I.28})$$

Recalling $\omega_0 = 2\pi f_0$ and $\omega_d = 2\pi f_d$, then Eqn. (I.28) can be:

$$\begin{aligned}
g_S^{du}(t, \omega_d) = & \left(1 - \frac{|\tau|}{T_c}\right) \cos(\pi f_d \tau) \sum_{n=-\infty}^{\infty} (-1)^n J_n(k_{S1}^{du}) \operatorname{sinc}\left[(2\pi f_0 + \pi f_d + 2n\theta)(T_c - |\tau|)\right] \\
& + \left(1 - \frac{|\tau|}{T_c}\right) \cos[\pi \tau (f_d + 2f_0)] \sum_{n=-\infty}^{\infty} (-1)^n J_{2n}(k_{S2}^{du}) \operatorname{sinc}\left[(\pi f_d + 2n\theta)(T_c - |\tau|)\right] \\
& - \left(1 - \frac{|\tau|}{T_c}\right) \sin[\pi \tau (f_d + 2f_0)] \sum_{n=-\infty}^{\infty} (-1)^n J_{2n+1}(k_{S2}^{du}) \operatorname{sinc}\left[(\pi f_d + 2n\theta + \theta)(T_c - |\tau|)\right]
\end{aligned} \quad (\text{I.29})$$

where $\theta = \frac{\pi\Omega}{2T_c}$, $k_{S1}^{du} = \frac{2BT_c}{\Omega} \sin(\theta\tau)$, $k_{S2}^{du} = \frac{2BT_c}{\Omega} \cos(\theta\tau)$

Curriculum Vitae

Name: Quan Wang

Post-secondary Education and Degrees: Hubei University of Technology,
Wuhan, Hubei Province, China
1998-2002 B.A.

Wuhan University of Technology
Wuhan, Hubei Province, China
2002-2005 M.A.

The University of Western Ontario
London, Ontario, Canada
2009-2015 Ph.D.

Honours and Awards: Best Student Paper Award at ISOFIC 2014
August 24th, 2014

Publications:

1. Quan Wang, Jin Jiang. "Performances of trigonometric chirp spread spectrum modulation in AWGN & Rayleigh channels". MSWiM 2013. 2013.11.
2. "Performance monitor, evaluation and diagnosis system for wireless sensor networks". US13/915,105. 2013.06.11.
3. Quan Wang, Liqian Li, etc. "Experimental evaluation of wireless communication channel under radiation environment". ISOFIC/ISSNP 2014. 2014.08.

Manuscripts under Preparation:

1. Quan Wang, Jin Jiang. "Technical Survey of Industrial Wireless Communication Standards". IEEE Communications Surveys and Tutorials (Submitted on April 2015, now is under revision).
2. Quan Wang, Jin Jiang. "Non-linear Chirps for the BOK CSS system". (Going to be submitted on June 2015).
3. Quan Wang, Jin Jiang. "Performance of the BOK CSS System by Using the Orthogonal Full Period Sine Chirps". (Going to be submitted on July 2015).